NATIONAL TRANSPORTATION SAFETY BOARD

Office of Research and Engineering
Washington, D.C. 20594

April 9, 2021

Aircraft Performance Study

by John O'Callaghan

Operator: Miami Air International flight 293

Location: Jacksonville Naval Air Station (KNIP), Jacksonville, Florida

Date: May 3, 2019

Time: 21:42 Eastern Daylight Time (EDT)
(01:42 Coordinated Universal Time (UTC), May 4, 2019)

Aircraft: Boeing 737-81Q, registration N732MA

NTSB#: DCA19MA143

TABLE OF CONTENTS

NATIONAL TRANSPORTATION SAFETY BOARD

Office of Research and Engineering
Washington, D.C. 20594

April 9, 2021

Aircraft Performance Study

by John O'Callaghan

A. ACCIDENT

Operator:	Miami Air International flight 293
Location:	Jacksonville Naval Air Station (KNIP), Jacksonville, Florida
Date:	May 3, 2019
Time:	21:42 Eastern Daylight Time (EDT) (01:42 Coordinated Universal Time (UTC), May 4, 2019)[1]
Aircraft:	Boeing 737-81Q, registration N732MA
NTSB#:	DCA19MA143

B. GROUP

Chairman: John O'Callaghan
National Resource Specialist - Aircraft Performance
National Transportation Safety Board (NTSB)
490 L'Enfant Plaza E, SW
Washington, DC 20594

Members: N/A

C. HISTORY OF FLIGHT

On May 3, 2019, at 21:42 eastern daylight time, Miami Air flight 293, a Boeing 737-81Q registration N732MA, was landing on runway 10 at Jacksonville Naval Air Station, Jacksonville, Florida, when it departed the end of the runway, contacted a stone embankment, and came to rest in shallow water in St. Johns River. The 2 pilots, 4 flight attendants, 1 mechanic, and 136 passengers were not seriously injured. The airplane was substantially damaged. Flight 293 was a non-scheduled passenger flight from Leeward Point Field, Naval Station Guantanamo Bay, Cuba (MUGM), operating under the provisions of 14 Code of Federal Regulations (CFR) Part 121 Supplemental. Instrument meteorological conditions prevailed at the time of the accident, and rain was occurring during the landing.

[1] Local time at KNIP on the day of the accident was Eastern Daylight Time (EDT). EDT = UTC - 4 hours. Times in this *Study* use EDT unless otherwise noted.

Objective and scope of the Aircraft Performance Study

The objective of this *Aircraft Performance Study* is to determine and analyze the motion of the airplane and the physical forces that produce that motion. In particular, the *Study* attempts to define the airplane's position and orientation during the relevant portion of the flight, and determine the airplane's response to control inputs, external disturbances, ground forces, and other factors that could affect its trajectory.

The data used to determine and analyze the airplane motion include the following:

- Wreckage location and condition.
- Ground scars / markings.
- Flight Data Recorder (FDR) data.
- Cockpit Voice Recorder (CVR) information.
- Runway macrotexture, cross-slope, and friction measurement information.
- Weather information.
- Airplane thrust and aerodynamic performance information.
- Output from aircraft performance computer programs and simulations.
- Models of braking friction on wet runways.
- Models of water drainage from runways.

This *Study* describes the results of using the data listed above in defining, as far as possible, the position of N732MA relative to the KNIP runway 10 threshold throughout the approach, landing, and overrun. The *Study* introduces the aircraft motion data collected during the investigation, describes the methods used to extract additional aircraft motion information from the FDR, and presents the results of these calculations.

In addition, this *Study* examines this accident within the larger context of the stopping performance of airplanes on wet runways. The *Study* notes that the maximum wheel braking friction coefficient (μ_B) developed by the airplane during the landing ground roll was significantly less than the μ_B underlying the wet-runway landing distances published in the Flight Crew Operating Manual (FCOM) (Reference 1) and computed by the Miami Air Onboard Performance Tool (OPT), and the μ_B predicted by a NASA model based on runway friction measurements that has successfully predicted the μ_B achieved in other accident landings investigated by the NTSB (see Reference 2). A μ_B lower than that assumed in the FCOM/OPT will result in landing distances longer than those presented in the FCOM/OPT. Possible explanations for the μ_B shortfall in this case are considered, including sidewise drift on the runway during the landing, the depth of water on the runway resulting from heavy rain, and the efficiency of the anti-skid braking system in low-μ_B conditions and in the presence of differential (left-to-right) and on/off brake application.

The landing distances in the FCOM are predicated not only on a μ_B model of the runway for a given runway surface condition,[2] but also on the conduct of the approach and landing

[2] The runway surface condition in the FCOM is characterized by a "reported braking action," as discussed in Section D-VII.

according to specified procedures and performance criteria. These include assumptions concerning approach speed, winds, the touchdown point, and the use of deceleration devices such as speedbrakes (spoilers), reverse thrust, and wheel brakes. The *Study* compares the conduct of the accident approach against these criteria, and quantifies how deviations from the assumed criteria affect the required landing distance.

Summary of results

The results of this *Study* indicate that the airspeed over the runway displaced threshold was closer to V_{REF30} + 20 knots instead of the nominal V_{REF30} + 5 knots; a tailwind of 6 to 12 knots was present over the runway; and touchdown occurred about 1,580 ft. past the displaced threshold, or 580 ft. beyond the nominal 1,000 ft. touchdown point. All these factors act to increase the required landing distance beyond the nominal distance published in the FCOM. Nonetheless, the *Study* also indicates that, even with these exacerbating factors, if the airplane had achieved the μ_B underlying the "good" braking action landing distances published in the FCOM, it still would have stopped on the runway pavement, with about 17% of the available runway remaining. Conversely, the airplane could not have stopped on the runway with the μ_B levels actually achieved during the accident landing, even if the approach speed had been the nominal V_{REF30} + 5 knots, the winds had been calm, and the touchdown point had been the nominal 1000 ft. past the displaced threshold; it would still have exited the pavement at a speed of about 12 knots.

These observations highlight the importance of understanding the reasons for the μ_B shortfall experienced during the accident landing, and of identifying when such a μ_B shortfall may occur. The circumstances of this accident also underscore the advice provided by the FAA in Safety Alert For Operators (SAFO) 19003, "Turbojet Braking Performance on Wet Runways" (Reference 4, dated 7/2/2019):

> When planning to land on a smooth runway under conditions of moderate or heavy rain, or when landing on a grooved or [Porous Friction Course] runway under heavy rain, pilots should consider that the surface may be contaminated with water at depth greater than 1/8 inch and adjust their landing distance assessment accordingly.

Summary of airborne performance during the approach and landing

This *Study* examines the performance of N732MA from the time it descended through about 1,400 ft. above mean sea level (MSL) on final approach, to its impact with the stone embankment (hereafter referred to as the "seawall") about 1,164 ft. past the end of runway 10. The summary descriptions of N732MA's performance during the approach, landing, and rollout provided in this and the following subsection are developed in greater detail, and with supporting plots and figures, in subsequent sections of the *Study*.

At 21:40:25, N732MA was configured for a flaps 30 landing with the landing gear extended as it descended through 1,390 ft. MSL (1,369 ft. above the touchdown zone elevation (TDZE) of 21 ft.) at an indicated airspeed of 158 knots and rate of descent of 1,062 ft./minute. Reference 5 notes that the Captain was the pilot flying (PF). The flaps 30 landing reference speed (V_{REF30}) at the airplane's landing weight of 143,200 lb. was 148

kt.; the nominal approach speed of V_{REF30} + 5 kt. was 153 kt.[3] The true airspeed at this time was 167 kt., and due to a 7 kt. tailwind, the ground speed was 174 kt.

At 21:40:25, N732MA was about 3.5 nautical miles (n.m.) from the KNIP runway 10 displaced threshold, and above a 3° glide path to the nominal touchdown point located 1,000 ft. past the displaced threshold. At this point, the Precision Approach Path Indicator (PAPI) lights would have appeared as four white lights.[4] The rate of descent was about 1,100 ft./min., and increased to 1,400 ft./min. at 21:40:30, before decreasing to 1,000 ft./min. at 21:40:40.

At 21:40:40, N732MA was at about 1,100 ft. MSL altitude and about 2.8 n.m. from the displaced threshold. The airplane was closer to the nominal 3° glide path, and the PAPI would have appeared as three white lights and one red light. The indicated airspeed had slowed to 153 kt. (the V_{REF30} + 5 speed) and the ground speed was 166 kt.

Between 21:40:46 and 21:41:39, the indicated airspeed increased steadily from 153 kt. to 170 kt., and the ground speed increased from 166 kt. to 180 kt. At 21:41:09, at about 680 ft. MSL altitude and about 1.6 n.m. from the displaced threshold, N732MA had deviated further above the 3° glide path, and the PAPI would again have appeared as four white lights, and retained that appearance throughout the rest of the approach. N732MA crossed the displaced threshold at 21:41:38, at an altitude of 140 ft. MSL (about 120 ft. above the runway), an indicated airspeed of 170 kt. (17 kt. above V_{REF30} + 5), a ground speed of 180 kt., and a rate of descent of 1,450 ft./min. The threshold crossing height on a 3° glide path to the nominal touchdown point is 52 ft. From 21:41:18 to 21:41:38, the flight path angle decreased from -2° to -5°, and multiple Ground Proximity Warning System (GPWS) “Sink Rate” alerts were recorded on the Cockpit Voice Recorder starting at 21:41:35, about when the rate of descent exceeded -1,450 ft./min. The descent rate peaked at -1,580 ft./min. at about 21:41:36.5.

Reference 5 notes that among the stabilized approach criteria cited in the Miami Air Flight Operations Manual (FOM), “no later than 1,000 feet [above field level], the airplane must be … at a sink rate of no greater than 1,000 feet per minute,” “stabilized at the proper approach speed,” and “on glideslope.” The FOM also states that “momentarily exceeding 1,000 feet per minute is permitted as long as the rate of descent is immediately reduced to at or below 1,000 feet per minute,” but that “if the aircraft is not stabilized by 1,000 feet AFL or at any point thereafter, a Missed Approach is MANDATORY” [emphasis in original].

---

[3] The flap setting, gear position, and airplane weight were recorded by the FDR. The V_{REF30} speeds are published in the FCOM. Reference 5 notes that the Miami Air 737 Operations Manual states that the “final approach speed is Vref plus one half the headwind plus all of the gusts. The minimum approach speed is Vref+5 with a maximum of Vref+20.” Airspeed corrections due to static port pressure errors, and the wind speed and direction present during the approach and landing, are presented in Section D-V of this *Study.*

[4] Reference 6 notes that the KNIP tower controller monitoring N732MA’s approach using Precision Approach Radar (PAR) stated that “At about 4-5 miles from touchdown, the aircraft climbed well above glide path, and after advising the pilot he began to descend back down and back on glidepath.” He also stated that “this was the first time he had ever had to say ‘well above glidepath’ while monitoring an RNAV approach with any aircraft.”

The airplane touched down at 21:41:43.1, about 1,580 ft. past the displaced threshold and 580 ft. beyond the nominal touchdown point. The short field arresting gear was rigged on runway 10, and its cable crossed the runway 1,186 ft. past the displaced threshold; hence the touchdown was 394 ft. beyond the cable.[5] At touchdown, the indicated airspeed was 164 kt. (11 kt. above V_{REF30} + 5) and the ground speed was 180 kt.

For most of the approach from 1,400 ft. MSL altitude (3.5 n.m. from the displaced threshold) to the displaced threshold, N732MA was offset about 100 ft. to the right of the extended runway centerline. At 21:41:17, about 1 n.m. from the displaced threshold, the roll angle dipped to 12° right and the airplane deviated further to the right, reaching 220 ft. right of centerline at 21:41:28, about 0.5 n.m. from the threshold and at 360 ft. MSL altitude. The airplane then rolled to about 9° left and corrected back towards the centerline, and touched down about 20 ft. right of centerline with a track angle of 87°, or 2.65° to the left of the runway bearing of 89.65°. After touchdown, N732MA continued moving left until reaching 10 ft. left of centerline, and then started moving back towards the right.

Summary of directional control and deceleration performance on the runway

At 21:41:47, about 4 seconds after touchdown, the speedbrake handle moved aft to 46° and the speedbrakes deployed. The speedbrake handle movement was most likely an automatic deployment from the "down" position, triggered by the movement of the right throttle into the idle reverse thrust detent[6] after main gear tire spin-up, as opposed to an automatic deployment from the "armed" position as the result of main gear compression and tire spin-up only; the position of the handle recorded on the FDR prior to touchdown indicates it was not in the "armed" position, as it would have had to have been for the deployment to be automatic following main gear compression and tire spin-up.[7] On the previous landing at MUGM, the speedbrake handle was in the armed position prior to touchdown, and it started moving aft to 46° within 1 second of touchdown, consistent with automatic deployment following main gear compression and tire spin-up. Consequently, on the accident landing the automatic deployment of the spoilers following the selection of reverse thrust was likely delayed by about 3 seconds compared to the automatic deployment following wheel spin-up that could have been obtained by arming the spoilers prior to touchdown.[8]

---

[5] The short field arresting gear includes a cable used to "trap" the tail hook of carrier-based aircraft landing at KNIP, in the same way arresting cables are used on aircraft carriers. Reference 7 states that arresting gear on runways place no limitations on Miami Air Boeing 737 takeoff or landing operations.

[6] The idle reverse thrust detent corresponds to a throttle resolver angle of about 26°.

[7] The "speedbrake armed light" parameter recorded on the FDR is also consistent with the speedbrake not being armed prior to touchdown. The speedbrake deployment could also have been performed manually by one of the pilots, but neither pilot mentioned manually deploying the speedbrakes in their interviews (see Reference 5). In any case, the timing of the spoiler handle movement is consistent with the timing of the movement of the right throttle into the first reverse thrust detent. A description of the Boeing 737 speedbrake system can be found at http://www.b737.org.uk/flightcontrols.htm.

[8] The CVR records the first officer stating "speedbrakes armed" during the landing checklist, but the speedbrake handle and speedbrake armed light parameters on the FDR (as well as the timing of the spoiler deployment following touchdown) indicate that the speedbrake was not in the armed position at touchdown.

Reference 5 notes that the left thrust reverser was inoperative and deferred per the FAA approved Minimum Equipment List (MEL). Consistent with this, the left reverser was not deployed after touchdown, but the right throttle commanded idle reverse thrust at about 21:41:46, and detent 2 reverse thrust[9] at about 21:41:48. Reverse thrust on the right engine and idle forward thrust on the left engine created an asymmetric thrust condition that acted to yaw the airplane nose right, and that would have had to be counteracted using rudder and possibly differential braking (though differential braking on a slippery runway is hard to achieve, for reasons described further in this *Study*). Between 21:41:55 and 21:41:58, maximum reverse thrust[10] was commanded on the right engine. Between 21:41:59 and 21:42:00, the right throttle moved briefly back to the forward idle thrust position, before full reverse thrust on the right engine was again commanded at 21:42:02. Maximum reverse thrust was maintained until 21:42:12, when the reverse thrust was reduced to about the detent 2 level, where it remained until the end of the data.

The FDR wheel brake pressures were steady near 0 psi until after 21:41:46. At 21:41:47, the left brake pressure increased to 905 psi, and the right brake pressure increased to 458 psi. The “autobrake applied” parameter on the FDR indicates that the autobrakes were applied during two samples of the parameter, at 21:41:48 and 21:41:49, suggesting that the wheel brakes were initially applied by the autobrake system, and then the PF applied manual brakes shortly thereafter.[11]

Throughout the landing roll, the left brake pressure was consistently higher than the right brake pressure (though at a couple of points the pressures were briefly matched), and left rudder pedal was consistently applied, suggesting that the PF might have intended to control the asymmetric reverse resulting from the operation of a single reverser using both rudder and differential braking. As noted above, at touchdown N732MA was tracking 2.65° left of the runway heading, and continued moving left until reaching 10 ft. left of centerline, before moving back towards the right. The airplane crossed the runway centerline from left to right at 21:41:50.3, about 3,650 ft. past the displaced threshold, and 2,070 ft. past the touchdown point. The airplane continued moving towards the right edge of the runway, reaching a maximum displacement from the centerline of 74 ft. at 21:42:01, 6,300 ft. past the displaced threshold.[12] N732MA then started moving back towards the centerline, and was about 55 ft. right of the centerline when it crossed the end of the runway at 21:42:10.4, 8,006 ft. past the displaced threshold. Thereafter, the airplane moved back towards the right, impacting the seawall at 21:42:19.2, 90 ft. to the right of the centerline, 9,170 ft. past the displaced threshold, and 1,164 ft. past the end of runway 10. Note that if the airplane had tracked the centerline of the runway, it would have impacted a steel approach light stanchion reaching into the St. Johns River past the seawall, potentially causing additional damage to the airplane.

---

[9] The detent 2 reverse thrust corresponds to a throttle resolver angle of about 10°.
[10] Maximum reverse thrust corresponds to a throttle resolver angle of about 6°.
[11] In his post-accident interview (see Reference 5), the Captain stated that the autobrakes were set to 2, and that the autobrakes disengaged. A description of the Boeing 737 autobrake system can be found at: http://www.b737.org.uk/landinggear.htm#Autobrakes.
[12] Runway 10 is 200 ft. wide, i.e., 100 ft. from the centerline to each edge.

As N732MA drifted back and forth from the centerline as it travelled down the runway, it developed a drift angle as high as 8° (the drift angle is the difference between the airplane's track over the ground and its heading). This drift or yaw angle developed a cornering force on the main gear tires, which helped the airplane correct back to the centerline; however, as discussed further below, the cornering demand on the tires might have reduced the tire braking friction available to slow the airplane.

The forces contributing to the deceleration of the airplane were aerodynamic drag, reverse thrust, and tire braking friction. The braking friction force on each tire is equal to the normal (vertical) force on the tire, multiplied by the braking friction coefficient (μ_B) between the tire and the runway. The calculation of μ_B from FDR data is described in detail below; here it suffices to note that the driving parameter in the calculation is the longitudinal load factor (n_x) recorded on the FDR, which is a measure of the airplane's deceleration.

At 21:41:45, about a couple of seconds after touchdown, the n_x was about -0.1 G's.[13] Following the spoiler deployment at 21:45:47, the n_x decreased to -0.24 G's, and attained its lowest value (maximum deceleration)[14] of -0.26 G's at 21:41:49.3, about 6.2 seconds after touchdown. At this point, the ground speed had decreased to 166 kt., and the airplane was 3,400 ft. past the displaced threshold, with 4,606 ft. of runway remaining.

From 21:41:49.3 to about 21:42:06 (about 17 seconds), the n_x steadily increased (i.e., the deceleration deteriorated). At 21:42:06, the n_x was -0.14 G's, the ground speed was 111 kt., and the airplane was 7,220 ft. past the displaced threshold, with 786 ft. of runway remaining. Between 21:42:06 and 21:42:11, the n_x varied between -0.14 and -0.17 G's, and the airplane departed the end of the runway at 21:42:10.4, at a ground speed of 98.5 kt. A 75-ft. wide paved overrun extended for 950 ft. past the end of runway 10, and pavement the width of the runway extended for 100 ft. past the end of the runway. N732MA was far enough to the right that its main gear missed the 75-ft. paved overrun, and instead entered the grass area to the right of the overrun, starting 100 ft. past the end of the runway. Deceleration improved in the grass area, with the n_x varying between -0.4 and -0.2 G's, with large oscillations (also reflected in the vertical load factor) indicative of a bumpy ride over the unimproved surface. The airplane impacted the seawall at 21:42:19.2 at a ground speed of about 61 kt.

As noted above, the μ_B attained during the ground roll was significantly less than both the μ_B implied in the unfactored wet-runway landing distances published in the FCOM, and the μ_B predicted by a NASA model based on friction measurements of the runway. At 21:41:48, about 5 seconds after touchdown, the computed μ_B was about 0.05, and decreased to about 0.04 at about 21:41:58, before jumping to about 0.08 at 21:42:00 (note that the μ_B on rolling, unbraked tires is about 0.02). Between 21:42:00 and 21:42:07, the

---

[13] Load factors are measured in units of acceleration (distance/time^2), normalized by the acceleration due to gravity (32.17 ft./s.^{2}), expressed in "G's." On the runway, positive n_x denotes acceleration (increasing speed), and negative n_x denotes deceleration (decreasing speed).

[14] This is the lowest n_x achieved on the runway; the lower n_x values attained in the grass and mud past the end of the runway are not considered here.

μ_B decreased to about 0.05, before increasing to about 0.09 at 21:42:11 just before the airplane departed the pavement into the grass. Consistent with the improvement in deceleration in grass, the μ_B achieved in the grass / mud varied with large oscillations between 0.14 and 0.30. The calculation of μ_B, and comparisons of the achieved μ_B with the μ_B levels underlying the FCOM landing distances and with various μ_B models for wet and flooded runways, are treated at length in Sections D-V and D-VII.

D. DETAILS OF THE INVESTIGATION

I. The Boeing 737-81Q Airplane

The Boeing 737-81Q is a 737-800, with the "1Q" designation identifying the delivery customer (in this case, CIT Aerospace Inc., a leasing company). Figure 1 shows a 3-view image of the Boeing 737-800, taken from Reference 8. Table 1 provides some dimensions of the airplane, as well as relevant mass properties for N732MA on the accident flight. The airplane weight at landing was determined from the FDR, and the center of gravity (C.G.) is an estimate provided by NTSB Operations Group staff.

Item	Value
Reference dimensions:	
Wing area	1,341 ft.^{2}
Wing span	112.58 ft.
Mean Aerodynamic Chord (MAC)	12.98 ft.
Mass properties for N732MA:	
FDR-recorded weight at landing	143,200 pounds (64,954 kg)
Estimated center of gravity (C.G.) position at landing	28% MAC

Table 1. Dimensions of the Boeing 737-800 airplane, and relevant mass properties for N732MA.

II. Ground Scars and Markings

KNIP runway 10 is 9,003 ft. long and 200 ft. wide, ungrooved, with a threshold elevation of 22.5 ft. The runway has a displaced threshold 997 ft. from the threshold (elevation 21.1 ft.), leaving a landing length of 8,006 ft. The elevation of the departure end of the runway is 7.9 ft., giving the runway an average gradient of -0.165% (downhill) over the 8,006 ft. landing length. The runway is concrete for the first 1,660 and last 1,000 ft., and asphalt in between. For additional details about KNIP and its runways, see Appendix A.

Several tire marks on the runway, and ruts or furrows in the grassy area to the right of the paved overrun past the end of the runway leading to the seawall, provided evidence of the trajectory of the airplane's landing gear following the initial touchdown. These items included:

- Light, white landing gear track marks on the pavement, starting 1,592 ft. from the displaced threshold (12 ft. past the computed touchdown point of 1,580 ft.), and ending at the end of the pavement and start of the grass area (see Figure 4).
- Landing gear “furrows” (tracks / scrapes in the grass) to the right of and beyond runway 10, leading from the end of the pavement to the breaks in the seawall between the field and the St. Johns River, just in front of the final resting place of the airplane (see Figures 3 and 5).

The tire tracks were surveyed using a handheld Trimble Geo7x survey-grade Global Navigation Satellite System (GNSS) receiver, supplemented with a 200-foot tape measure. The GNSS position of one of the main gear tire tracks was surveyed with the Geo7x, and the distances from that main gear track to the nose gear and the other main gear track (along a line perpendicular to the tracks) were measured with the tape measure.

After post-processing differential correction of the recorded GNSS positions, the reported 68% horizontal and vertical position precision[15] of the GNSS points is 0.3 ft.

The results of the tire mark survey are shown in Figure 2, which plots the surveyed items over a plan view of the runway environment in “runway axes.” The runway 10 x axis originates at the displaced threshold and extends down the runway (east) to the threshold of runway 28. The runway 10 y axis originates at the displaced threshold and extends to the right (south) normal to the centerline of the runway.

The top plot in Figure 2 depicts the full length of runway 10 to scale, with the surveyed tire marks overlaid. The bottom plot of Figure 2 is identical to the top plot, but with the runway y axis scale expanded to show greater detail in that dimension.

The tracks of all three landing gear from a point 3,900 ft. from the displaced threshold to the end of the tracks at the seawall (9,170 ft. from the displaced threshold) were surveyed using both the Geo7x and tape measure, as described above, with the Geo7x recording the position of the left main landing gear (LMG). Only the track of the right main landing gear (RMG) was surveyed, using the Geo7x, from a point 1,592 ft. past the displaced threshold (12 ft. beyond the computed touchdown point) to a point 4,200 ft. from the displaced threshold. There is a 300 ft. overlap between the LMG and RMG tracks surveyed with the Geo7x. The positions of the nose landing gear (NG) and LMG from 1,592 ft. to 4,200 ft. from the displaced threshold were estimated from the surveyed positions of the RMG, using the nominal distance between the main gears (18.75 ft; this assumption is perfect when there is no drift or crabbing of the airplane, though as noted above, the actual drift angle was as high as 8°). The estimated tracks are depicted in Figure 2 with dashed lines.

[15] The 68% precision value indicates that there is at least a 68% chance that the true position is within the stated precision of the measured position.

III. Surveillance data

N732MA was tracked by both ground-based radar stations, and by the Automatic Dependent Surveillance – Broadcast (ADS-B) system. ADS-B capability enables aircraft to broadcast their three-dimensional position (latitude, longitude, and altitude) to other ADS-B equipped aircraft and to ADS-B ground stations. ADS-B latitude and longitude are determined by GNSS, including Global Positioning System (GPS) satellites, and altitudes determined both barometrically and by GNSS are included in ADS-B messages. The GNSS positions are very accurate compared to radar data; radar range uncertainty alone (without even considering azimuth uncertainty) is about ±1/16 nmi, or ±380 ft., and GNSS positions are generally accurate to within 60 ft. (see Reference 11). Furthermore, ADS-B data is available at a higher frequency (typically 1 sample/second) than radar data (at best, 1 sample every 4.5 seconds). Consequently, only the ADS-B surveillance data for N732MA are used in this *Study*. The ADS-B positions serve as "target" positions for the calculation of kinematically consistent airplane positions through mathematical integration of the load factors (accelerations) recorded by the FDR, as described in Section D-V.

The recorded ADS-B data includes the following parameters:

- UTC time of the ADS-B report, in hours, minutes, and seconds. EDT = UTC – 4 hours.
- Aircraft identifying information.
- Latitude and longitude, to a resolution of 0.01 arc-seconds (≈1 ft.)
- Pressure altitude in feet, to the nearest 25 ft. (an uncertainty band of ± 12.5 ft.)
- Geometric (GNSS) altitude in feet, to the nearest 25 ft.
- North-south and east-west components of ground speed, to a resolution of 1 kt.
- Rate of climb, to a resolution of 1 ft./min.
- Numerous parameters documenting the quality and accuracy of each reported GNSS position.

The sample rate of this data is a consistent 1 sample / sec (1 Hz). The ADS-B data is presented along with recorded flight data in subsequent sections of this *Study*.

IV. Recorded flight data

FDR and CVR data description

The aircraft cockpit voice recorder (CVR) and flight data recorder (FDR) were recovered and sent to the NTSB Recorders Laboratory in Washington, DC for readout.

Descriptions of the FDR and CVR and the recorder readout processes can be found in References 9 and 10, respectively. The FDR readout results in tabulated and plotted values of the recorded flight parameters versus time. The CVR readout results in a transcript of the CVR events, a partial list of which is shown in Table 2. The paraphrased version of the selected CVR events listed in Table 2 are also presented along with other information in various Figures throughout this *Study*. For the complete transcript and CVR report, see Reference 10.

Reference 10 notes that the audio quality of the CVR recording was “poor.” As a result, there is likely much conversation between the pilots, and other cockpit sounds, that investigators were not able to properly hear or understand and transcribe, and so are missing from the CVR transcript. For example, in his post-accident interview the Captain stated that the airplane had automatic (electronic voice) callouts for 50, 40, 30, 20, and 10 feet above the runway, and also for 100 ft. above minimums, and that he thought he heard the callouts on the flight (see Reference 5); however the CVR transcript only contains electronic voice altitude callouts at 500 and 10 ft. In addition, the CVR transcript only specifies times of events to the nearest second, which results in a relatively coarse placement of the CVR events on the Figures presented in this *Study*, and in particular in Figures 2 and 6. The uncertainty resulting from the poor CVR quality, and the consequent potential for missing statements and sounds in the transcript, should be considered when reviewing the CVR content presented in this *Study.*

FDR time (EDT)	Selected CVR items full transcript text	Paraphrased text on plots
21:40:25	[CAM] [sound of autopilot disconnect warning].	[CAM] [autopilot disconnect]
21:40:33	[CAM-2] * landing checklist. * * ah. * * * * speedbrakes ah armed, landing gear down three green, flaps thirty.	[CAM-2] Landing checklist.
21:41:10	[CAM-1] field in sight. report it.	[CAM-1] field in sight
21:41:16	[HOT] five hundred [electronic voice].	[HOT] 500. [elec. voice]
21:41:23	[HOT] minimums. [electronic voice].	[HOT] minimums [elec. voice]
21:41:35	[HOT] sink rate, sink rate, sink rate, sink rate, sink rate [electronic voice].	[HOT] mult. sink rate [elec. voice]
21:41:42	[HOT] ten. [electronic voice].	[HOT] 10. [elec. voice]
21:41:42	[HOT] sink rate [electronic voice].	[HOT] sink rate [elec. voice]
21:41:52	[HOT-1] oh.	[HOT-1] Crew utterance.
21:42:04	[HOT-1] oh we're going *.	[HOT-1] Comment re: overrun
21:42:10	[CAM] [sounds consistent with departure from prepared surface].	[CAM] [departing paved surface]

Table 2. Full CVR transcript text corresponding to paraphrased text on plots in this *Study*. Audio sources are: [CAM] = Cockpit Area Microphone; [CAM-1] = Captain’s voice on CAM; [CAM-2] = First Officer’s voice on CAM; [HOT] = Captain’s or FO’s hot microphone; [HOT-1] = Captain’s hot microphone.

Correlation of FDR and CVR Times

The FDR and CVR record their information with respect to time, but these recorded times are not synchronized. To use these data sources together, their times must be synchronized to a single reference time. This reference time is based on the UTC parameters recorded on the FDR (FDR time), converted into EDT. (The plot of ADS-B pressure altitude vs. ADS-B time matches the plot of FDR pressure altitude vs. FDR time (see Figure 7), indicating that FDR and ADS-B times are synchronized as received, and so FDR time does not need adjustment to match ADS-B time.)

Time on the FDR is measured in terms of the Subframe Reference Number (SRN), with one SRN equivalent to one second of time. Comparing the FDR SRNs associated with the recorded UTC parameters results in the following relationship:

$$\text{(Seconds elapsed since midnight EDT)} = \text{(FDR SRN)} - 19870.707 \text{ seconds} \qquad [1]$$

Equivalently,

21:40:00 EDT FDR time = 97870.707 FDR SRN [2]

The correlation between the FDR and CVR times is described in Reference 9. The CVR transcript provided in Reference 10 uses the FDR EDT time.

Several of the plots in this *Study* portray selected CVR content. For example, plots of data vs. time include CVR content overlaid on vertical lines that intersect the x axis of the plot at the times that the content was recorded. The content portrayed on the plots is not the verbatim CVR transcript text, but rather a paraphrase or shorthand code for this text. The full CVR transcript text associated with each paraphrase or code is shown in Table 2.

V. Performance Calculations based on FDR Data

Overview

The FDR records many, but not all, performance parameters of interest. Many additional parameters can be derived from the FDR parameters; however, the FDR parameters themselves can suffer from inherent measurement errors[16] and must be corrected before being used in these calculations.

This section describes the corrections applied to the FDR data, and the calculations used to derive additional performance parameters from the corrected data. The airplane weight and CG used in these calculations are 143,200 lb. and 28% MAC, respectively.[17] Further details about the derivation of the equations and calculation methods used in this *Study* can be found in Appendix A of Reference 12.

The FDR corrections discussed in this Study attempt to remove the following errors:

- Static pressure errors during the landing flare and rollout that introduce errors in the recorded calibrated airspeed and pressure altitude.
- Accelerometer bias errors.
- Magnetic heading errors.

The additional performance parameters derived from the corrected FDR data include:

- True airspeed and altitude.
- Kinematically consistent positions and velocities from accelerometer integration.
- Wind speed and direction while airborne, and headwind / tailwind on the ground.
- Braking friction coefficient developed during the ground roll.

---

[16] "Measurement error" in this context means the difference between the actual true value of the property being measured and the measured or recorded value. It does not necessarily imply defects or malfunctions in the measurement and recording equipment itself. This difference can result from, among other things, limitations in the sensor accuracy and / or resolution, or from the necessity of measuring a property that is only approximately equal to the desired property (for example, the static pressure measured at the airplane's static ports may not exactly equal the freestream static pressure, which is the desired property).

[17] See Table 1.

The results of these corrections and derivations for the period from the airplane's descent through 1,000 ft. above the runway to its departure off the end of the runway are presented in Figures 6 – 26.[18]

True airspeed calculation

True airspeed equals Mach number multiplied by the speed of sound; the speed of sound is a function of the static temperature. Static temperature is obtained from total temperature and Mach number.

Mach number can be computed from calibrated airspeed and static pressure. Calibrated airspeed and total temperature are recorded directly by the FDR, and the static pressure can be determined from the pressure altitude recorded by the FDR (which is based on the standard sea-level pressure of 29.92 "Hg).

Figure 9 shows the results of the true airspeed calculation, compared with the indicated (calibrated) airspeed recorded by the FDR. Figure 8 shows that the airplane departed the end of the runway at about 21:42:10.4; at this time, Figure 9 shows that the FDR airspeed is 85.7 knots calibrated airspeed (KCAS) as recorded, and 89.3 KCAS after correcting for static port pressure errors (this correction is described below). The recorded and corrected true airspeeds are up to 2 knots higher than the corresponding calibrated airspeeds. Figure 9 also shows the ground speed recorded by the FDR, and the ground speed computed from integration of the accelerometer data (this calculation is also described below); the integrated ground speed at 21:42:10.4 (when the airplane departed the runway) is about 98.5 kt. During the time the airplane is rolling down the runway, the ground speed is about 5 to 13 kt. greater than the corrected true airspeed, indicating a tailwind in this range. This tailwind component is consistent with the 21:45 EDT KNIP special weather observation taken shortly after the accident, as shown in Table 3). A more rigorous calculation of the winds during the approach and rollout is described below, and presented in Figure 16.

Parameter / Report	KNIP SPECI 21:05 EDT	KNIP SPECI 21:22 EDT	KNIP SPECI 21:45 EDT	KNIP METAR 21:53 EDT
Sky condition	800 ft. scattered 3,000 ft. broken CB 25,000 ft. broken	800 ft. scattered 1,800 ft. broken CB 3,000 ft. overcast	800 ft. scattered 1,500 ft. broken CB 3,200 ft. overcast	1,000 ft. scattered 2,100 ft. broken CB 3,500 ft. overcast
Visibility	10 statute miles	5 statute miles	3 statute miles	2 statute miles
Winds	080° @ 3 kt.	350° @ 4 kt.	290° @ 8 G 16 kt.	130° @ 3 kt.
Temperature / Dew Point	25°C / 23°C	24°C / 22°C	24°C / 22°C	23°C / 21°C
Altimeter setting	29.97 "Hg	29.98 "Hg	29.99 "Hg	29.98 "Hg
Precipitation	Light rain, thunderstorms	Heavy rain, thunderstorms, mist	Heavy rain, thunderstorms, mist	Heavy rain, thunderstorms, mist

Table 3. Weather observations at KNIP surrounding the time of the accident. CB = cumulonimbus.

[18] Several Figures in this *Study* have an "a" and a "b" version, which present the same information but at different scales, or with different background images. When the *Study* refers to a Figure with two or more versions without specifying the version, all versions are meant to be included in the reference.

Pressure-based true altitude and density altitude calculations

The altitude recorded by the FDR is pressure altitude; i.e., it is the altitude in the standard atmosphere corresponding to the pressure sensed at the airplane's static pressure ports. The altitude in the actual atmosphere corresponding to the local static pressure generally does not equal the pressure altitude, and it is insufficient to simply adjust the pressure altitude for the local sea level pressure because, in general, the lapse rate of pressure with altitude does not match the lapse rate in the standard atmosphere.

To estimate the actual altitude of N732MA, the recorded pressure altitude is first adjusted to account for a 29.98" Hg altimeter setting (see Table 3).[19] During the approach, the change in altitude corresponding to a change in static pressure is calculated by solving the hydrostatic equation continuously (the hydrostatic equation describes the pressure increment across a differential element of air required to balance the weight of the element). With static pressure and the static temperature values from the speed calculations, the density and weight of the air elements can be calculated.

The result of this calculation is shown in Figures 6 and 7 as the blue line labeled "Barometric altitude corrected for non-standard pressure and temperature and shifted to match radio altitude + terrain." As the label implies, the altitude computed by solving the hydrostatic equation is shifted upwards to match the known altitude of the airplane while it is on the runway (the need for this shift results from static pressure measurement errors, as described below). Accounting for the higher-than-standard temperature of the day changes the rate of change of altitude with distance (Figure 6) or time (Figure 7) slightly.[20]

The indicated altitude is the altitude shown on the airplane's altimeters. Note that the indicated altitude places the airplane below the terrain elevation during the time the airplane is on the ground; this is evidence that there is some error in the pressure measured at the airplane's static pressure ports. The dashed green line in Figures 6 and 7 is the indicated altitude corrected for the static port pressure error (the correction is described below), and correctly places the airplane slightly above the terrain while on the ground. Likewise, the altitude derived from the hydrostatic equation (blue line in Figures 6 and 7) is also shifted upwards to correctly place the airplane on the runway. Note that the corrected indicated altitude (dashed green line) deviates slightly from the hydrostatic-derived altitude (blue line) as altitude increases; this deviation results from the non-standard lapse rate of pressure with altitude.

The density altitude is the altitude in the standard atmosphere corresponding to the actual air density at each point in the flight. Because of the warmer-than-standard day, and temperature variations during the descent, the density altitude during the approach and landing was 540 to 1,000 ft. higher than the true MSL altitude.

---

[19] Table 3 indicates that at 21:45, the reporting time closest to the accident, the altimeter setting was actually 29.99" Hg, with the reports immediately preceding and following showing 29.98" Hg. The indicated altitude would be about 9 ft. higher at 29.99" Hg than at 29.98" Hg.

[20] The standard-day temperature at the field elevation of about 21 ft. is 14.9° C (58.9° F); at 24° C (75.2° F), the temperature was 9.1° C (16.3° F) higher than standard.

True altitude based on radio altimeter and terrain elevation data

The brown line in Figures 6 and 7 labeled "Radio altitude + terrain elevation + 14 ft." is the altitude that results from adding the height of the airplane's main gear tires above the ground (measured by the radio altimeter) to the elevation of the terrain underneath the airplane. The added 14 ft. is about the distance from the bottom of the main gear tires to the top of the cockpit windshield. The terrain elevation is determined by using the ADS-B latitude and longitude data to define the airplane's track over the ground, and then by obtaining the terrain elevation underneath the airplane's track from Shuttle Radar Topography Mission (SRTM) elevation data provided by the United States Geological Survey (USGS). The USGS provides SRTM digital elevation data with a resolution of 1 arc-second (about 100 ft.) for the United States and 3 arc-seconds (300 ft.) for global coverage[21]. The resolution of the terrain data used in this *Study* is 1 arc-second.

Note that the "Radio altitude + terrain elevation + 14 ft." altitude is well-behaved during the flare and touchdown, whereas the FDR pressure altitude exhibits unrealistic "waviness" in this area. The waviness of the FDR pressure altitude is the result of static pressure sensing errors, which are likely due to ground effects and the pitch rates present during the flare and landing.

While the radio altimeter-based altitude is better behaved than the FDR pressure altitude during the landing flare and rollout, on approach the radio altimeter-based data shows oscillations that are likely due to undulations in the terrain or other terrain features (such as buildings), and do not indicate variations in the airplane's MSL altitude. The oscillations are reduced near the runway, where the terrain is flatter. In turn, the FDR pressure altitude is well-behaved at higher altitudes, but exhibits unrealistic waviness near touchdown. Consequently, a better estimate of the altitude during the entire approach and landing would use a pressure-based altitude during the approach, transitioning to the radio-based altitude near the runway; this is the method used to construct the blue "Barometric altitude corrected for non-standard pressure and temperature and shifted to match radio altitude + terrain" line in Figures 6 & 7. However, the altitude constructed in this way may not be entirely kinematically consistent with the load factor data recorded on the FDR. In addition, while the FDR ground speed parameter is relatively accurate, it may not be entirely kinematically consistent with the FDR load factor data or the ADS-B position data. "Kinematically consistent" means that the mathematical relationships between acceleration (measured by load factor parameters), speed (measured by the ground speed and heading parameters), and position (measured by the ADS-B position parameters) hold in the three dimensions of the airplane's motion. In practice, the FDR parameters as recorded are only approximately kinematically consistent, as a result of inherent measurement errors and uncertainties.

In light of these errors and uncertainties, a better, kinematically consistent solution for the airplane's altitude, position, and speed throughout the approach and landing can be obtained by integrating the load factor data recorded on the FDR. This calculation is described below.

---

[21] See http://viewer.nationalmap.gov/viewer/.

Accelerometer data corrections and integration

The red line in Figures 6 and 7 labeled "Altitude from accelerometer integration" is the altitude that results from integrating[22] the FDR load factor data twice to derive aircraft position. It is a better estimate of the actual path of the airplane since it does not suffer from the static pressure sensing errors inherent in the FDR pressure-based altitude data.

An accurate estimate of the flight path of the airplane during relatively short intervals (about 30 to 60 seconds) can be obtained by integrating the accelerations recorded at the CG of the airplane. In general, the accelerometers are not located exactly on the CG, and so the accelerations at the CG must be computed by adjusting the FDR-recorded load factors for the effects of angular rates and accelerations. In the present case, the angular rates and accelerations are sufficiently small that this correction is negligible.

However, accelerometers generally contain small offsets, or "biases," that produce large errors in speed and position if not removed prior to integration.[23] In addition, the initial values of speed, rate of climb, and track angle are required during the integration process (these are essentially the "constants of integration" when integrating acceleration to get speeds). The constants of integration and the values of the accelerometer biases can be estimated by selecting them such that the aircraft position that results from the integration agrees with known "target" positions determined from another source.

The accelerometer biases are not necessarily constant over an entire flight, but can drift over time. It is for this reason that integrating the accelerometers works best over relatively short intervals, during which the accelerometer biases are approximately constant. In order to obtain an integrated flight path for N732MA's approach, landing, and rollout, the flight path was divided into three segments (approach, landing, and rollout), and the accelerometer data was integrated separately for each segment. For each segment, the "target" positions for the accelerometer integration are defined by the ADS-B data points shown in Figure 8, and by the blue "Barometric altitude …" line shown in Figure 7. In addition, the solution is forced to be continuous (no discontinuities in position or speed) at the boundaries between segments. The integration is solved in "reverse," starting at the end of the data (assumed coincide with the impact of the airplane with the seawall), and progressing backwards in time, ending at about 1,400 ft. MSL altitude. Solving the problem in reverse makes it easier to match the known end point at the seawall.

For the rollout segment, the constants of integration (the initial ground speed, track angle, and rate of climb) are chosen to minimize the root-mean-square difference between the integrated path and the target path throughout the entire segment. For the landing and approach segments, the constants of integration are defined by the end values of the corresponding parameters in the previous segment. Since the integration is performed in reverse, the "initial" conditions for the rollout segment are those at the seawall (the actual

[22] In the following discussion, "integrating" the load factor data refers to mathematical integration with respect to time, per the theorems of Calculus.

[23] For details about the equations to be integrated and the bias correction technique described in this *Study*, see Appendix A of Reference 12.

end of the rollout); the initial conditions for the landing segment are those at the start of the rollout; and the initial conditions for the approach segment are those at the start of the landing. The accelerometer biases in each segment are chosen to minimize the error between the integration and the target at the end point of the integration; i.e., the biases are chosen so that the integrated path and target path coincide at the end of the integration over each segment.

The approach segment starts at about 1,392 ft. MSL and ends at 445 ft. MSL; the landing segment starts at the end of the approach segment, and ends shortly after all the FDR weight on wheel parameters stabilize in the "on ground" state; and the rollout segment starts at the end of the landing segment, and ends at the end of the data at the seawall. The beginning and end times, constants of integration, and accelerometer biases used for the three segments are shown in Table 4. The constants of integration for the rollout segment are expressed as increments, or biases, on the initial ground speed, track, and rate of climb that would be computed using the target trajectory. For the landing and approach segments, the initial ground speed and rate of climb are set equal to the values of these parameters at the boundary with the adjacent segment, and so the increment or bias is not applicable.

Segment	Start time (EDT)	End time (EDT)	Speed bias, knots	Track bias, degrees	Rate of climb bias, ft/min	n_x bias, G's	n_y bias, G's	nlf bias, G's
Approach	21:40:25	21:41:23	n/a	n/a	n/a	-0.00839	0.00470	-0.00474
Landing	21:41:23	21:41:50	n/a	n/a	n/a	-0.00012	0.00707	-0.00577
Rollout	21:41:50	21:42:19.2	-2	0.92	72.88	-0.00715	0.00958	-0.00475

Table 4. Constants of integration and accelerometer biases for accelerometer integrations.

Accelerometer integration results and consequent PAPI indications

The airplane position and altitude resulting from the final integrated trajectory for all three segments (approach, landing and rollout) are shown in Figures 2, 6, 7, and 8 as the lines with the "Accelerometer integration" label. The ground speed and rate of climb resulting from the integrated trajectory are plotted in Figure 9.

The corrected load factors are compared to the load factors recorded by the FDR in Figure 10.

The dashed gray lines in Figure 6 depict the runway 10 Precision Approach Path Indicator (PAPI) light beam boundaries. The PAPI lighting system provides visual vertical flight path guidance to runway 10. The FAA *Aeronautical Information Manual* (AIM, Reference 13) describes the PAPI system as follows:

> **Precision Approach Path Indicator (PAPI).** The precision approach path indicator (PAPI) uses light units … installed in a single row of either two or four light units. These lights are visible from about 5 miles during the day and up to 20 miles at night. The visual glide path of the PAPI typically provides safe obstruction clearance within plus or minus 10 degrees of the extended runway centerline and to 4 SM from the runway threshold. Descent, using the PAPI, should not be initiated until the aircraft is visually

> aligned with the runway. The row of light units is normally installed on the left side of the runway and the glide path indications are as depicted [in Figure 6]. Lateral course guidance is provided by the runway or runway lights. In certain circumstances, the safe obstruction clearance area may be reduced due to local limitations, or the PAPI may be offset from the extended runway centerline. This will be noted in the Airport/ Facility Directory (AIM paragraph 2-1-2 (b)).

Technical specifications for the design of the PAPI system, including the flight path angle ranges corresponding to each combination of light displays, are contained in FAA Advisory Circular (AC) 150/5340-30G, *Design and Installation Details for Airport Visual Aids* (Ref. 14). Section 7.5(d) of this AC addresses the design of the PAPI, and Table 7-2 of the AC describes the aiming of Type L-880 (4 Box) PAPI relative to the pre-selected flight path angle. For a standard installation, the four PAPI lights are aimed 30' (minutes of arc) above, 10' above, 10' below, and 30' below the nominal glide path. In Figure 6, the nominal glide path is 3°, and the PAPI lights are located 1,000 ft. from the runway 10 displaced threshold, based on measurements taken from *Google Earth* satellite imagery.

The labels in the top left corner of Figure 6 depict the PAPI presentation provided within each of the regions defined by the dashed gray PAPI light beam lines. Above the top PAPI line, four white lights would be presented ("WWWW"), indicating that the airplane is well above the 3° glide path, which is depicted by the gray dash-dot line. Between the two top lines, three white and 1 red light would be presented; between the two middle lines, 2 white and 2 red lights would be presented; and so on. The Figure indicates that within 3.5 nm of the displaced threshold, three white lights and one red light would have been presented between about 3.2 nm and 1.6 nm from the displaced threshold, and four white lights would have been presented everywhere else. This indicates that at times during the final approach, the airplane was well above the nominal 3° glide path specified by the RNAV (GPS) instrument approach to runway 10 (see Figure 11).

Figure 2 indicates that the path over the runway resulting from the accelerometer integration is in good agreement with both the ADS-B position data and the tire marks measured on the runway, and is therefore a satisfactory solution.

Flight path angle (γ), angle of attack (α), and sideslip angle (β) calculations

The flight path angle is defined by

$$\gamma = \sin^{-1}\left(\frac{\dot{h}}{V}\right) \qquad [3]$$

where γ is the flight path angle, $\dot{h}$ is the rate of climb, and V is speed. Using true airspeed gives γ relative to the airmass, and using ground speed gives γ relative to the Earth. If $\dot{h}$ and V from the pressure-based altitude[24] and true airspeed calculations described above are used in Equation [3], the resulting γ is very noisy (i.e., it contains unrealistic "spikes" and oscillations). A better (smoother) calculation of γ results from using $\dot{h}$ and V from integrated accelerometer data. The γ relative to the Earth using $\dot{h}$ and ground speed from

[24] This is the altitude labeled "Barometric altitude …" in Figures 6 and 7.

the accelerometer integration is shown as the red line in the top plot of Figure 12. The γ relative to the airmass using the same $\dot{h}$ and the corrected true airspeed described above is shown as the green line in the top plot of Figure 12. The $\dot{h}$ used in these calculations is shown as the red line in the bottom plot of Figure 9.

The sideslip angle (β) is the angle that the velocity vector of the airplane relative to the airmass makes with the airplane's plane of symmetry (see Figure 13). This angle is required to resolve the airspeed of the airplane into components along each of the airplane's axes, which in turn are required to estimate the atmospheric wind from the FDR data. Consequently, the behavior of β during the approach is of interest.

β is not sensed or recorded by the FDR, but an estimate of β (while the airplane is airborne) can be made if the side force (Y) characteristics of the airplane are known and if the side force generated during the flight can be calculated. The most significant contributors to the side force are β and rudder deflection (δ_r):

$$C_Y = \frac{Y}{\frac{1}{2}\rho V^2 S} = \frac{\partial C_Y}{\partial \beta}\beta + \frac{\partial C_Y}{\partial \delta_r}\delta_r + \{smaller\ terms\} \quad [4]$$

Where C_Y is the side force coefficient, ρ is the air density, V is true airspeed, and S is the wing reference area. Ignoring the smaller terms, Equation [4] can be solved for an estimate of β:

$$\beta \cong \frac{C_Y - \frac{\partial C_Y}{\partial \delta_r}\delta_r}{\frac{\partial C_Y}{\partial \beta}} \quad [5]$$

The derivatives $\partial C_Y/\partial\beta$ and $\partial C_Y/\partial\delta_r$ are aerodynamic characteristics of the airplane.

The side force Y can be calculated using

$$Y = (W)(n_y) \quad [6]$$

Where W is the weight of the airplane and n_y is the lateral load factor recorded by the FDR, corrected to the CG location and for accelerometer bias, as described above.

In the present case, the corrected n_y during the approach is very small, as is the rudder angle δ_r. Consequently, Y and β are also very small. This *Study* assumes that $\beta \cong 0$.

Once γ and β are computed, they can be used along with the pitch angle (θ) and roll angle (ϕ) recorded by the FDR to compute the angle of attack, α:

$$\alpha = \tan^{-1}\left(\frac{\tan\theta}{\cos\phi}\right) - \sin^{-1}\left(\frac{\sin\gamma + \sin\beta\cos\theta\sin\phi}{\cos\beta\sqrt{1-\cos^2\theta\sin^2\phi}}\right) \quad [7]$$

Note that when $\beta = \phi = 0$, Equation [7] simplifies to the well-known result that

$$\alpha = \theta - \gamma \quad [8]$$

As shown in Figure 10, during the approach $|\phi| < 12°$, and so Equation [8] is an excellent approximation (the difference between the results of Equations [7] and [8] is at most 0.04°). The α resulting from Equation [8], using γ relative to the airmass based on $\dot{h}$ from the accelerometer integration, is presented as the blue line in the top plot of Figure 12.

Static pressure error correction

The static pressure measurement error used in this *Study* is defined as

$$\Delta P = P_{TRUE} - P_{MEASURED} \quad [9]$$

where P_{TRUE} is the actual freestream static pressure, and $P_{MEASURED}$ is the static pressure sensed at the airplane static ports, as determined from the FDR pressure altitude data.

To calculate P_{TRUE}, the known static pressure on the ground and the altitude resulting from the accelerometer integration are used in the hydrostatic equation to compute the lapse of static pressure with altitude. As noted above, the hydrostatic equation describes the pressure increment across a differential element of air required to balance the weight of the element:

$$dP = -(\rho)(g)dh \quad [10]$$

Where dP is the differential pressure change, g is gravitational acceleration, dh is the differential altitude change, and ρ is air density:

$$\rho = \frac{P}{RT} \quad [11]$$

Where P is the static pressure, T is the static temperature, and R is the gas constant of air. Substituting Equation [11] into Equation [10] gives

$$dP = -\left(\frac{P}{RT}\right)(g)dh \quad [12]$$

Equation [12] can be integrated to obtain P_{TRUE} as a function of altitude using the initial P on the ground, T from the FDR data, and dh from the accelerometer integration.

The error in the total pressure (P_{TOTAL}) sensed by the airplane's pitot tubes is assumed to be small. The total pressure can be calculated correctly from the uncorrected static pressure measurement and FDR calibrated airspeed.

Once P_{TRUE} and P_{TOTAL} have been calculated, the Mach number, static temperature, speed of sound, and true airspeed calculations can be redone. The results are shown in Figures 6, 7, 9 and 16 as the data labeled "corrected for static pressure error."

Magnetic heading correction

The nose and main gear tire gear marks left by N732MA on the runway (depicted in Figure 2) and the geometry of the B737-800 (depicted in Figure 1) can be used to determine the heading of the airplane in the areas covered by the marks. These calculations, as well as a comparison of the recorded heading during the takeoff from MUGM with the takeoff runway heading, indicate that the recorded heading is shifted 2.3° to the left of the actual heading. The heading calculations use the KNIP runway 10 and MUGM runway 10 true headings (89.65° and 91.14°, respectively), as measured in *Google Earth*. The FDR records magnetic heading, and the FDR true heading at KNIP and MUGM is computed using the magnetic variation at those airports determined using the International Geomagnetic Reference Field (IGRF) model.[25] For May 3, 2019, this model specifies a magnetic variation of 6.5° west at KNIP and 8.9° west at MUGM.

The tire mark locations depicted in Figure 2 correspond to the approximate center of the associated landing gear struts, i.e., the midpoint between the two tires mounted on each strut. Placing a scaled drawing of the B737-800 over an identically scaled drawing of the tire marks allows the orientation of the airplane relative to the runway to be determined, which in turn defines the airplane's heading (see Figure 14).

The results of the heading calculations are shown in Figure 15. The top plot shows the 2.3° adjustment required to make the FDR heading recorded during the takeoff roll match the takeoff runway heading. Similarly, the middle plot shows that the FDR heading matches the heading deduced from the images in Figure 14 better when it is shifted 2.3° to the right. The slope of the main tire marks provides the "Track angle from tire marks" data shown in the Figure, which matches the track computed from the accelerometer integration well. The bottom plot in Figure 13 shows the drift angle computed using both the original and corrected FDR heading. The drift angle is computed as

$$\psi_{DRIFT} = \psi_{TTRK} - \psi_{THDG} \qquad [13]$$

Where ψ_{TTRK} is the true track angle (determined from the accelerometer integration) and ψ_{THDG} is the true heading. The "Drift from tire marks" data in Figure 15 is the result of computing ψ_{DRIFT} using the "Track angle from tire marks" and "Heading from tire marks" data in Equation [13]. The ψ_{DRIFT} computed using ψ_{TRACK} from the accelerometer integration matches the "Drift from tire marks" data better when the corrected ψ_{THDG} is used instead of the FDR ψ_{THDG} in Equation [13].

[25] See https://www.ngdc.noaa.gov/geomag/calculators/magcalc.shtml#declination.

Wind calculations

Airspeed, ground speed, and wind are related as follows:

$$\vec{V}_W = \vec{V}_G - \vec{V} \quad [14]$$

where $\vec{V}$ is the airspeed vector, $\vec{V}_G$ is the ground speed vector and $\vec{V}_W$ is the wind vector. The components of $\vec{V}_G$ in body axes result from the integration of the accelerometer data described above. The components of the airspeed $\vec{V}$ in body axes, as indicated by Figure 13, are related to α and β as follows:

$$u = V\cos(\beta)\cos(\alpha) \quad [15a]$$
$$v = V\sin(\beta) \quad [15b]$$
$$w = V\cos(\beta)\sin(\alpha) \quad [15c]$$

where in the present case $\beta \cong 0$ and α is computed using Equation [8]. Once the components of $\vec{V}_W$ in the airplane body axes are computed using Equation [15], they can be transformed into Earth axes using the known θ, ϕ, and true heading (ψ_{THDG}). The results of the wind calculations are shown in Figure 16, computed using V *uncorrected* for the static pressure measurement error. Figure 16 also presents the winds recorded on the FDR, from both the Flight Management Computer (FMC) and Inertial Reference Unit (IRU) sources; the computed wind speed and direction agree well with these sources.

Once the airplane is on the ground, it is hard to determine the true value of β, and so Equations [14] and [15] cannot be used to determine the winds. Consequently, the wind calculation in Figure 16 ends when the airplane reaches the runway. However, in the present case what is of most interest (affecting landing distance) is the tailwind component. On the runway, this is computed as

$$\text{Tailwind} = \text{Ground speed} - \text{True airspeed} \quad [16]$$

Where the ground speed used is the result of the accelerometer integration. The solid magenta line in Figure 16 shows Equation [16] evaluated with the true airspeed uncorrected for the static pressure measurement error, and the dashed magenta line is Equation [16] evaluated using the corrected true airspeed. Note that the correction reduces the tailwind component by about 3 to 4 knots. The corrected tailwind averages about 5 knots during the approach and about 10 knots on the runway, with variations on the runway between about 4 and 13 knots.

The middle plot in Figure 16 shows the computed and recorded wind direction, which indicate winds from 290° to 320° (giving a left crosswind component for runway 10, that has a true heading of about 90°). The calculation shows the wind direction veering into the west close to touchdown, resulting in a more direct tailwind component, which might explain the increase in tailwind between 21:41:33 and 21:41:47.

Braking friction calculations

The record of the post-accident interview with the Captain (see Reference 5, Attachment 1), states that

> The flight touched down and [the Captain] believed it was a soft landing, deployed the thrust reverser, brakes and nothing happened. [The Captain] stepped on the brakes after that to the point that his back hurt. He had a good reverser but did not feel there was any deceleration whatsoever. He said they were "going over" to the First Officer (FO) and mechanic [in the jumpseat] and the rest was history.
> …
> [The Captain] thought they touched down not far from the 1,000 feet displaced threshold. The airplane was a bit to the right of the centerline on touchdown and he was able to correct to centerline. Autobrakes were set to 2 which was the correct setting given the information they were given. As far as he knew, the runway was not contaminated. After touchdown, he knew pretty quickly that they were not decelerating. He was the pilot flying. He pushed the brakes, and nothing happened. He looked at the autobrake disarm light to make sure it was illuminated; it was illuminated meaning he had manual braking. He did not ask the FO to get on the brakes because he was doing manual braking himself. He did not recall if the FO made the required callouts. There were no other lights on the landing roll.
>
> The number 1 thrust reverser was MEL'd.
>
> At the very beginning of the landing roll the airplane did slide to the right. He never let go of the brakes but was able to get it back to the center, which he thought was with the rudder. He remembered never letting go of the brakes. It happened right after touchdown, but he seemed to have rudder effectiveness.

As noted earlier in this *Study* and in the citation above, the left engine thrust reverser was inoperative and deferred per the MEL, and only the right thrust reverser was available to supplement the deceleration provided by the wheel brakes. The Captain's statement that "nothing happened" when he stepped on the brakes and that he "did not feel there was any deceleration whatsoever" underscore the importance of determining the retarding forces produced by the right thrust reverser and wheel brakes during the landing rollout.

Consequently, it is of interest to determine the braking friction coefficient (μ_B) generated on the runway, and compare the μ_B levels achieved with those that would be expected on a wet runway given current industry models, and the wet runway landing distances published in the B737-800 FCOM and computed by the Miami Air electronic Onboard Performance Tool (OPT).[26] This sub-section presents various FDR parameters relevant to the braking system operation and performance, and describes a method for computing μ_B using FDR-based parameters and additional information about the airplane provided by Boeing. The results of the μ_B calculation are also presented. The computed μ_B is compared with μ_B levels assumed in the FCOM, OPT, and various wet-runway friction models in Section D-VII.

Several FDR parameters relevant to the airplane's braking and deceleration performance are presented in Figures 17 and 18, including:

[26] The FCOM and OPT landing distances are described further in Section D-VII.

- Cockpit flight control positions (column, wheel, rudder pedals, speedbrake handle)
- Control surface positions (elevators, ailerons, rudder, spoilers)
- Speedbrake armed light discrete
- Speedbrake “do not arm” light discrete
- Ground spoiler deployment discrete
- Throttle resolver angle (TRA) and engine N1
- Thrust reverser deployed discrete
- Left and right wheel brake pressures
- Autobrake applied discrete
- Wheel braking friction coefficient (μ_B)

(The calculation of the μ_B plotted in Figure 18 is described below.)

Unfortunately, the main wheel rotational speeds, which are critical parameters (together with the runway surface conditions) affecting the μ_B achieved by the tires, are not recorded by the FDR. The wheel speed and airplane ground speed determine the wheel slip ratio:

$$s = 1 - \frac{V_{WHEEL}}{V_G} \quad [17]$$

Where V_G is the airplane’s ground speed, and V_{WHEEL} is the tangential speed of the tire:

$$V_{WHEEL} = \omega_{WHEEL} r_{TIRE} \quad [18]$$

Where ω_{WHEEL} is the angular velocity of the wheel, and r_{TIRE} is the effective radius of the tire (the distance from the center of rotation of the wheel to the point where the tire contacts the runway). Per Equation [17], when the tires are free-rolling and $V_{WHEEL} = V_G$, then $s = 0$. Conversely, when the tires are locked and $V_{WHEEL} = 0$, then $s = 1$. The significance of the slip ratio in the generation of braking forces on the tire is illustrated in Figures 20 and 35 and discussed further below.

The result of the μ_B calculation is presented along with the engine N1 speeds recorded by the FDR, and the n_x achieved during the landing roll, in Figure 18. As described further below, the engine thrust, which is measured by N1, and the achieved n_x are used in the μ_B calculation.

The μ_B can be computed from n_x, engine N1, and knowledge of the airplane’s aerodynamic and thrust characteristics. Figure 19 is a free-body diagram showing the forces and moments acting on the airplane during the braking portion of the ground roll. The lift, pitching moment, drag, and thrust forces shown in Figure 19 can be estimated based on the recorded FDR data, and the known aerodynamic and thrust properties of the airplane. The vertical and longitudinal reaction forces at the main and nose gear (N_N, F_N, N_M, and F_M) are unknown, but can be computed by solving the following system of equations:

$$F_N = \mu_N N_N \quad [19]$$

$$F_M = \mu_B N_M \quad [20]$$

$$\sum F_x = W n_x + W_x = W(n_x - \sin\theta) \quad [21]$$

$$\sum F_z = W n_z + W_z = W(n_z + \cos\theta) \quad [22]$$

$$\sum M_y = 0 \quad [23]$$

Where:

N_N = vertical reaction at nose gear
μ_N = rolling friction coefficient at nose gear
F_N = longitudinal reaction at nose gear (rolling friction on nose gear)
N_M = vertical reaction at main gear
μ_B = wheel braking friction coefficient at main gear
F_M = longitudinal reaction at main gear (braking friction on main gear)
$\sum F_x$ = sum of forces along body x-axis
W = airplane weight
W_x = component of airplane weight along body x-axis
n_x = longitudinal load factor
θ = airplane pitch angle
$\sum F_z$ = sum of forces along body z-axis
W_z = component of airplane weight along body z-axis
n_z = vertical load factor (= normal load factor multiplied by -1)
$\sum M_y$ = sum of moments about body y-axis

Assuming the rolling friction on the nose gear (μ_N) is 0.02,[27] Equations [19]-[23] can be reduced to three equations for the three unknowns N_N, N_M, and μ_B. As is evident in Figure 19, the geometry of the landing gear, thrust line, CG location, and aerodynamic reference point of the airplane must be known. This geometry, as well as aerodynamic coefficient and thrust data for the B737-800, were provided to the NTSB by Boeing.

For the μ_B calculation, the θ recorded on the FDR was used, and a runway gradient of -0.165% was assumed (downhill, as determined from the runway threshold elevations at each end[28]). Tables of forward and reverse thrust as a function of Mach number and engine N1 for the pressure and temperature conditions of the accident were provided by Boeing. The engine N1 and thrust reverser position data shown in Figure 18, and the Mach number computed from the FDR calibrated airspeed and static pressure, were used with these tables to compute the forward thrust from the left engine (with an inoperative thrust reverser) and forward and reverse thrust from the right engine during the ground roll.

The result of solving Equations [19]-[23] for μ_B is shown in Figure 18, and in several subsequent Figures discussed in Section D-VII.

---

[27] Boeing uses a rolling μ of 0.0125 at the speeds relevant in this *Study*; another aircraft manufacturer, Embraer, uses a rolling μ of 0.03. Hence, the value of 0.02 used here is about an "average" of the values used by these manufacturers.
[28] See https://enasr.faa.gov/eNASR/nasr/Current/Airport/4834 and Appendix A.

VI. Regulations and guidance concerning operations on wet runways

Overview

Section D-VII of this *Study* compares the actual μ_B achieved during the landing roll (as described above and presented in Figure 18) with the μ_B that would be predicted on a wet runway by various models in use in the aerospace industry and specified in certain airplane certification regulations, and with the μ_B underlying the unfactored[29] landing distances published in the B737-800 FCOM, for different runway "reported braking action" levels[30] and braking effort settings[31] under the weight, wind, temperature, and pressure conditions of the accident. Braking action levels are not associated with particular runway surface conditions directly; however, different runway conditions will result in different braking action levels, and the methodology in the FCOM assumes that the braking action for a particular landing will be reported to the flight crew by ATC or other means, if warranted.

In addition, since October 2016, within the U.S.A. runway surface conditions and associated braking performance have been described and reported using the Takeoff And Landing Performance Assessment (TALPA) Runway Condition Assessment Matrix (RCAM) framework, which differs from the "braking action" level framework used in the FCOM. Operators must use an accepted method to "translate" RCAM "Runway Condition Codes" (RwyCCs) into the FCOM reported braking action levels and associated landing distances. One such method, used by Miami Air, employs an Apple iPad-based application (the Onboard Performance Tool, or OPT) to compute landing distances based on information in a Boeing-provided operational performance computing module called the Boeing Landing Module (BLM).

The BLM contains the same calculations and data as the certified B737-800 Airplane Flight Manual - Digital Performance Information (AFM-DPI) computer software, but can also compute additional operational landing distance information. In the case of FAA-certified and registered aircraft, the AFM-DPI does not contain non-dry, non-wet landing distances; however, the BLM does, and this information is available in the Miami Air OPT.

The additional operational landing distance information available in the BLM is a combination of 1) data based on contaminant type, contained in the AFM-DPI of European-certified and registered aircraft, and 2) braking-action-based landing distance information, contained in the Boeing FCOM. Operators can customize the operational landing distance information provided by the BLM by specifying certain options such as the assumed air distance for the landing (the distance from the runway threshold to touchdown), and different braking coefficient options.

---

[29] The "unfactored" landing distance means the actual distance from the runway threshold required to land the airplane and bring it to a stop, without any safety factors applied.

[30] The FCOM reported braking action levels are Dry Runway, Good, Medium, and Poor.

[31] The FCOM braking effort settings are Max Manual, Autobrake Max, Autobrake 3, Autobrake 2, and Autobrake 1.

The RCAM levels, FCOM braking actions, OPT options, and the μ_B models they imply are described in Section D-VII. The relevance of the μ_B models, their associated landing distances, and of the landing distances published in the FCOM is determined both by the accuracy of these models and data, and by how this information is used to operate the airplane.

The B737 is certificated to the transport category airworthiness standards specified in 14 CFR Part 25,[32] and is typically used for Part 121 "Domestic, Flag, and Supplemental" operations (as in this accident). Part 25 dictates that landing distance data must be published in the Airplane Flight Manual (AFM).[33] As discussed below, the AFM landing distances are based on maximum-performance (minimum possible distance) landings conducted on smooth, dry runways during flight testing. Part 121 requires that these distances, with applied factors, be used during flight planning and dispatch to establish the minimum runway length required at the destination and alternate airports, or alternatively, the maximum takeoff weight at departure.

The landing distances published in the FCOM (for different braking efforts and runway conditions) are not required by FAA regulations, but are "advisory" data[34] provided by the manufacturer to assist flight crews in conducting en-route landing distance assessments (after the airplane has taken off) in case conditions at the destination airport change. (However, some foreign regulators *do* require that the AFM contain landing distances for contaminated runways, as discussed below.) The advisory data in the FCOM (and BLM) does not need to be established by flight test, but can be determined by calculation.

To provide context for the presentation of the wet-runway μ_B models and the landing distances that follow from those models, this Section will briefly outline the airplane certification standards that govern the required landing distance data presented in the AFM, the advisory data provided in the FCOM, and the operating regulations and guidance that govern how these data sources are to be used.

---

[32] In the following discussion, "Part" will be used as shorthand for Parts of Title 14 of the Code of Federal Regulations (14 CFR), governing Aeronautics and Space. Part 23 specifies airworthiness standards for normal, utility, acrobatic, and commuter category airplanes. Part 25 specifies airworthiness standards for transport category airplanes. Part 91 specifies general operating and flight rules, and includes Part 91K, governing fractional ownership operations. Part 135 specifies operating requirements for commuter and on-demand operations. Part 121 specifies operating requirements for domestic, flag, and supplemental operations. See 14 CFR for further details about airplane categories and the different types of operations.

[33] The AFM is a document approved by the FAA as part of the airplane's certification (see the following footnote for a definition of FAA "approval"). The FCOM is a document authored by Boeing to assist flight crews in operating the airplane. The FCOM is not part of the airplane's certification, like the AFM is, but its content is consistent with the AFM.

[34] "Advisory" data provided by an aircraft manufacturer can be contrasted with data "approved by" the regulator. In this context, "approved by" means the data is required to be and has been reviewed and formally approved by the FAA (or appropriate Civil Aviation Authority). Approvals are granted only by letter, by a stamp of approval, or by other official means. "Advisory" data is not subject to these requirements.

Required AFM landing distance data for Part 25 transport category airplanes

14 CFR §25.1587, "Performance Information," dictates the landing distance information that must be presented in the Airplane Flight Manual (AFM) of airplanes certificated under Part 25.[35] The regulation reads, in part:

> (b) Each Airplane Flight Manual must contain the performance information computed under the applicable provisions of this part (including §§25.115, 25.123, and 25.125 for the weights, altitudes, temperatures, wind components, and runway gradients, as applicable) within the operational limits of the airplane, and must contain the following:
> …
> (3) The following performance information (determined by extrapolation and computed for the range of weights between the maximum landing weight and the maximum takeoff weight):
> …
> (iii) Landing distance.

The landing distance is defined in §25.125 as "the horizontal distance necessary to land and come to a complete stop … from a point 50 feet above the landing surface." Furthermore, §25.125(c) states that "for landplanes and amphibians, the landing distance on land must be determined on a level, smooth, dry, hard-surfaced runway."

As noted above, these landing distances are established by flight testing without using reverse thrust, and represent the minimum distance required to land and stop the airplane without reverse thrust. For the B737-800, the landing distance data required by §25.125 is contained in the AFM-DPI, which is part of the approved AFM.

For Part 25 airplanes intended to be operated on contaminated runways in Europe, contaminated landing distances must be presented in the European AFM and computed per the methods described in the European Aviation Safety Agency (EASA) Acceptable Means of Compliance (AMC) document 25.1591, *The derivation and methodology of performance information for use when taking-off and landing with contaminated runway surface conditions* (AMC 25.1591). AMC 25.1591 provides one acceptable means of compliance with the provisions of EASA Certification Specification (CS) 25.1591, *Performance Information for Operations with Contaminated Runway Surface Conditions*, which states

> (a) Supplementary performance information applicable to aeroplanes operated on runways contaminated with standing water, slush, snow or ice may be furnished at the discretion of the applicant. If supplied, this information must include the expected performance of the aeroplane during take-off and landing on hard-surfaced runways covered by these contaminants. If information on any one or more of the above contaminated surfaces is not supplied, the AFM must contain a statement prohibiting operation(s) on the contaminated surface(s) for which information is not supplied. Additional information covering operation on contaminated surfaces other than the above may be provided at the discretion of the applicant.

[35] The parallel requirement for Part 23 airplanes is §23.1587, and refers to landing distances determined under §23.75.

> (b) Performance information furnished by the applicant must be contained in the AFM. The information may be used to assist operators in producing operational data and instructions for use by their flight crews when operating with contaminated runway surface conditions. The information may be established by calculation or by testing.
>
> (c) The AFM must clearly indicate the conditions and the extent of applicability for each contaminant used in establishing the contaminated runway performance information. It must also state that actual conditions that are different from those used for establishing the contaminated runway performance information may lead to different performance.

Note that EASA CS 25.1591, which prohibits operations on contaminated runways unless performance data is provided for those surface conditions, has no counterpart in the American Federal Aviation Regulations (14 CFR). FAA regulations do *not* require the publication of landing distances on other than dry runways, though applicants may choose to present this information as "advisory" data in order to satisfy foreign regulations that do require this information (this is the case with the B737-800 AFM-DPI). The wet and contaminated runway data is not necessarily based on flight tests (largely because of the difficulty of achieving a consistent "wet" or "contaminated" runway surface), but is derived from calculations such as those specified in AMC 25.1591.

It should be noted that a runway that is merely wet (not flooded with at least 3 mm of standing water[36]) is not considered "contaminated" and hence is not covered by CS 25.1591. Consequently, neither the EASA CS or American 14 CFR regulations specify methods or μ_B models for computing landing distances on wet (but not contaminated) runways.

However, 14 CFR §25.109 defines the accelerate-stop distance for transport category airplanes, and describes how this distance is to be determined. In particular, §25.109(c) defines the μ_B to be assumed in the calculation of the accelerate-stop distance for a smooth, wet runway, such as runway 10 at KNIP on the day of the accident; however, Part 25 does not prescribe the μ_B to be used when calculating the *landing* distance on a wet runway. Part 25 does not require the publication of wet-runway landing distances in the AFM, though applicants may choose to provide this information as advisory data.

In December 2015, the FAA published AC 25-32, titled *Landing Performance Data for Time-of-Arrival Landing Performance Assessments* (Reference 3). This AC prescribes using the §25.109 μ_B model for computing wet landing distances that are (optionally) provided in Part 25 AFMs, and is discussed in greater detail below.[37]

---

[36] European operational regulations (EU OPS 1.480(a)(2)) consider a runway "contaminated" with standing water (i.e., "flooded") when more than 25% of the runway surface is covered with surface water more than 3 mm (0.118 inches) deep.

[37] In April 2009, the Takeoff/Landing Performance Assessment Aviation Rulemaking Committee (TALPA ARC) presented several recommendations to the FAA to increase the safety of operations on wet and contaminated runways. Among these recommendations was a requirement for manufacturers of Part 25 airplanes to provide wet-runway landing distances based on the μ_B computed per the method described in §25.109. The TALPA ARC recommendations were ultimately implemented through ACs 25-31 and AC 25-32, which are non-regulatory documents.

Operational regulations concerning dispatch and arrival landing distance assessments

The accident flight was conducted under the provisions of Part 121. The corresponding regulation governing the runway lengths required at a destination airports is §121.195, "Airplanes: Turbine engine powered: Landing limitations: Destination airports," which states, in part,

> (a) No person operating a turbine engine powered transport category airplane may take off that airplane at such a weight that (allowing for normal consumption of fuel and oil in flight to the destination or alternate airport) the weight of the airplane on arrival would exceed the landing weight set forth in the Airplane Flight Manual for the elevation of the destination or alternate airport and the ambient temperature anticipated at the time of landing.
>
> (b) Except as provided in paragraph (c), (d), or (e) of this section, no person operating a turbine engine powered transport category airplane may take off that airplane unless its weight on arrival, allowing for normal consumption of fuel and oil in flight (in accordance with the landing distance set forth in the Airplane Flight Manual for the elevation of the destination airport and the wind conditions anticipated there at the time of landing), would allow a full stop landing at the intended destination airport within 60 percent of the effective length of each runway described below from a point 50 feet above the intersection of the obstruction clearance plane and the runway.

The factored dry runway landing distances in the B737-800 AFM are based on the actual (unfactored) landing distances for a dry runway, multiplied by the mandated safety factor of 1/0.6 ≅ 1.67; this guarantees that the actual demonstrated dry runway landing distance is at most 60% of the factored dry distance. For Part 121 operations, the factored dry distances in the AFM are used during flight planning and dispatch to determine the dry-runway field length required and / or the maximum allowable takeoff weight.

If, prior to takeoff, the destination runway is not forecast to be dry, then §121.195(d) applies:

> (d) Unless, based on a showing of actual operating landing techniques on wet runways, a shorter landing distance (but never less than that required by paragraph (b) of this section) has been approved for a specific type and model airplane and included in the Airplane Flight Manual, no person may takeoff a turbojet powered airplane when the appropriate weather reports and forecasts, or a combination thereof, indicate that the runways at the destination airport may be wet or slippery at the estimated time of arrival unless the effective runway length at the destination airport is at least 115 percent of the runway length required under paragraph (b) of this section.

Hence, when the destination runway is forecast to be wet, the wet factored landing distance is the dry factored distance in the AFM, multiplied by an additional safety factor of 1.15. This results in a required landing distance of about 1.92 times the actual, unfactored demonstrated dry runway distance ((unfactored distance / 0.6) x 1.15 ≅ unfactored distance x 1.92). Note that this wet-runway landing distance is obtained by applying safety factors to demonstrated dry runway performance, not on actual demonstrated wet-runway landing performance.

The B737-800 BLM module used by the Miami Air OPT includes advisory data (which is also in the EASA version of AFM-DPI) based on EASA CS 25.1591/AMC 25.1591. This data provides landing distances for runways covered with wet ice, compacted snow,

standing water, slush and snow.[38] However, this advisory data is not required to be used for flight planning or dispatch; for dispatch purposes, the additional 15% safety factor prescribed by §121.195(d) is considered sufficient to address all "slippery" (neither dry nor wet) runways. Instead, the advisory data in the BLM are primarily intended to be used by the flight crew to perform en-route landing distance assessments when conditions at the destination have deteriorated from those assumed at dispatch. Nonetheless, Miami Air did use the advisory data in the OPT to compute the required landing distance when dispatching flights to runways that were forecast to be "slippery" at the time of arrival (see below).

En-route landing distance assessments: CAT.OP.MPA.300 & FAA SAFOs 06012 & 19001

European operational regulation CAT.OP.MPA.300 requires what amounts to an en-route landing distance assessment, i.e., a determination by the pilot while in flight as to whether or not a successful landing can be made at the intended destination, considering the best information available concerning the expected weather and condition of the runway at the time of arrival. However, other than specifying that this determination must be made "having regard to the performance information contained in the operations manual," CAT.OP.MPA.300 does not provide guidance for making the determination. Challenges pilots may face in this regard include evaluating the runway condition based on weather, friction, or braking action reports, and selecting a safety factor to apply to landing distances computed from FCOM guidance material.

There is no equivalent to CAT.OP.MPA.300 in the 14 CFR. However, following the Southwest Airlines landing overrun accident involving a Boeing 737-700 at Chicago Midway Airport (KMDW) in December 2005, the FAA performed an internal audit of regulations and guidance information concerning landing distance requirements, and on August 31, 2006 issued Safety Alert For Operators (SAFO) 06012, titled *Landing Performance Assessments at Time of Arrival (Turbojets)*. While a SAFO is not regulatory, it "contains important safety information and may include recommended action. SAFO content should be especially valuable to air carriers in meeting their statutory duty to provide service with the highest possible degree of safety in the public interest." SAFO 06012

> urgently recommends that operators of turbojet airplanes develop procedures for flightcrews to assess landing performance based on conditions actually existing at time of arrival, as distinct from conditions presumed at time of dispatch. Those conditions include weather, runway conditions, the airplane's weight, and braking systems to be used. Once the actual landing distance is determined an additional safety margin of at least 15% should be added to that distance. Except under emergency conditions flightcrews should not attempt to land on runways that do not meet the assessment criteria and safety margins as specified in this SAFO.

The SAFO also notes that "the FAA has undertaken rulemaking that would explicitly require the practice described above." In December 2015, the FAA issued ACs 25-31 and 25-32 in lieu of the rulemaking contemplated in SAFO 06012.

---

[38] The runway condition options included in the Miami Air OPT en-route landing distance calculation are described below.

SAFO 06012 points out that the dry-runway landing distances established during flight test, and that are the basis for the factored landing distances used for dispatch, are shorter than the landing distances achieved in practice. In addition, FCOM landing distances for wet and contaminated runways may also be based on the minimum dry distances obtained during flight tests. Consequently, landing distances on wet or contaminated runways computed from FCOM data with little or no additional safety margin may be too short for normal operations. The SAFO recommends a conservative approach to assessing the landing distance requirements, including using the most adverse reliable braking action report or expected conditions for the runway, and using values for air distances and approach speeds that are representative of actual operations. The SAFO recommends that a 15% safety margin be then added to the computed (unfactored) landing distance, as "the FAA considers a 15% margin between the expected actual airplane landing distance and the landing distance available at the time of arrival as the minimum acceptable safety margin for normal operations."

Reference 2 discusses NTSB recommendations concerning en-route landing distance assessments and SAFO 06012, as well as NTSB comments on the content of ACs 25-31 and 25-32.

SAFO 06012 was cancelled and replaced by SAFO 19001, published on March 11, 2019. SAFO 19001 (see Appendix C) updates the information presented in SAFO 06012 to incorporate the TALPA RCAM framework and the corresponding contaminated runway performance guidance provided in ACs 25-31 and 25-32. As stated in SAFO 19001,

> After a Boeing 737-700 runway overrun accident at Chicago Midway Airport in December 2005, the FAA convened the Takeoff and Landing Performance Assessment (TALPA) Aviation Rulemaking Committee (ARC). The Federal Aviation Administration (FAA) adopted certain recommendations of the ARC (which became known as "TALPA"), and implemented them into the National Airspace System on October 1, 2016. This SAFO provides information and guidelines to airplane operators on utilizing the safety benefits TALPA provides.

In addition,

> The TALPA ARC discovered significant gaps in information needed to determine if a safe landing can be made. The ARC produced consistent terminology and runway assessment criteria, and recommended usage of non-dry, non-wet performance data for takeoff and time of arrival landing calculations. The TALPA ARC did not recommend any changes in the *preflight* landing distance requirements.[39]

Like SAFO 06012, SAFO 19001 recommends a conservative approach to assessing landing distance requirements, including using the most adverse reliable braking action report or runway condition code, values for air distances and approach speeds that are representative of actual operations, and a safety margin of at least 15%. However, compliance with SAFOs is not mandatory, and so the FAA can only "encourage" operators to adopt the practices recommended in the SAFO:

[39] A subsequent Aviation Rulemaking Advisory Committee (ARAC) has in fact recommended an addition to preflight (or dispatch) landing distance requirements, to account for the shortfall in the expected runway friction observed in a number of wet runway landing overruns; see Section D-VII.

> There is no specific regulation requiring operators to assess landing distance requirements at time of arrival, however the FAA encourages operators to adopt such procedures to ensure that a safe landing can be made. Additionally, the FAA highly encourages operators to use their FAA-approved landing performance data and any associated manufacturer-provided supplemental/advisory data in concert with the AC 91-79-generated RCAM Braking Action Codes to conduct an adequate landing distance assessment at the time of arrival. This is particularly important when the landing runway is contaminated or not the same runway analyzed for preflight calculations.

Miami Air International Flight Operations Manual Requirements

The certification of air carriers in the USA is governed by 14 CFR Part 119 §119.33, which states in part that "a person may not operate as a direct air carrier unless that person … obtains operations specifications that prescribe the authorizations, limitations, and procedures under which each kind of operation must be conducted." The content of operations specifications is defined in §119.49.

Miami Air held[40] operations specifications (OpsSpecs) for its air carrier operations conducted under 14 CFR Part 121. Miami Air's Flight Operations Manual (FOM, Reference 15) states that

> Miami Air has been issued Operations Specifications (OpSpecs) which describe the authorizations, limitations and procedures under which each kind of operation must be conducted.
>
> Pertinent excerpts from the OpSpecs are clearly identified in the FOM and must be complied with completely. Miami Air is approved for electronic OpSpecs. These OpSpecs are accessible via computer at the corporate address and satisfy the requirement for a complete and separate manual …. Compliance with each operations specifications requirement is mandatory.

The dispatch landing distances and associated limitations on landing weight required by the FOM are equivalent to those of 14 CFR §121.195. In addition, the FOM states that "as standard practice, landing weights at all airports are predicated on 'wet runway' conditions, as provided in the takeoff / landing analysis (OPT)." Consistent with this practice, the dispatcher that checked the landing distance and weight calculations for the accident flight told investigators that "there was an OPT software that he used to determine the performance numbers. They were already calculated for the accident flight [by the previous dispatcher on duty], but he still did the numbers and it was ok for a wet landing" (see Reference 5, Attachment 2).

The Miami Air FOM also includes requirements for a landing distance assessment:

> Compute the enroute landing distance if conditions have worsened since dispatch. The enroute landing distance computation is not required if:
>
> - Runway length at least 7,000 feet,
> - Airport elevation no greater than 3,000 feet,
> - Airport temperature not greater than 40°C,
> - Braking action good or better,
> - Landing flaps 30° or 40°,

[40] Miami Air International ceased operations on May 8, 2020.

- Tailwind no greater than 5 knots,
- No more than one thrust reverser inoperative and,
- Max manual braking.

Since Miami Air flights are dispatched assuming wet runway conditions at arrival, the presence of rain at KNIP during the landing did not in itself constitute a "worsened condition" requiring an en-route landing distance assessment per the FOM. Among the criteria in the list above that are required to render an en-route landing distance assessment unnecessary even when "worsened conditions" are clearly present, three that might not have been satisfied are the following:

- Braking action good or better: There were no braking action reports available to the accident flight crew. Hence, while there were no reports to the contrary, no "good" or better braking action reports existed.[41]

- Max manual braking: Reference 5 notes that the Captain told investigators that the flight crew "briefed the autobrake setting as 2," not "maximum manual braking." In addition, Figure 18 indicates that the brake pressures on both the left and right brakes did not in fact reflect "maximum manual braking" until about 21:42:01, about 14 seconds after touchdown. In practice, however, the low friction available on the runway would have made the maximum available μ_B attainable at brake pressures much lower than the maximum pressure that could be commanded from the brake pedals (this effect is discussed further below).

- Tailwind no greater than 5 knots: Reference 6 indicates that at 21:40, when the flight crew contacted the "radar final" controller, the controller reported the wind as 240° at 10 knots. This wind results in a 7.7 knot tailwind component for runway 10. This tailwind component is less than the maximum 10 knots allowed for any landing (with certain exceptions) in the FOM, but is greater than the maximum 5 knots allowed in the criteria that preclude the requirement for an en-route landing distance assessment. In addition, the 7.7 knot tailwind component itself might be considered a "worsened condition" from the dispatch assumptions that should have triggered the requirement for an en-route landing distance assessment.[42]

Guidance concerning braking performance on wet runways: SAFOs 15009 and 19003

Reference 2 presents the μ_B achieved in six accidents in which the airplane overran the runway after landing in wet conditions. In all of these accidents, the achieved μ_B was

[41] Reference 6 notes that the crew of a Navy P8 (a military variant of the Boeing 737) that landed on KNIP runway 28 at 21:08 told NTSB investigators that "no degradation in braking action was observed" during their landing. However, a braking action report was neither requested by or provided to ATC at the time.

[42] 14 CFR 121.195(b) states:

> For the purpose of determining the allowable landing weight at the destination airport the following is assumed:
> (1) The airplane is landed on the most favorable runway and in the most favorable direction, in still air.
> (2) The airplane is landed on the most suitable runway considering the probable wind velocity and direction and the ground handling characteristics of the airplane, and considering other conditions such as landing aids and terrain.

significantly lower than the μ_B predicted by industry-standard models, and the μ_B required to match the manufacturer's published unfactored, wet-runway landing distances.

In recognition of the unexpectedly low μ_B achieved in some of the accidents described in Reference 2 (among others), the FAA issued SAFOs 15009 and 19003 in August 2015 and July 2019, respectively. SAFO 15009 "warns airplane operators and pilots that the advisory data for wet runway landings may not provide a safe stopping margin under all conditions," and states that

> Landing overruns which occur on wet runways typically involve multiple contributing factors such as long touchdown, improper use of deceleration devices, tailwind and less available friction than expected. Several recent runway landing incidents/accidents have raised concerns with wet runway stopping performance assumptions. Analysis of the stopping data from these incidents/accidents indicates the braking coefficient of friction in each case was significantly lower than expected for a wet runway as defined by the Federal Aviation Administration (FAA) in Federal Air Regulation (FAR) 25.109 and Advisory Circular (AC) 25-7C methods. These incidents/accidents occurred on both grooved and un-grooved or non-Porous Friction Course overlay (PFC) runways. The data indicates that applying a 15% safety margin to wet runway time-of-arrival advisory data, as recommended by SAFO 06012, may be inadequate in certain wet runway conditions.

This statement summarizes the findings in the wet-runway overrun events described in Reference 2. The SAFO states that there are typically "multiple contributing" factors to wet-runway overruns, only one of which is "less available friction than expected." The other contributors include a long touchdown, tailwind, and "improper use of deceleration devices."

SAFO 15009 goes on to say that

> The root cause of the wet runway stopping performance shortfall is not fully understood at this time; however issues that appear to be contributors are runway conditions such as texture (polished or rubber contaminated surfaces), drainage, puddling in wheel tracks and active precipitation. Analysis of this data indicates that 30 to 40 percent of additional stopping distance may be required in certain cases where the runway is very wet, but not flooded.

Based on examinations of the runways involved, rubber contamination, drainage, and puddling in wheel tracks were *not* contributors in the overrun accidents described in Reference 2.[43]

SAFO 15009 states that "data contained in the Aircraft Flight Manuals (and/or performance supplemental materials) may underestimate the landing distance required to land on wet, ungrooved runways." The SAFO recommends that

> Directors of safety and directors of operations (Part 121); directors of operations (part 135, and 125), program managers, (Part 91K), and Pilots (Part 91) should take appropriate action within their operation to address the safety concerns with landing performance on wet runways discussed in this SAFO.

[43] For one of the accidents described in Reference 2, it is not possible to exclude drainage and puddling problems or rubber deposits on the runway as contributors to the accident, though dynamic hydroplaning in that event can be ruled out (dynamic hydroplaning is described below).

The SAFO also suggests some ways of taking "appropriate action" to address the safety concerns, such as "assuming a braking action of medium or fair when computing time-of-arrival landing performance or increasing the factor applied to the wet runway time-of-arrival landing performance data."

SAFO 19003 (see Appendix D) "cancels and replaces SAFO 15009 and warns airplane operators and pilots that the advisory data for wet runway landings may not provide a safe stopping margin especially in conditions of Moderate or Heavy Rain." This language is nearly identical to that in SAFO 15009, but specifies that the loss of friction might be associated with moderate or heavy rain conditions. In addition, SAFO 19003 updates the discussion in SAFO 15009 to refer to SAFO 19001 (which replaced SAFO 06012) and address the TALPA RCAM framework, and focuses on the risk of heavy rain events transitioning runways from a "wet" condition to a flooded ("contaminated") condition:

> These [landing] incidents/accidents occurred on both grooved and un-grooved runways. The data indicates that applying a 15% safety margin to wet runway time-of-arrival advisory data, as recommended by SAFO 19001 (or current guidance), may be inadequate in certain wet runway conditions. Takeoff and Landing Performance Assessment (TALPA) procedures implemented by the FAA on October 1, 2016, added new insight as to how flightcrews can evaluate runway braking performance prior to landing. TALPA defines WET as "includes damp and 1/8-inch depth or less of water," while CONTAMINATED is "greater than 1/8-inch of water."
>
> **Discussion:** These overruns have occurred on grooved and smooth runways during periods of moderate to heavy rain. Analysis of these incidents/accidents indicates that the braking coefficient of friction in each case was significantly lower than expected, and that 30 to 40 percent of additional stopping distance may be required if the runway transitions from wet to contaminated based on the rainfall intensity or reported water contamination (greater than 1/8-inch depth). For the operational in-flight landing assessment, determining whether the runway is wet or potentially contaminated is the pilot's responsibility.

As discussed further below, in the Miami Air accident, it likely that the runway "transition[ed] from wet to contaminated based on the rainfall intensity" present shortly before the landing, consistent with the scenario described in SAFO 19003.

SAFO 19003 continues:

> The FAA recommends that airports report "Wet" conditions. However, airports are not required to report when a runway is only wet. Further, an airport may not be able to generate a Field Condition NOTAM (FICON) for sudden rain showers that result in water on the runway more than 1/8 of an inch in depth (contaminated). Rainfall intensity may be the only indication available to the pilot that the water depth present on the runway may be excessive. The 1/8-inch threshold that separates a wet runway with a RWYCC of 5 from runway contaminated with water depth greater than 1/8-inch a RWYCC of 2 is based on possibility of dynamic hydroplaning. This can be especially true in moderate rain if the runway is not properly crowned, grooved, constructed with a porous friction course (PFC) overlay, or when water run-off becomes overwhelmed. During heavy rain events, this may be true even on a properly maintained grooved or PFC runway.
>
> The TALPA RCAM recommends using landing performance data associated with medium to poor braking or RwyCC of 2, if greater than 1/8-inch of water is anticipated to be on the runway. When planning to land on a smooth runway under conditions of moderate or heavy rain, or when landing on a grooved or PFC runway under heavy rain, pilots should consider that the surface may be contaminated with water at depth greater than 1/8 inch and adjust their landing distance assessment

> accordingly. Pilots should use all available resources to determine what condition they may expect upon landing to include Air Traffic Control (ATC), FICONs (as some airports do report Wet conditions), flight visibility, and/or onboard weather radar.
>
> > **Note:** A Special Weather Observation (SPECI) will only be generated if a Thunderstorm begins. A SPECI is not generated when rainfall rates simply change.
>
> Knowing ahead of time whether your aircraft can or cannot stop within the Landing Distance Available if runway conditions deteriorate to a medium to poor condition (RwyCC = 2) is critical when operating in moderate or heavy rain. Go-around, holding, or diversion may be necessary if rainfall intensity increases beyond what might be acceptable for the intended operation.
> …
> Unless the pilot or operator is knowledgeable of the runway's maintenance program, and that the runway is grooved or is a PFC surface that can provide good runway friction during periods of active moderate or heavy rain, they should consider basing their time-of-arrival assessment on the above recommendations. Aircraft operators should also clarify their reporting needs to the airport operator as it relates to "Wet" runway conditions.

Significantly, SAFO 19003 notes that pilots cannot rely on the airport to know of and / or inform them of flooded (standing water) conditions resulting from heavy rainfall, and it is the rainfall intensity itself that "may be the only indication available to the pilot that the water depth present on the runway may be excessive." Hence, the pilot's observation of heavy rain and recognition of its potential effect on braking performance is the last line of defense against sudden flooded conditions that can defeat the dispatch landing distance safety factors required by 14 CFR §121.195 and the operator's Flight Operations Manual.

Flight Test Harmonization Working Group wet runway regulatory recommendations

As indicated by SAFOs 15009 and 19003, the FAA has recognized that the actual μ_B achieved on some wet runways may be less than that specified in §25.109(c), and that the runway length required to stop on these runways may exceed the lengths specified in AFMs. On March 8, 2013, the FAA assigned an additional task addressing wet runway stopping performance to the Transport Airplane Performance and Handling Characteristics Aviation Rulemaking Advisory Committee (ARAC). The notice in the *Federal Register* announcing this assignment (Reference 17) states:

> The FAA tasked ARAC to consider several areas within the airplane performance and handling qualities requirements of the 14 CFR part 25 airworthiness standards and guidance for possible revision. The task includes prioritizing the list of topic areas provided in this notice based on prioritization criteria established by the [Flight Test Harmonization Working Group (FTHWG)]. The prioritization criteria should consider harmonization of regulatory requirements and associated guidance material for airworthiness certification of airplane designs. Recommendations may result in subsequent ARAC taskings for standards recommendations in follow-on phases. ARAC may also recommend additional topics in the general area of airplane performance and handling qualities that are not on the list provided in this notice.
>
> The working group will provide a draft report to ARAC recommending focus areas and work plans to address those areas the FTHWG identified as high priorities for airworthiness standards development relative to new airplane designs. This report will provide the rationale for the priority recommended as well as identify those items for which coordination with other working groups or experts outside the FTHWG may be needed. The report will also include a proposed schedule for accomplishment of the plan, including whether multiple topics can be worked simultaneously. If there

> is disagreement within the working group, those items should be documented, including the rationale from each party and the reasons for the disagreement. The following subject areas should be considered:
>
> 1. *Fly-by-wire (FBW) Flight Controls*. …
>
> 2. *Takeoff and Landing Performance*. Regulatory requirements and associated guidance material for airworthiness certification in the following areas listed below. (Note: This topic area excludes items addressed by the Takeoff and Landing Performance Assessment Aviation Rulemaking Committee.)
>
> a. Flight test methods used to determine maximum tailwind and crosswind capability. ...
>
> b. Wet runway stopping performance. Recent landing overruns on wet runways have raised questions regarding current wet runway stopping performance requirements and methods. Analyses indicate that the braking coefficient of friction in each case was significantly lower than expected for a wet runway (i.e., lower than the level specified in FAA regulations). Consideration should also be given to the scheduling of landing performance on wet porous friction course and grooved runway surfaces. Recommendations may include the need for additional data gathering, analysis, and possible rulemaking.

Because the tasking assigned to the FTHWG was very broad, the FTHWG decided to conduct the technical deliberations on each topic individually, and adopted the topic numbers from the original list of topics as identifiers for each topic. Wet runway landing performance was identified as "Topic 9." [44]

The FTHWG started its review of wet runway stopping performance and associated μ_B models in September, 2015. In March 2018, the FTHWG published its final report on this topic, titled *FAA Aviation Rulemaking Advisory Committee FTHWG Task 9: Wet Runway Stopping Performance Final Report: Recommendation Report, March 16, 2018* (Reference 18). The report recommends the creation of a new 14 CFR Part 25 transport airplane certification requirement (§25.126) to determine landing distances on wet runways, to supplement the existing requirement to determine landing distances on dry runways (§25.125). In addition, the report proposes modifying the 14 CFR 121.195 operating rule to account for the wet runway landing distances required by the new §25.126 rule when dispatching airplanes to runways forecast to be wet at the time of arrival.

In general, the wet landing distances required by the recommended new §25.126 rule would have to be determined by calculation, assuming the μ_B defined by §25.109(c), and incorporate a 10% safety margin (see Reference 18 for details about exceptions to this requirement, such as the use of μ_B values determined by flight test). In addition, reverse thrust could be used when determining the wet-runway landing distances (in contrast to the dry-runway landing distances required by §25.125, which must be determined without the use of reverse thrust).

The recommended change to the §121.195 operating rule would require that to dispatch a flight to a runway forecast to be wet at the time of arrival, the landing distance available

[44] See Reference 19.

must be at least 115% of the wet-runway landing distance determined per the recommended new §25.126 rule. Hence, the landing distance required at dispatch to a wet runway would be equal to the unfactored landing distance determined using the μ_B defined by §25.109(c) and including the effect of reverse thrust, multiplied by a total safety factor of 1.1 x 1.15 = 1.265. (The 1.1 factor is from the recommended new §25.126 rule, and the 1.15 factor is from the recommended change to §121.195.)

Even if the accident flight had been required to comply with these FTHWG recommendations, N732MA could still have been dispatched to KNIP with one thrust reverser inoperative because runway 10/28, even when wet, is long enough to satisfy the recommended requirements, which assume that the airplane will achieve the μ_B defined by §25.109(c). For example, Table 12a (described below) indicates that at the nominal flaps 30 approach speed of 153 KCAS and with a 10 kt. tailwind, the Miami Air OPT computes a non-factored landing distance of 6,284 ft. with one thrust reverser inoperative and a "WET (5)" runway condition (this condition uses the μ_B defined by §25.109(c)). The required wet-runway dispatch distance under the new recommendations would therefore be 6,284 ft. x 1.265 = 7,949 ft., which is 57 ft. less than the 8,006 ft. runway length available. The required distance in calm winds, and / or at flaps 40, would of course be even shorter.

VII. Comparison of wet-runway μ_B models and resulting landing distances

Overview

This Section presents several methods for modeling the physics underlying the μ_B achievable on wet runways, and compares the μ_B achieved during the accident landing roll (presented in Section D-V) with the μ_B that would be predicted using several wet-runway friction models. These models include the μ_B assumed in the TALPA Runway Condition Assessment Matrix (RCAM) for wet and flooded runway conditions, and the μ_B implicit in the various "reported braking action" levels associated with the landing distances published in the B737-800 FCOM and computed by the Miami Air OPT. This Section also summarizes the historical development of the TALPA RCAM in the context of other TALPA recommendations, and its presentation in AC 25-32.

In addition, this Section compares the landing distance that would be required given the actual μ_B achieved during the landing roll to the distances computed using the FCOM and OPT data, and to the distances computed using other μ_B models.

It will be shown that the computed μ_B is well below all the wet-runway μ_B models considered, and even below the μ_B specified in a Boeing simulation model for runways flooded with standing water, though this model comes closest to matching the computed μ_B. The water depth on the runway is estimated using a model based on the recorded rainfall rate preceding the accident and measured runway characteristics. This estimate, and the poor μ_B achieved during the landing, suggest that portions of the runway may in fact have been flooded, unlike the runways associated with the landing accidents described in Reference 2. In those accidents, a shortfall in the achieved μ_B was observed

on runways that were wet, but not flooded; in this accident, the poor μ_B might be attributable primarily to water depths that approach the definition of a "flooded" runway. The implication that the KNIP runway is not simply "slippery when wet" like the other runways in Reference 2 is supported by Continuous Friction Measuring Equipment (CFME) tests on the KNIP runway, and by the μ_B achieved during a different Miami Air B737-800 landing at KNIP in December 2019, when the runway was clearly wet (but not flooded). The CFME tests and December 2019 landing are discussed further below.

Physical parameters affecting μ_B

As indicated by Equation [20], the retarding force provided by the main gear tires during braking is equal to the normal force on the gear, N_M (acting perpendicular to the runway surface), multiplied by μ_B. N_M is approximately proportional to the weight of the airplane, minus the lift provided by the wings (see Figure 19). The lift depends on the flap setting, pitch attitude on the runway, dynamic pressure (airspeed and air density), and the position of the spoilers or speedbrakes (if the airplane is so equipped). Deploying the spoilers or speedbrakes after landing greatly improves braking by reducing the airplane's lift, thereby increasing N_M.

The physical parameters affecting μ_B have been the object of much study over the last 50 years. The NTSB *Aircraft Performance Study* for the EMB-505 landing overrun accident in Conroe, Texas in September, 2014 (Reference 20) provides a detailed review of the findings of this research, and a summary of how different physical parameters affect μ_B. Reference 20 gives particular attention to the factors affecting μ_B on wet runways, and includes a discussion of the three types of hydroplaning (viscous, dynamic, and reverted rubber hydroplaning).

Much of Reference 20's detailed discussion of these topics will not be repeated here; instead, the relevant points or findings are simply listed below. Readers interested in additional evidence supporting these findings are referred to Reference 20.

The μ_B behavior described in Reference 20 can be summarized as follows:

- μ_B increases above the rolling (unbraked) coefficient of friction (μ_N in Equation [19]) when the slip ratio s (see Equation [17]) of the main gear tires increases above 0.
- μ_B increases to a maximum ($\mu_{B,MAX}$) at a slip ratio $s_{\mu,MAX}$, and then decreases to the locked-wheel skidding coefficient of friction ($\mu_{B,SKID}$) at s = 1 (see Figure 20).
- The shape of the curve of μ_B against s is affected by surface texture and tire tread pattern and is particularly variable in the region between $\mu_{B,MAX}$ and $\mu_{B,SKID}$.
- $\mu_{B,MAX}$ and $\mu_{B,SKID}$ are affected by:
    - Tire design and construction (tread material, tread pattern; the tire tread pattern influences the tire's ability to move water away from the footprint of the tire).

- Tire inflation pressure: on dry and wet runways, μ_B tends to decrease with increasing inflation pressure; however, higher inflation pressure will increase the hydroplaning speed in standing water (see below).
- Runway surface material and texture (roughness), including large or macro-scale texture (macrotexture), and small or micro-scale texture (microtexture).
- Water depth on runway: on wet runways, μ_B is a strong function of forward speed. When, in addition, the runway is flooded (water deeper than 3 mm or 0.1 inches above the top of the surface asperities), then hydroplaning is possible (see below).
- Runway surface deposits (loose surface deposits such as sand, grit or dust decrease μ_B on a dry surface, and may increase or decrease μ_B on a wet surface depending on the surface texture and water depth.
- Rubber deposits, hardened smears of asphalt binder, and paint: these deposits "can cover large areas of busy runways, particularly near the touch-down region … in dry conditions no appreciable effects are observed. In wet conditions, large reductions may occur in both $\mu_{B,MAX}$ and $\mu_{B,SKID}$- depending in part on the initial texture of the underlying surface" [Reference 21].
- Forward speed: "In general, $\mu_{B,MAX}$ and $\mu_{B,SKID}$ decrease with increase in forward speed" [Reference 21], though this effect is much more pronounced on wet runways than on dry ones. The effect of speed on μ_B on a wet runway is described further below.
- Tire wear: "For the aircraft operator, tire wear is a most important factor … the available μ_B in wet conditions decreases as a tire wears. For a typical aircraft-type, rib-tread tire, when groove depths have been reduced to about 20% or less of the unworn value, the remaining tread may be 'flattened out' under load and the tire may then behave as if smooth" [Reference 21]. Reference 23 states that the range of tread depths measured on N732MA's tires after the accident were from 7/32"-8/32" on tire 1 (left outboard), 9/32"-12/32" on tire 2 (left inboard), 6/32"-8/32" on tire 3 (right inboard), and 2/32"-5/32" on tire 4 (right outboard). The groove depth on new tires is 0.4" or 13/32"; hence, an 80% worn tire would have a groove depth of about 0.08" or between 2/32" and 3/32". One of the center two grooves on tire 4 had worn to 2/32", but all the other grooves on the tires were 4/32" or deeper.

- $s_{\mu,MAX}$ usually lies between 0.1 and 0.2. Modern anti-skid braking systems are designed to detect and operate near $s_{\mu,MAX}$, but they cannot do so perfectly. The ability of these systems to operate at $s_{\mu,MAX}$ is a measure of their efficiency (η_{AS}).
- The §25.109(c) μ_B model assumes a constant η_{AS} of 80% for modern, "fully-modulating" anti-skid braking systems, over the full speed range of the airplane, and independent of the $\mu_{B,MAX}$ that can be attained on the runway. However, the research presented in Reference 20 suggests that η_{AS} can decrease as $\mu_{B,MAX}$ decreases, and may even be as low as 0.5 at $\mu_{B,MAX}$ = 0.3.

- On a wet runway, μ_B decreases precipitously with forward speed, particularly on runways with relatively low macrotexture and / or microtexture.
- Reference 20 documents six wet runway overrun events as well as the results of two wet runway braking test programs, and notes that in each case the μ_B achieved was less than the μ_B predicted by the §25.109(c) μ_B model. Reference 20 concludes that the reduced μ_B can be explained by (1) a wet-runway η_{AS} that is significantly less than 80%; (2) a wet-runway $\mu_{B,MAX}$ that is significantly less than what would be expected based on the pavement macrotexture and airplane tire inflation pressure in each case; or (3) a combination of these factors.

μ_B on wet runways

Reference 21 explains the decrease in μ_B with forward speed on wet runways as follows:

> The presence of a fluid, which is usually water, on a runway decreases the available tire-ground coefficient of friction.
>
> The tire-ground contact area in wet conditions can be divided into three zones, as illustrated in Figure [21a].
>
> *Zone 1* is the region where impact of the tire with the surface fluid generates sufficient pressure to overcome the inertia of the fluid. Much of the fluid is either ejected as spray or forced beneath the tire into the tread grooves (if present) or into the drainage paths provided by the surface texture. Throughout Zone 1 a continuous, relatively thick fluid layer exists between the tire and the runway surface and the only retarding force developed is that due to fluid drag ….
>
> *Zone 2* is a transition region. After the bulk of the fluid is displaced, a thin film remains between the tire and the surface. At the rear of Zone 1, and in Zone 2, a rapid outflow of fluid is prevented, and fluid pressures are maintained, by viscous effects. The thin film first breaks down at points where the local bearing pressure is high, e.g. at sharp surface asperities. In the presence of a lubricant such as water, the coefficient of friction of rubber on hard surfaces is greatly reduced from the dry surface value and varies little with changes in sliding speed and temperature …. Thus, in general, very little frictional force is generated wherever a thin film of fluid persists.
>
> *Zone 3* is the region of predominantly dry contact and, although obviously smaller than the contact area in dry conditions, it is here that most of the braking force is generated ….
>
> In wet conditions, the tire-ground coefficient of friction depends on the relative sizes of Zones 1, 2 and 3. These are determined by the surface texture, the depth, density and viscosity of the fluid, the tread pattern and inflation pressure of the tire and the time [required] … for a tread element to pass through the contact area ….
>
> Figure [21] also shows the effect of increased forward speed on the relative sizes of Zones 1, 2 and 3. In Figure [21b] the tire forward speed is higher than in Figure [21a] so that Zone 1 extends farther back into the contact area and Zones 2 and 3 occupy a horseshoe-shaped region at the rear. In Figure [21c], at a still higher speed, contact with the ground is all but lost. In this condition the tire develops very little braking force. Finally, in Figure [21d], the tire is moving at a speed such that Zone 1 extends throughout the contact area. (When dry contact with the ground ceases, the tire is said to be "planing".)

Hydroplaning on wet runways

The discussion of hydroplaning in Reference 20 can be summarized as follows:

- There are three types of hydroplaning: viscous hydroplaning, dynamic hydroplaning, and reverted-rubber hydroplaning.

- "Viscous hydroplaning" is associated with the buildup of water pressure under the tire due to viscosity in a thin film of water between a portion of the tire footprint and the runway surface. This is the kind of hydroplaning inferred when a surface is described as "slippery when wet," e.g., a wet bathtub. $\mu_{B,MAX}$ is greatly reduced under the water film (as shown in Figure 21c).

- "Dynamic hydroplaning" is associated with the buildup of water pressure due to water density and the tire's forward speed; in this condition, the tire is lifted entirely off the surface of the runway, and a continuous, relatively thick layer of water lies between the tire and the runway surface (as shown in Figure 21d). Dynamic hydroplaning is commonly referred to simply as "hydroplaning," and can be experienced by driving a car through a deep puddle at high speed. Under dynamic hydroplaning conditions, $\mu_{B,MAX}$ is further reduced, with the tire developing very little braking force, and the only retarding force being that due to fluid drag.

- A water depth of 3 mm above the top of the runway macrotexture is considered the minimum required to support dynamic hydroplaning. Consistent with this understanding, the TALPA RCAM and European operational regulations (EU OPS 1.480(a)(2)) consider a runway "contaminated" with standing water (i.e., "flooded") when more than 25% of the runway surface is covered with surface water more than 3 mm (0.118 inches) deep.

- If the water depth is sufficient, dynamic hydroplaning will occur when the tire's forward speed is greater than or equal to the hydroplaning speed. In Reference 22, W.B. Horne identifies three "zones" of hydroplaning risk based on water depth; these zones are illustrated in Figure 23 and discussed further below.

- For rotating tires (e.g., airplanes aborting a takeoff roll), the hydroplaning speed is given by

$$V_{p,spin\ down} = 9\sqrt{p} \quad \text{(rotating tire)} \qquad [24a]$$

  Where V_p is in knots and p is the tire inflation pressure in psi. Reference 40 notes that the tire tread depth can affect the hydroplaning speed, with higher tread depths corresponding to higher hydroplaning speeds.

- For nonrotating tires (e.g., airplanes on approach to landing), the hydroplaning speed is given by

$$V_{p,spin\ up} = 7.7\sqrt{p} \quad \text{(nonrotating tire)} \qquad [24b]$$

For the 205 psi tire pressure of the B737-800, Equation [24b] yields $V_{p,spin\ up}$ = 110 knots.

- On a wet runway, $\mu_{B,MAX}$ decreases with increasing speed due to viscous hydroplaning. If the water depth is sufficient and the speed increases to V_p, then dynamic hydroplaning will occur and μ_B will decrease to a minimum value (≈0.05; the unbraked rolling μ_B is typically modeled as 0.0125 to 0.03).

- Tires in a dynamic hydroplaning condition may experience "spin-down," in which unbraked wheels slow down or stop completely. This effect is due to both the absence of a spin-up moment due to friction, and the presence of a spin-down moment resulting from a shift in the center of pressure towards the front of a hydroplaning tire. This "spin-down" will cause the anti-skid system to limit the hydraulic pressure to the wheel brake to a very low level until the wheel "spins-up."

- "Reverted-rubber" hydroplaning occurs during locked-wheel skids on wet runways when the tire rubber in the skid patches reverts to an uncured state. In this condition, $\mu_{B,MAX}$ decreases to very low values, and the tire leaves white streaks on the runway (as opposed to black streaks on dry runways resulting from molten rubber deposited in the wheel track). The low $\mu_{B,MAX}$ during reverted-rubber hydroplaning is relatively insensitive to airplane speed and runway texture.

The tires from N732MA do not show any evidence of reverted-rubber hydroplaning, such as skid patches or areas of molten rubber (see Reference 23). The airplane did leave white tire marks or streaks down the length of the runway (see Figures 2 and 4), indicating that the tires were in contact with the runway, but these marks can be evidence of viscous hydroplaning as well as reverted rubber hydroplaning. Since N732MA's tires were in contact with the runway from the touchdown point onwards, dynamic hydroplaning (in which the tires are lifted off the pavement by water pressure) can be ruled out in this case; and since the tires do not exhibit skid patches or areas of molten rubber, reverted rubber hydroplaning can also be ruled out. Additional evidence against dynamic hydroplaning is the lateral load factor (n_y) developed during the landing roll, which likely resulted from cornering forces on the main gear tires as the pilot used the rudder to return the airplane towards the runway centerline (see Figures 2, 10, and 17); no significant cornering forces would be developed under dynamic hydroplaning conditions. Hence, the skid marks, tire evidence, and performance of the airplane are most consistent with viscous hydroplaning, in which large portions of the tires are in the "Zone 2" depicted in Figure 21.

Water depth on KNIP runway 10 at the time of the accident

N732MA touched down at about 180 kt. ground speed, above the $V_{p,spin\ up}$ of 110 kt. given by Equation [24b]. If the depth of water on the runway was sufficient to support dynamic hydroplaning, then between touchdown and the time that the airplane decelerated through 110 kt. (at 21:42:06.3, 7,278 ft. from the displaced threshold), conditions that could have

supported dynamic hydroplaning were present. As argued above, the skid marks and n_y evidence indicate contact of the tires with the pavement and preclude dynamic hydroplaning; nonetheless, the poor braking performance indicates that the tires might have been in the condition depicted in Figure 21c, in which “contact with the ground is all but lost” and “the tire develops very little braking force” (Reference 21). Consequently, it is of interest to determine the possible water depths on the runway during the accident.

Once equilibrium conditions are met during a rain event over a runway, the water depth at a given point from the runway centerline is constant (neither increasing nor decreasing). In this condition, the amount of water flowing towards that point from the crown (centerline) of the runway equals the amount of water flowing away from the point towards the runway edge. The volume of water per unit runway length flowing past a given point from the centerline is proportional to the speed of the water times the water depth. The water volume will increase with rainfall rate and distance from the centerline (the further from the centerline, the more runway area is available for collecting water that flows towards the point in question), and the water speed will increase with the runway cross-slope (the steeper the slope, the faster the flow). Thus, for a given slope, the water depth will increase with distance from the runway centerline (to accommodate the increasing volume of water) and with rainfall rate. At a given rainfall rate and distance from the centerline, the water depth will decrease as the runway cross-slope increases, since the increased speed of the water accommodates the same volume of water flow at a lesser water depth.

The runway macrotexture depth is the average depth of irregularities in the surface of the runway, produced by the coarseness of the surface texture. The greater the number and magnitude of these irregularities, the more “channels” are provided for water to flow through, and the higher the rainfall rate required to submerge the “peaks” of the irregularities. On a grooved runway, mechanically created grooves provide additional “macro-texture” to facilitate this drainage and increase the rainfall rate the runway can accept before the water depth rises above the peaks. Reference 32 notes that “cutting or forming grooves in existing or new pavement is a proven and effective technique for providing skid-resistance and prevention of hydroplaning during wet weather.” KNIP runway 10/28 is not grooved. A January 2020 Naval Safety Center study notes that only 7 of 31 primary Navy airfields have grooved runways, and recommends that the Navy take steps to “modernize Naval airport runways in compliance with FAA standards,” including grooving runways to reduce the risk of hydroplaning (see Reference 42).

Under some conditions, the required water depth to accommodate the volume of water flow will be less than the average macrotexture depth of the runway; in this case, the tips of the macrotexture irregularities will be above the water. If the required water depth is greater than the macrotexture depth, then the tips of the macrotexture irregularities will be below the water.

Reference 24 documents the results of experiments performed at the Texas Transportation Institute (TTI) that quantified the water depths resulting from various combinations of rainfall intensity, pavement cross slope, surface texture, and drainage

length. The TTI report provides the following equation to describe the experimental results:[45]

$$d = (0.00338)\left(\frac{1}{T}\right)^{-0.11}(L)^{0.43}(I)^{0.59}\left(\frac{1}{S}\right)^{0.42} - T \qquad [25]$$

where:

d = average water depth above the top of the macrotexture irregularities (inches);
T = average macrotexture depth, inches;
L = drainage path-length (i.e., distance from runway centerline), feet;
I = rainfall intensity (inches / hour)
S = runway cross slope, ft/ft (= slope in % divided by 100)

While on-scene at KNIP, the NTSB and parties to the investigation measured the runway macrotexture depth T, and the runway cross slope S. The cross-slope and macrotexture were measured at the runway x and y coordinates indicated in Table 5. The cross-slope was measured by placing a digital inclinometer on top of a 78-inch level placed perpendicular to the runway centerline, about halfway between the centerline and the runway edge. The macrotexture was measured using an ELAtextur macrotexture scanner.[46] The results of both measurements are shown in Table 5.

The runway is concrete for the first 1,660 and last 1,000 ft., and asphalt in between.[47] The measurements in Table 5 indicate that the macrotexture on the last (eastern) 1,000 ft. concrete section of runway 10 tends to be lower than that on the asphalt section. In addition, the southern cross slope is not as steep as the northern cross slope, and is less steep over the concrete section than over the asphalt section. Hence, it can be expected that water depths will be greater over the southeastern portion of the runway than over other portions. In addition, as the cross-slope gets shallower, the longitudinal slope of the runway (averaging 0.165% downhill) will affect the water drainage path more, causing the water to flow at other than a 90° angle to the centerline and increasing the water depth at a given distance from the centerline above that specified in Equation [25]. Wind over the runway can also affect the drainage path and resulting water depths.

The Department of Defense *Unified Facilities Criteria (UFC) 3-260-01: Airfield and Heliport Planning and Design* document (Reference 43) specifies that the minimum runway cross-

---

[45] Other models for the rain-induced water depth on pavements exist, including a 1979 update to the TTI model that incorporates test data from pavements with deeper macrotexture depths than those typically found on ungrooved runways. The documentation of the update recommends that Equation [25] be used to compute water depths rather than the updated equation that incorporates the additional data. In addition, Reference 28 describes a completely different model for water depth on a runway, but warns that "it is recommended that caution be exercised when considering the use of the model in conditions where the time rate of rainfall exceeds 50 mm/hr (approximately 2 in/hr), at distances greater than some 30 ft (9.1 m) from the crown of a runway." Indeed, tests of this model for the accident conditions reveal that the computed water depths agree relatively well with Equation [25] within about 40 ft. of the runway centerline, but start to increase exponentially (and unrealistically) a little beyond that distance.

[46] The ELAtextur scanner is described at https://iwsmesstechnik.de/en/texture/elatextur/ (accessed 6/3/20).

[47] The first 1,660 ft. of runway 10, measured from the threshold, is concrete; the displaced threshold (the origin of the runway x coordinate in this *Study*) is 1,000 ft. from the threshold, and so the western concrete portion of the runway ends at x = 660 ft. from the displaced threshold.

slope should be 1%. Tables 5 and 6 indicate that the southern slope of KNIP runway 10 did not satisfy this criteria, with measured cross-slopes of 0.3% to 0.9%.

Runway 10 x coordinate (feet)	Runway 10 y coordinate (feet)	ELAtextur Estimated Texture Depth (mm)	North cross slope (%)	South cross slope (%)
1600	-20	0.57	1.0	0.9
	-10	0.43		
	10	0.47		
	20	0.66		
	43	0.58		
2870	-20	0.67	1.1	0.5
	-10	0.80		
	10	0.83		
	20	0.64		
	40	0.54		
5000	-20	0.71	1.1	0.9
	-10	0.92		
	10	0.75		
	20	0.62		
	40	0.55		
6990	-20	1.04	Not measured	Not measured
	-10	0.83		
	10	0.57		
	20	0.85		
	40	0.62		
7025	Not measured	Not measured	0.6	0.3
7740	-20	0.35	0.9	0.3
	-10	0.35		
	10	0.37		
	20	0.36		
	40	0.44		

Table 5. Runway 10 macrotexture and cross-slope measurement results. Cells with white background indicate measurements on the asphalt portion of runway; cells with gray background indicate measurements on the concrete portion of runway.

The macrotexture depth values shown in Table 5 are the “estimated texture depth” (ETD) values reported by the ELAtextur laser scanning device used to take the measurements. However, the device does not measure ETD directly; the “mean profile depth” (MPD) is the actual physical measurement taken by the device, and ETD is computed from MPD according to the equation

$$ETD = 0.80*(MPD) + 0.20 \text{ mm} \quad [26]$$

With both ETD and MPD in millimeters. Furthermore, macrotexture measurements taken on runway 3/21 at the Roswell International Air Center (KROW) using a variety of methods (including measurements with the ELAtextur device) indicate that Equation [26] does not provide the best correlation between the MPD measured by the device, and the ETD measured using other methods (the “NASA Grease Sample” and “Water Outflow Meter”

methods; see Reference 25).[48] Instead, the measurements indicate that a better correlation between ETD and MPD is that given in Reference 26:

$$ETD' = 0.91*(MPD) + 0.053 \text{ mm} \quad [27]$$

Where the symbol ETD' is used to distinguish the ETD computed using Equation [27] from that computed using Equation [26]. Solving Equation [26] for MPD and substituting the result into Equation [27] gives ETD' in terms of the reported ETD:

$$ETD' = 1.1375*(ETD) - 0.1745 \text{ mm} \quad [28]$$

The ETD' computed using Equation [28] and the ETD in Table 5 is shown in Table 6 in the column labeled "ELAtextur Corrected Texture Depth (mm)."

Runway 10 x coordinate (feet)	Runway 10 y coordinate (feet)	ELAtextur Corrected Texture Depth (mm)	North cross slope (%)	South cross slope (%)
1600	-20	0.47	1	0.9
	-10	0.31		
	10	0.36		
	20	0.58		
	43	0.49		
2870	-20	0.59	1.1	0.5
	-10	0.74		
	10	0.77		
	20	0.55		
	40	0.44		
5000	-20	0.63	1.1	0.9
	-10	0.87		
	10	0.68		
	20	0.53		
	40	0.45		
6990	-20	1.01	Not measured	Not measured
	-10	0.77		
	10	0.47		
	20	0.79		
	40	0.53		
7025	Not measured	Not measured	0.6	0.3
7740	-20	0.22	0.9	0.3
	-10	0.22		
	10	0.25		
	20	0.24		
	40	0.33		

Table 6. Runway 10 cross-slope and *corrected* macrotexture measurement results. Cells with white background indicate measurements on the asphalt portion of runway; cells with gray background indicate measurements on the concrete portion of runway. Macrotextures are corrected per Equation [28].

[48] Reference 25 documents the NASA Grease Sample and Water Outflow Meter measurements taken at KROW in January 2012; the ELAtextur device measurements on KROW runway 3/21 were taken by an NTSB investigator in January 2013 and are recorded in an internal NTSB document.

Using the data in Table 6, the overall average ETD' (or T, to use the variable in Equation [25]) is 0.53 mm (0.0209"). The average T over the asphalt portion of the runway is 0.60 mm (0.0236"); the average T over the eastern concrete portion is 0.25 mm (0.0098").

The rainfall amounts at KNIP on the day of the accident were recorded by an automated Airport Surface Observation System (ASOS) at both 1 minute and 5 minute intervals (see Reference 27). The rainfall rate computed from the ASOS 1 and 5 minute rainfall data is shown in Figure 22 for the 7 minutes preceding and 3 minutes following the accident. The area highlighted in red in Figure 22 indicates the time span during which the airplane was on the runway. Figure 22 indicates that between 21:38:00 and 21:39:00, about 4 minutes before the accident, the 1-minute rainfall rate was as high as 2.4 in./hr. Between 21:35:00 and 21:41:00, the 5-minute rainfall rate nearly tripled, from 0.6 in./hr. to over 1.6 in./hr. At 21:41:00, about 1 minute before the accident, the 1-minute rainfall rate was 1.2 in./hr., dropped to 0.6 in./hr. at 21:42:00, and then increased to 1.8 in./hr. at 21:43:00.

Note in Table 3 that the KNIP SPECI weather observations at 21:22, 21:45, and 21:53 all reported the precipitation condition as "heavy rain." Per Reference 41, "heavy rain," the most intense rainfall rate descriptor available, corresponds to rainfall rates of 0.3 in./hr. and greater. As described above, the actual rainfall rates around the time of the accident were 2 to 8 times this threshold. The available precipitation descriptors fail to describe the significant difference between a rainfall rate of 2.4 in./hr. (8 times the "heavy rain" threshold) and 0.3 in./hr. (the threshold itself). Consequently, a report of "heavy rain" might not communicate to flight crews the true intensity of the rainfall at the airport, thereby impairing their ability to make a sound assessment of the runway conditions (e.g., "wet" vs. "flooded"), and the required landing distance.

Figure 23 shows the computed water depth on the runway as a function of distance from the runway centerline, at various rainfall rates, using Equation [25], for two combinations of T and S, corresponding to the different average characteristics of the asphalt and concrete portions of the pavement: [49]

Portion of KNIP runway 10	Macrotexture depth T, inches	Cross-slope S, %
Asphalt (660 ft. < x < 7,000 ft.)	0.0236	0.9
Concrete (x ≥ 7,000 ft.)	0.0098	0.3

Table 7. Macrotexture depth and cross-slope used for runway water depth calculations.

Per Figure 1, the lateral span of the main gear (from strut to strut) is 18.75 ft., so if the airplane tracks the centerline of the runway, both main gears should be within 10 ft. of the centerline. Figure 23 indicates that within this distance of the centerline, at a rainfall rate of 2 in./hr. the maximum water depth would be about 0.042" over the asphalt portion of the

[49] Equation [25] assumes that rain can drain from the edges of the runway with no obstructions. The drainage of water from the runway during a rainstorm was observed during the on-scene portion of the investigation, and no significant pooling of the water at the runway edges was observed.

runway, and about 0.085" over the concrete portion of the runway.[50] These values are within the "Safe" and "Caution" hydroplaning risk zones identified by W.B. Horne in Reference 22. However, Figure 2 indicates that the airplane deviated as far as 70 ft. to the right of the runway centerline during the ground roll, and was 60 ft. to the right of the centerline when it crossed the end of the runway. Figure 23 indicates that at a rainfall rate of 2 in./hr., the water depth over both the asphalt and concrete portions of the runway would be in the Reference 22 "hydroplaning danger zone." Even at a rainfall rate of 1.5 in./hr., which may be more representative of the conditions immediately preceding the accident, the water depths at 60 to 80 ft. from the runway centerline would be significant. As discussed above, the tire marks on the runway indicate that the tires were in contact with the pavement, and so could not have been lifted from the surface as occurs during dynamic hydroplaning. Nonetheless, the water depth (and speed) might have been sufficient to make dynamic hydroplaning imminent, and to place the tires in the condition shown in Figure 21c (where there is no dry Zone 3 under the tires, and the thin, viscous water film between the pavement and the tires in Zone 2 significantly reduces μ_B).

If a runway is not specifically identified as flooded (contaminated with at least 3 mm of standing water over 25% of its surface) or categorized as "Slippery When Wet" (a TALPA RCAM term discussed further below), then per the RCAM framework, in obviously wet (raining) conditions, the runway condition will simply be classified as "wet" and assumed to provide the μ_B defined by 14 CFR §25.109(c). Hence, it is of interest to compare the μ_B achieved during the accident landing with the μ_B defined by §25.109(c), and other models of μ_B for runways that are wet, but not flooded. Several of these models are described in detail in Reference 20, and are summarized below.

Definition of 14 CFR §25.109 wet runway braking friction coefficients

14 CFR §25.109 defines the accelerate-stop distance for transport-category airplanes, and describes how this distance is to be determined. The accelerate-stop distance is the distance required to accelerate from a stop to V_1,[51] and then bring the airplane back to a stop in the remaining runway length.[52] §25.109(a) defines the accelerate-stop distance on a dry runway, and §25.109(b) defines the accelerate-stop distance on a wet runway. §25.109(c) defines the μ_B to be assumed in the calculation of the accelerate-stop distance for a smooth, wet runway (the μ_B for wet runways that are grooved or treated with porous friction course material are defined in §25.109(d)).

---

[50] Note that some runways are not crowned, but are "tilted slabs" that have a constant cross-slope from one edge to the other. On such runways, the water depth in the wheel tracks will be greater than on crowned runways since the length of the drainage path will be from the edge of the runway to the gear location.

[51] Per 14 CFR 1.2, V_1 "means the maximum speed in the takeoff at which the pilot must take the first action (e.g., apply brakes, reduce thrust, deploy speed brakes) to stop the airplane within the accelerate-stop distance. V_1 also means the minimum speed in the takeoff, following a failure of the critical engine at V_{EF}, at which the pilot can continue the takeoff and achieve the required height above the takeoff surface within the takeoff distance."

[52] This simplified definition suffices for the intent of this *Study*; §25.109 defines additional details regarding how this maneuver is to be accomplished, that account for engine failures and pilot reaction times.

For a smooth, wet runway, §25.109(c) defines the μ_B as follows:

> The wet runway braking coefficient of friction for a smooth wet runway is defined as a curve of friction coefficient versus ground speed and must be computed as follows:
>
> (1) The maximum tire-to-ground wet runway braking coefficient of friction is defined as:

Tire Pressure (psi)	Maximum Braking Coefficient (tire-to-ground)
50	$\mu_{t/g_{MAX}} = -0.0350\left(\frac{V}{100}\right)^3 + 0.306\left(\frac{V}{100}\right)^2 - 0.851\left(\frac{V}{100}\right) + 0.883$
100	$\mu_{t/g_{MAX}} = -0.0437\left(\frac{V}{100}\right)^3 + 0.320\left(\frac{V}{100}\right)^2 - 0.805\left(\frac{V}{100}\right) + 0.804$
200	$\mu_{t/g_{MAX}} = -0.0331\left(\frac{V}{100}\right)^3 + 0.252\left(\frac{V}{100}\right)^2 - 0.658\left(\frac{V}{100}\right) + 0.692$
300	$\mu_{t/g_{MAX}} = -0.0401\left(\frac{V}{100}\right)^3 + 0.263\left(\frac{V}{100}\right)^2 - 0.611\left(\frac{V}{100}\right) + 0.614$

> Where—
>
> Tire Pressure = maximum airplane operating tire pressure (psi);
> $\mu_{t/gMAX}$ = maximum tire-to-ground braking coefficient;
> V = airplane true ground speed (knots); and
>
> Linear interpolation may be used for tire pressures other than those listed.
>
> (2) The maximum tire-to-ground wet runway braking coefficient of friction must be adjusted to take into account the efficiency of the anti-skid system on a wet runway. Anti-skid system operation must be demonstrated by flight testing on a smooth wet runway, and its efficiency must be determined. Unless a specific anti-skid system efficiency is determined from a quantitative analysis of the flight testing on a smooth wet runway, the maximum tire-to-ground wet runway braking coefficient of friction determined in paragraph (c)(1) of this section must be multiplied by the efficiency value associated with the type of anti-skid system installed on the airplane:

Type of anti-skid system	Efficiency value [η_{AS}]
On-Off	0.30
Quasi-Modulating	0.50
Fully Modulating	0.80

Consequently, §25.109(c) defines the wet runway braking coefficient as

$$\mu_B = (\mu_{t/gMAX})(\eta_{AS}) \qquad [29]$$

Where $\mu_{t/gMAX}$ (or μ_{max})[53] and the anti-skid efficiency η_{AS} are defined in the rule as shown above.

FAA AC 25-7D, *Flight Test Guide for Certification of Transport Category Airplanes*, dated 05/04/2018 (Reference 36), describes the three types of anti-skid braking systems

[53] Throughout this *Study*, $\mu_{t/gMAX}$ and μ_{max} are used equivalently.

identified in §25.109.[54] The B737-800 is equipped with a "fully modulating" anti-skid system, and so the applicable η_{AS} is 0.80 for this airplane.

The history of the §25.109 μ_B model described above, and its development from a μ_B model documented in Reference 29, is described in Reference 37.

The nominal inflation pressure of the main tires for the B737-800 is 205 psi. Interpolating the $\mu_{t/gMAX}$ tables above for a tire pressure of 205 psi gives

$$\mu_{t/gMAX} = -0.0335\left(\frac{V_G}{100}\right)^3 + 0.2526\left(\frac{V_G}{100}\right)^2 - 0.6557\left(\frac{V_G}{100}\right) + 0.6881 \qquad [30]$$

Where V_G is the ground speed in knots. The μ_B resulting from multiplying the $\mu_{t/gMAX}$ defined in Equation [30] by the nominal η_{AS} of 0.80 (for a fully-modulating anti-skid braking system) is shown in Figures 24 and 25 as the magenta line labeled "14 CFR 25.109(c) μ_B (205 psi / η_{AS} = 0.80)."

Comparison of achieved and modeled μ_B, and corresponding landing distances

Figures 24 and 25 compare the μ_B achieved during the accident landing roll ("Computed main gear μ_B," also plotted as a function of time in Figure 18) with the μ_B defined by various friction models. The §25.109(c) μ_B model is described above; the other μ_B lines plotted in Figure 24a are described below.

Figure 25 is similar to Figure 24, but compares the achieved μ_B with various μ_B models as a function of the runway x coordinate (distance from the displaced threshold). The value of μ_B at each point on the "14 CFR 25.109(c) μ_B (205 psi / η_{AS} = 0.80)" line in Figure 25 is computed using Equations [29] and [30], with V_G equal to N732MA's ground speed at the corresponding x coordinate value in the plot.

Note that the §25.109 μ_B curves in Figures 24 and 25 are substantially higher than the computed μ_B based on the accident data, indicating that the achieved μ_B fell well short of that specified by §25.109 for an ungrooved, wet runway (that is not flooded).

The jump in the achieved μ_B from about 0.04 to about 0.08 at 130 kt. shown in Figure 24a (and at time 21:41:59 in Figure 18) is noteworthy, and coincides with both the stowing of the right engine thrust reverser, and with the nearly simultaneous application of the left and right brakes after a brief period during which both brakes had been released. At the same time, the plot of n_x in Figure 18 doesn't show much change in response to these events. The stable n_x as the thrust reverser is stowed results in the computed μ_B jump: to keep n_x approximately the same, the total friction force from the tires has to increase to compensate for the loss of retarding force from the thrust reverser. That an increase in friction would almost exactly, and at the right moment, compensate for the stowing of the reverser seems very coincidental and improbable. Nonetheless, the n_x behavior indicates

[54] See AC 25-7D, paragraph 4.3.7.4, "Classification of Types of Anti-Skid Systems."

that either this is the case, or that the level of reverse thrust did not change when the reverser was stowed, or that one or several FDR parameters are in significant error.

To quantify the effect of reverse thrust on the μ_B calculation, the μ_B computed per Equations [19]-[23], but assuming zero reverse thrust, is plotted in Figures 24b and 25b. Note that the μ_B in these Figures is higher than in Figures 24a and 25a (since friction now is presumed to provide the retarding force previously provided by reverse thrust), does not jump at the time the reverser is stowed, and in general matches the "Boeing flooded μ_B" line fairly well (the "Boeing flooded μ_B" model is described below). While this μ_B behavior seems more reasonable than that plotted in Figures 24a and 25a, it derives from the assumption that, in spite of the FDR evidence to the contrary, the right engine was not producing reverse thrust. There is no other evidence to support such an assumption, or to entertain doubts about the validity of the FDR reverser position or engine N1 data.

Even so, the jump in μ_B that coincides with the stowing of the thrust reverser remains a remarkable coincidence. A possible explanation for the jump in μ_B is the application of the left and right brakes at around the same time. This brake application, following a brief period during which both brakes were released, might have resulted in a higher η_{AS} than had been achieved previously; research concerning η_{AS} is discussed further below.

Figure 26 plots ground speed vs. distance from the runway 10 displaced threshold for the accident data (accelerometer integration), and compares this curve with those corresponding to simulated ground rolls that assume different μ_B models for the runway. The top plot in Figure 26 presents simulations starting from a touchdown airspeed of V_{REF30} + 5 KCAS (the nominal approach speed), and the bottom plot presents simulations starting from a touchdown airspeed of V_{REF30} + 20 KCAS (the accident condition).[55] A tailwind of 10 knots is assumed for all the simulations, consistent with the corrected tailwind component on the runway shown in Figure 16. In addition, all the simulations assume a touchdown point 1,580 ft. from the runway 10 displaced threshold, to match the touchdown point in the accident.

Note that the "*PAVEMENT END"* line in Figures 25 and 26 corresponds to the point where N732MA exited the pavement into the grass. This point is 100 ft. past the runway end and about 18 ft. to the right of the right edge of the 75 ft.-wide paved runway overrun, which extends 950 ft. past the runway end (see Figure 2).

The bottom plot of Figure 26 indicates that everything else being equal, had the airplane achieved the μ_B specified by §25.109(c) for an ungrooved, wet runway, it would have stopped on the runway with about 930 ft. to spare, or about 12% of the 8,006 ft. runway length available.[56] This is the case even though the touchdown point was 580 ft. beyond

[55] The indicated airspeed at touchdown was 164 kt. (16 kt. above the V_{REF30} of 148 kt.); however, due to the static pressure error, the actual calibrated airspeed was 4 kt. greater, or 168 kt. The true airspeed was 169 kt., 1 kt. higher than the calibrated airspeed.

[56] The x coordinate plotted in Figures 25 and 26 corresponds to the position of the airplane's main gear tires, close to the CG. The nose gear is 51 ft. ahead of the main gear (see Figure 1), so 51 ft. should be added to

the FCOM "nominal" touchdown point (1,000 ft. from the displaced threshold), the touchdown speed was 18 KCAS higher than the nominal V_{REF30} + 5 KCAS approach speed, it took 4 seconds to deploy the spoilers (twice as long as normal[57]), and there was a 10-knot tailwind over the runway. The top plot of Figure 26 indicates that had the airplane been on-speed (at V_{REF30} + 5 KCAS) and achieved the §25.109(c) μ_B, it could have stopped about 6,300 ft. from the displaced threshold, with about 1,700 ft. (21% of the runway) to spare. The 1.265 dispatch safety factor in the new FTHWG proposals described above would have made the required dispatch landing distance (assuming the §25.109(c) μ_B model) 6,300 ft. x 1.265 = 7,970 ft., and so would not have precluded dispatching the flight to the 8,006 ft. long runway. In fact, the dispatch calculations would probably have assumed zero or favorable winds (not a 10 kt. tailwind), and so the required landing distance under the proposed new rules would have been even shorter.

In contrast, the red lines in Figure 26 labeled "0.6 x Boeing flooded μ_B (N732MA match)" depict the simulated landing distance required using a μ_B that approximately matches the μ_B achieved during the accident (see Figures 24 and 25), and indicate that with this μ_B level the airplane would not have stopped on the runway even if it had been on speed, touched down only 1,000 ft. from the displaced threshold,[58] and deployed the spoilers in the nominal 2 seconds. The dashed red line in the top plot of Figure 26 shows the simulation results with the same μ_B, but with zero wind (i.e., no tailwind), an on-speed approach, a 1,000 ft. touchdown point, and nominal spoiler deployment time; the airplane departs the end of the runway at a speed of about 12 knots even in this case.

The red line in the bottom plot of Figure 26 doesn't lie on top of the black "N732MA accelerometer integration line" (which would be a perfect match) because the simulation deploys the spoilers and applies the brakes 2 seconds after touchdown (corresponding to the times assumed in the Boeing FCOM for manual brake and spoiler application), whereas in the accident the spoilers did not deploy until about 4 seconds after touchdown. The change in slope of the speed vs. distance lines due to spoiler deployment is clearly seen in Figure 26. Even though the black and red lines do not match, the *slope* of the lines match well after spoiler deployment, indicating that the μ_B depicted by the red dashed lines in Figures 24 and 25 is a good approximation to the actual μ_B achieved on the runway.

In light of the results shown in Figure 26, the poor μ_B achieved on the runway can be considered a greater contributor to the runway overrun than the deviations from the nominal approach speed, touchdown point, and nominal spoiler deployment time. Nonetheless, the tailwind, high approach speed, longer than nominal touchdown point, and delay in spoiler deployment increased the speed at which the airplane departed the runway and impacted the seawall, and hence contributed to the severity of the accident.

---

the x coordinate values in the Figures to determine the location of the nose gear, and the available runway remaining at zero ground speed, as measured from the nose gear.

[57] The landing distance data in the FCOM assumes that it takes 2 seconds after touchdown to manually deploy the speedbrakes. For automatic speedbrakes, the deployment time is 1 second (see Table 11).

[58] The simulation was run with a touchdown point of 1,580 ft. from the threshold, but the resulting line in Figure 26 can be "backed up" 580 ft. to see the result with a 1,000 ft. touchdown point; the speed in this case is still greater than zero at the end of the runway. The "Boeing flooded μ_B" model is discussed below.

The additional μ_B models presented in Figures 24-26, including the "Boeing flooded" μ_B that is the basis of the model used to match the accident μ_B, are discussed further below. A matrix of landing distances from the FCOM and OPT that supplement the results of Figure 26 by considering different runway surface conditions (μ_B models) and operational criteria (winds, approach speeds, and deceleration device usage) is also presented below.

NASA μ_B model based on Continuous Friction Measurement Equipment (CFME) data

References 2 and 20 discuss the investigations of six other landing accidents or incidents on wet runways (all involving turbojet airplanes) in which the airplane did not achieve the μ_B implied in the manufacturer's FCOM landing distances, or that would be predicted by the §25.109 model. These six accidents are:

- The BAe 125-800A accident in Owatonna, MN (KOWA), on 7/31/2008 (NTSB #DCA08MA085) (Reference 37 is the *Airplane Performance Study* for this accident)
- The American Airlines flight 331 accident in Kingston, Jamaica, on 12/22/2009 (NTSB #DCA10RA017)
- The United Express flight 8050 accident in Ottawa, Ontario, on 6/16/2010 (NTSB # DCA10RA069)
- The Southwest Airlines flight 1919 incident in Chicago, IL (KMDW), on 4/26/2011 (NTSB #DCA11SA047)
- The EMB-505 accident in Conroe, TX (KCXO), on 9/19/2014 (NTSB #CEN14FA505) (Reference 20 is the *Airplane Performance Study* for this accident)
- The EMB-500 accident in Sugarland, TX (KSGR), on 11/21/2014 (NTSB # CEN15LA057)

The μ_B levels achieved in these events (and numerous events not investigated by the NTSB[59]) are below those underlying the wet runway landing distances published in the airplanes' FCOMs and the μ_B specified by 14 CFR §25.109. However, the achieved μ_B levels *are* generally consistent with the μ_B predicted using a National Aeronautics and Space Administration (NASA) model that is based on runway friction measurements taken with a CFME device. Significantly, however, the runways in five of these events were determined *not* to be flooded,[60] while as shown in Figure 23, portions of the KNIP runway were likely very close to or over the 3 mm water depth that defines a "flooded" runway. This sub-section of the *Study* describes the CFME μ_B model, the CFME tests performed on KNIP runway 10/28, and the resulting μ_B predicted by the CFME model and plotted in Figures 24 and 25.

[59] The foreign events were noted in comments by the FAA on a draft version of this *Study*.

[60] For the Ottawa accident, it is not possible to exclude drainage and puddling problems or rubber deposits on the runway as contributors to the accident, though dynamic hydroplaning in that event can be ruled out. The NASA CFME μ_B model overestimates the achieved μ_B in this accident, though it is much closer to the actual μ_B than the §25.109 model (see Reference 2).

As documented in Reference 30, on May 6, 2019 (three days after the accident) the Florida Department of Transportation (FDOT) conducted CFME friction tests on KNIP runway 10/28 using a Dynatest Model 6875 Runway Friction Tester (RFT) vehicle.[61] Seventeen runs of the RFT were performed, at different speeds and offsets from the runway centerline, as shown in Table 8 and Figure 27. The results of these measurements are presented in Figures 28 and 30.[62] The legends in the plots indicate the runway direction, speed and runway y-coordinate of the run; for example, "RWY10_OFF20_V40" indicates a test on runway 10, performed at a lateral offset of 20 ft. (i.e., 20 ft. right of the runway centerline), at a speed of 40 mph. Note that all the "offsets" from the centerline are to the right, so runs on runway 28 are offset to the *left* of runway 10. The k_B parameter plotted in Figure 30 is defined below.

Appendix B of this *Study* is a paper prepared by Mr. Thomas Yager, Distinguished Research Associate at the NASA Langley Research Center (retired), documenting the details of the NASA method for computing μ_B for aircraft based on CFME data. This paper was prepared for the NTSB in support of the investigation of the Hawker Beechcraft BAe 125-800A accident in Owatonna, MN, on July 31, 2008 (NTSB #DCA08MA085). The method is also presented in Reference 31.

Run #	Vehicle speed (mph)	Runway offset
1	40	10 ft. right of runway 10 centerline
2	40	10 ft. right of runway 28 centerline
3	40	20 ft. right of runway 10 centerline
4	40	20 ft. right of runway 28 centerline
5	60	10 ft. right of runway 10 centerline
6	60	10 ft. right of runway 28 centerline
7	60	20 ft. right of runway 10 centerline
8	60	20 ft. right of runway 28 centerline
9	50	10 ft. right of runway 10 centerline
10	50	10 ft. right of runway 28 centerline
11	50	20 ft. right of runway 10 centerline
12	50	20 ft. right of runway 28 centerline
13	25	10 ft. right of runway 10 centerline
14	25	10 ft. right of runway 28 centerline
15	25	20 ft. right of runway 10 centerline
16	25	20 ft. right of runway 28 centerline
17	40	60 ft. right of runway 10 centerline

Table 8. CFME runs performed by FDOT.

The NASA method for computing airplane μ_B values from the CFME data consists of computing the ratio of the wet-runway μ (μ_{wet}) to the dry-runway μ (μ_{dry}) based on the CFME μ (which measures μ_{wet}) and a μ_{dry} for the test vehicle, and assuming that this

[61] A description of the Dynatest CFME device can be found at: https://www.dynatest.com/runway-friction-tester-rft

[62] The lines in Figure 28 labeled "MIN LEVEL," "MAINT LEVEL," and "NEW LEVEL" indicate the μ values corresponding to runway friction maintenance levels defined in FAA AC 150/5320-12C (Reference 32).

ratio also applies to the μ_{wet}/μ_{dry} ratio of the braked airplane tires. The μ_{dry} of the airplane tires is a function of the tire inflation pressure (see Appendix B). The selection of μ_{dry} for the RFT vehicle is discussed below.

The airplane ground speed associated with each μ_{wet} value is similarly based on computing the ratio of the ground speed (V_G) to the spin-down hydroplaning speed ($V_{p,spin\ down}$) of the test vehicle, and then applying that same ratio to the spin-down hydroplaning speed of the aircraft tires. The $V_{p,spin\ down}$ of both the test vehicle and airplane tires are a function of each vehicle's tire inflation pressure (see Equation [24a]).

One product of this method, which is based on similarity of the μ_{wet}/μ_{dry} and $V_G/V_{p,spin\ down}$ ratios between the friction test vehicle and an airplane, is the maximum wet friction coefficient that the runway can provide (μ_{max}), as a function of V_G for an airplane. As described in §25.109(c), the actual μ_B achieved by an aircraft is less than μ_{max} because the braking systems of aircraft are not 100% efficient. In the NASA method, μ_B is computed from μ_{max} using the following equations:

For μ_{max} < 0.7: $\mu_B = 0.2\ \mu_{max} + 0.7143\ (\mu_{max})^2$ [31a]

For μ_{max} ≥ 0.7: $\mu_B = 0.7\ \mu_{max}$ [31b]

The computation of μ_B from μ_{max} to account for the braking system efficiency of the airplane is similar to the method prescribed in §25.109 for the computation of μ_B by multiplying $\mu_{t/gMAX}$ by η_{AS} (see Equation [29]). The η_{AS} implied in Equations [31a] and [31b] can be gleaned by dividing these equations by μ_{max}:

For μ_{max} < 0.7: $\eta_{AS} = \mu_B/\mu_{max} = 0.2 + 0.7143\ \mu_{max}$ [32a]

For μ_{max} ≥ 0.7: $\eta_{AS} = \mu_B/\mu_{max} = 0.7$ [32b]

Note that the η_{AS} defined by these equations is a function of μ_{max} (and is never greater than 0.7), and does not depend on the type of anti-skid braking system, as does the anti-skid efficiency value defined in §25.109. Significantly, Equation [32a] indicates that η_{AS} deteriorates with μ_{max}; so, as the runway gets more slippery, the anti-skid system becomes less able to take advantage of the available friction that remains – in effect, a double penalty. Reference 20 presents additional evidence that η_{AS} deteriorates with μ_{max}, contrary to the constant η_{AS} assumed in the §25.109 μ_B model.

Figure 28 indicates that the μ measured by the RFT on KNIP runway 10/28 was not constant over any given test run, but varied considerably during each run. Not surprisingly, this indicates that the μ_{max} available from a runway can depend on both speed *and* the location (runway x and y coordinates) in question. Of note, the RFT runs indicate a substantial reduction in μ between about 1,000 ft. and 2,000 ft. from the runway 10 displaced threshold (during the accident landing, N732MA overflew about half of this "slippery" area, touching down 1,580 ft. from the displaced threshold).

The RFT test speeds of 25, 40, 50, and 60 mph transform into airplane ground speeds of 57, 91, 114, and 136 knots, respectively, using an RFT tire pressure of 30 psi and an airplane tire pressure of 205 psi. Consequently, the maximum RFT speed of 60 mph is not sufficient to determine the airplane μ_B at airplane ground speeds above 136 knots. As shown in Figure 9, the speed range of interest (while N732MA was on the pavement) is from 180 to about 90 knots, so a substantial portion of the higher speed range is not covered by the RFT tests. Nonetheless, References 2 and 20 present a method for estimating the airplane μ_B across the entire speed range of interest based on a combination of the §25.109 model and CFME runs that address only part of the desired speed range. That method is used to here to estimate the airplane μ_B as a function of both airplane ground speed and position on the runway; the result of this calculation is shown in Figures 24 and 25 as the line labeled "NASA CFME μ_B." The method itself is described below, after some necessary preliminary discussion about the CFME μ values defined in FAA AC 150/5320-12C, and how these values are used to compute a μ_{dry} for the RFT vehicle (this μ_{dry} is needed for converting RFT μ measurements into airplane μ_B values using the NASA method, as described above). AC 150/5320-12C also describes the use of CFME devices for runway pavement maintenance, and defines the "NEW," "MAINT," and "MIN" friction levels depicted in Figure 28.

CFME μ values defined in AC 150/5320-12C

FAA AC 150/5320-12C (Reference 32) notes that the μ_{max} on a given runway will deteriorate over time, and recommends that airports that support turbojet traffic monitor the μ_{max} on the runways through the use of CFME:

> Over time, the skid-resistance of runway pavement deteriorates due to a number of factors, the primary ones being mechanical wear and polishing action from aircraft tires rolling or braking on the pavement and the accumulation of contaminants, chiefly rubber, on the pavement surface. The effect of these two factors is directly dependent upon the volume and type of aircraft traffic. Other influences on the rate of deterioration are local weather conditions, the type of pavement ([Hot Mix Asphalt or Portland Cement Concrete]), the materials used in original construction, any subsequent surface treatment, and airport maintenance practices.
> …
>
> All airports with turbojet traffic should own or have access to use of CFME. Not only is it an effective tool for scheduling runway maintenance, it can also be used in winter weather to enhance operational safety (see AC 150/5200-30). Airports that have few turbojet traffic operations may be able to borrow the CFME from nearby airports for maintenance use, share ownership with a pool of neighboring airports, or hire a qualified contractor.

The CFME μ values corresponding to runway friction levels that warrant specific maintenance actions are defined in Section 3 of the AC. Three friction levels are defined, corresponding to the "NEW," "MAINT," and "MIN" lines shown in Figure 28. The AC describes these friction levels as follows:

> 3-20.EVALUATION AND MAINTENANCE GUIDELINES. The following evaluation and maintenance guidelines are recommended based on the friction levels classified in [Figure 29]. These guidelines take into account that poor friction conditions for short distances on the runway do not pose a safety

problem to aircraft, but long stretches of slippery pavement are of serious concern and require prompt remedial action.

a. Friction Deterioration Below the Maintenance Planning Friction Level [MAINT LEVEL] (500 ft). When the average Mu value on the wet runway pavement surface is less than the Maintenance Planning Friction Level but above the Minimum Friction Level [MIN LEVEL] in [Figure 29] for a distance of 500 feet (152 m), and the adjacent 500 foot (152 m) segments are at or above the Maintenance Planning Friction Level, no corrective action is required. These readings indicate that the pavement friction is deteriorating but the situation is still within an acceptable overall condition. The airport operator should monitor the situation closely by conducting periodic friction surveys to establish the rate and extent of the friction deterioration.

b. Friction Deterioration Below the Maintenance Planning Friction Level (1000 ft). When the averaged Mu value on the wet runway pavement surface is less than the Maintenance Planning Friction Level in [Figure 29] for a distance of 1000 feet (305 m) or more, the airport operator should conduct extensive evaluation into the cause(s) and extent of the friction deterioration and take appropriate corrective action.

c. Friction Deterioration Below the Minimum Friction Level [MIN LEVEL]. When the averaged Mu value on the wet pavement surface is below the Minimum Friction Level in [Figure 29] for a distance of 500 feet (152 m), and the adjacent 500 foot (152 m) segments are below the Maintenance Planning Friction Level, corrective action should be taken immediately after determining the cause(s) of the friction deterioration. Before undertaking corrective measures, the airport operator should investigate the overall condition of the entire runway pavement surface to determine if other deficiencies exist that may require additional corrective action.

d. New Design/Construction Friction Level for Runways [NEW LEVEL]. For newly constructed runway pavement surfaces (that are either saw cut grooved or have a PFC overlay) serving turbojet aircraft operations, the averaged Mu value on the wet runway pavement surface for each 500 foot (152 m) segment should be no less than the New Design/Construction Friction Level in [Figure 29].

The drop in μ measured by the RFT between 800 and 2,600 ft. shown in Figure 28 for the 60 mph run conducted 10 ft. to the right of the centerline of runway 28 (the black line in the second plot) satisfies the description in paragraph (c) above, indicating that "corrective action should be taken immediately after determining the cause(s) of the friction deterioration."

Table 3-2 from AC 150/5320-12C is included here as Figure 29, and can be used along with information included in Appendix B to determine μ_{dry} for the RFT vehicle used to test KNIP runway 10/28. As descried above, this μ_{dry} is needed to convert RFT μ measurements into airplane μ_B values using the NASA method. Appendix B lists values of μ_{dry} for several CFME devices, but the Dynatest RFT is not one of them. However, the values of μ_{dry} for the "Friction Tester" CFME device listed in Appendix B (corresponding to the Sarsys Airport Surface Friction Tester, or SFT[63]) can be used along with Figure 29 to determine the μ_{dry} for the RFT. This determination rests on the observation that independent calculations of airplane μ_B, each starting from μ measurements collected with different types of CFME devices, should match. Figure 29 is a table of μ values for different

[63] See https://www.sarsys-asft.com/measuring-system (accessed 06/10/2020). This device has a test tire incorporated into the structure of a Saab car, and is called the Saab Friction Tester in the text of Appendix B, and is listed simply as the "Friction Tester" in Table I of Appendix B.

CFME devices that correspond to “equivalent” runway friction levels, so the airplane μ_B computed using the μ values in Figure 29 for different devices should produce identical results for the same combinations of speed and runway friction level. The CFME devices listed in Figure 29 include both the Sarsys SFT and the Dynatest RFT; hence a correspondence between the RFT and the SFT can be established, and the μ_{dry} of the SFT (listed in Appendix B) can be used to determine the μ_{dry} of the RFT.
The RFT is represented by the “Dynatest Consulting, Inc. Runway Friction Tester” device entry in Figure 29, and the SFT is represented by the “Airport Surface Friction Tester” device entry. The RFT trailer and SFT have similar operational characteristics: a 30 psi measurement tire inflation pressure, operated at a slip ratio between 10% (for the SFT) and 14% (for the RFT). Table I of Appendix B lists the μ_{dry} for the SFT as 1.1.

As argued above, for each friction classification level in Figure 29, the resulting μ_B for an airplane should be the same, regardless of the CFME device used to measure μ. The μ_B is given by Equation [31], with μ_{max} from the NASA CFME model given by

$$\mu_{max} = \frac{\mu_{CFME}}{\mu_{dry,CFME}} \mu_{dry,airplane} \quad [33]$$

Where:

μ_{CFME}= runway μ measured by the CFME device;
$\mu_{dry,CFME}$= μ_{dry} of the CFME device; and
$\mu_{dry,airplane}$= μ_{dry} of the airplane (a function of the airplane tire p).

Since the μ_{max} computed from RFT and SFT measurements should be the same, we can write

$$\frac{\mu_{RFT}}{\mu_{dry,RFT}} \mu_{dry,airplane} = \frac{\mu_{SFT}}{\mu_{dry,SFT}} \mu_{dry,airplane} \quad [34]$$

Where:

μ_{RFT} = runway μ measured by the RFT device;
$\mu_{dry,RFT}$= μ_{dry} of the RFT device;
μ_{SFT} = runway μ measured by SFT device; and
$\mu_{dry,SFT}$= μ_{dry} of the SFT device.

From Equation [34] it follows that

$$\mu_{dry,RFT} = \frac{\mu_{RFT}}{\mu_{SFT}} \mu_{dry,SFT} \quad [35]$$

Equation [35] can be used to compute $\mu_{dry,RFT}$ based on the μ_{RFT} and μ_{SFT} values in Figure 29, and $\mu_{dry,SFT}$ = 1.1. The results are shown in Table 9.

Friction Level	40 mph	60 mph
MIN	1.1	1.33
MAINT	1.1	1.26
NEW	1.1	1.07

Table 9. $\mu_{dry,RFT}$ values computed using Equation [35] with inputs from Figure 29.

Since the data in Figure 29 at 40 mph are the same for the RFT and the SFT, the RFT $\mu_{dry,RFT}$ values at 40 mph match the $\mu_{dry,SFT}$ of 1.1. The 60 mph data in Figure 29 are different for the two CFME devices, and so at 60 mph the $\mu_{dry,RFT}$ is different than the $\mu_{dry,SFT}$. Table 9 shows that at 60 mph the computed $\mu_{dry,RFT}$ values for the MIN and MAINT friction levels are about the same ($\mu_{dry,RFT} \cong 1.3$), but the value for the NEW level differs from these ($\mu_{dry,RFT} = 1.07$). Since in this accident we are interested in the μ_B at high speeds (above 90 kt.), and Figure 28 shows that the μ measured by the RFT on runway 10/28 at 60 mph was closest to the MAINT level, this *Study* uses $\mu_{dry,RFT} = 1.3$ to compute μ_B from the RFT μ. If $\mu_{dry,SFT} = 1.1$ were used instead, then the μ_{max} computed using Equation [33] would increase by a factor of 1.3/1.1 = 1.18. As shown in Figures 24 and 25, the μ_B predicted by the NASA CFME model (using $\mu_{dry,RFT} = 1.3$) is already much greater than the actual μ_B achieved, so using $\mu_{dry,SFT} = 1.1$ would not change this result.

Expected μ_B for accident landing based on combined NASA CFME and §25.109 models

As noted above, References 2 and 20 present a method for estimating the airplane μ_B across the entire speed range of interest based on a combination of the §25.109 model and CFME runs that address only part of the desired speed range. That method is described in this sub-section, and is used to estimate the (expected) airplane μ_B as a function of both airplane ground speed and position on the runway.

The RFT runs can be used to predict the expected airplane μ_B along the RFT tracks at airplane ground speeds of 57, 91, 114, and 136 knots, per the NASA CFME method described above. The §25.109 model also predicts the airplane μ_{max} at these speeds, per Equation [30] (the resulting μ_{max} is independent of the position on the runway, unlike the CFME-based μ_B). The CFME prediction, which is based on measurements of the actual runway, can be used to compute an "effective" η_{AS} that should be applied to the §25.109 μ_{max}, which models runways in general. This effective η_{AS}, termed k_B, is defined as

$$k_B = \frac{\mu_{B,CFME}}{\mu_{max,25.109}} \quad [36]$$

Where:

$\mu_{B,CFME}$ = μ_B obtained from the RFT runs using the NASA CFME method
$\mu_{max,25.109}$ = μ_{max} from the §25.109(c) model (Equation [30])

Since $\mu_{B,CFME}$ varies with position on the runway, k_B also varies along the runway. Figure 30 plots k_B computed using Equation [36] as a function of distance from the runway 10 displaced threshold for all the RFT runs. Figure 30a is the raw calculation, which is as

noisy as the RFT μ measurements plotted in Figure 28; Figure 30b plots k_B filtered using a fast-Fourier filtering algorithm with a low-pass cutoff frequency of 0.01 Hz.

Figure 30b indicates that k_B is a function of runway x position, runway y position, and RFT vehicle speed. In this *Study*, we are primarily interested in the airplane μ_B at higher speeds, and along a track offset to the right of runway 10 (see Figure 2). Consequently, for simplicity, only the filtered k_B corresponding to the 60 mph RFT run offset 20 ft. to the right of runway 10 (the light green line labeled "RWY10_OFF20_V60" in the bottom plot of Figure 30b) is used to compute the expected μ_B during the landing roll, based on the RFT measurements.

Accordingly, the "NASA CFME μ_B" line plotted in Figures 24 and 25 is obtained by multiplying the μ_{max} from Equation [30] by the "RWY10_OFF20_V60" k_B line in Figure 30b. Note that when k_B is greater than 0.8 (the η_{AS} assumed in Equation [29]), then the NASA CFME μ_B is greater than the §25.109(c) μ_B. Where the NASA CFME μ_B no longer oscillates (below 116 kt. in Figure 24 and beyond 6,900 ft. in Figure 25), there is no RFT measurement for the corresponding point on the runway (see Figure 30) and the last available k_B value is "held." In general, the NASA CFME μ_B is only slightly lower than the §25.109(c) μ_B, indicating that in this case, unlike in the other overrun events mentioned above, the poor μ_B achieved by the airplane is more likely the result of the depth of the water on the runway, as opposed to the underlying condition of the pavement.

AMC 25.1591 flooded runway μ_B

As noted above, AMC 25.1591 provides one acceptable means of compliance with EASA regulation CS 25.1591, *Performance Information for Operations with Contaminated Runway Surface Conditions*. AMC 25.1591, paragraph 7.3.1 indicates that for runways contaminated with standing water, the "effective braking coefficient of an anti-skid controlled braked wheel/tyre" is given by

$$\mu_B = -0.0632\left(\frac{V}{100}\right)^3 + 0.2683\left(\frac{V}{100}\right)^2 - 0.4321\left(\frac{V}{100}\right) + 0.3485 \qquad [37]$$

Where V is the ground speed in knots.
Note: For V greater than the aquaplaning [hydroplaning] speed, use μ = 0.05 constant.

Other paragraphs of AMC 25.1591 describe additional forces acting on the airplane during operations on contaminated runways, including contaminant drag (water displacement drag and water spray impingement drag).

As noted above, the spin-up hydroplaning speed for 205 psi tires is 110 kt., so per the AMC 25.1591 model, above this speed, the μ_B should be set to 0.05 to represent full dynamic hydroplaning conditions. The μ_B defined by Equation [37] is presented in Figures 24 and 25 as the purple lines labeled "AMC 25.1591 (flooded) μ_B" and AMC 25.1591 (hydro) μ_B." The "hydro" line incorporates the drop of μ_B to a constant 0.05 above 110 kt.; the "flooded" line applies Equation [37] at all speeds. The stopping distances under the

accident conditions (at both V_{REF30} + 5 and V_{REF30} + 18) associated with both the "flooded" and "hydro" μ_B are shown Figure 26. If the approach speed had been the nominal V_{REF30} + 5 kt. and the μ_B defined by Equation [37] alone ("flooded" line) been attained, the airplane would have stopped about 7,600 ft. from the displaced runway threshold, or about 400 ft. before the end of the runway. If the μ_B defined by the "hydro" line had been attained, the airplane would have crossed the runway end at 42 kt. At the actual approach speed of V_{REF30} + 18 kt., the airplane would have crossed the runway end at about 50 kt. if the "flooded" μ_B had been attained, and at about 77 kt. if the "hydro" μ_B had been attained.

Note that Figures 24-26 indicate that the actual μ_B achieved during the landing is lower even than the flooded μ_B defined by Equation [37], but matches the μ_B = 0.05 representing full dynamic hydroplaning above 110 kt. rather well. Since the tire mark and n_y evidence indicates that the tires were in contact with the runway and therefore likely not experiencing full dynamic hydroplaning, the constant μ_B of 0.05 that matches the achieved μ_B suggests that this low μ_B can result even without the tire being lifted entirely off the runway surface. This is consistent with the discussion of the water depth on the runway presented earlier, which notes that the very low μ_B achieved during the accident indicates that the tires might have been in the viscous hydroplaning condition depicted in Figure 21c, in which "contact with the ground is all but lost" and "the tire develops very little braking force" (Reference 21).

Notably, References 2 and 20 conclude that some wet runways appear to only support the μ_B level defined by Equation [37], *even though they may not be flooded*. These References document cases in which the rainfall rate and runway characteristics preclude concluding that the runways involved were flooded, but in which the μ_B attained by the aircraft was much less than that defined by the §25.109 μ_B model, and closer that given by Equation [37]. This observation also underlies the concerns expressed in SAFOs 15009 and 19003.

Boeing simulator model flooded runway μ_B

Reference 33 is a technical description of the algorithms and data underlying Boeing's B737 engineering simulator model. Chapter 9 of this document concerns the friction and cornering forces developed by the landing gear, and includes a table of μ_B vs. ground speed for several runway conditions, including dry, wet, flooded, icy, melting ice, snowy, and "wet on rubber residue." The data for the "flooded" conditions are plotted in Figures 24 and 25 as the brown line labeled "Boeing flooded μ_B." This μ_B line is lower than the "AMC 25.1591 (flooded) μ_B" line, and therefore closer to the achieved μ_B, though it is still somewhat higher than the achieved μ_B.

The simulated landing distances computed using the Boeing flooded μ_B are shown in Figure 26, and indicate that with this μ_B the airplane would not stop on the runway with either of the approach speeds considered in Figure 26. The actual μ_B achieved during the accident is approximately 60% of the Boeing flooded μ_B level.

Effect of drift angle on μ_B

The airplane's tires not only provide braking forces, but also cornering forces that help to "steer" the airplane down the runway. These cornering forces are side forces on the tires produced when the tires are yawed relative to the direction of travel. The side forces increase with angle of yaw, up to a point. As with car tires, the friction available at the tire-pavement interface must be "shared" between braking and cornering forces; the more friction is used for braking, the less is available for cornering, and vice-versa. Reference 33 describes the way these cornering and braking forces are modeled in the B737NG engineering simulator. In response to a request from the NTSB, Boeing exercised the B737NG simulator model to determine the reduction in μ_B resulting from yaw on the tires, considering that during the accident landing, the drift angle on the runway reached 8° (see Figures 12 and 15). Boeing's report transmitting the results of the simulations reads:

> The purpose of this investigation was to determine the effect of airplane skidding at a constant yaw angle on braking force. To do this the Boeing 737NG simulation was used to determine an analytical value for braking friction with the airplane put into a drift condition using rudder input with an initial ground speed of 220 knots. This was done for drift angles of 2°, 4°, 6°, and 8° for dry, wet, and flooded runway conditions. In general it was found that there was a roughly linear reduction in friction coefficient as a percentage of the 0° yaw braking coefficient …. It was also found that the percentage reduction in braking coefficient was relatively constant for a given yaw angle regardless of ground speed.
>
> Caution should be exercised when using the information provided in this analysis. There is no flight test data for braking with an airplane in a drift condition. The effect of yaw on braking implemented in the 737NG simulation is based on NASA testing and is primarily meant to simulate taxi conditions with relatively low ground speeds. Boeing has not however performed any in depth investigation into braking combined with airplane steering since the simulation has been judged sufficient for training purposes.

Table 10 presents the reduction in μ_B as a function of drift angle (ψ_{DRIFT}) determined from the simulations:

Drift Angle (°)	**Average % Reduction in Braking Coefficient**		
	Dry Runway	Wet Runway	Flooded Runway
2	5.5	1.2	2.1
4	11	5.8	5.4
6	16.6	15.8	11.4
8	22.1	24.4	17.4

Table 10. Effect of drift angle on μ_B, from B737NG simulations performed by Boeing.

While bearing the caveats stated in Boeing's report in mind, the results shown in Table 10 reflect the expectation that μ_B decreases with increasing drift angle. For a wet runway, Table 10 indicates that μ_B can be reduced by about 24% at ψ_{DRIFT} = 8°. Assuming that the μ_B achieved during the accident landing roll was reduced as a result of cornering force demand on the tires, the results of Table 10 can be used to estimate the μ_B that the airplane *might* have achieved in the absence of the cornering demand. Let $\mu_{B,\psi}$ be the μ_B corresponding to a non-zero ψ_{DRIFT}; then

$$\mu_{B,\psi} = \mu_B k_\psi \quad [38]$$

Where k_ψ is a correction factor due to ψ_{DRIFT}. Using the 24.4% reduction in μ_B at ψ_{DRIFT} = 8° from Table 10, we can write (with ψ_{DRIFT} in degrees)

$$k_\psi = 1 - (0.0305)\psi_{DRIFT} \quad [39]$$

The μ_B at non-zero ψ_{DRIFT} can then be computed by dividing the achieved μ_B by k_ψ. The result of this calculation in shown in Figures 24 and 25 as the dashed black line labeled "Main gear μ_B/k_ψ." This correction increases the "achieved" μ_B between 130 and 120 knots to approximately the level of the AMC 25.1591 (flooded) μ_B model, but outside of this region the corrected μ_B remains well below all of the wet and flooded μ_B models.

The "sharing" of the available pavement friction between cornering and braking components is sometimes conceptualized as the "friction circle."[64] The available friction coefficient is visualized as a circle with radius μ_{max} centered on a Cartesian axis system where the x axis represents longitudinal friction (braking, and acceleration for cars), and the y axis represents cornering friction. The friction available for any combined cornering and braking event is limited to points within the circle, and for events that extract the maximum friction, to points on the circle. Hence, a pure braking event lies entirely on the x axis and the maximum braking friction available (μ_B, ignoring η_{AS}) is μ_{max}. A pure cornering event lies entirely on the y axis and the maximum cornering friction coefficient (μ_C) is μ_{max}. A combined braking and cornering event, that uses all the available friction, will lie on the circle with an x component of μ_B and a y component of μ_C, where

$$(\mu_B)^2 + (\mu_C)^2 = (\mu_{max})^2 \quad [40]$$

Hence, another way of estimating the μ_B that *might have been* available to N732MA in the absence of the cornering developed during the landing roll is to compute μ_C, and then the implied μ_{max} per Equation [40]. The resulting μ_{max} is the μ_B available when μ_C = 0.

μ_C can be computed using an approach similar to that described in Equations [19]-[23] for computing μ_B. The lateral load factor (n_y) is a measure of the sum of all the non-gravitational forces acting along the airplane's y body axis:

$$\sum F_y = Y + T_y + F_C + W_y = W n_y + W_y \quad [41]$$

Where:

Y = aerodynamic side force
$\sum F_y$ = sum of forces along body y-axis
T_y = component of thrust along body y-axis
F_C = cornering force from landing gear (component of gear forces along body y-axis)
W_y = component of airplane weight along body y-axis

[64] See, for example, https://www.autoweek.com/car-life/columns/a32034304/what-is-the-friction-circle/.

The cornering force F_C is given by

$$F_C = N_M \mu_{C,M} + N_N \mu_{C,N} = (N_M + N_N)\mu_{C,AP} \quad [42]$$

Where:

N_M = vertical reaction at main gear
N_N = vertical reaction at nose gear
$\mu_{C,M}$ = cornering friction coefficient at main gear
$\mu_{C,N}$ = cornering friction coefficient at nose gear
$\mu_{C,AP}$ = "total airplane" cornering friction coefficient

The aerodynamic side force Y is given by Equation [4]. Assuming T_y = 0 and combining Equations [4], [41], and [44] gives

$$\mu_{C,AP} = \frac{W n_y - C_Y \bar{q} S}{N_M + N_N} \quad [43]$$

The aerodynamic side force coefficient C_Y can be computed using Equation [4] if the sideslip angle β, rudder deflection δ_r, and the derivatives $\partial C_Y/\partial\beta$ and $\partial C_Y/\delta_r$ are known. On the runway, β can be assumed to be approximately equal to the drift angle ψ_{DRIFT} computed from the accelerometer integration and plotted in Figures 12 and 15. δ_r is recorded on the FDR, and the aerodynamic derivatives were computed from C_Y data provided by Boeing based on simulator tests. The vertical reaction forces N_M and N_N are available from the μ_B calculations described above.

Note that because the cornering friction coefficient of the nose gear ($\mu_{C,N}$) is unknown and cannot realistically be assumed (unlike the rolling friction μ_N of the nose gear), the cornering friction coefficient of the main gear alone ($\mu_{C,M}$) cannot be computed; instead, only a "total airplane" corning friction coefficient ($\mu_{C,AP}$) can be calculated. $\mu_{C,AP}$ is analogous to the "airplane braking friction coefficient" μ_{AP} described below.

Figure 31 shows the result of the $\mu_{C,AP}$ calculation, along with various terms that contribute to the calculation, as a function of distance from the runway 10 displaced threshold. The "$\mu_{B,AP}$" plotted in the bottom graph of Figure 32 is identical to the μ_{AP} described below and plotted in Figures 24 and 25 as "computed μ_{AP}." The "$\mu_{T,AP}$" plotted in the bottom graph of Figure 31 is the total available airplane friction coefficient computed from $\mu_{C,AP}$ and $\mu_{B,AP}$ using Equation [40]. Note that the resulting $\mu_{T,AP}$ matches the main gear μ_B/k_ψ, computed as described above very well, suggesting that the reduction in μ_B due to drift angle modeled in the Boeing simulator is representative of this case.

The TALPA RCAM and AC 25-32

As noted in SAFO 06012, following the Southwest Airlines accident at KMDW, the FAA initiated rulemaking that would require the practice recommended in the SAFO. In October 2007, FAA order 1110.149 established the "Takeoff/Landing Performance Assessment

Aviation Rulemaking Committee" (TALPA ARC). According to the order, the objectives and scope of the TALPA ARC were to

> … provide a forum for the U.S. aviation community to discuss the landing performance assessment methods provided in SAFO 06012. Additionally, takeoff performance for contaminated runway operations and issues relevant to part 139, Certification of Airports, will be discussed. These discussions will be focused on turbine powered aircraft including both turbojet and turboprop airplanes operated under parts 121, 135, 125, and 91 subpart K.

In addition, the TALPA ARC "will provide advice and recommendations to the Associate Administrator for Aviation Safety. The committee will act solely in an advisory capacity." Furthermore,

> the committee will discuss and present information, guidance, and recommendations that the members of the committee consider relevant to disposing of issues. Discussion will include, but is not limited to, the following:
>
> (1) Operational objectives, recommendations, and requirements.
> (2) Recommendations for rulemaking necessary to meet objectives.
> (3) Guidance material and the implementation process.
> (4) Global harmonization issues and recommendations.

The TALPA ARC presented landing performance recommendations to the FAA in April, 2009; these recommendations are presented in detail in Reference 20. Reference 20 also describes internal disagreements between TALPA ARC participants representing Part 91K, 125, and 135 operators on the one hand, and the FAA and most other TALPA ARC participants on the other, concerning the operational assumptions and safety margins to be used for landing distance assessments on contaminated runways.

As described in Reference 20, the regulatory changes proposed by the TALPA ARC would codify many of the provisions of SAFO 06012, and introduce a new "Runway Condition and Braking Action Reports" table that would provide a mapping between a six-level runway "code" and corresponding runway contaminant type and depth, Continuous Friction Measuring Equipment (CFME) measured friction coefficient values, airplane wheel braking coefficient values, and pilot braking action reports. The runway codes range from "6," for a dry runway, to "0," for runways contaminated with various forms of wet ice, and for which braking action is "minimal to non-existent." Aircraft manufacturers would have to supply data from which "operational" (i.e., unfactored) landing distances could be calculated for runway codes 6 through 1; operations would be prohibited on code "0" runways. The methods and assumptions to be used for generating this data would be specified in new regulations added to 14 CFR Part 25, "airworthiness standards: transport category airplanes." Specifically, the new rules would require that the braking coefficients on wet, ungrooved runways be computed per the method described in 14 CFR §25.109.

In addition, pilots would be required to perform an en-route landing distance assessment prior to landing. This assessment would "consider the runway surface condition, aircraft landing configuration, and meteorological conditions, using approved operational landing performance data in the Airplane Flight Manual supplemented as necessary with other data acceptable to the Administrator." A 15% safety margin would be added to the

computed operational landing distance to determine the runway length required for landing.

The FAA declined to pursue rulemaking to codify the TALPA ARC recommendations, deciding instead to encourage adoption of the practices recommended by the TALPA ARC through non-regulatory means (see Reference 20 for a detailed description of this evolution). These efforts culminated in the publication of AC 25-32, *Landing Performance Data for Time-of-Arrival Landing Performance Assessments*, in December 2015.[65] This AC provides guidance and standardized methods that data providers, such as type certificate (TC) holders, supplemental type certificate (STC) holders, applicants, and airplane operators can use when developing contaminated runway landing performance data for transport category airplanes. In addition, the AC includes a Runway Condition Assessment Matrix (RCAM) that is the outgrowth of the "Runway Condition and Braking Action Reports" table proposed by the TALPA ARC. The RCAM promotes the use of consistent terminology for runway surface conditions used among data providers and FAA personnel, and is presented here as Figure 32. The FAA officially started reporting runway conditions for Part 139 airports using the RCAM in October 2016.

Note that while AC 25-32 provides guidance for the development of airplane landing performance data on contaminated runways, it does not include any operational guidance as to how this data should be used for en-route landing distance assessments, or recommend that any specific safety factor be applied to the data (whereas the TALPA ARC specifically recommended *requiring* that a safety margin of 15% be added to landing distance assessments). Similarly, the 15% safety margin and en-route landing distance assessment practice is *recommended* by SAFO 19001, but is not *required*. The NTSB expressed concern regarding these points, and about the non-regulatory approach to the TALPA ARC recommendations in general, in comments submitted to the FAA during the AC 25-32 draft comment period (see Reference 20).

Several of the runway condition codes (RwyCCs) and corresponding μ_B models listed in Figure 32 are relevant to the N732MA accident, and are discussed below.

RwyCC 5: This RwyCC is associated with a pilot-reported braking action of "good," and includes a runway surface that is "wet (includes damp ⅛″ (3 mm) depth or less of water)." From a pilot's point of view, absent pilot braking action reports or other information to the contrary (such as a field condition report or, as a last resort, familiarity with the contents of SAFO 19003), the RwyCC 5 runway surface condition might describe KNIP runway 10 on the night of the accident, and all but one of the other wet runways involved in the overrun events discussed in Reference 20. This raises the question of how pilots can know that a wet runway is worse than RwyCC 5, when nobody else appears to know, and the approach recommended in SAFO 19003 (to assume "a RwyCC of '2' whenever there is the likelihood of moderate or greater rain on a smooth runway") is not part of the operator's Flight Operations Manual or other guidance.

[65] At the same time, the FAA published *Advisory Circular AC 25-31, Takeoff Performance Data for Operations on Contaminated Runways*, containing guidance for developing takeoff performance data on contaminated runways.

For a RwyCC 5 runway, Figure 32 indicates that the μ_B should be computed "per [the] method defined in §25.109(c)." As stated above and discussed in detail References 2 and 20, and acknowledged in SAFOs 19003 and 15009, the §25.109(c) μ_B model can significantly overestimate the μ_B available on some wet runways. In comments on the draft versions of ACs 25-31 and 25-32 (Reference 34), the NTSB expressed concern with the use of the §25.109(c) μ_B model for code 5 runways, given the evidence from multiple events that this model is insufficiently conservative:

> One technical problem that should be addressed within the ACs is their reliance, in part, on the wheel braking coefficient model codified in Section 25.109(c) for wet runway stopping performance calculations. However, the Section 25.109(c) model has never been validated by flight test data. To its credit, the FAA has recognized that the wheel braking coefficient model in Section 25.109(c) might be insufficiently conservative, as evidenced by the recent FAA Aviation Rulemaking Advisory Committee (ARAC) tasked to provide recommendations regarding new or updated standards for airplane performance and handling qualities. Under the subject area of Takeoff and Landing Performance, subtask (b) addresses wet runway stopping performance ….
>
> The NTSB encourages the FAA to perform flight tests on representative domestic and international runways that support turbine-powered airplane operations in order to validate the wet-ungrooved and wet-grooved wheel braking coefficient models in Section 25.109(c). …

The results of the ARAC task mentioned in these comments are the FTHWG wet runway regulatory proposals discussed in Section D-VI. In their response to the NTSB's comments, the FAA also noted that "FAA Flight Standards (AFS-200) has also addressed this topic to some degree in SAFO 15009, dated 8/11/15."

RwyCC 3: This RwyCC is associated with a pilot-reported braking action of "medium," and includes a "Slippery When Wet" (SWW) runway. The μ_B for this condition is modeled as a constant 0.16. A SWW runway is defined in Advisory Circular 150/5200-30D, *Airport Field Condition Assessments and Winter Operations Safety* (Reference 35):

> 1.12.19 Slippery When Wet Runway
> 1.12.19.1. For runways where a friction survey (conducted for pavement maintenance) indicates the averaged Mu value at 40 mph on the wet pavement surface failed to meet the minimum friction level classification specified in AC 150/5320-12, *Measurement, Construction, and Maintenance of Skid Resistant Airport Pavement Surfaces*, the airport operator must reports [sic] via the NOTAM system a RwyCC of '3' for the entire runway (by thirds: 3/3/3) when the runway is wet. The runway condition description "Slippery When Wet" is used for this condition. **Do not report a "Wet" runway when a "SLIPPERY WHEN WET" NOTAM is in effect.** When a "SLIPPERY WHEN WET" NOTAM is in effect, report the runway condition "Slippery When Wet" instead of "Wet" for the relevant thirds. If airport operator judgment deems a downgrade is necessary, the downgrade must be made such that all three runway thirds match (i.e. 3/3/3, 2/2/2, 1/1/1). An airport may discontinue the use of this NOTAM when the runway minimum friction level classification has been met or exceeded [emphasis in original].
>
> 1.12.19.2. Slippery When Wet is only reported when a pavement maintenance evaluation indicates the averaged Mu value on the wet pavement surface is below the Minimum Friction Level classification specified in Table 3-2 of AC 150/5320-12 [Figure 29]. Some contributing factors that can create this condition include rubber buildup, groove failures/wear, and pavement macro/micro textures.

A friction survey fails to meet "the minimum friction level classification specified in AC 150/5320-12" when, as specified in that AC, "the averaged Mu value on the wet pavement surface is below the Minimum Friction Level in [Figure 29] for a distance of 500 feet (152 m), and the adjacent 500 foot (152 m) segments are below the Maintenance Planning Friction Level." By this definition, Figure 28 indicates that KNIP runway 10/28 might have been classified SWW based on the CFME measurements taken after the accident. The measured μ at 40 mph, 10 ft. to the left of the centerline of runway 10 is below the MIN level between about 1,100 ft. and 2,000 ft. from the displaced threshold (a distance of 900 ft.), and below the MAINT level between about 1,000 ft. and 2,400 ft. (a distance of 1,400 ft., with occasional short sections above the MAINT level on the edges of the 1,400 ft. section). So, the μ is below the MIN level for the 500 ft. segment between 1,500 ft. and 2,000 ft., and (arguably) below the MAINT level for the 500 ft. segment preceding and the 400 ft. segment following that segment, coming very close to satisfying the SWW criteria. While the section of pavement where the μ is mostly below the MAINT level is about 100 ft. short of the length required to satisfy the SWW criteria, it is to be hoped that these μ measurements, if observed, would in fact result in a SWW classification, given how close they come to the SWW definition.

In any case, KNIP is a Naval Air Station and does not use the TALPA framework to report runway conditions, and so no NOTAM identifying runway 10 as SWW would have been required even if CFME measurements known to airfield operators clearly satisfied the SWW criteria. If the runway *had* been identified as SWW and assigned a RwyCC of 3 ("medium" braking action with a constant μ_B of 0.16), then the Miami Air OPT en-route landing distance calculation for flaps 30 (which includes a 15% safety margin) would have reported that the "predicted enroute field length exceeds landing distance available"), with a calculated operational landing distance of 8,457 ft. with zero wind. (The OPT calculations are described further below.) The corresponding OPT landing distance for flaps 40 is 7,942 ft., 64 ft. less than the 8,006 ft. runway length. Presumably, since the Miami Air dispatcher reported checking the landing distance with the OPT, he would have noted that the flight could only be dispatched under the planned conditions or airplane weight if flaps 40, and not flaps 30, were used for landing. Furthermore, a SWW designation would mean that the TALPA braking action was "Medium" (i.e., less than "Good"), and so the Miami Air FOM would have prohibited the flight crew from attempting the approach with *any* tailwind component (the FOM states that "no landing will be attempted with a tailwind when the braking action is reported as anything less than 'Good'").

As noted, KNIP does not use the TALPA framework for reporting runway conditions, even though CFME is used to monitor the pavement friction for maintenance purposes, and so did not identify runway 10 as SWW (or very close to SWW). In general, a practical operational difficulty in identifying SWW runways is determining whether a wet (but not flooded) runway corresponds to condition code 5 or 3, in the absence of a prior CFME test or a current pilot braking report. This difficulty was addressed in the NTSB comments on the draft versions of ACs 25-31 and 25-32 (Reference 34):

> Designating a runway as "Slippery When Wet" requires that it be tested using a calibrated Continuous Friction Measuring Equipment (CFME) device, and the resulting friction coefficient found to be below some threshold value. However, because the wet runway friction coefficients specified

> in Section 25.109(c) have never been validated by flight test, the association of these coefficients with airplane stopping performance capability on runways with CFME friction measurements above a target threshold is unproven. Furthermore, many international runways and smaller domestic runways that support turbojet operations will not have a friction maintenance program, and might therefore not get tested. The NTSB believes that untested runways should be designated as "Slippery When Wet" until and unless (1) the runways have been tested and shown to meet the minimum CFME friction coefficient threshold, and (2) the CFME measurements have been shown to correlate to a minimum wheel braking coefficient developed by airplanes on wet runways deemed to be adequately maintained. This procedure would result in more conservative estimates of airplane stopping distance required on runways with undocumented friction characteristics until a proper CFME friction survey could be conducted and the results could be reliably correlated to airplane stopping performance.

The FAA's response to these comments as follows:

> As to the inclusion of "Slippery when Wet," the FAA agrees with many of the NTSB's specific points. However, the TALPA ARC felt, and the FAA concurs, that it is better at a minimum to supply some guidance that has the potential of identifying a worse than nominal wet runway and, therefore, have operators take actions to mitigate the possible worse than expected wheel braking on a wet runway. We recognize the tools to do this are less than optimal and are optimistic the ARAC working group will be able to determine a better course of action for the future.

In May 2020, NTSB staff asked the FAA for some statistics regarding runways in the U.S.A. identified as "Slippery When Wet" per AC 150/5200-30D. The FAA noted that a runway that meets the SWW criteria won't be identified as SWW until a rain event at the airport triggers a Field Condition Notice to Airmen (FICON NOTAM), designating the runway SWW with a TALPA RwyCC of 3/3/3 (a RwyCC of 3 for each third of the runway). There is no database that identifies which runways *would be* identified as SWW via a FICON *if* a rain event were to occur. However, the FAA did provide a count of the number of runways identified as SWW by FICON NOTAMs during the 12-month period from July 9, 2019 to July 9, 2020. There were 573 SWW FICONs noted in the period, associated with 72 individual runways (many runways had multiple FICONs associated with them). These runways included both asphalt and concrete grooved runways at major Part 139 airports, as well as ungrooved runways at smaller airports. Hence, "slippery when wet" is not an extremely rare or uncommon runway condition.[66] However, it should be noted that the SWW FICONs issued for most runways appeared only a few times during the 12-month period, indicating that either these were the only times that it rained at those airports, or that at some point rubber removal or other maintenance was performed on the runways to address the SWW condition (thereby eliminating the need for a SWW FICON when it rained).

NTSB staff also asked the FAA about the number of airports in the U.S.A. that are known to perform pavement maintenance evaluations that gather the information required to determine whether or not a runway is SWW, as described in AC 150/5200-30D. The FAA responded that

[66] Per information provided by the FAA, 3,704 runways in the U.S.A. support turbine airplane traffic (1,037 of which correspond to 14 CFR Part 139 airports). 2,635 paved runways are over 5,000 ft. long, which is the length considered necessary to support turbojet traffic.

> This question cannot be obtained without individually inquiring with each airport in question. That being said, federally obligated airports are required to maintain their airports in a safe and serviceable condition in accordance with FAA grant assurances. 14 CFR Part 139 airports may have additional requirements and procedures outlined in their Airport Certification Manual or their snow and ice control plan that provides specificity to procedures to perform maintenance evaluations relative to slippery when wet. FAA advisory circulars also provide an acceptable means of compliance that many airports choose to follow.

The FAA also noted that KNIP is "a [Department of Defense] installation and it is our understanding they do not use the NOTAM term SWW."

It cannot be determined based on this information alone whether only 72 runways had SWW FICONS associated with them during the 12-month period described above because all the runways in the U.S.A. have been tested and only these 72 were found to meet the definition of SWW, or because many runways simply haven't been tested and their status is unknown. It also cannot be determined whether more SWW runways would be identified if all runways were tested.

RwyCC 2: This RwyCC is associated with a pilot-reported braking action of "medium to poor," and includes a flooded runway (i.e., greater than 1/8 inch (3 mm) of water), on which dynamic hydroplaning is possible. The μ_B for this condition is similar to the AMC 25.1591 flooded runway model given in Equation [37]. At speeds at and above 85% of the hydroplaning speed,[67] μ_B is constant at 0.05; and below 85% of the hydroplaning speed, μ_B is modeled as "50% of the wheel braking coefficient determined in accordance with §25.109(c), but no greater than 0.16." As can be seen in Figure 24, half of the §25.109(c) μ_B is close to the μ_B defined by Equation [37] in the AMC 25.1591 flooded runway model.

RwyCC 1: This RwyCC is associated with a pilot-reported braking action of "poor," and is associated with an ice-covered runway. μ_B is modeled as a constant 0.08. As shown in Figures 24 and 25, the actual μ_B achieved in the accident is below even this level for much of the landing roll.

RwyCC 0: This RwyCC is associated with a pilot-reported braking action of "nil," and is associated with wet ice, water on top of compacted snow, and dry or wet snow over ice. The μ_B for this RwyCC is not modeled because it is "not applicable. (No operations in Nil conditions.)" The data in Figures 24 and 25 indicate that the achieved μ_B during the landing roll best matches a RwyCC between 0 and 1.

Airplane braking friction coefficient (μ_{AP})

The airplane braking friction coefficient (μ_{AP}) is similar to the wheel braking friction coefficient (μ_B) in that it quantifies the runway friction force acting on the airplane's tires, but it differs in that it is a simpler calculation that it does not isolate the braking forces and corresponding friction on the braked main gear alone, but accounts for the total frictional

[67] 85% of the spin-down hydroplaning speed, defined in Equation [24a], is equivalent to the spin-up hydroplaning speed, defined in Equation [24b]. AC 25-32 defines the "hydroplaning speed" as the spin-down hydroplaning speed (Equation [24a]).

forces acting on the airplane, which result from both the braked main gear and the rolling nose gear:

$$\mu_{AP} = \frac{F_M+F_N}{N_M+N_N} = \frac{\mu_B N_M+\mu_N N_N}{N_M+N_N} \quad [44]$$

Whereas, from Equation [20],

$$\mu_B = \frac{F_M}{N_M} \quad [45]$$

Note that as μ_B approaches the rolling friction coefficient μ_N, $\mu_B \cong \mu_N$, $F_M \cong \mu_N N_M$ and

$$\mu_{AP} \cong \frac{\mu_N N_M+\mu_N N_N}{N_M+N_N} = \frac{\mu_N(N_M+N_N)}{N_M+N_N} = \mu_N \cong \mu_B \quad [46]$$

This result is reflected in Figures 24 and 25, which show very little difference between the "Computed main gear μ_B" and "Computed μ_{AP}" lines, and both relatively close to the value of 0.02 assumed for μ_N. Boeing performed an independent calculation of μ_{AP}, which is shown as the "Boeing μ_{AP}" line in Figures 24 and 25, and is in good agreement with the "Computed μ_{AP}" line (both indicating very poor friction achieved during the landing roll).

The results of research into runway friction (such as References 2, 3, 19, 20, 21, 22, 28, 29, and 31) is presented in terms of the wheel braking friction coefficient (μ_B), not the airplane braking friction coefficient (μ_{AP}). Likewise, 14 CFR 25.109 and AC 25-32 specify values of μ_B, not μ_{AP}, and so this *Study* analyzes the friction on the runway in terms of μ_B.

μ_B "requested" via brake application

The FDR recorded left and right brake pressure parameters, which measure the brake pressure commanded by the pilots' brake pedals upstream of the anti-skid system. The anti-skid system modulates the pressure actually delivered to the brake calipers, reducing it intermittently in order to prevent locking up the wheels and skidding the tires. The lower the μ_B, the lower the brake pressure at the calipers required to lock the wheels, and so in very poor friction conditions (such as in this case) the actual pressure delivered to the calipers might be far below the pressure commanded by the brake pedals. Determining the performance and efficiency of the anti-skid system in these conditions is an interesting problem, but beyond the scope of this *Study*. However, the NASA CFME model presumes that η_{AS} decreases with μ_B (see Equation [32a]), and additional evidence to this effect is presented below.

Although the anti-skid system likely reduces the pressure delivered to the brake calipers, the recorded brake pressures can be used to determine the braking level – effectively, the μ_B – "requested" by the pilots through the brake pedals. Where this "requested" μ_B exceeds the achieved μ_B, it is reasonable to conclude that the anti-skid system is reducing the pressure delivered to the brakes, and the airplane's braking is "friction limited" – that is, the anti-skid system is extracting as much braking performance from the runway as possible (η_{AS} being what it may), and any increase in pressure at the brakes would result in a skid, with a resultant further drop in μ_B and, possibly, directional control problems.

The requested μ_B is that value of μ_B that results in a frictional force at the tire that generates a torque about the wheel axle that exactly balances the torque the brakes are able to apply to the wheel with the commanded brake pressure. Boeing provided the NTSB with a table defining the applied brake torque as a function of brake pressure. With this information, for the left and right brakes we can write

$$T_L = f(p_L) = \mu_{reqL}\left(\frac{N_M}{4}\right) r_{TIRE} \quad [47a]$$

$$T_R = f(p_R) = \mu_{reqR}\left(\frac{N_M}{4}\right) r_{TIRE} \quad [47b]$$

Where:

T_L = Torque applied by the brakes on one of the two left wheels
T_R = Torque applied by the brakes on one of the two right wheels
$f(p_x)$ = Brake torque as a function of brake pressure p_x, per Boeing table; x indicates left (L) or right (R) brakes
μ_{reqx} = Requested μ_B by brake system x (L or R)
N_M = vertical reaction at main gear
r_{TIRE} = effective radius of main gear tires

Equation [47] is the torque about *one* wheel. The two left wheels are assumed to develop the same braking torque as a function of p_L, and the two right wheels are assumed to develop the same braking torque as a function of p_R. The vertical reaction force N_M is assumed to be distributed evenly across all four main gear tires. Solving Equation [47] for μ_{reqx},

$$\mu_{reqL} = \frac{4f(p_L)}{r_{TIRE}N_M} \quad [48a]$$

$$\mu_{reqR} = \frac{4f(p_R)}{r_{TIRE}N_M} \quad [48b]$$

The results of evaluating Equation [48] are shown in Figures 24 and 25 as the lines labeled "Left brake requested μ_B" and "Right brake requested μ_B." The "Brake torque limit μ_B" line in the Figures is the result of evaluating Equation [48] with the maximum brake pressure that can be commanded from the pedals (3,000 psi); this is the maximum μ_B that the brakes would be able to sustain. Any higher μ_B on the runway would overcome the brakes, increasing V_{WHEEL} and forcing the wheels to a lower slip ratio s (see Equation [17]).

Figures 24 and 25 indicate that μ_{reqL} is consistently above μ_{reqR} from the moment of brake application onwards (starting about 2,500 ft. from the displaced threshold), suggesting that the pilot intended to use differential braking to assist with directional control, or that he inadvertently applied more pressure to the left brake pedal than to the right brake pedal in the course of applying left rudder (see Figure 17b). In those parts of the Figures where both μ_{reqL} and μ_{reqR} are above the achieved μ_B, both the left and right tires are friction-limited, developing the same maximum possible braking force, and not providing any *differential* braking at all. Between 4,250 ft. and 4,550 ft. from the displaced threshold, the

right brakes were released while μ_{reqL} remained above the achieved μ_B. Between 5,500 ft. and 5,900 ft. from the threshold, both the left and right brakes were released briefly.

Anti-skid system efficiency dependence on μ_B

As noted above, in the NASA CFME μ_B model the anti-skid system efficiency η_{AS} decreases linearly with μ_{max}, and is at most 0.7, less than the 0.8 value assumed in the §25.109(c) model. AC 25-7C, *Flight Test Guide For Certification Of Transport Category Airplanes* (Reference 36) also indicates that the η_{AS} of "quasi-modulating" anti-skid systems may deteriorate on wet runways, if the anti-skid system has not been properly "tuned" for such a runway:

> The effectiveness of quasi-modulating systems can vary significantly depending on the slipperiness of the runway and the design of the particular control system. On dry runways, these systems typically perform very well; however, on wet runways their performance is highly dependent on the design and tuning of the particular system.

Reference 37 indicates that η_{AS} might also deteriorate with decreasing μ_{max} even for "fully-modulating" anti-skid systems, such as that on the Boeing 737-200 ADV.[68] In analyzing the results of several wet-runway landing tests conducted at Roswell, NM, in 1973 with a Lockheed L-1011 airplane and a Boeing 737-200 ADV airplane (originally documented in Reference 38), Reference 37 concludes that the B737 landing data "indicate that the η_{AS} of even fully-modulating systems decreases as the runway becomes more slippery."

The authors of Reference 38 arrived at a similar conclusion by examining the relationships between the μ measured by ground vehicles and the stopping performance of various aircraft during flight tests (including the L-1011 and 737 tested at Roswell):

> The theoretical aircraft braking efficiency, η, lines … are related to a μ_{max} value for a low friction wet surface and have been obtained from a current NASA/FAA digital computer simulation study. This comparison indicates a considerable reduction in braking efficiency of the aircraft as the wet runway surface exhibits lower friction values. This trend is confirmed by the data previously shown in [the Roswell B737-200 ADV μ_B data] wherein the aircraft effective braking friction coefficient was shown to be closer to the level of μ_{skid} than to μ_{max} [Reference 38].

The development of the §25.109(c) μ_B model is described in Reference 37, which explains that the method is based on wet runway friction data from the Engineering Sciences Data Unit (ESDU), NASA, and the aerospace industry. In particular, ESDU 71026 (Reference 29) contains extensive information about the maximum μ (μ_{max}), as a function of ground speed, obtainable on wet and dry runways of various textures, with different tire tread depths and at various tire inflation pressures. The polynomials in §25.109(c) from which Equation [30] is derived are based on information presented in ESDU 71026.

ESDU 71026 also addresses anti-skid system efficiency, and includes the chart duplicated here as Figure 33, which shows the range of η_{AS} values for "on-off" and "adaptive" type anti-skid systems. The chart indicates that, for values of μ_{max} from 0.25 – 0.30, "adaptive"

[68] Per an email from Boeing to NTSB dated 12/08/2010, the B737-200 ADV is equipped with a Hydro-Aire Mark III anti-skid braking system, which is an analog, fully modulating system.

systems have a “maximum likely value” of η_{AS} from 0.80 – 0.85, comparable to the η_{AS} specified by §25.109(c).[69] However, these maximum values do “not allow for installation and undercarriage suspension effects.” In discussing this chart, ESDU 71026 states that

> *Values of* μ_{eff} [equivalent to μ_B in this *Study*] *and* μ_{max} obtained or deduced from tests with a ground vehicle and aircraft are shown as the shaded areas in Figure [33]. The scatter indicated by these shaded areas reflects differences between types of brake system and also the differences resulting from the application of these systems to particular undercarriage and test vehicle configurations.
>
> *The efficiencies that may be expected* from current automatic braking systems are represented in Figure [33] by the curves labelled, "adaptive system" and "on-off system". These curves are derived principally from dynamometer tests and do not include any measure of the effects introduced when a brake system is incorporated as part of an aircraft undercarriage …. Where no further information is available, these curves should be used to estimate μ_{eff} once μ_{max} has been determined …. [emphasis in original].

ESDU 71026 goes on to include an equation for the effective braking force that is equivalent to modeling η_{AS} as follows:

$$\eta_{AS} = (k)\left(\eta_{AS,Fig.33}\right) \qquad [49]$$

Where $\eta_{AS,Fig.33}$ is the η_{AS} determined from Figure 33, and

> The factor k is included in Equation [49] to allow for possible reductions in braking efficiency due to, for example, normal load fluctuations, undercarriage vibration and suspension effects - none of which are usually simulated in dynamometer tests. Experience and the data presented as shaded areas in Figure [33], suggest that until values of η_{AS} based on aircraft trials are available, k should be assumed to lie in the range $0.8 \leq k < 1.0$ …. Where more precise information is available, either from aircraft braking trials or from brake manufacturers' tests, it should be used.

In allowing an η_{AS} of 0.80 for “fully-modulating” anti-skid systems, §25.109(c) effectively assumes that ***both*** terms in Equation [49] ($\eta_{AS,Fig.33}$ and k) will achieve the maximum values contemplated in ESDU 71026, implying that these systems will always operate at the “maximum likely value” level shown in Figure 33, and that there will be no reduction in efficiency due to “normal load fluctuations, undercarriage vibration and suspension effects.” However, Figure 33 indicates that when these effects are taken into account, the resulting η_{AS} can be as low as 0.50 at μ_{max} = 0.3. If the lower bound of k given in ESDU 71026 (0.8) is applied to the §25.109(c) η_{AS} of 0.80, the overall η_{AS} is $(0.8)^2 = 0.64$, close to the η_{AS} = 0.63 value that makes the §25.109(c) μ_B match the actual μ_B achieved during the accident discussed in Reference 37. This is evidence cited in References 2 and 20 that the η_{AS} = 0.80 value allowed by §25.109(c) might be unreasonably high.

On the other hand, ESDU 71026 notes that “where more precise information is available, either from aircraft braking trials or from brake manufacturers' tests, it should be used.” It is likely that over the long history of the B737, many flight tests have validated a value of η_{AS} = 0.8 (or higher) on wet runways. However, it is not clear that these tests account for

---

[69] On the basis of this observation, the “adaptive” systems referred to in ESDU 71026 can be considered equivalent to the “fully modulating” systems referred to in §25.109(c).

the possible range of μ_{max}, and consequent sensitivity of η_{AS} to μ_{max}, over different runways with different macrotextures, microtextures, and water depths, or for the presence of drift, or variations in piloting technique, such as the differential braking and on/off braking inputs seen in this accident. The results of Reference 38 included data from a B737 airplane, and Boeing's report regarding the effect of drift angle on μ_B states that "there is no flight test data for braking with an airplane in a drift condition." Evaluating the effects of μ_{max} and the other factors just cited on the η_{AS} of an operative anti-skid system is beyond the scope of this *Study*; however, this subject is deserving of further research, since a proper μ_B model must account for both μ_{max} *and* η_{AS} correctly. An observed shortfall in μ_B, improperly attributed to a decrease in μ_{max} rather than in η_{AS}, can contribute to a confused understanding of the behavior of μ_{max}, and to an unwarranted confidence in the invariability of η_{AS}.

ESDU 05011 μ_{max} & implied accident η_{AS}

In February 2013, ESDU issued item 10015, titled *Model for performance of a single aircraft tyre rolling or braking on dry and precipitate contaminated runways* (Reference 39). Whereas ESDU 71026 (Reference 29) presents a semi-empirical method for determining μ_{max}, based on curves of μ_{max} vs. ground speed for different tire pressures and runway macrotexture (roughness) "classes," ESDU 10015 presents a completely mathematical method for computing μ_B as a function of the slip ratio s (see Equation [17] for the definition of s). The equations required to compute μ_B on contaminated runways as a function of s, contaminant depth, macrotexture depth, and various tire parameters per the model described in ESDU 10015 are summarized in ESDU item 05011, titled *Aircraft tyre rolling or braking on dry or precipitate contaminated runways: Summary of the model* (Reference 28). ESDU items 05011 and 10015 are published through IHS Markit (see https://ihsmarkit.com/index.html). IHS Markit provided the NTSB with draft copies of recent revisions to ESDU 10015 and 05011; the calculations presented below are based on these draft documents.

Figure 34 presents the μ_{max} computed per the method of ESDU 05011 as a function of ground speed for water depths of 1, 2, and 3 mm on a runway with a macrotexture depth of 0.60 mm (0.0236"), corresponding to the asphalt portion of KNIP runway 10. μ_{max} was determined from the peaks of the μ_B vs. s curves generated by the ESDU 05011 model at each ground speed (see Figure 35). (Here, μ_{max} is identical to $\mu_{B,MAX}$ in Figure 20.)

The efficiency of the anti-skid system measures how closely the system maintains the slip ratio s near the value $s_{\mu,MAX}$ required to obtain μ_{max}. As seen in Figure 35, $s_{\mu,MAX}$ varies with ground speed and water depth, and so the anti-skid system needs to adjust the brake pressure to match $s_{\mu,MAX}$ as conditions change. The actual s will generally vary to the left or the right of $s_{\mu,MAX}$, resulting in an achieved μ_B that is less than μ_{max}, and a loss in efficiency.

The red line labeled "0.6 x Boeing flooded μ_B (N732MA match)" in Figure 34 is the same μ_B plotted in Figures 24-26 that approximately matches the μ_B achieved in the accident, as discussed above. Assuming that the ESDU 05011 μ_{max} values plotted in Figure 34

reflect the true μ_{max} available on the runway, these μ_{max} values and the "N732MA match" μ_B can be used to compute the anti-skid efficiency achieved in the accident:

$$\eta_{AS} = \frac{(N732MA\ match\ \mu_B)}{ESDU\ 05011\ \mu_{max}} \quad [50]$$

Since the ESDU 05011 μ_{max} decreases with increasing water depth, the η_{AS} computed per Equation [50] increases with increasing water depth. At a water depth of 2 mm, Figure 34 shows η_{AS} varying between about 0.29 and 0.38 for μ_{max} values varying between about 0.12 and 0.29, consistent with the η_{AS} behavior depicted in Figure 33.

N732MA braking performance during previous landing at MUGM

The very poor μ_B achieved during the accident landing (even compared to the most pessimistic flooded runway models) raises the possibility of a problem or failure in the brake system itself. The dependence of η_{AS} on μ_B, discussed above, is a separate question, concerning the response of a healthy, functioning system, per its design, to a combination of very low μ_B conditions and complex brake application (differential braking, on/off braking). This sub-section is concerned with a mechanical failure that precludes normal brake function.

The NTSB Systems Group examined N732MA's brake system, and their findings are documented in the System Group Factual Report (Reference 23). The NTSB Systems Group Chairman asked the NTSB Aircraft Performance Specialist to examine N732MA's previous landing at MUGM for evidence of any non-normal or unexpected braking performance. In response to this request, Figure 36 plots the left and right "requested" μ_B (computed per Equation [48]) compared to the achieved μ_B during the MUGM landing (computed per Equations [19]-[23]). The MUGM runway was dry during the previous landing, so the wet-runway μ_B models described above are not relevant for this landing.

Figure 36 indicates differential braking during the MUGM landing, consistent with an effort to compensate for the yawing moment from the MEL'd left thrust reverser. The total requested μ_B, computed as the average of the μ_B requested by the left and right brakes, matches the achieved μ_B very well until about 60 knots; below this speed, the achieved μ_B is actually *higher* than the computed requested μ_B, and matches the μ_B requested by the left brakes alone below 50 knots. The reason for this is unknown, but it is possible that the torque applied by the brakes on the wheels depends not only on the brake pressure (as modeled), but also on ground speed; if the torque for a given brake pressure increases at lower ground speeds, that could explain the high μ_B achieved at these lower speeds. In comments on a draft version of this *Study*, Boeing noted that

> Boeing simulator models do show that braking torque can increase at low speeds, although our data suggest that the amount of increase is somewhat stochastic, and heavily dependent on factors like brake condition, energy absorption rates, and other factors.
>
> The Boeing simulator document models this as a factor that ramps linearly from 1.0 at 20 kt. to 1.2 at 0 kt.

In any case, Figure 36 indicates that the brakes were performing as expected during the previous MUGM landing.

μ_B achieved on wet KNIP runway 10 by N733MA during a landing on 12/20/2019

On December 23, 2019, Miami Air forwarded to the NTSB an email that one of their pilots had sent to the company expressing concern over the amount of water he observed on KNIP runway 10 following a landing on December 20. The email stated:

> I landed NIP at 22:18Z and weather was 2 miles Light rain and Mist. The weather at the start of decent was 10 miles and VFR. I asked ground handler if a cell passed over airport prior to our arrival and he said no just a light rain and mist. The left side of this runway is holding water and this is a trap for a pilot landing at night who can't see runway conditions. The water was worse on approach end of 10 but I couldn't stop and get my camera out. I stopped on runway and quickly snapped a picture and turned off immediately. I will file a safety report tomorrow.

The pictures included with the email are shown here in Figure 37, and indicate that the runway is indeed wet, though the rainfall rates recorded at the time of the landing are minimal (0.01" of rain over the hour from 21:53 UTC to 22:53 UTC). A SPECI weather observation at 22:19 (the time of the landing) stated:

Wind 030° at 13 knots, visibility 4 statute miles, light rain, mist, scattered clouds at 1,300 ft., broken clouds at 3,000 ft., overcast ceiling at 5,500 ft., temperature 14° C, dew point 12° C, altimeter setting 30.36" Hg.

The requested and achieved μ_B for this landing, computed using Quick Access Recorder (QAR) data provided by Miami Air, are shown in Figure 38, and as in the MUGM landing, show good agreement with each other. Consequently, even though the runway was wet, the braking was not friction-limited; the airplane was achieving the μ_B level requested by the brake pressures. Note that the airplane for this December 20 landing (N733MA) had two operational thrust reversers, and so the braking is symmetrical until near the end of the calculation at QAR time 195,539 sec., where the ground speed had decreased to 50 kt. As seen in the MUGM landing, at low speeds the achieved μ_B actually exceeds the requested μ_B (again, possibly because the torque applied by the brakes at low speeds is higher than is modeled using only brake pressure).

Between QAR time 195,523 and 195,533 sec., the requested and achieved μ_B are about 0.15, much higher than the μ_B achieved during the accident landing. The μ_B corresponding to the §25.109(c) and NASA CFME models are also shown, and indicate that the requested μ_B was always below the §25.109(c) level, and below the NASA CFME level from QAR time 195,526 sec. onwards (briefly matching that level at 195,540 sec.) Prior to QAR time 195,526 sec., the achieved μ_B was higher than the NASA CFME level, which decreases to about 0.05; this decrease corresponds with the low μ region between 1,000 ft. and 2,000 ft. from the displaced threshold shown in Figure 28. It is possible (even likely) that the low-friction region on runway 10 was addressed following the N732MA accident, and so a better NASA CMFE μ_B calculation for the December 20 landing could be obtained using CFME measurements taken closer to that date. The NTSB requested updated

CFME data for runway 10/28 from the KNIP airfield manager and the Naval Safety Center to support this calculation, but received no response.

In any case, the μ_B achieved during the December 20 landing indicates that when wet KNIP runway 10/28 is capable of supporting higher μ_B values than those achieved during the accident. This suggests that the very low accident μ_B is likely the result of the heavy rainfall at the time, which produced water depths on the runway close to or exceeding the "flooded" criteria on portions of the runway. As noted above, the efficiency of the anti-skid system under the combination of these runway conditions and the braking technique used might also have reduced the μ_B achieved during the accident.

Boeing 737-800 FCOM & Miami Air OPT landing distances for the accident conditions

Perhaps the most relevant μ_B models, from an operational point of view, are those underlying the wet-runway stopping distances in the B737-800 Flight Crew Operating Manual (FCOM) and the On-board Performance Tool (OPT) iPad application. These sources contain performance data that operators can use to ensure compliance with dispatch requirements and to perform en-route landing distance assessments.

In response to an inquiry from the NTSB, Boeing described[70] some of the differences between the FCOM and OPT, and the landing distances each presents, as follows:

> For the 737NG, a software called Airplane Flight Manual - Digital Performance Information (AFM-DPI) replaces the airplane performance charts in section four (4) of the airplane flight manual as the sole source of AFM certified performance. OPT uses the operational performance databases for takeoff and landing which are created from the "AFM-DPI" databases. AFM-DPI and OPT use the same calculation engine, Boeing Takeoff Module (BTM) & Boeing Landing Module (BLM), to perform the takeoff and landing calculations.
>
> In OPT, the calculation is a first principle 'point' calculation, taking into account all of the variables including their interactions. For example, if there is runway slope the calculation takes into account the runway slope for the given weight, temperature, wind, etc. being used in the calculation. First principles means the fundamental equations of motion and the parameters defining the airplane (thrust, lift, drag, etc.) are used to calculate the performance directly, yielding a more exact solution. Advanced mathematical optimization techniques are used in order to maximize the performance available. In addition, the user can customize the calculation for calculating the operational landing distance via the OPT Administrator tool. For example, the operator can choose to apply a factor to the final operational landing distance calculation i.e. 15%, or/and change the flare distance used by fixing the flare value (i.e. 1,500 ft.)
>
> The reason why the normal and non-normal landing distances calculated using OPT might not match the distances obtained from the tables in the QRH [Quick-Reference Handbook] is because the FCOM-QRH normal landing distance data is based off a reference weight, maximum manual braking with no adjustments, and does not take credit for thrust reversers. The FCOM-QRH adjustments are then run independent from each other, and are based on varying a single parameter such as weight or wind, and observing the change in runway required relative to the reference conditions. As such, when multiple adjustments are made, there is usually a difference between the FCOM/QRH results and the OPT/BLM results.

[70] In an email to the NTSB Aircraft Performance specialist dated June 10, 2020.

The OPT/BLM results would be considered more representative of the combined effects of multiple parameters being changed relative to the reference conditions than would the FCOM/QRH results.

The FCOM and OPT advisory data for landing distances corresponding to different runway conditions and braking action reports also differ in the μ_B and other parameters assumed in the underlying calculations. The landing distance for a given airplane weight and approach speed depends not only on the achieved μ_B, but also on the air distance (from 50 ft. above the runway threshold to touchdown) and the time required to engage the deceleration devices (wheel brakes, speedbrakes, and reverse thrust). The FCOM and OPT assume the same values for these parameters, except for the air distance; the FCOM uses a fixed air distance of 1,000 ft., but the air distance in the OPT "uses the database calculation (based on a fixed time [4.3 seconds from the threshold to touchdown] that matches the AFM)."[71] The OPT also includes an optional safety factor.

Table 11 shows the values of various parameters used in the FCOM and OPT calculations.

Item (times are from touchdown)	FCOM	Miami Air OPT
Touchdown distance from threshold	1,000 ft.	Time-based (4.3 sec. from threshold to touchdown)
Speed reduction from approach speed to touchdown speed	$V_{touchdown}$ = (0.9902)$V_{approach}$	$V_{touchdown}$ = (0.9902)$V_{approach}$
Time to wheel brake application (autobrakes)	0 sec.	0 sec.
Time to wheel brake application (manual wheel brakes and auto speedbrakes)	1 sec.	1 sec.
Time to wheel brake application (manual wheel brakes and manual speedbrakes)	2 sec.	2 sec.
Time to speedbrake deployment (auto speedbrakes)	1 sec.	1 sec.
Time to speedbrake deployment (manual speedbrakes)	2 sec.	2 sec.
Time to reverse thrust selected	2 sec.	2 sec.
Time to full reverse thrust deployment	4 sec.	4 sec.
Reverse thrust detent used (normal landing)	Detent 2	Detent 2
Reverse thrust reduced / removed	Starting @ 60 kt., decrease to reverse idle by 30 kt.	Starting @ 60 kt., decrease to reverse idle by 30 kt.
Safety factor applied	None	15% (Miami Air option)

Table 11. Assumptions used in the calculation of FCOM and OPT landing distances.

The FCOM predates the TALPA ARC and AC 25-32, and so the different runway conditions it considers are not described in terms of the TALPA RwyCCs listed in Figure 32, but in terms of "reported braking action." Constant μ_{AP} values are assumed for each

[71] Per Boeing's June 10 email. The email also noted that the operator can change the assumed air distance to a fixed value, but that the default method uses the time-based database calculation. Examination of the outputs of the Miami Air OPT indicate that it uses the default method.

braking action: 0.4 for “dry,” 0.2 for “good,” 0.1 for “medium,” and 0.05 for “poor.” [72] The results of an NTSB simulation of a landing roll for the accident conditions with a constant 0.2 μ_{AP} is shown in Figure 26 as the blue line labeled “Boeing FCOM ‘good’ μ_{AP}.” The FCOM landing distances for different combinations of touchdown conditions, reverse thrust, and runway braking action reports are shown in Table 12.

The runway condition options presented in the Miami Air OPT appear to include those corresponding to the braking action reports in the FCOM, *and* those corresponding to the TALPA RwyCCs listed in Figure 32. The runway condition options in the OPT are:

DRY (6), WET (5), STANDING WATER, SLUSH, COMPACT SNOW, DRY SNOW, GOOD (5), GOOD-MEDIUM (4), MEDIUM (3), MEDIUM – POOR (2), POOR (1).

(See Figure 39.) However, the Miami Air FOM indicates that pilots are not to use several of these options. The section of the FOM titled “Takeoff and Landing Performance Assessment (TALPA)” describes the RCAM RwyCCs, and states in a sub-section titled “Matrix RCC and Pilot Braking Action Equivalent” that:

> Upon receiving a [Runway Condition Code (RCC)] report, Miami Air pilots will “translate” the report into an equivalent braking action (e.g. good, good to medium, medium, medium to poor, poor or nil) for the OPT calculation.
>
> **NOTE: If the PIREP braking action category is “Good to Medium” use the “Medium” for OPT computations. If the PIREP braking action category is “Medium to Poor,” use “Poor” for OPT computations.**
>
> **NOTE: If the RCC report includes multiple codes, use the most restrictive. For a RCC report of 5, 5, 3, a pilot should use “3” for OPT computations.**
>
> **NOTE: Pilots should use “Dry,” “Wet,” “Slippery Good,” “Slippery Medium” or “Slippery Poor” for OPT computations. Do not use “Standing Water,” “Slush,” “Compact Snow” or “Dry Snow.”**
>
> **NOTE: Use the RCC that is applicable to the runway length being used. For example, assume an aircraft is landing on a very long runway (e.g. 12,000 feet), the aircraft is light weight and the aircraft will be stopped well before the last 1/3 of the runway. Assume also the RCC is 5, 5, 3. It would not be necessary to compute the landing distance based on the RCC of 3. Only the first 2/3rd of the runway would be used and therefore, only an RCC of 5 should be used for OPT computations.**
>
> [emphasis in original]

The FOM also states that “no landing will be attempted with a tailwind when the braking action is reported as anything less than ‘Good.’”

Per the FOM, the only relevant runway condition options in the OPT are “Dry,” “Wet,” “Slippery Good,” “Slippery Medium” or “Slippery Poor.” Confusingly, however, the actual

[72] The dry runway μ_B is actually a Boeing proprietary model based on flight test data; the same data is used to build both the OPT calculator and the FCOM tables. For a typical 737-800 landing, the dry runway μ_{AP} is approximately 0.40. The non-dry braking action μ_{AP} values are in fact modeled as the constants indicated.

options that appear in the OPT (listed above) do not include the word “slippery.” It appears that “Slippery Good” in the FOM refers to “GOOD (5)” in the OPT, and that “Slippery Medium” and “Slippery Poor” refer to “MEDIUM (3)” and “POOR (1),” respectively.

The Miami Air FOM also notes that

> Military bases report braking action as Runway Condition Reading or RCR values according to the following table:
>
> | | *… Runway Condition Reading (RCR)* |
> |---|---|
> | 02-05 | Nil |
> | Poor | Poor |
> | Fair | Fair |
> | Good | Good |

However, the FOM does not indicate which OPT runway condition options should be associated with each of these military Runway Condition Readings. In any case, during the accident flight, the flight crew did not receive a Runway Condition Reading from ATC.

In response to NTSB inquiries, Boeing indicated that the μ_B underlying the OPT “WET (5)” option is the §25.109(c) model (consistent with TALPA RwyCC 5 as shown in Figure 32), and that the μ_B underlying the OPT “GOOD (5)” option is a constant value of 0.2 (consistent with the FCOM “good braking action” level shown in Figure 37). Presumably, the μ_B underlying the “MEDIUM (3)” and “POOR (1)” OPT options are constant values of 0.1 and 0.05, respectively, corresponding to the FCOM “medium” and “poor” braking action levels.

As noted in Table 11, the Miami Air OPT adds a 15% safety factor to the landing distances computed by the BLM, whereas the FCOM distances shown in Figure 37 do not include any safety factor. FCOM and OPT landing distances for various conditions are compared in Table 12; the OPT distances shown in this table include a column of the distances output by the OPT divided by 1.15, to represent unfactored distances comparable to the FCOM distances.

The invariant conditions for the landing distances presented in Table 12 are as follows:

- Airport elevation 22 ft. MSL
- Runway slope -0.165% (downhill)
- Temperature 24° C
- Airplane gross weight = 143,200 lb. (64,954 kg.)
- Flaps 30 (accident configuration, Table 12a); flaps 40 (Table 12b)
- V_{REF30} = 148 KCAS (approach speed varies in Table 12a)
- V_{REF40} = 140 KCAS (approach speed varies in Table 12b)
- Nominal air distance (1,000 ft. for FCOM, time-based for OPT)
- Maximum manual braking
- Auto speedbrakes

FLAPS 30 / V_{REF30} = 148 kt. (accident configuration)							
Approach speed (KCAS)	**Tailwind (knots)**	**Number of thrust reversers**	**FCOM braking action**	**FCOM landing distance (feet)**	**OPT runway condition**	**OPT landing distance (feet)**	**OPT landing distance/1.15 (feet)**
153	10	1	Good	5537	WET (5) GOOD (5)	7227 7206	6284 6266
168	10	1	Good	6017	WET (5) GOOD (5)	8350 8122	7261 7063
153	0	1	Medium	6981	MEDIUM (3)	8457	7354
168	0	1	Medium	7611	MEDIUM (3)	9545	8300
153	0	1	Poor	9630	POOR (1)	11420	9930
168	0	1	Poor	10380	POOR (1)	12641	10992
153	10	2	Good	5307	WET (5) GOOD (5)	6807 6834	5919 5943
168	10	2	Good	5787	WET (5) GOOD (5)	7826 7690	6805 6687
153	0	2	Medium	6361	MEDIUM (3)	7670	6670
168	0	2	Medium	6991	MEDIUM (3)	8654	7525
153	0	2	Poor	8320	POOR (1)	9773	8498
168	0	2	Poor	9070	POOR (1)	10851	9436
153	10	0	Good	5817	WET (5) GOOD (5)	7767 7667	6754 6667
168	10	0	Good	6297	WET (5) GOOD (5)	9029 8658	7851 7529
153	0	0	Medium	7841	MEDIUM (3)	9564	8317
168	0	0	Medium	8471	MEDIUM (3)	10795	9387
153	0	0	Poor	11750	POOR (1)	14151	12305
168	0	0	Poor	12500	POOR (1)	15571	13540

Table 12a. Comparison of FCOM and OPT Flaps 30 landing distances for different combinations of approach speed, tailwind, thrust reversers, and runway conditions. Red highlights indicate non-factored distances longer than the runway length. Yellow highlights indicate OPT distances including a 15% safety factor that are longer than the runway length. KNIP runway 10 available landing length = 8,006 ft. The landing distances shown include the air distance from 50 ft. above the runway threshold to touchdown.

FLAPS 40 / V_{REF40} = 140 kt.							
Approach speed (KCAS)	**Tailwind (knots)**	**Number of thrust reversers**	**FCOM braking action**	**FCOM landing distance (feet)**	**OPT runway condition**	**OPT landing distance (feet)**	**OPT landing distance/1.15 (feet)**
145	10	1	Good	5318	WET (5) GOOD (5)	6743 6841	5863 5941
160	10	1	Good	5828	WET (5) GOOD (5)	7859 7779	6834 6764
145	0	1	Medium	6620	MEDIUM (3)	7942	6906
160	0	1	Medium	7250	MEDIUM (3)	9038	7859
145	0	1	Poor	9078	POOR (1)	10729	9330
160	0	1	Poor	9828	POOR (1)	11911	10357
145	10	2	Good	5108	WET (5) GOOD (5)	6378 6500	5546 5652
160	10	2	Good	5618	WET (5) GOOD (5)	7396 7396	6431 6431
145	0	2	Medium	6060	MEDIUM (3)	7232	6289
160	0	2	Medium	6690	MEDIUM (3)	8226	7153
145	0	2	Poor	7898	POOR (1)	9773	8498
160	0	2	Poor	8648	POOR (1)	10289	8947
145	10	0	Good	5568	WET (5) GOOD (5)	7204 7260	6264 6313
160	10	0	Good	6078	WET (5) GOOD (5)	8450 8274	7348 7195
145	0	0	Medium	7380	MEDIUM (3)	8927	7763
160	0	0	Medium	8010	MEDIUM (3)	10161	8836
145	0	0	Poor	10948	POOR (1)	13144	11430
160	0	0	Poor	11698	POOR (1)	14504	12612

Table 12b. Comparison of FCOM and OPT Flaps 40 landing distances for different combinations of approach speed, tailwind, thrust reversers, and runway conditions. Red highlights indicate non-factored distances longer than the runway length. Yellow highlights indicate OPT distances including a 15% safety factor that are longer than the runway length. KNIP runway 10 available landing length = 8,006 ft. The landing distances shown include the air distance from 50 ft. above the runway threshold to touchdown.

Table 12a indicates that with one thrust reverser, and good braking action (FCOM) or WET (5) or GOOD (5) runway conditions (OPT), and a 10 knot tailwind, the airplane could stop on the runway, even at an approach speed of 168 kt. (equal to V_{REF30} + 20, the speed flown in the accident), and an air distance up to about 700 ft. longer than nominal.

Table 12 does not include data with a tailwind for braking actions / runway conditions worse than “good” because the Miami Air FOM prohibits landing in these conditions. At flaps 30, with one thrust reverser, zero tailwind, and medium braking action, the FCOM indicates that the airplane could have stopped on the runway even at the high approach speed if it had touched down at the nominal 1,000 ft. from the displaced threshold; however, with the 580 ft. longer touchdown achieved in the accident, it would not have stopped on the runway. The OPT indicates that with a MEDIUM (3) runway condition, the

airplane could have stopped on the runway if it had maintained the nominal flaps 30 approach speed (153 KCAS), but not with the higher approach speed. Even for the nominal speed, however, the OPT indicates that the required 15% safety margin would not have been available with flaps 30, and so the landing attempt would have been prohibited by the FOM. At the nominal flaps 40 approach speed of 145 KCAS, the OPT indicates that the airplane could have landed with a 15% safety margin, and the approach would have been allowed.

At flaps 30, with either one or two thrust reversers, zero tailwind, and poor braking action or runway conditions, both the FCOM and OPT indicate that the airplane could not have stopped on the runway, even with the nominal approach speed and air distance. At flaps 40, with the nominal approach speed and air distance, and two reversers operating, the FCOM data indicates the airplane could have stopped in poor braking action conditions with only 108 ft. remaining. However, the OPT data indicates the airplane would overrun the runway by 492 ft. in these conditions.

The data in Table 12 support the findings drawn from Figure 26 and discussed above: the poor μ_B achieved on the runway can be considered a greater contributor to the runway overrun than the deviations from the nominal approach speed, touchdown point, and nominal spoiler deployment time.

Additional observations concerning the data in Table 12 are as follows:

- The FCOM distances indicate that the benefit of thrust reversers becomes more pronounced as the runway friction deteriorates. However, in this case the airplane could not have stopped on the runway in poor braking action conditions even if the left engine thrust reverser had also been operational.

- The OPT landing distances corresponding to “WET (5)” and “GOOD (5)” runway conditions are both longer than those corresponding to the FCOM “good” braking action.

- The OPT landing distances corresponding to the “WET (5)” runway condition are generally longer than those corresponding to the “GOOD (5)” runway condition, and the difference is greater at higher speeds. At the nominal flaps 40 approach speed, the “WET (5)” distances are shorter than the “GOOD (5)” distances.

- Part of the reason the OPT landing distances are longer than the FCOM landing distances for similar conditions is that the air distance used by the OPT is time-based and hence depends on the ground speed, whereas the FCOM air distance is fixed at 1,000 ft. Table 13 presents the air distances computed by the OPT for different combinations of approach speed and tailwind.

FLAPS 30 / V_{REF30} = 148 kt. (accident configuration)		
Approach speed, KCAS	**Tailwind, knots**	**Air distance computed by OPT, feet**
153	10	1290
168	10	1405
153	0	1180
168	0	1296

Table 13a. Flaps 30 air distances computed by OPT.

FLAPS 40 / V_{REF40} = 140 kt.		
Approach speed, KCAS	**Tailwind, knots**	**Air distance computed by OPT, feet**
145	10	1234
160	10	1350
145	0	1123
160	0	1239

Table 13b. Flaps 40 air distances computed by OPT.

E. CONCLUSIONS

Summary

The material in this *Study* supports a number of observations and conclusions regarding the performance of N732MA during its approach and landing on KNIP runway 10. Section C of this *Study* summarizes the motion of the airplane during the approach and landing, and the surprisingly poor braking performance achieved during the landing roll.

In addition, the results of this *Study* underscore the recommendation in SAFO 19003 that

> Directors of Safety and Directors of Operations (Part 121); Directors of Operations (parts 135, and 125), Program Managers, (Part 91K), and Pilots (Part 91) should ensure pilots verify, prior to initiating an approach, that the aircraft can stop within the Landing Distance Available using a RwyCC of “2” whenever there is the likelihood of moderate or greater rain on a smooth runway or heavy rain on a grooved/PFC runway.

This accident also highlights that unless the language or intent of SAFO 19003 is incorporated into operators’ Operations Specifications and Flight Operations Manuals, flight crews are likely to use a RwyCC of “5” (corresponding to a wet runway), instead of “2” (corresponding to a flooded runway), when performing en-route landing distance assessments “whenever there is the likelihood of moderate or greater rain on a smooth runway or heavy rain on a grooved/PFC runway” (unless braking action reports from other flight crews change this assessment).

The *Study* indicates that the rainfall rate at the time of the accident and the runway macrotexture depth and cross slope could have produced water depths on portions of the runway close to or exceeding the 3 mm (1/8”) considered to be a flooded condition that

can support dynamic hydroplaning. However, white tire marks on the runway over the entire length of the landing roll, and the lateral load factor developed on the runway, indicate that the tires were in contact with the runway (likely through a thin film of water), as opposed to being lifted entirely off the runway as occurs during dynamic hydroplaning. The combination of the evidence against dynamic hydroplaning with the extremely low achieved μ_B suggests that the airplane was experiencing viscous hydroplaning with the tires in the condition depicted in Figure 21c.

Previous NTSB Aircraft Performance Studies of wet-runway overrun accidents (see References 2 and 20) conclude that the μ_B achieved during these events was significantly less than the wet-runway μ_B predicted by industry-accepted models, and less than the μ_B assumed in the wet-runway landing distance advisory data provided in the manufacturers' Airplane Flight Manuals. While this is the case in this accident as well, the depth of water on the KNIP runway exceeds the depths in the other events considerably; the other runways were not flooded, but portions of the KNIP runway might have been. The concern raised by the previous events about lower-than-expected μ_B on *non-flooded* wet runways is therefore not as relevant in this accident.

Even so, the achieved μ_B is lower than the flooded-runway μ_B models described in the TALPA RCAM RwyCC 2 (Figure 32), AMC 25.1591, and Boeing's B737NG simulation model for non-dynamic hydroplaning conditions (see Figures 24 and 25; the achieved μ_B does match the μ_B = 0.05 constant used to model dynamic hydroplaning conditions, but as noted, other evidence argues against dynamic hydroplaning in this case). The reasons for the extremely low μ_B in the absence of dynamic hydroplaning might be associated with the viscous hydroplaning condition depicted in Figure 21c (as noted above), but might also be associated with a loss in anti-skid system efficiency in the presence of the water depth, airplane drift, and braking technique (differential braking and on/off braking inputs) seen in this accident. Evaluating the effects of these factors on η_{AS} is beyond the scope of this *Study*; however, this subject is deserving of further research, since a proper μ_B model must account for both μ_{max} *and* η_{AS} correctly. An observed shortfall in μ_B, improperly attributed to a decrease in μ_{max} rather than in η_{AS}, can contribute to a confused understanding of the behavior of μ_{max}, and to an unwarranted confidence in the invariability of η_{AS}.

As stated above, in this accident the depth of water on the KNIP runway considerably exceeds those in other wet-runway overrun events investigated by the NTSB. A runway becomes flooded when the rainfall rate overwhelms the runway's drainage capacity. A runway's drainage capacity can be maximized by increasing the runway cross-slope and macrotexture depth. Runway grooving, which effectively increases the macrotexture depth dramatically, "is a proven and effective technique for providing skid-resistance and prevention of hydroplaning during wet weather" (Reference 32). KNIP runway 10/28 is not grooved, and its southern cross-slope is less than the 1% minimum grade specified in *UFC 3-260-01: Airfield and Heliport Planning and Design* (Reference 43).

Relative effects of operational factors and runway friction on stopping performance

The NTSB Operational Factors / Human Performance Factual Report (Reference 5) notes that among the stabilized approach criteria cited in the Miami Air FOM, “no later than 1,000 feet [above field level], the airplane must be … at a sink rate of no greater than 1,000 feet per minute,” “stabilized at the proper approach speed,” and “on glideslope.” The FOM also states that “momentarily exceeding 1,000 feet per minute is permitted as long as the rate of descent is immediately reduced to at or below 1,000 feet per minute,” and that “if the aircraft is not stabilized by 1,000 feet AFL or at any point thereafter, a Missed Approach is MANDATORY” [emphasis in original].

Section C of this *Study* indicates that below 1,000 ft. AGL during the approach, the indicated airspeed, glide path, and sink rate of the airplane violated some of the stabilized approach criteria specified in the Miami Air FOM. The airspeed reached 170 KCAS (17 kt. above the nominal V_{REF30} + 5 speed), the PAPI lights would have displayed 4 white lights (indicating the airplane was well above the glideslope), and the rate of descent peaked at -1,580 ft./min., triggering multiple GPWS “Sink Rate” alerts.

The airplane touched down about 1,580 ft. past the displaced threshold, or about 580 ft. beyond the nominal touchdown point assumed in the FCOM. As a result of the fast approach and an 11 kt. tailwind, the ground speed was 180 kt. at touchdown. In addition, the speedbrake deployment occurred 4 seconds after touchdown (vs. the nominal 2 seconds for manual speedbrake deployment, or 1 second for automatic speedbrake deployment). Nonetheless, the results of this *Study* indicate that had the airplane achieved the μ_B specified by §25.109(c) for an ungrooved, wet runway, or the μ_B underlying the FCOM “good” braking action landing distances, it would have stopped on the runway, even with the actual fast approach, tailwind, touchdown point, and speedbrake delay. Conversely, with the μ_B level actually achieved during the landing, the airplane would not have stopped on the runway even if it had been on speed, touched down only 1,000 ft. from the displaced threshold, and deployed the spoilers in the nominal 2 seconds.

In light of these findings, the poor μ_B achieved on the runway can be considered a greater contributor to the runway overrun than the deviations from the nominal approach speed, touchdown point, and nominal spoiler deployment time. Nonetheless, the tailwind, high approach speed, longer than nominal touchdown point, and delay in spoiler deployment increased the speed at which the airplane departed the runway and impacted the seawall, and hence contributed to the severity of the accident. Note that if the airplane had tracked the centerline of the runway, it would have impacted a steel approach light stanchion reaching into the St. Johns River past the seawall, potentially causing additional damage to the airplane.

Need for rainfall rate descriptors to address rainfall much heavier than “heavy rain”

The KNIP SPECI weather observations at 21:22, 21:45, and 21:53 all reported the precipitation condition as “heavy rain,” the most intense rainfall rate descriptor available, corresponding to rainfall rates of 0.3 in./hr. and greater. The actual rainfall rates around

the time of the accident were 2 to 8 times the 0.3 in./hr. "heavy rain" threshold. The available precipitation descriptors fail to describe the significant difference between a rainfall rate of 2.4 in./hr. (8 times the "heavy rain" threshold) and 0.3 in./hr. (the threshold itself). Consequently, a report of "heavy rain" might not communicate to flight crews the true intensity of the rainfall at the airport, thereby impairing their ability to make a sound assessment of the runway conditions (e.g., "wet" vs. "flooded"), and the required landing distance. Additional rainfall rate descriptors, that cover rainfall rates that can be significantly greater than the "heavy rain" threshold, could help address this problem.

Although this accident involved a runway that was likely partially flooded as a result of the rainfall rate at the time, some of the observations and findings noted in References 2 and 20 stemming from other wet-runway overrun accidents on non-flooded runways are relevant here as well. These observations are presented below.

Need for more conservative μ_B models for computing FCOM wet-runway landing distances

The μ_B deficit observed in other accidents makes the stopping performance of the airplanes involved more consistent with FCOM landing distances for runways contaminated with standing water, than for runways that are merely "wet." For this reason, observers may be (understandably) quick to conclude that the runways involved must be more contaminated (contain a greater depth of water) than assumed in the wet runway models underlying the FCOM distances. However, in those accidents, examination of the runways involved, including an examination of their macrotexture and cross-slope, did not support a conclusion that the runways could have been flooded given the rainfall rates during the accidents in question. Furthermore, the μ_B actually achieved in a number of these accidents *was* consistent with the NASA CFME model for a wet – not flooded – runway. In other words, the NASA CFME model for a wet runway is more conservative than those underlying the airplane FCOMs, and moreover, matches the actual airplane performance achieved during the accidents better than those underlying the FCOMs. The NASA CFME model is also more conservative than the §25.109(c) model.

In this accident, portions of the runway may well have been flooded, but the μ_B achieved is still below various accepted μ_B models for ***flooded*** runways, as noted above. Hence, these models – and/or the behavior of η_{AS} on these runways – should be reviewed. In particular, the validity of the models (for both flooded and non-flooded runways) at high speeds (above 120 kt.) should be examined; many μ_B models are derived from publicly-available test data conducted at relatively low speeds, and so may overestimate μ_B at higher speeds. Test data at higher speeds exist, but are the intellectual property of aircraft manufacturers or other private organizations.[73]

The FAA has recognized and addressed the reality of the μ_B deficit on wet runways in several documents and actions. For example, SAFO 19003 warns operators that

> Several recent runway-landing incidents/accidents have raised concerns with wet runway stopping performance assumptions. Analysis of the stopping data from these incidents/accidents indicates

[73] Per comments from the FAA on a draft version of this *Study*.

> the braking coefficient of friction in each case was significantly lower than expected for a wet runway as defined by Title 14 of the Code of Federal Regulations (14 CFR) part 25 § Section 25.109 and Advisory Circular (AC) 25-7D methods.

SAFO 19003 also advises that

> When planning to land on a smooth runway under conditions of moderate or heavy rain, or when landing on a grooved or PFC runway under heavy rain, pilots should consider that the surface may be contaminated with water at depth greater than 1/8 inch and adjust their landing distance assessment accordingly.

Moreover, the Transport Airplane Performance and Handling Characteristics ARAC, through the FTHWG, has recommended new 14 CFR Part 25 and Part 121 rules to help cover for potentially lower-than-expected wet runway μ_B at the time of dispatch (these proposals would not have affected the dispatch of N732MA on the accident flight, however).

In addition, AC 25-32, *Landing Performance Data for Time-of-Arrival Landing Performance Assessments*, incorporates many of the recommendations of the TALPA ARC, including the RCAM. However, wet (not flooded) runways can either be classified as RwyCC 5 (associated with μ_B levels defined by the §25.109(c) model), or as RwyCC code 3 "Slippery When Wet" (for which μ_B = 0.16 constant). The "Slippery When Wet" designation applies when the average CFME μ of the runway falls below the minimum runway friction maintenance level defined in Advisory Circular 150/5320-12C – a condition that 72 runways in the U.S.A. were found to meet during a 12-month period from July 2019 to July 2020, and a condition that KNIP runway 10 came very close to meeting based on CFME measurements taken after the accident.[74] The μ_B levels achieved on the non-flooded runways considered in Reference 2 and 20 was *between* those specified by RwyCCs 5 and 3, and the μ_B achieved in this accident was below that specified by RwyCC 2. Consequently, the RCAM as currently specified in AC 25-32 will likely overestimate the μ_B that can actually be achieved on some operational, wet runways. Of note, however, had KNIP reported runway 10 as "slippery when wet" per the TALPA framework, the airplane could only have been dispatched from MUGM under the planned conditions or airplane weight if flaps 40, and not flaps 30, were used for landing, and the Miami Air FOM would have prohibited the flight crew from attempting a landing with *any* tailwind component.

While it is clear that some wet runways cannot provide the μ_B levels specified by the RCAM, it is likely that many can. Hence, there is an operational disadvantage to penalizing "good" runways with more conservative (and unnecessary) μ_B models intended to account for the reduced performance attainable on "poor" runways. To resolve the tension between ensuring safety on *all* runways while maximizing the utilization of high-performing runways, the actual μ_B achievable on any individual runway, for any realistic rainfall rate, must be predictable. To this end, research efforts are required to better understand the physics of how friction is created on wet runways, and to develop tools with which airport operators can reliably predict and report the performance of their runways when wet.

---

[74] Technically, the CFME μ measurements did not perfectly satisfy the definition of "Slippery When Wet;" see the discussion of these measurements in Section D-VII.

Need for "closed-loop" demonstration of μ_B

For a μ_B model to be correct, the product of μ_{max} and η_{AS} must be correct. For non-flooded runways, the NASA CFME model produces an accurate estimate of μ_B with μ_{max} values that are somewhat higher than those assumed in §25.109(c), and with η_{AS} values that are substantially lower than the 0.80 allowed in §25.109(c) for fully-modulating braking systems. The resulting NASA CFME μ_B values are significantly lower than those predicted by §25.109(c), but match the μ_B values actually achieved during the other landing overrun events and flight tests described in References 2 and 20 relatively well.

Given these results, either the assumption of η_{AS} = 0.80 in §25.109(c) (regardless of μ_{max} and / or braking technique), the μ_{max} specified in §25.109(c), or both, must be considered suspect. The reduced μ_B documented in this accident and those considered in References 2 and 20 might be explained by:

- A wet or flooded-runway η_{AS} that is significantly less than 80% (even for fully-modulating anti-skid systems);
- A wet-runway μ_{max} that is significantly less than that specified in §25.109(c), and a flooded-runway μ_B (in non-dynamic hydroplaning conditions) that is less than that specified in AMC 25.1591 or TALPA RwyCC 2;
- A combination of these factors.

NTSB staff discussions with staff at airplane and brake system manufacturers indicate that these organizations are very confident that the wet-runway η_{AS} of fully-modulating anti-skid systems is at least 80%, and that the methods outlined in AC 25-7C for demonstrating η_{AS} are valid.[75] It is likely that these organizations would be skeptical of the suggestion that η_{AS} could be significantly lower than 80%, as it is modeled in the NASA CFME model (see Equation [32]). On the other hand, the NASA CFME and ESDU models, reflecting research results, indicate that η_{AS} decreases as μ_{max} decreases, even for fully-modulating systems; but this behavior is not reflected in the §25.109(c) model. Furthermore, while §25.109(c) requires a demonstration that the anti-skid braking system operates as expected, there is no requirement to demonstrate that the μ_{max} specified by §25.109(c), when combined with the η_{AS} assumed (or "demonstrated") by the manufacturer, is consistent with the stopping distance actually obtained during flight tests on wet runways. While in practice the μ_{max} attainable on different wet runways will likely be different due to differences in runway textures and / or water depth, this very fact underscores the importance of demonstrating that the assumed combination of μ_{max} and η_{AS}, together with the relevant operational safety factors, can reliably account for these variations.

The μ_{max} available from a wet runway at a given V_G depends on the water depth and the runway surface macrotexture and microtexture, as well as the presence of rubber and loose surface deposits, such as sand or grit. Macrotexture can be measured by a number of methods. Microtexture has a strong influence on $\mu_{max,}$ but the research reviewed in References 2 and 20 does not identify a means for measuring this quantity directly.

[75] These methods are described in Reference 20.

However, developments since these References were written suggest that a means for measuring microtexture is now available.[76] If the reduced μ_B documented in this *Study* and References 2 and 20 is partially the result of fine microtextures on the runway surfaces involved, then this too indicates the inadequacy of the §25.109(c) model, since that model does not account for the range of microtextures that are possible on existing runways.

References 2 and 20 indicate that the μ_B predicted by the NASA CFME model matches the μ_B actually attained in other non-flooded wet runway landing overrun events, and wet runway flight tests, much better than the §25.109(c) model and the μ_B levels implicit in the airplane FCOMs. Furthermore, the NASA model is rooted in a measurement of μ on the runway in question (via a CFME device). Factors that act to reduce or increase the CFME μ will affect μ_{max} in a similar way; for example, reductions in macrotexture and microtexture, and greater rubber contamination, all act to reduce *both* the CFME μ and the runway μ_{max}. In addition, AC 150/5320-12C indicates that CFME runs at different speeds can help identify the effects of both macrotexture (from 40 mph runs) and microtexture (from 60 mph runs).

A disadvantage of the NASA CFME model is that the measurement speeds of the CFME device typically transform to a relatively narrow range of airplane ground speeds. The "combined" μ_B model described in this *Study* (and in References 2 and 20) scales the §25.109(c) μ_B (which is defined across a large speed range) to match the better, CFME-based estimate of μ_B in a narrow speed range, yielding an improved estimate of μ_B across the larger speed range.

On non-flooded runways, the combined μ_B model provides an improved means for estimating the final airplane μ_B, even when the details of the runway macrotexture, microtexture, and rubber contamination are unknown. Nonetheless, measurements of runway macrotexture, cross-slope, and rubber contamination are always useful, in order to estimate water depths using the TTI model (so as to evaluate the possibility of flooded conditions and dynamic hydroplaning), and to help understand the surface condition that produced the CFME measurements. Hence, the development of methods for measuring microtexture directly significantly improves the potential for understanding poor μ_B performance on wet runways, and research employing these methods should be pursued.

Any future research concerning wet-runway stopping performance should include "closed-loop" evaluation of the μ_B models underlying FCOM wet and flooded runway landing distances, and of the NASA method for computing μ_B from CFME measurements. This evaluation would consist of demonstrating that the landing distances computed from the assumed μ_{max} and η_{AS} match the landing distances actually achieved on a wet runway. In particular, the behavior of η_{AS} as μ_{max} decreases, and with different braking techniques (including differential and intermittent braking), should be tested so as to correctly model the performance of the anti-skid system over a range of μ_{max} and braking behaviors.

[76] See, for example, https://amesengineering.com/products/laser-texture-scanner-model-9400/ (accessed 6/19/2020).

While the NASA CFME model provides good estimates of the μ_B achieved in the non-flooded wet-runway overrun accidents considered in References 2 and 20, the method fails to predict the extremely low μ_B achieved in this accident. The reason for this might be that the model breaks down (either in its estimate of μ_{max} or η_{AS}) as the depth of the water approaches the 3 mm that defines a "flooded" runway. Likewise, the flooded-runway μ_B models provided by AMC 25.1591 (Equation [37]) and TALPA RwyCC 2 also overestimate the μ_B achieved in this accident below the hydroplaning speed. Hence, establishing the range of water depths and other conditions (runway textures, airplane speed) for which these models are valid, and / or correcting the models to account for a broader range of water depths and conditions, are also worthy research goals.

_____

John O'Callaghan
National Resource Specialist – Aircraft Performance
Office of Research and Engineering

F. REFERENCES

1. The Boeing Company, *737-700/-800/-900ER Flight Crew Operations Manual, C.I.T. Leasing Corporation,* Document # D6-27370-8BK-TCI, Revision # 26, Revision date March 21, 2019.

2. O'Callaghan, John J., *Slippery When Wet: The Case for More Conservative Wet Runway Braking Coefficient Models.* Presented at the 16th American Institute of Aeronautics and Astronautics Aviation Technology, Integration, and Operations Conference, Washington, D.C., June 17, 2016. Paper # AIAA-2016-4364, available at https://goo.gl/rWfoUc

3. Federal Aviation Administration, *Advisory Circular No. 25-32: Landing Performance Data for Time-of-Arrival Landing Performance Assessments,* dated December 22, 2015. Available at https://www.faa.gov/regulations_policies/advisory_circulars/index.cfm/go/document.information/documentID/1028656.

4. Federal Aviation Administration, *Safety Alert for Operators (SAFO) 19003: Turbojet Braking Performance on Wet Runways,* dated July 2, 2019. Available at https://www.faa.gov/other_visit/aviation_industry/airline_operators/airline_safety/safo/all_safos/media/2019/SAFO19003.pdf.

5. National Transportation Safety Board, Office of Aviation Safety, *Operational Factors / Human Performance Group Chairman's Factual Report, Miami Air International Flight 293, Boeing 737-81Q, N732MA, Jacksonville, Florida, May 3, 2019, NTSB Accident # DCA19MA143*. (Washington, D.C., January 14, 2020.) (Contact NTSB at pubinq@ntsb.gov.)

6. National Transportation Safety Board, Office of Aviation Safety, *Air Traffic Control Group Chairman's Factual Report, Miami Air International Flight 293, Boeing 737-81Q, N732MA, Jacksonville, Florida, May 3, 2019, NTSB Accident # DCA19MA143*. (Washington, D.C., May 5, 2020.) (Contact NTSB at pubinq@ntsb.gov.)

7. Miami Air International, *B737-800 Aircraft Operations Manual I Bulletin 19-09, "Aircraft Arresting Cables,"* dated 05/20/2019.

8. The Boeing Company, *737-600/700/700IGW(BBJ)/800/900 Airplane Recovery Document*, Document # D626A004, March 31 2016 (Boeing proprietary document).

9. National Transportation Safety Board, Office of Research and Engineering, *Flight Data Recorder Specialist's Factual Report, Miami Air International Flight 293, Boeing 737-81Q, N732MA, Jacksonville, Florida, May 3, 2019, NTSB Accident # DCA19MA143*. (Contact NTSB at pubinq@ntsb.gov.)

10. National Transportation Safety Board, Office of Research and Engineering, *Cockpit Voice Recorder Specialist's Factual Report, Miami Air International Flight 293, Boeing 737-81Q, N732MA, Jacksonville, Florida, May 3, 2019, NTSB Accident # DCA19MA143*. (Contact NTSB at pubinq@ntsb.gov.)

11. International Civil Aviation Organization (ICAO), *The Tenth Meeting of Automatic Dependent Surveillance – Broadcast (ADS-B) Study and Implementation Task Force (ADS-B SITF/10) Agenda Item 6: Review States' activities and interregional issues on trials and implementation of ADS-B and multilateration: ADS-B / GPS Accuracy (Presented by Australia)*. Singapore, 26-29 April 2011. Document available at https://www.icao.int/APAC/Meetings/2011_ADS_B_SITF10/IP10_AUS%20AI.%206%20-%20GPS%20Accuracy.pdf.

12. National Transportation Safety Board, Office of Research and Engineering, *Group Chairman's Aircraft Performance Study, American Airlines Flight 587, Airbus A300B4-605R, Belle Harbor, New York, November 12, 2001*, NTSB Accident Number DCA02MA001, Docket Item 188 (Washington, DC: NTSB, October 10, 2002). (Contact NTSB at pubinq@ntsb.gov).

13. Federal Aviation Administration, *Airman's Information Manual (AIM)*, *Change 1,* Effective January 30, 2020. Available at https://www.faa.gov/air_traffic/publications/atpubs/aim_html/index.html.

14. Federal Aviation Administration, *Advisory Circular 150/5340-30G, Design and Installation Details for Airport Visual Aids*, dated September 21, 2012. Available at: https://www.faa.gov/documentLibrary/media/Advisory_Circular/150_5340_30g.pdf.

15. Miami Air International, *Flight Operations Manual (FOM)*, document # MAISYS-00000-00180-01, Revision No. 005. (Miami Air International proprietary document.)

16. National Transportation Safety Board, Office of Aviation Safety, *Operational Factors / Human Performance Group Chairman's Factual Report, Miami Air International Flight 293, Boeing 737-81Q, N732MA, Jacksonville, Florida, May 3, 2019, NTSB Accident # DCA19MA143*: *Attachment #2: Miami Personnel Interview Summaries and Transcript* (Washington, D.C., January 31, 2020.) (Contact NTSB at pubinq@ntsb.gov.)

17. *Federal Register* Vol. 78, No. 46 / Friday, March 8, 2013 / Notices, page 15112.

18. Federal Aviation Administration (FAA) Aviation Rulemaking Advisory Committee (ARAC) Flight Test Harmonization Working Group (FTHWG), *Task 9: Wet Runway Stopping Performance Final Report, Recommendation Report,* March 16, 2018. Available at https://www.faa.gov/regulations_policies/rulemaking/committees/documents/media/FTHWG-%20Wet%20Runway%20Topic9%20Final%20Report.pdf.

19. Federal Aviation Administration (FAA) Aviation Rulemaking Advisory Committee (ARAC) Flight Test Harmonization Working Group (FTHWG): *Phase 2 Recommendation Report – REV A*, April, 2017. Available at: https://www.faa.gov/regulations_policies/rulemaking/committees/documents/media/09%20-%20FTHWG_Final_Report_Phase_2_RevA__Apr_2017.pdf.

20. National Transportation Safety Board, Office of Research and Engineering, *Group Chairman's Aircraft Performance Study, Embraer EMB-505, N322QS, Conroe, TX (Lone Star Executive Airport (KCXO)), September 19. 2014*, NTSB Accident Number CEN14FA505 (Washington, DC: NTSB, April 20, 2016). (Contact NTSB at pubinq@ntsb.gov).

21. Engineering Science Data Unit (ESDU) Item 71025, *Frictional and Retarding Forces on Aircraft Tyres, Part I: Introduction*, issued October 1971. Sponsored by the Royal Aeronautical Society. For ESDU items see https://ihsmarkit.com/index.html.

22. Horne, Walter B. *Wet Runways*, NASA Technical Memorandum TM-X-72650, NASA Langley Research Center, Hampton, VA, April 1975. Available at https://ntrs.nasa.gov/archive/nasa/casi.ntrs.nasa.gov/19750012279.pdf.

23. National Transportation Safety Board, Office of Aviation Safety, *Systems Group Chairman's Factual Report, Miami Air International Flight 293, Boeing 737-81Q, N732MA, Jacksonville, Florida, May 3, 2019, NTSB Accident # DCA19MA143*. (Contact NTSB at pubinq@ntsb.gov.)

24. B. Gallaway, R. Schiller, Jr., and J. Rose, *The Effects of Rainfall Intensity, Pavement Cross Slope, Surface Texture, and Drainage Length on Pavement Water Depths*. Texas Transportation Institute (TTI) Research Report 138-5, May 1971.

25. Renze, K. J., Yager, T. J, Stimson, D, Smith, M. H., Stephens, A. T., and Raby, C., *Runway Pavement Macrotexture Retest*, *Pavement Macrotexture Measurements (NASA Grease Sample Method and Water Outflow Meter), Runway 3/21, Roswell, NM (KROW)*, National Transportation Safety Board (NTSB) Public Docket, NTSB No. DCA12SS002, August 2012. (Contact NTSB at pubinq@ntsb.gov).

26. National Cooperative Highway Research Program, *Synthesis 291: Evaluation of Pavement Friction Characteristics,* Transportation Research Board – National Research Council, Washington, D.C., 2000, page 22.

27. National Transportation Safety Board, Office of Aviation Safety, *Meteorology Factual Report, Miami Air International Flight 293, Boeing 737-81Q, N732MA, Jacksonville, Florida, May 3, 2019, NTSB Accident # DCA19MA143*. (Washington, D.C., January 24, 2020.) (Contact NTSB at pubinq@ntsb.gov.)

28. Engineering Science Data Unit (ESDU) Item 05011, *[Draft] Aircraft tyre rolling or braking on dry or precipitate contaminated runways: Summary of the model,* ESDU P791/1, first draft November 2019. For ESDU items see https://ihsmarkit.com/index.html.

29. Engineering Science Data Unit (ESDU) Item 71026, *Frictional and Retarding Forces on Aircraft Tyres*, *Part II: estimation of braking force (friction data updated – 1981),* with Amendments A and B, August 1981. Sponsored by the Royal Aeronautical Society. For ESDU items see https://ihsmarkit.com/index.html.

30. Florida Department of Transportation (FDOT), State Materials Office, *Memorandum: Continuous Friction Measurements / Runway 10/28,* May 13, 2019.

31. Yager, Thomas J., Vogler, William A., & Baldasare, Paul, *Evaluation of Two Transport Aircraft and Several Ground Test Vehicle Friction Measurements Obtained for Various Runway Surface Types and Conditions: A Summary of Test Results From Joint FAA / NASA Runway Friction Program.* NASA Technical Paper 2917, NASA Office of Management, Scientific and Technical Information Division, February 1990.

32. Federal Aviation Administration, *Advisory Circular 150/5320-12C: Measurement, Construction, and Maintenance of Skid-Resistant Airport Pavement Surfaces,* dated March 18, 1997. Available at: http://www.faa.gov/regulations_policies/advisory_circulars/index.cfm/go/document.information/documentID/22107

33. The Boeing Company, *Landing Gear Systems and Ground Handling Data for the 737NG and 737MAX Training Simulator*, Boeing document # D611A019 (Boeing proprietary document).

34. NTSB letter to FAA transmitting comments on draft Advisory Circulars 25-31 and 25-32, March 4, 2015, accessible at http://www.ntsb.gov/safety/safety-recs/_layouts/ntsb.recsearch/Recommendation.aspx?Rec=A-07-057

35. Federal Aviation Administration, *Advisory Circular 150/5200-30D, Airport Field Condition Assessments and Winter Operations Safety*, March 8, 2017. Available at: https://www.faa.gov/documentLibrary/media/Advisory_Circular/AC_150_5200-30D_with_chg1.pdf

36. Federal Aviation Administration, *Advisory Circular 25-7D – Flight Test Guide For Certification Of Transport Category Airplanes*, dated May 4, 2018. Available at: https://www.faa.gov/documentLibrary/media/Advisory_Circular/25-7D.pdf

37. National Transportation Safety Board, Office of Research and Engineering, *Group Chairman's Aircraft Performance Study Addendum #1 (Errata #2), Hawker Beechcraft BAe 125-800A, registration N818MV, Owatonna, MN, July 31, 2008*, NTSB Accident Number DCA08MA085 (Washington, DC: NTSB, February 25, 2011). Available at: http://dms.ntsb.gov/pubdms/search/document.cfm?docID=344186&docketID=46427&mkey=68571

38. Merritt, Leslie R. (Program Manager), *Concorde Landing Requirement Evaluation Tests.* U.S. Dept. of Transportation, FAA Technical Report # FAA-FS-160-74-2, August 1974. Document available to the public through the National Technical Information Service, Springfield, VA, 22151.

39. Engineering Science Data Unit (ESDU) Item 10015, *[Draft] Model for performance of a single aircraft tyre rolling or braking on dry and precipitate contaminated runways,* ESDU P792/1, first draft November 2019. For ESDU items see https://ihsmarkit.com/index.html.

40. Wray, Gilbert A., *A Systematic Experimental Investigation of Significant Parameters Affecting Model Tire Hydroplaning,* NASA CR-132346, Davidson Laboratory Report SIT-DL-72-1602, July 1973. Available at: https://ntrs.nasa.gov/archive/nasa/casi.ntrs.nasa.gov/19740003931.pdf

41. U.S. Department of Commerce / National Oceanic and Atmospheric Administration (NOAA), Office of the Federal Coordinator for Meteorological Services and Supporting Research (OFCM), *Federal Meteorological Handbook No. 1: Surface Weather Observations and Reports*, document FCM-H1-2019, Washington, D.C., July 2019. Available at https://www.ofcm.gov/publications/fmh/FMH1/fmh1_2019.pdf.

42. Naval Safety Center, *Naval Runway Surfaces ~ it's about time the Navy got its groove on*, January 24, 2020.

43. United States Department of Defense, *Unified Facilities Criteria: Airfield and Heliport Planning and Design*, document UFC 3-260-1, dated February 4, 2019, Change 1 dated May 5, 2020. Available at: https://www.wbdg.org/FFC/DOD/UFC/ufc_3_260_01_2019_c1.pdf

G. GLOSSARY

Acronyms

AC	Advisory Circular
ADS-B	Automatic Dependent Surveillance – Broadcast
AFE	Above Field Elevation
AFM	Airplane Flight Manual
AFM-DPI	Airplane Flight Manual - Digital Performance Information
AIM	Airman's Information Manual
AMC	Acceptable Means of Compliance (EASA)
ARC	Aviation Rulemaking Committee
ARAC	Aviation Rulemaking Advisory Committee
ASOS	Airport Surface Observation System
ATC	Air Traffic Control
ATIS	Automatic Terminal Information Service
BLM	Boeing Landing Module
CFME	Continuous Friction Measurement Equipment
CFR	Code of Federal Regulations
CG	Center of Gravity
CS	Certification Specification (EASA)
CVR	Cockpit Voice Recorder
EASA	European Aviation Safety Agency
EDT	Eastern Daylight Time
ESDU	Engineering Science Data Unit
EU OPS	European operational regulation(s)
FAA	Federal Aviation Administration
FCOM	Flight Crew Operating Manual
FDOT	Florida Department of Transportation
FDR	Flight Data Recorder
FMC	Flight Management Computer
FO	First Officer
FOM	Miami Air International Flight Operations Manual
GNSS	Global Navigation Satellite System
GPS	Global Positioning System
IGRF	International Geomagnetic Reference Field magnetic variation model
IRU	Inertial Reference Unit

KNIP	Jacksonville Naval Air Station, Jacksonville, Florida
KROW	Roswell International Air Center, Roswell, New Mexico
LMG	Left main landing gear
MAC	Mean Aerodynamic Chord
MEL	Minimum Equipment List
METAR	Meteorological Terminal Air Report
MPD	Mean profile depth
MUGM	Leeward Point Field, Naval Station Guantanamo Bay, Cuba
NASA	National Aeronautics and Space Administration
NG	Nose gear
NTSB	National Transportation Safety Board
OpsSpec	Operations Specification(s)
OPT	Miami Air International Onboard Performance Tool (iPad application)
PAPI	Precision Approach Path Indicator
PF	Pilot Flying
QAR	Quick Access Recorder
RCAM	Runway Condition Assessment Matrix
RFT	Dynatest Model 6875 Runway Friction Tester CFME device
RMG	Right main landing gear
RwyCC	RCAM runway condition code
SAFO	Safety Alert For Operators
SPECI	Special meteorological report or forecast
SRN	Subframe Reference Number
SRTM	Shuttle Radar Topography Mission
SFT	Sarsys Airport Surface Friction Tester CFME device
STC	Supplemental Type Certificate
TALPA	Takeoff And Landing Performance Assessment
TC	Type Certificate
TDZE	Touchdown Zone Elevation
TRA	Throttle resolver angle
TTI	Texas Transportation Institute
USA	United States of America
USGS	United States Geological Survey
UTC	Coordinated Universal Time

English symbols

C_Y	Side force coefficient
d	Average water depth above the top of the runway macrotexture
dh	Differential altitude element
ETD	Estimated texture depth, converted from MPD using Equation [21]
ETD'	Estimated texture depth, converted from MPD using Equation [22]
F_C	Cornering friction force provided by landing gear
F_N	Longitudinal reaction force at nose gear
F_M	Longitudinal reaction force at main gear
F_x	Force along body x-axis
F_y	Force along body y-axis
F_z	Force along body z-axis

g	Gravitational acceleration
h	Altitude
$\dot{h}$	Rate of climb
I	Rainfall intensity
k_B	Effective η_{AS} for scaling §25.109(c) μ_{max} to μ_B from CFME runs
k_ψ	Factor for reducing μ_B due to tire cornering forces
L	Runway drainage path-length (distance from runway centerline)
M_y	Moment about body y-axis
n_x	Longitudinal load factor
n_y	Lateral load factor
N_N	Vertical reaction force at nose gear
N_M	Vertical reaction force at main gear
P	Air pressure
P_{TOTAL}	Total pressure at pitot tube
P_{TRUE}	True freestream static pressure (vs. static pressure at static ports)
p	Tire pressure, or atmospheric pressure (depending on context)
p_L	Left brake pressure
p_R	Right brake pressure
R	Gas constant of air
r_{TIRE}	Effective tire radius
s	Wheel slip ratio
$s_{\mu,MAX}$	Wheel slip ratio for $\mu_{B,MAX}$
S	Wing reference area, or runway cross slope (depending on context)
T	Air temperature, or runway macrotexture depth (depending on context)
T_L	Torque applied by the brakes on one of the two left wheels
T_R	Torque applied by the brakes on one of the two right wheels
T_y	Component of thrust along body y-axis
u	Component of airspeed along body x-axis
v	Component of airspeed along body y-axis
V	Airplane speed (airspeed or ground speed depending on context)
$\vec{V}$	Airspeed vector
V_1	Takeoff decision speed
V_{REF30}	Flaps 30 landing reference speed
V_{WHEEL}	Wheel velocity at tire effective radius
V_G	Ground speed
$\vec{V}_G$	Ground speed vector
V_p	Hydroplaning speed (for dynamic hydroplaning)
$V_{p,spin\ down}$	Spin-down hydroplaning speed (rotating tire)
$V_{p,spin\ up}$	Spin-up hydroplaning speed (nonrotating tire)
$\vec{V}_W$	Wind speed vector
V_{WHEEL}	Tangential speed of tire
w	Component of airspeed along body z-axis
W	Airplane weight
W_x	Component of airplane weight along body x-axis
W_y	Component of airplane weight along body y-axis
W_z	Component of airplane weight along body z-axis

x	Runway x coordinate
Y	Side force
y	Runway y coordinate

Greek symbols

α	Angle of attack
β	Sideslip angle
δ_r	Rudder deflection
γ	Flight path angle
η_{AS}	Anti-skid braking system efficiency
θ	Pitch angle
μ	Friction coefficient
μ_{AP}, $\mu_{B,AP}$	Airplane braking coefficient
μ_B	Wheel braking friction coefficient
$\mu_{B,av}$	Average μ_B in the range of 0.1 ≤ s ≤ 0.5
$\mu_{B,MAX}$	Maximum wheel braking friction coefficient (at $s_{\mu,MAX}$)
$\mu_{B,SKID}$	Wheel braking friction coefficient with locked wheels (i.e., at s =1)
μ_C	Cornering friction coefficient
$\mu_{C,AP}$	"Total airplane" cornering friction coefficient
$\mu_{C,M}$	Cornering friction coefficient at main gear
$\mu_{C,N}$	Cornering friction coefficient at nose gear
μ_{CFME}	Runway μ measured by a CFME device
μ_{dry}	Dry-runway μ
μ_N	Rolling friction coefficient at nose gear
μ_{max}, $\mu_{t/gMAX}$	Maximum μ available on runway
μ_{reqx}	Requested μ_B by brake system x (L or R)
$\mu_{T,AP}$	Total available airplane friction coefficient computed from $\mu_{C,AP}$ and $\mu_{B,AP}$
μ_{wet}	Wet-runway μ
ρ	Air density
ϕ	Roll angle
ψ_{DRIFT}	Drift angle
ψ_{THDG}	True heading angle
ψ_{TTRK}	True track angle
ω_{WHEEL}	Wheel angular velocity

FIGURES

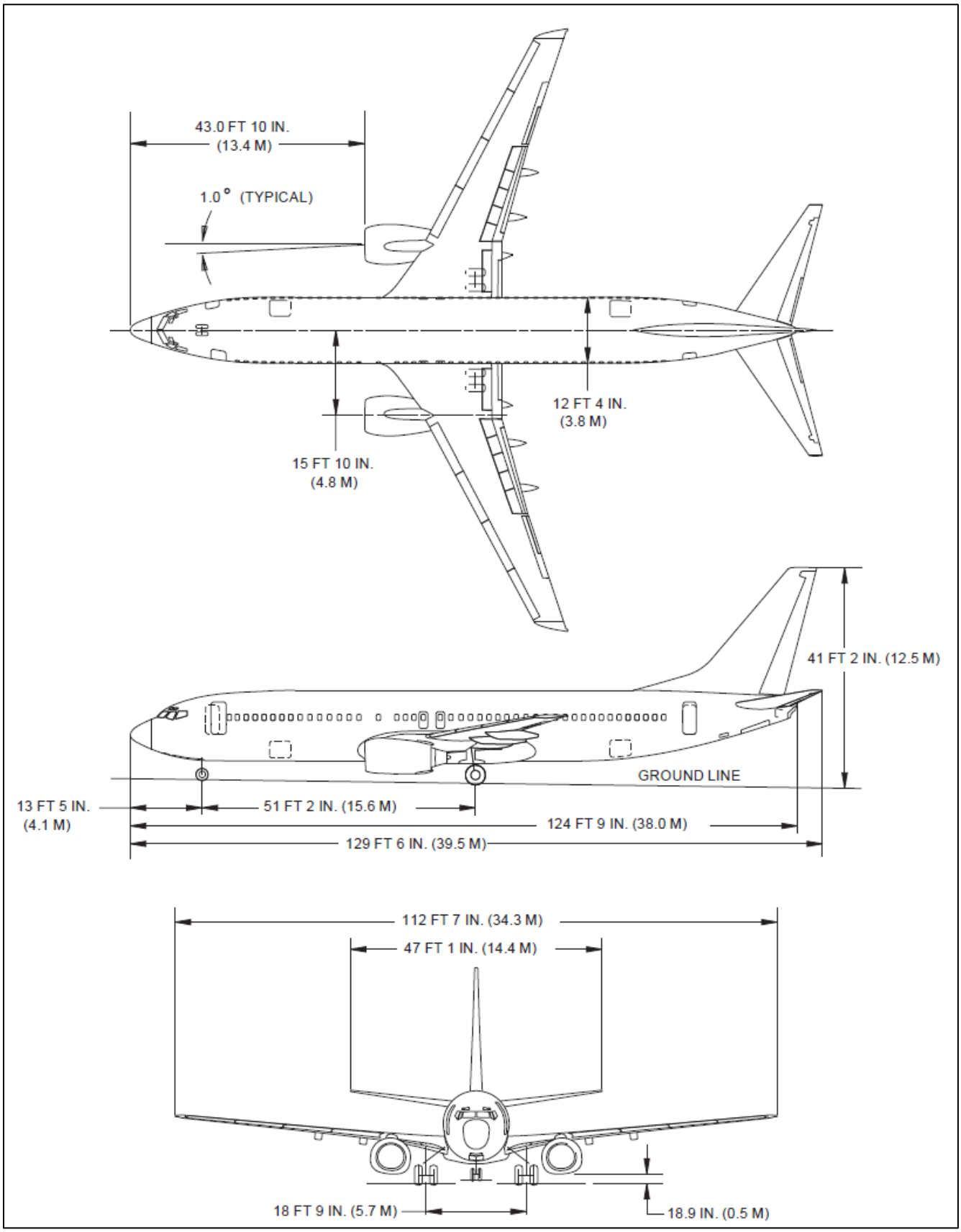

Figure 1. 3-view of Boeing 737-800 airplane (from Reference 8).

DCA19MA143: Miami Air flight 293, Boeing 737-800 N732MA, Jacksonville, FL, May 3, 2019

Tire track survey results

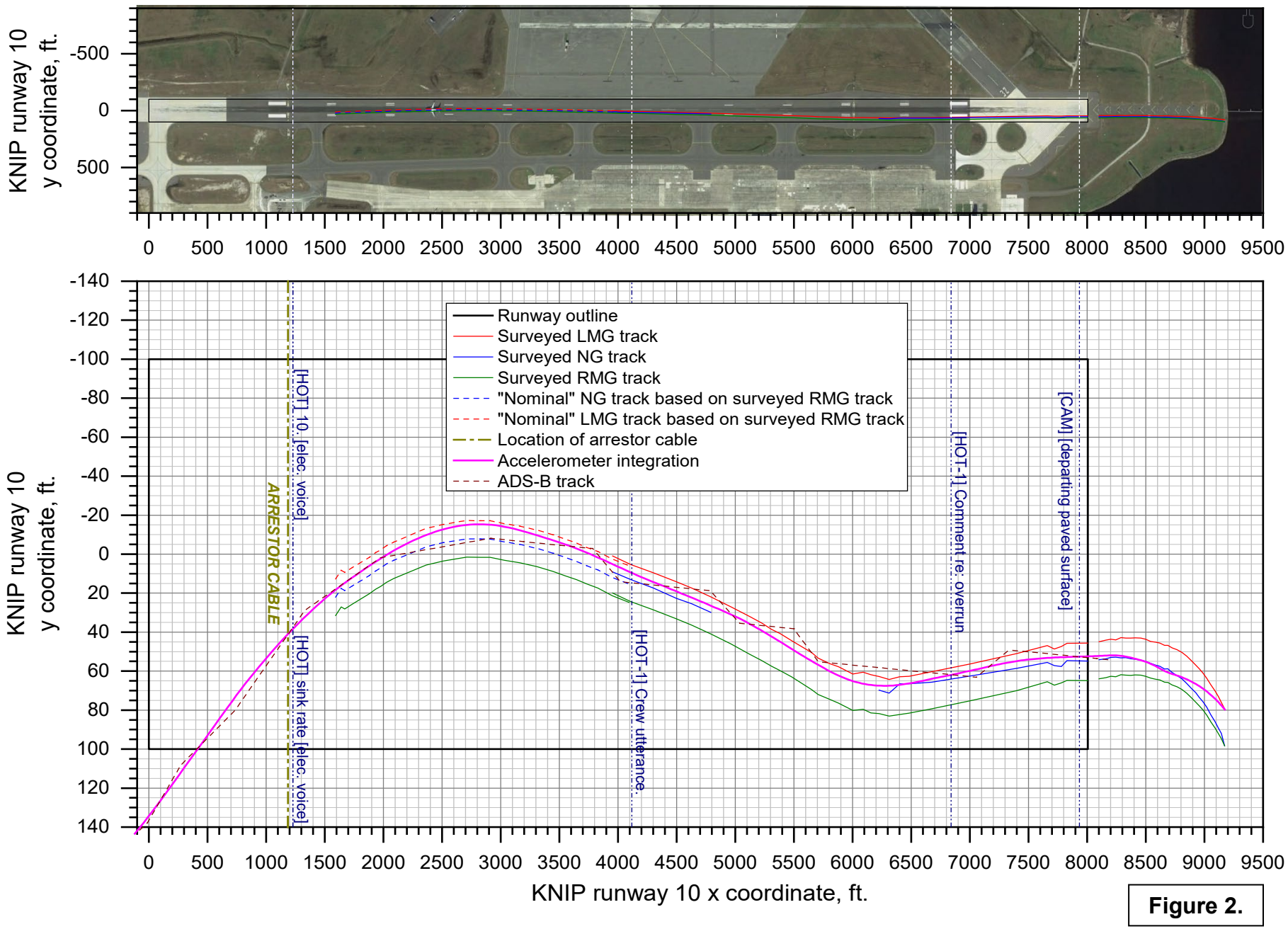

Figure 2.

(a)

(b)

Figure 3 (1 of 2). N732MA at rest in St. Johns River past the end of the runway and seawall.

(c)

(d)

(e)

Figure 3 (2 of 2). N732MA at rest in St. Johns River past the end of the runway and seawall.

(a)

(b)

(c)

Figure 4. Example landing gear tracks on pavement.

(a)

(b)

Figure 5. Landing gear tracks leading from end of pavement to seawall.

DCA19MA143: Miami Air flight 293, Boeing 737-800 N732MA, Jacksonville, FL, May 3, 2019

Plan & profile views of final approach, landing, and rollout

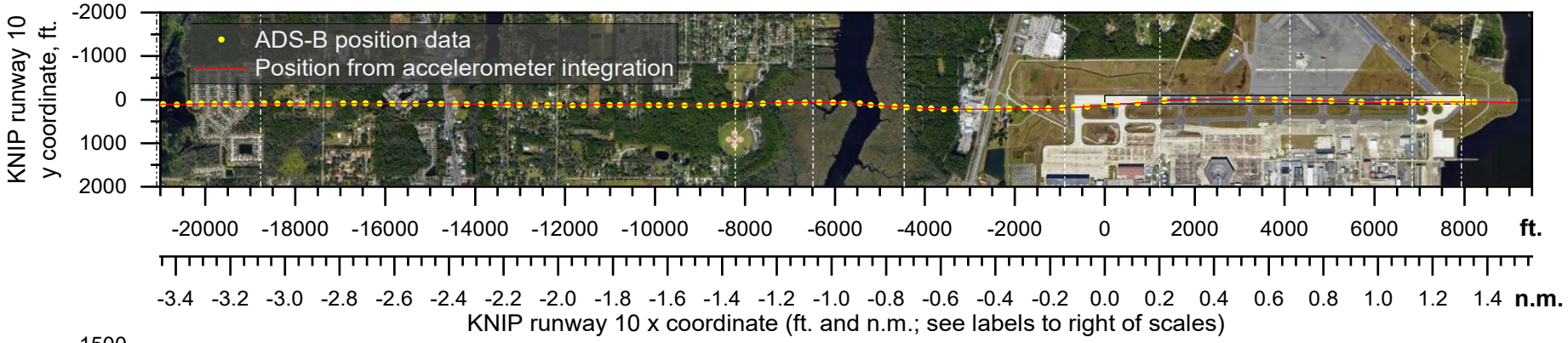

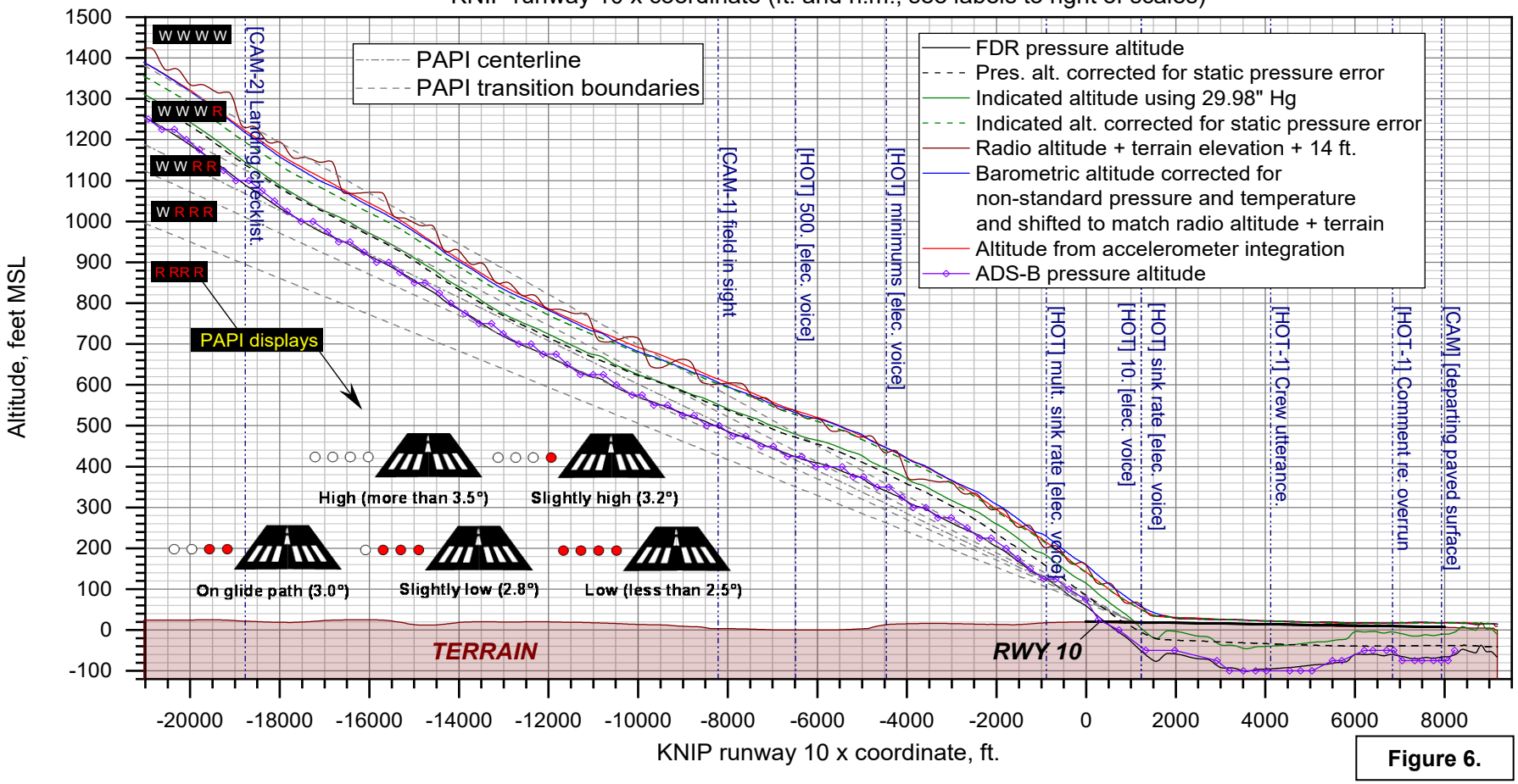

Figure 6.

DCA19MA143: Miami Air flight 293, Boeing 737-800 N732MA, Jacksonville, FL, May 3, 2019

Altitude vs. time during final approach, landing, and rollout

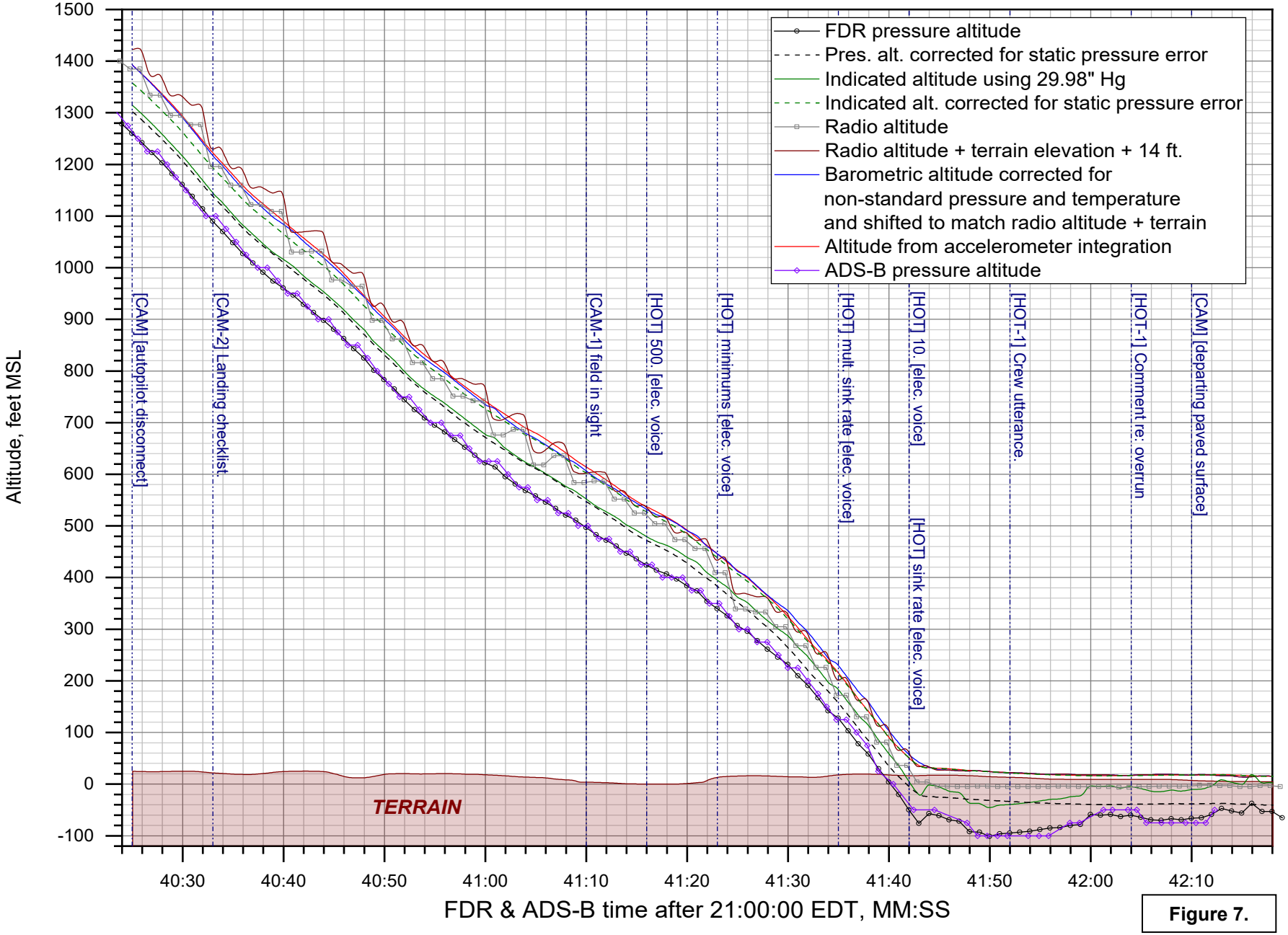

Figure 7.

DCA19MA143: Miami Air flight 293, Boeing 737-800 N732MA, Jacksonville, FL, May 3, 2019

Runway coordinates during final approach, landing, and rollout

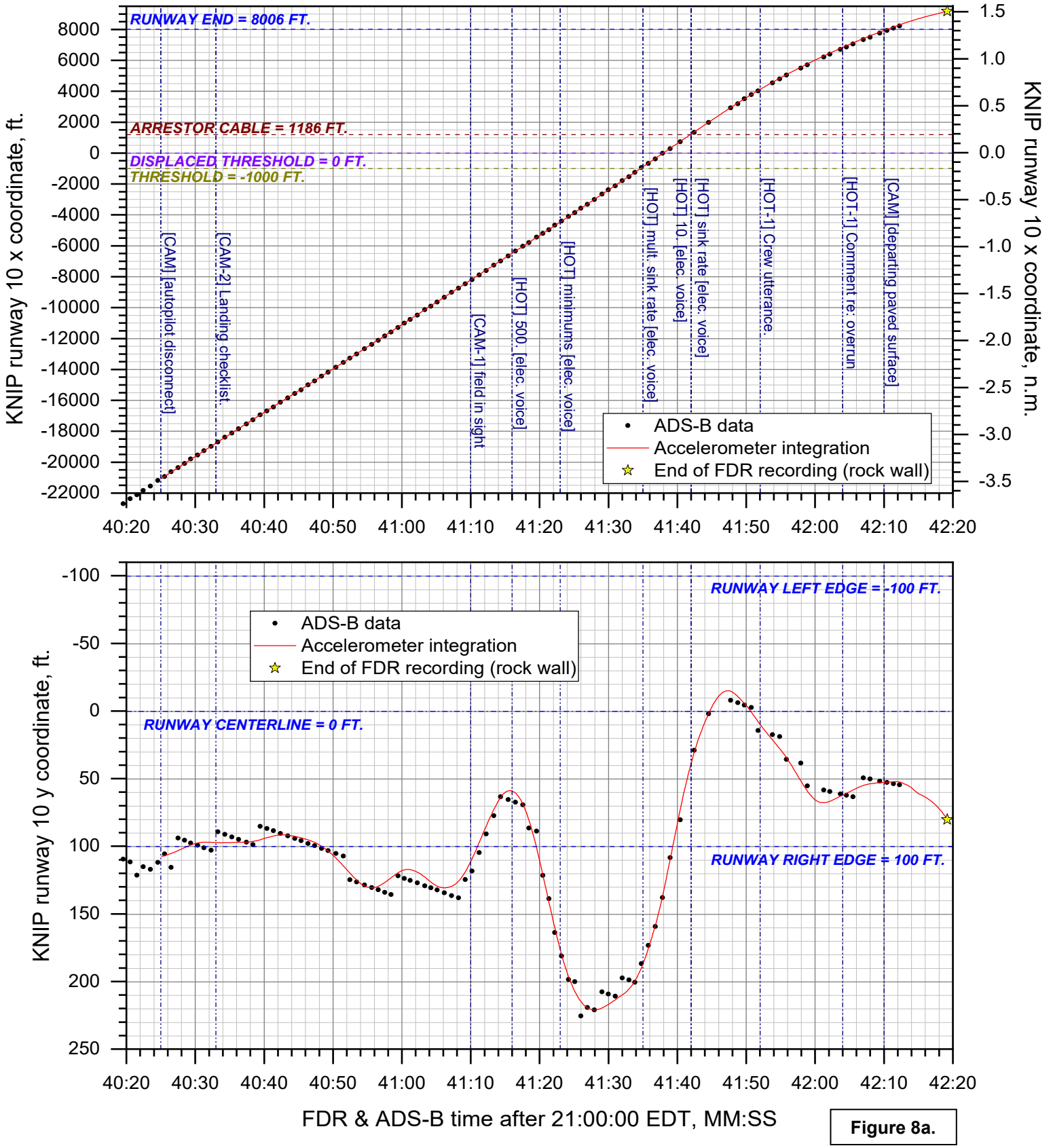

Figure 8a.

DCA19MA143: Miami Air flight 293, Boeing 737-800 N732MA, Jacksonville, FL, May 3, 2019

Runway coordinates during final approach, landing, and rollout (detail)

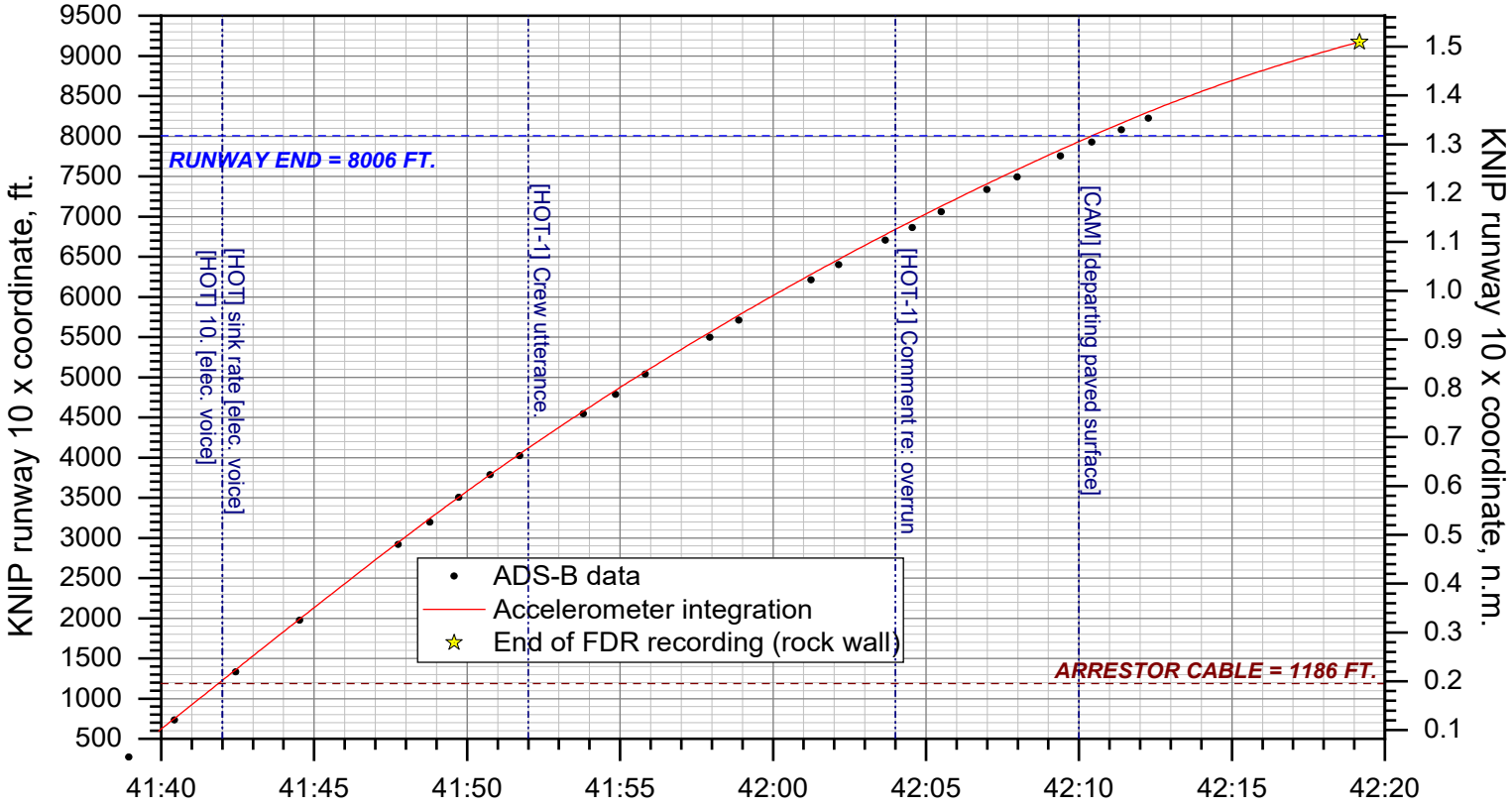

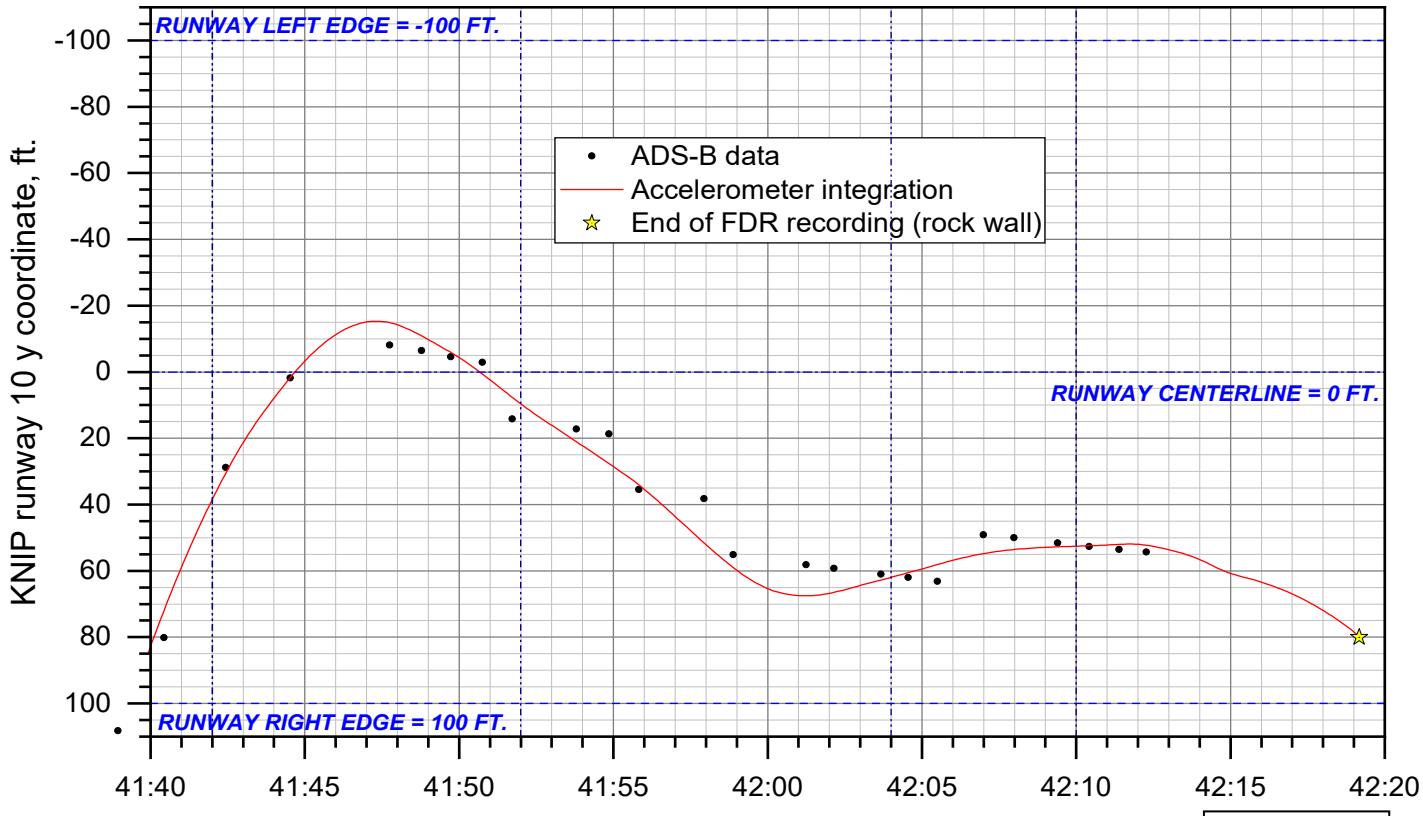

Figure 8b.

DCA19MA143: Miami Air flight 293, Boeing 737-800 N732MA, Jacksonville, FL, May 3, 2019

Speed and rate of climb during final approach, landing, and rollout

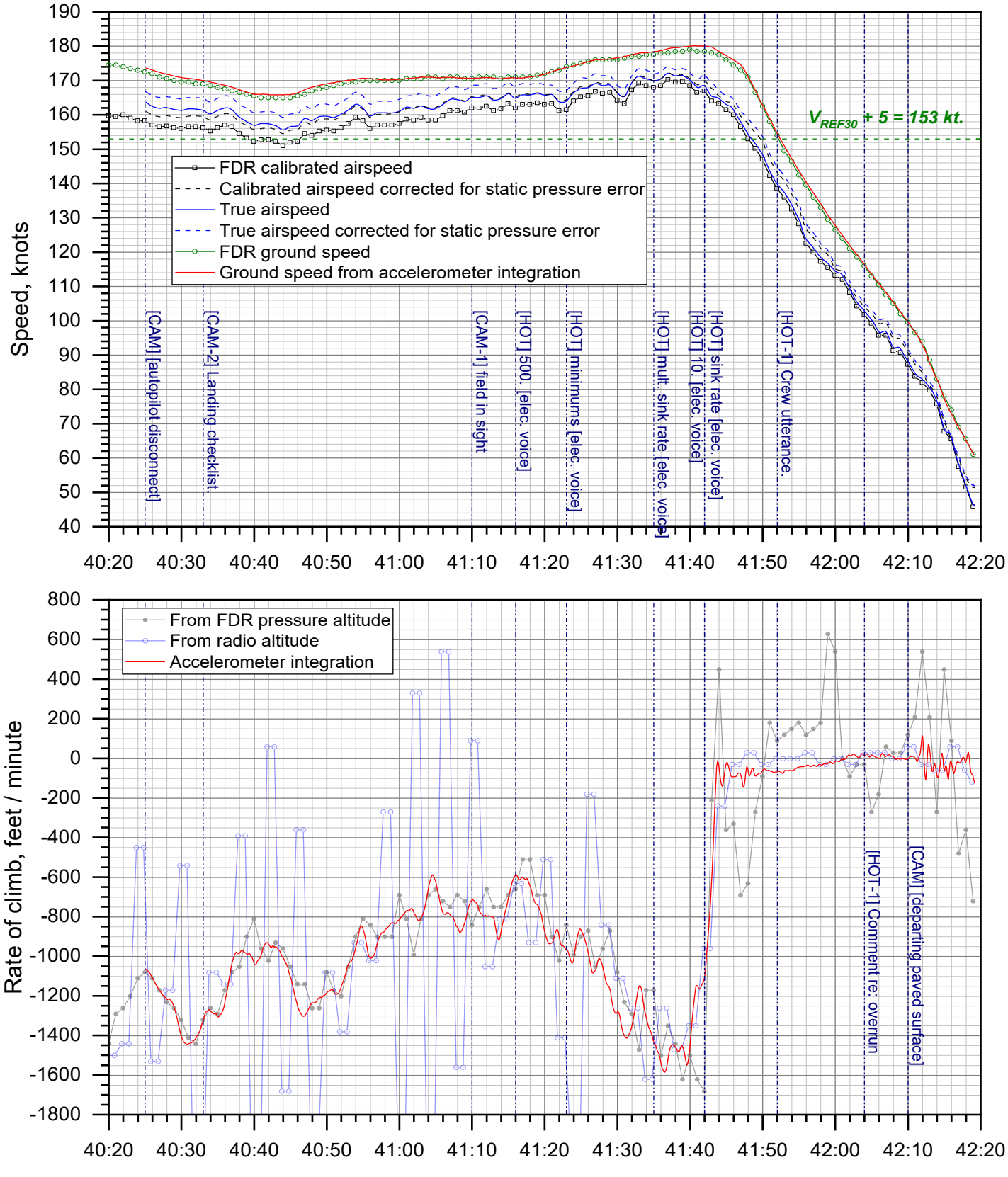

Figure 9a.

DCA19MA143: Miami Air flight 293, Boeing 737-800 N732MA, Jacksonville, FL, May 3, 2019

Speed and rate of climb during final approach, landing, and rollout (detail)

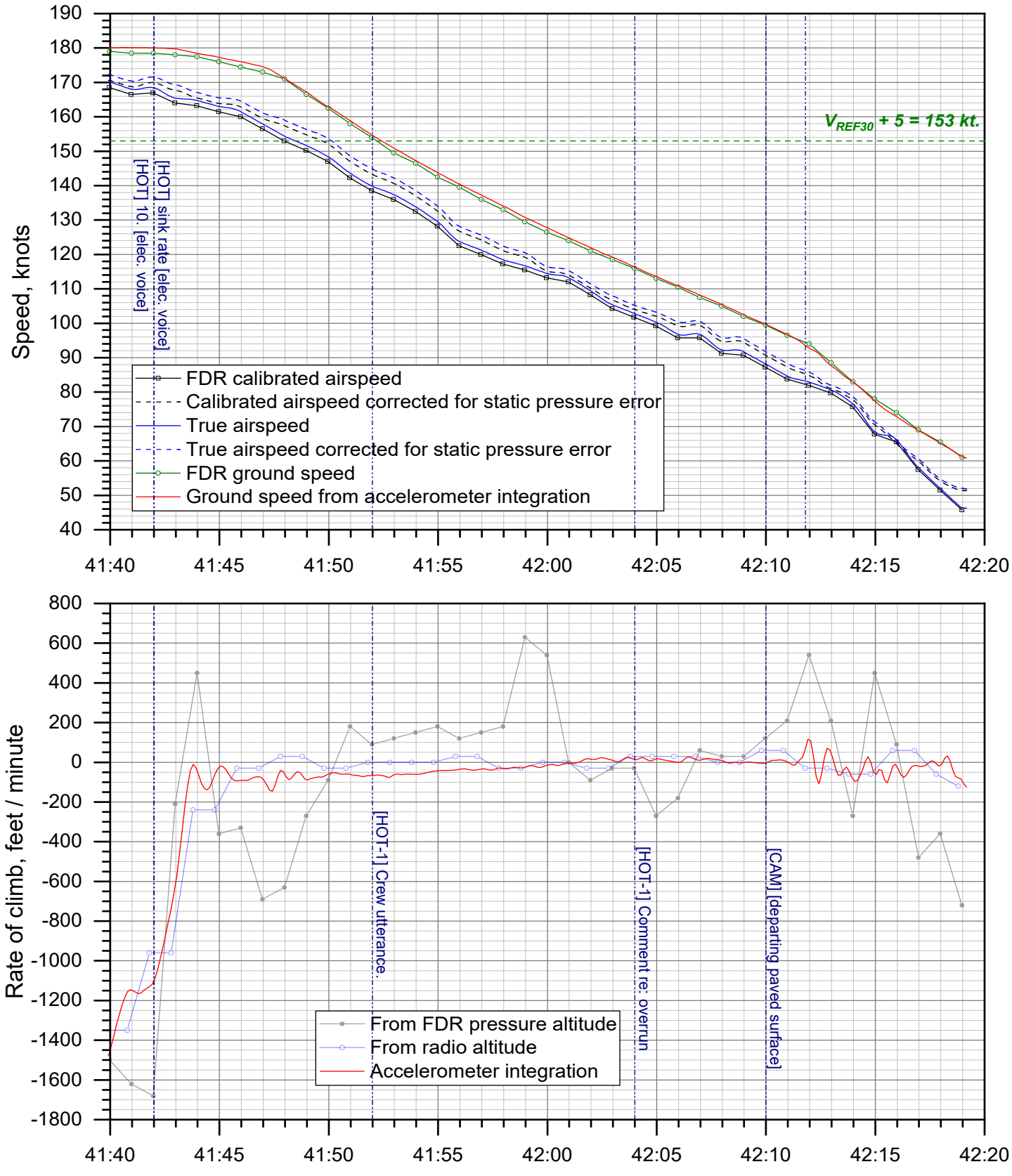

Figure 9b.

DCA19MA143: Miami Air flight 293, Boeing 737-800 N732MA, Jacksonville, FL, May 3, 2019

Load factors during final approach, landing, and rollout

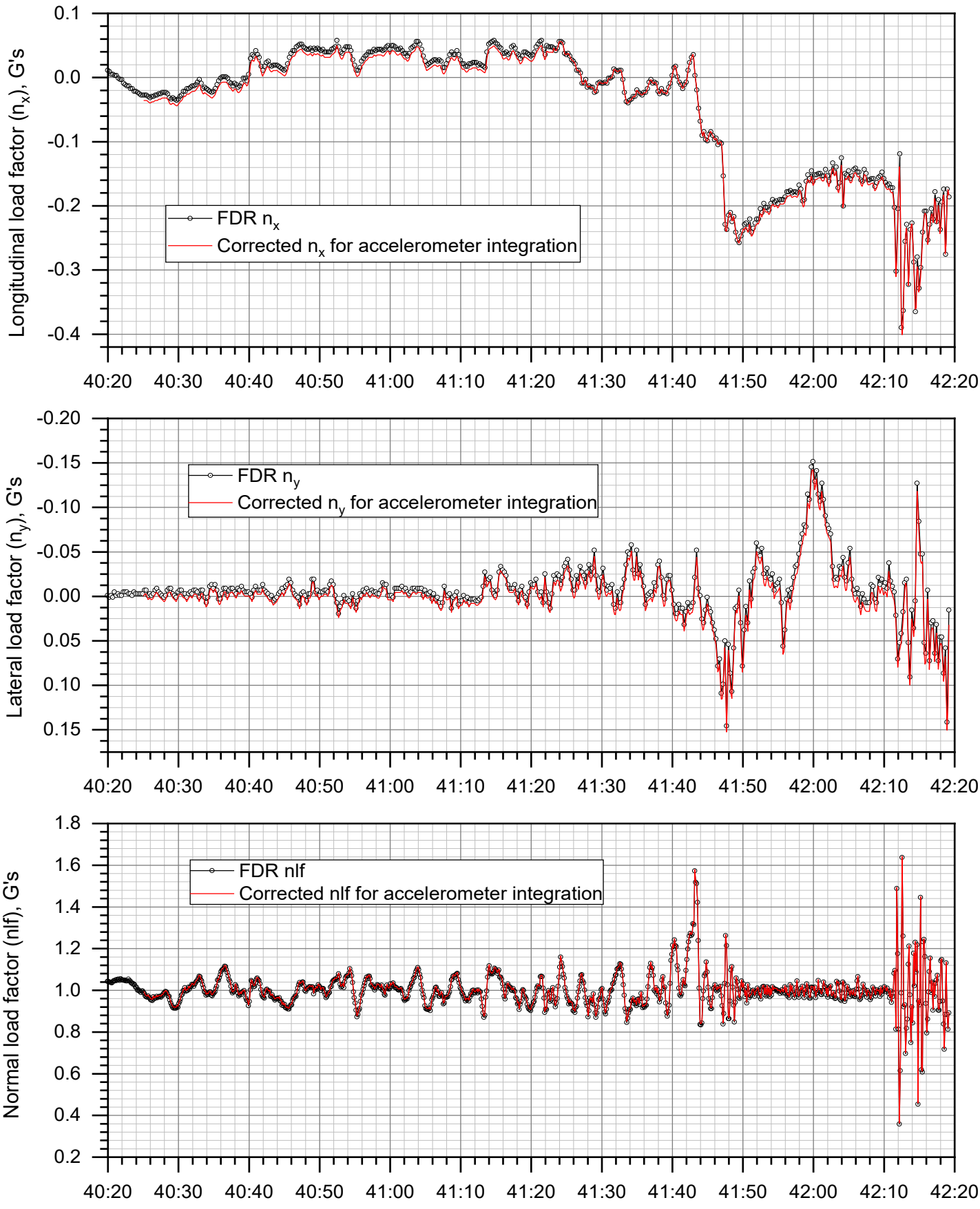

Figure 10a.

DCA19MA143: Miami Air flight 293, Boeing 737-800 N732MA, Jacksonville, FL, May 3, 2019

Load factors during final approach, landing, and rollout (detail)

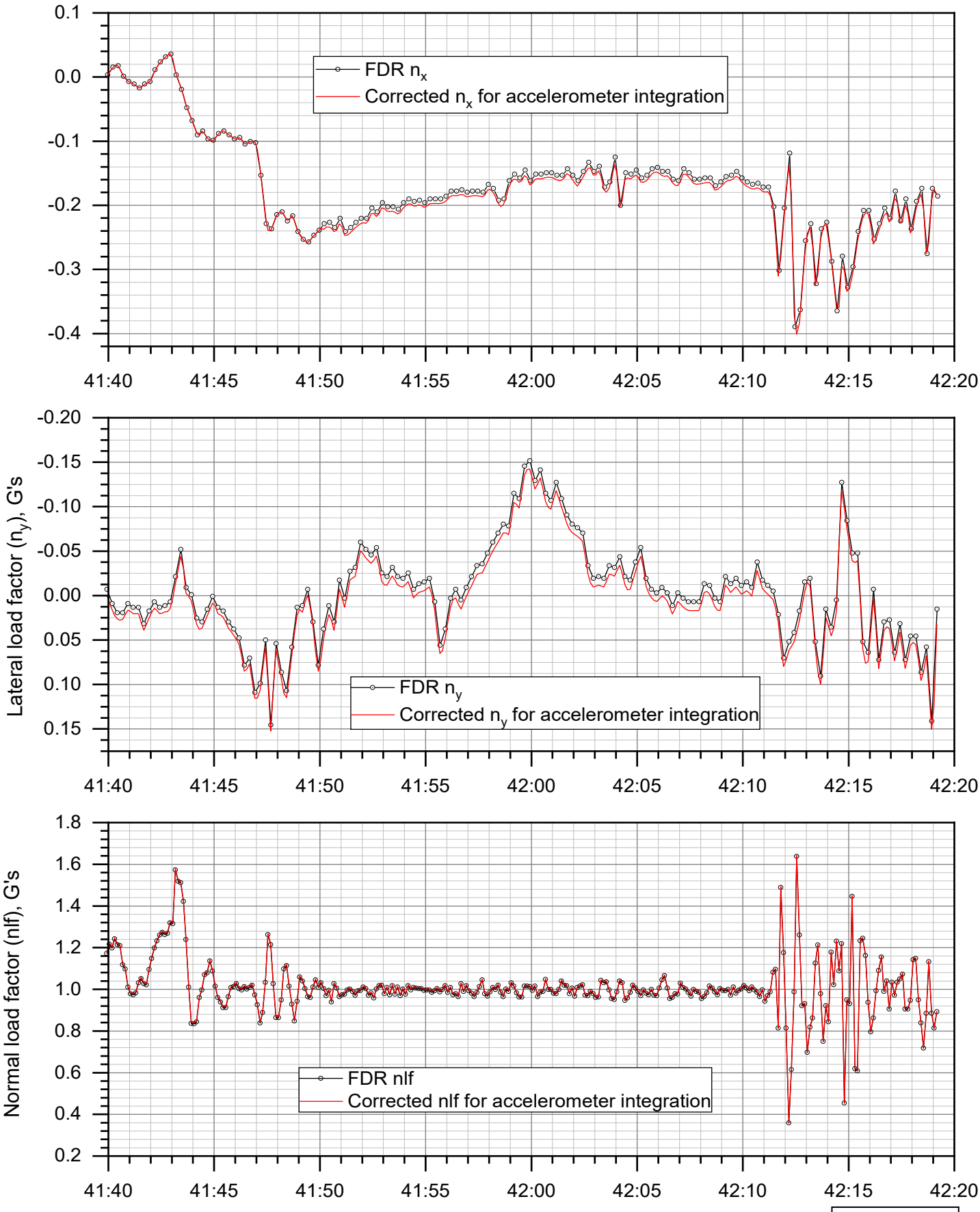

Figure 10b.

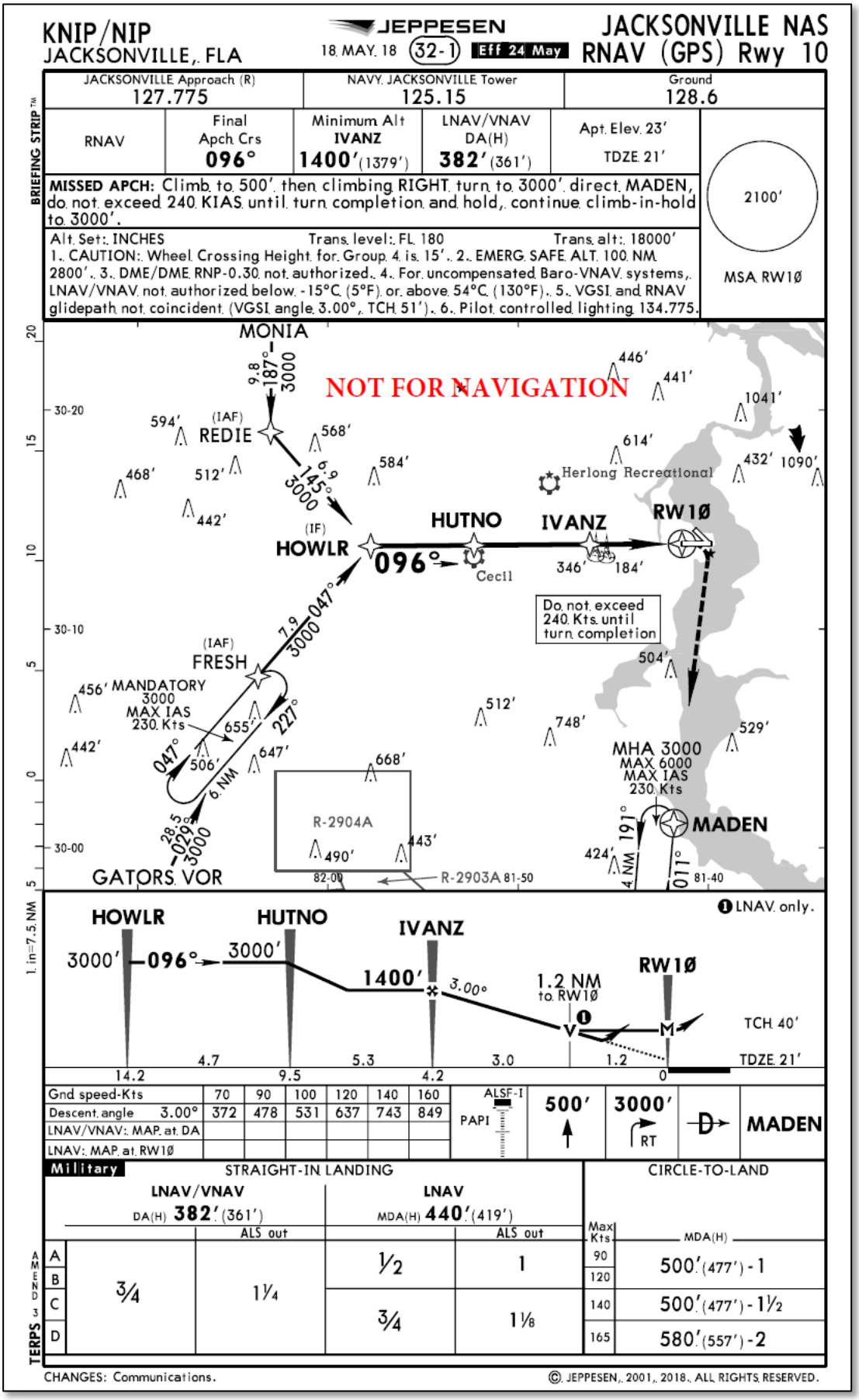

Figure 11. KNIP RNAV (GPS) Rwy 10 instrument approach plate.

DCA19MA143: Miami Air flight 293, Boeing 737-800 N732MA, Jacksonville, FL, May 3, 2019

Euler angles during final approach, landing, and rollout

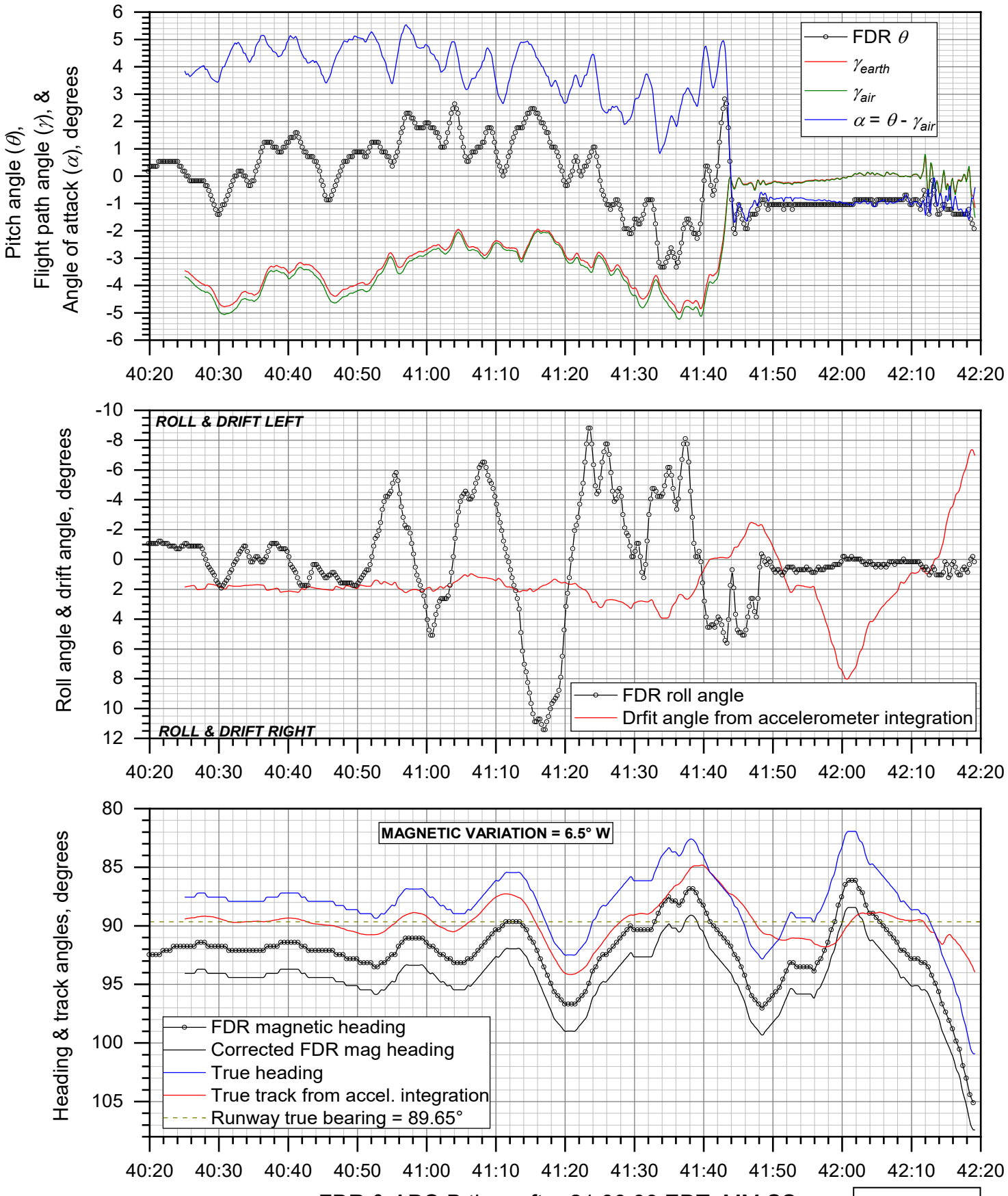

Figure 12a.

DCA19MA143: Miami Air flight 293, Boeing 737-800 N732MA, Jacksonville, FL, May 3, 2019

Euler angles during final approach, landing, and rollout (detail)

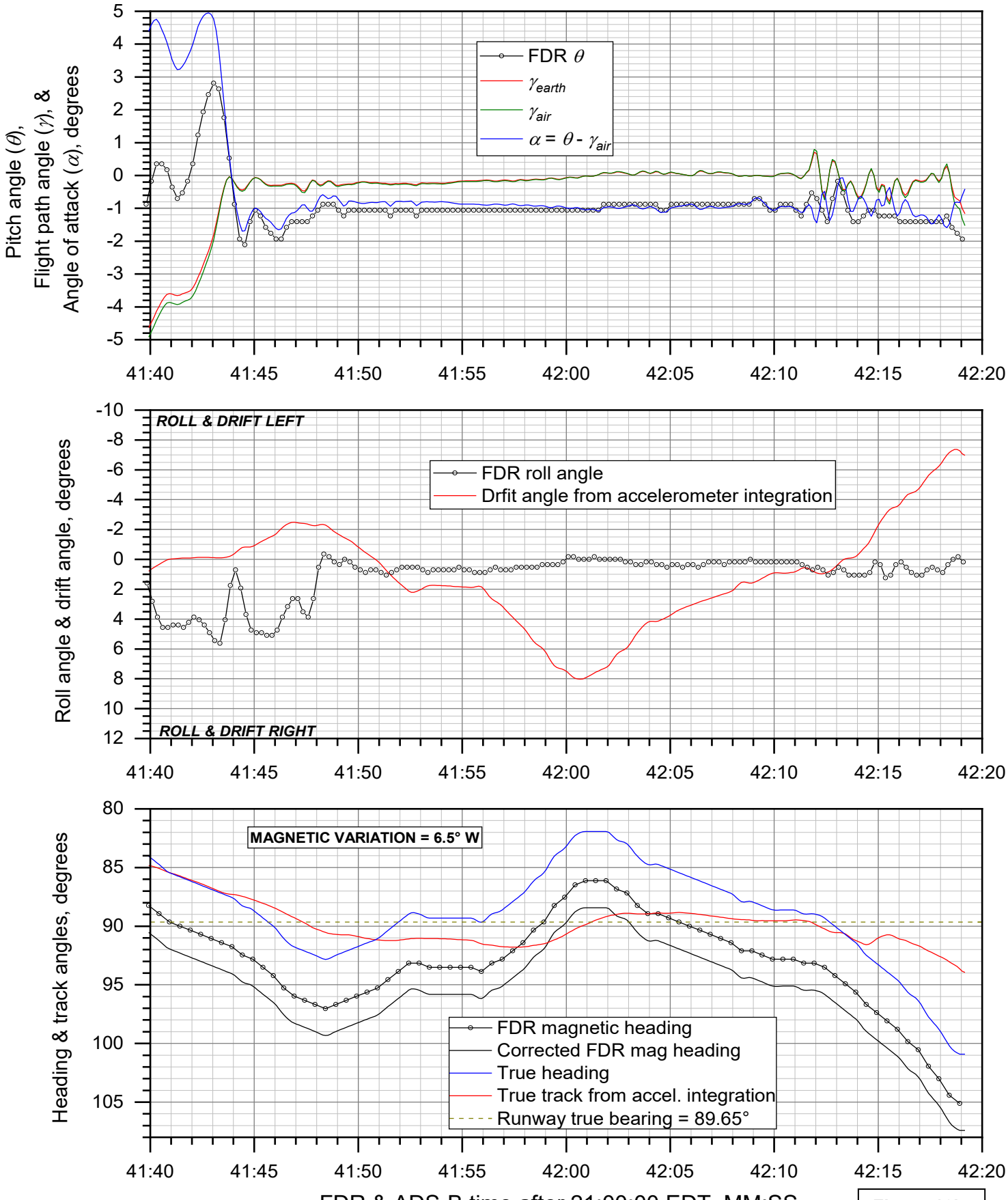

Figure 12b.

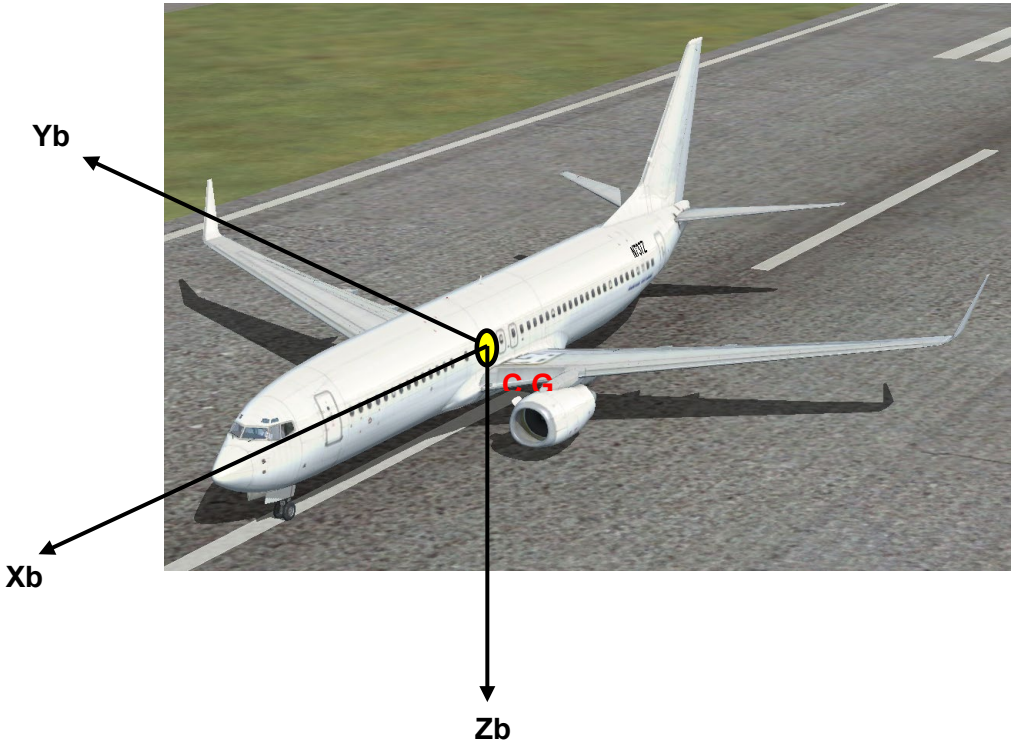

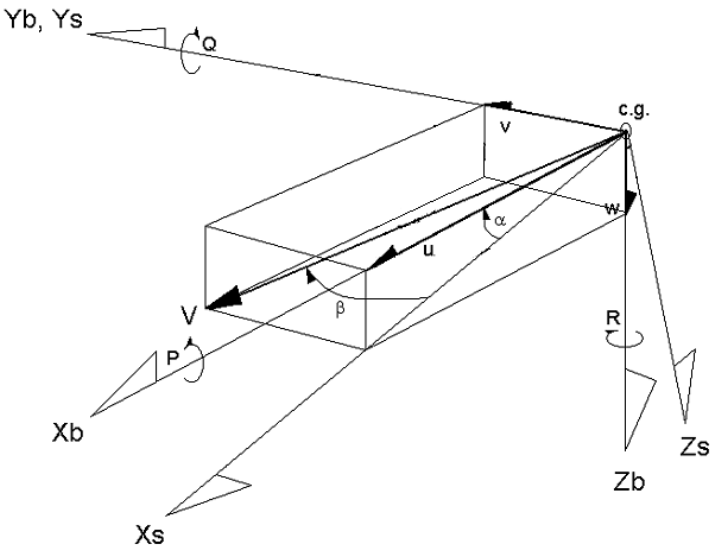

C.G. = center of gravity

{Xb, Yb, Zb} = body axis system

{Xs, Ys, Zs} = stability axis system

V = velocity vector

α = angle of attack

β = sideslip angle

P = body axis roll rate

Q = body axis pitch rate

R = body axis yaw rate

u = component of V along Xb

v = component of V along Yb

w = component of V along Zb

Figure 13. Airplane body axis system, body-axis components of linear and angular velocities, and definitions of α and β.

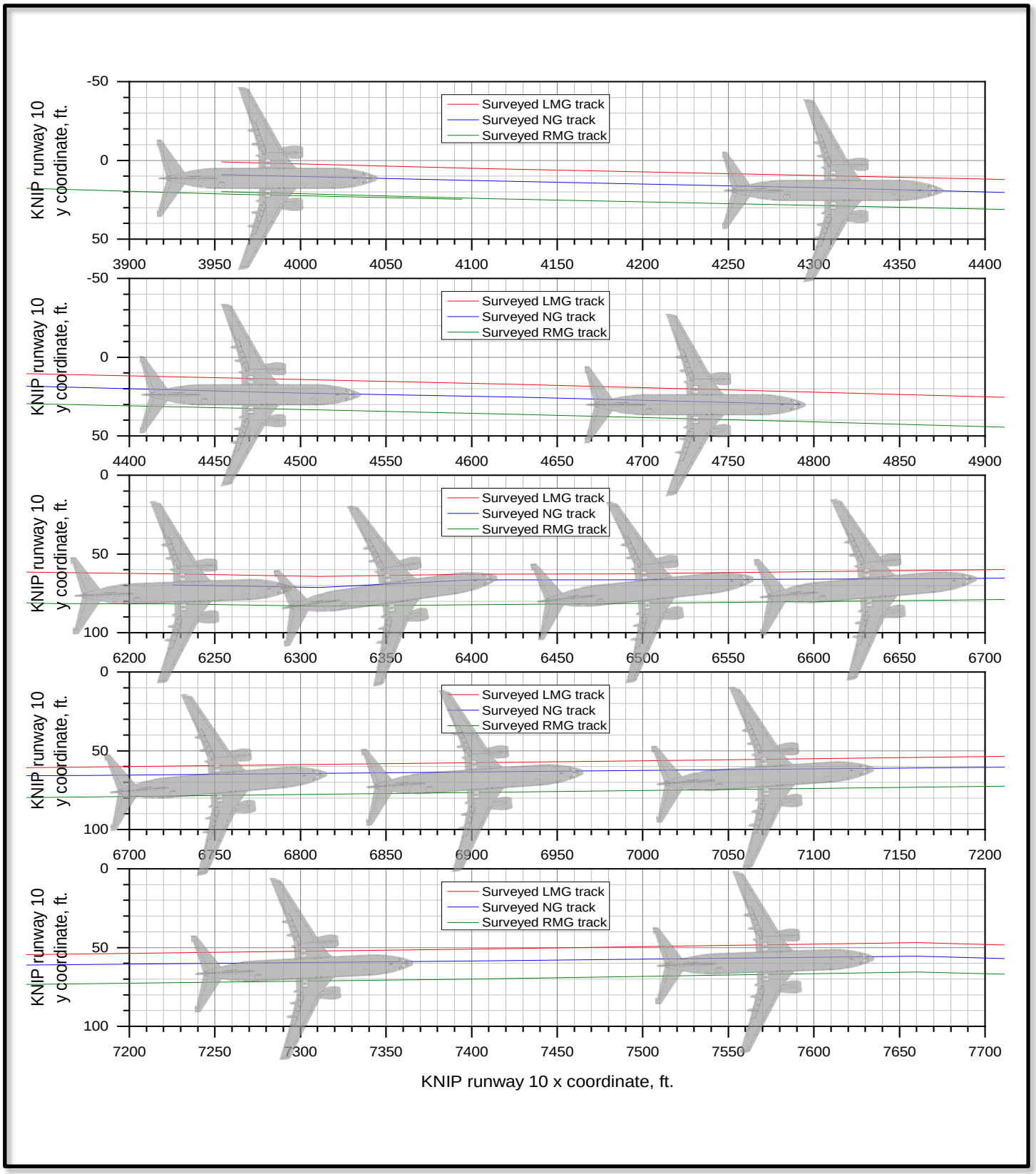

Figure 14. Determining airplane heading by overlaying to-scale drawings of the airplane over tire mark measurements.

DCA19MA143: Miami Air flight 293, Boeing 737-800 N732MA, Jacksonville, FL, May 3, 2019

Heading correction based on takeoff from MUGM and tire marks at KNIP

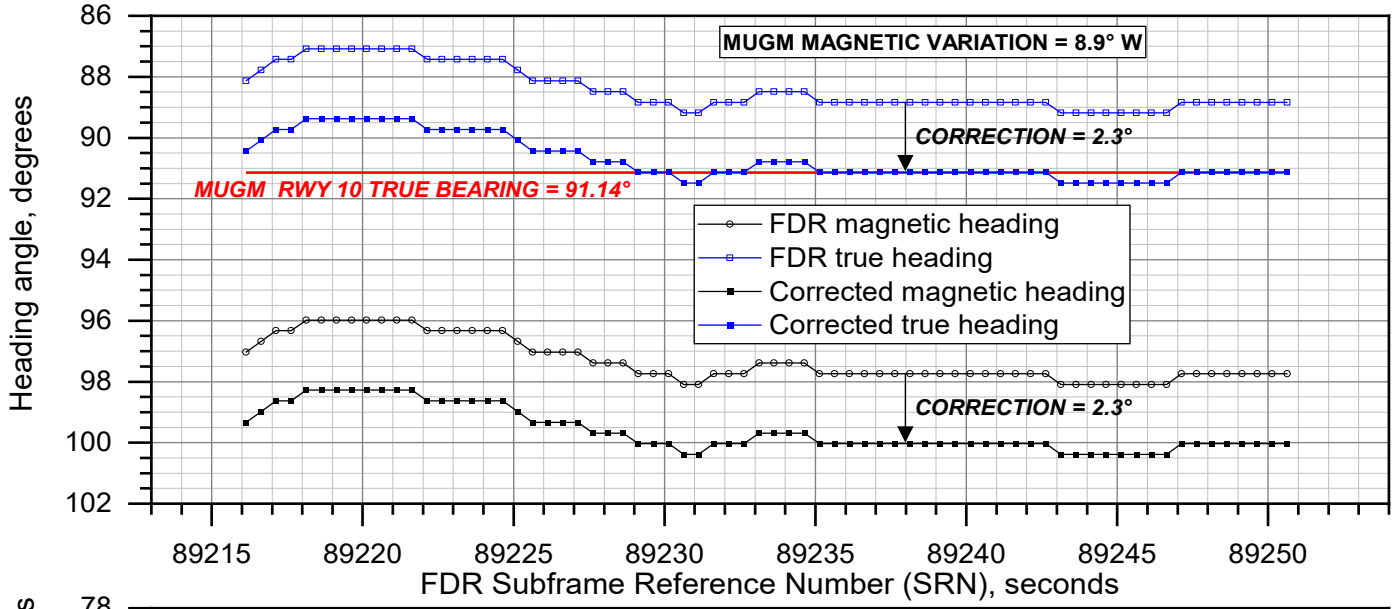

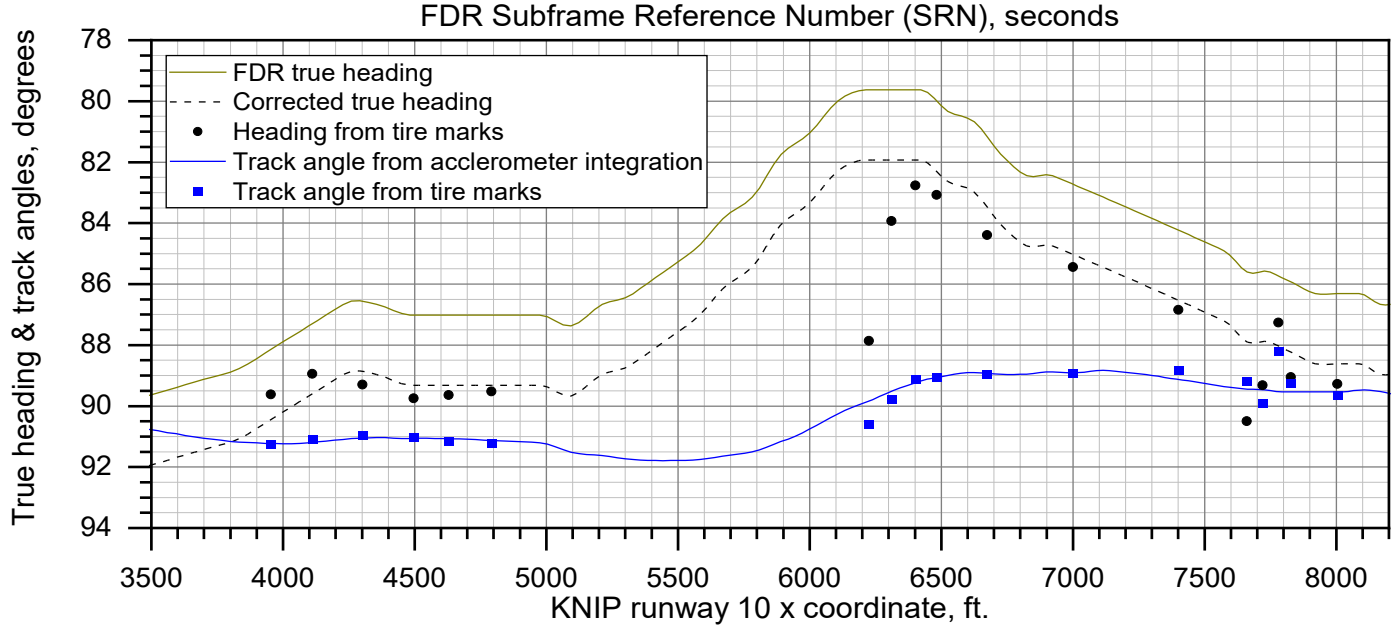

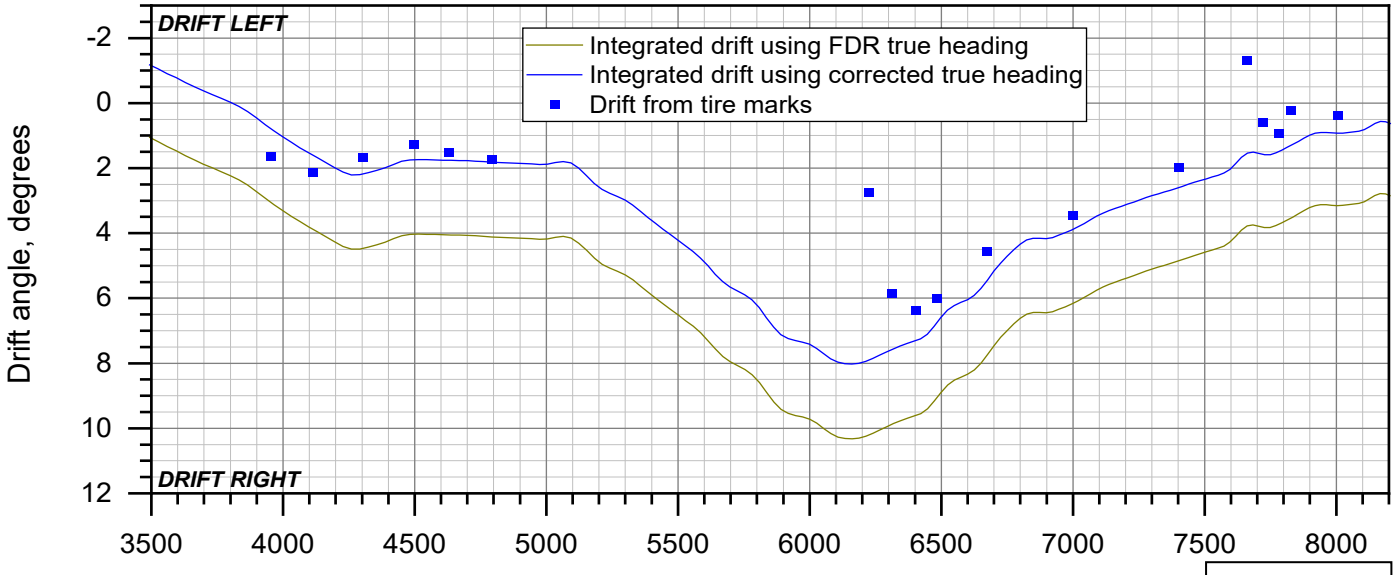

Figure 15.

DCA19MA143: Miami Air flight 293, Boeing 737-800 N732MA, Jacksonville, FL, May 3, 2019

Winds during final approach, landing, and rollout

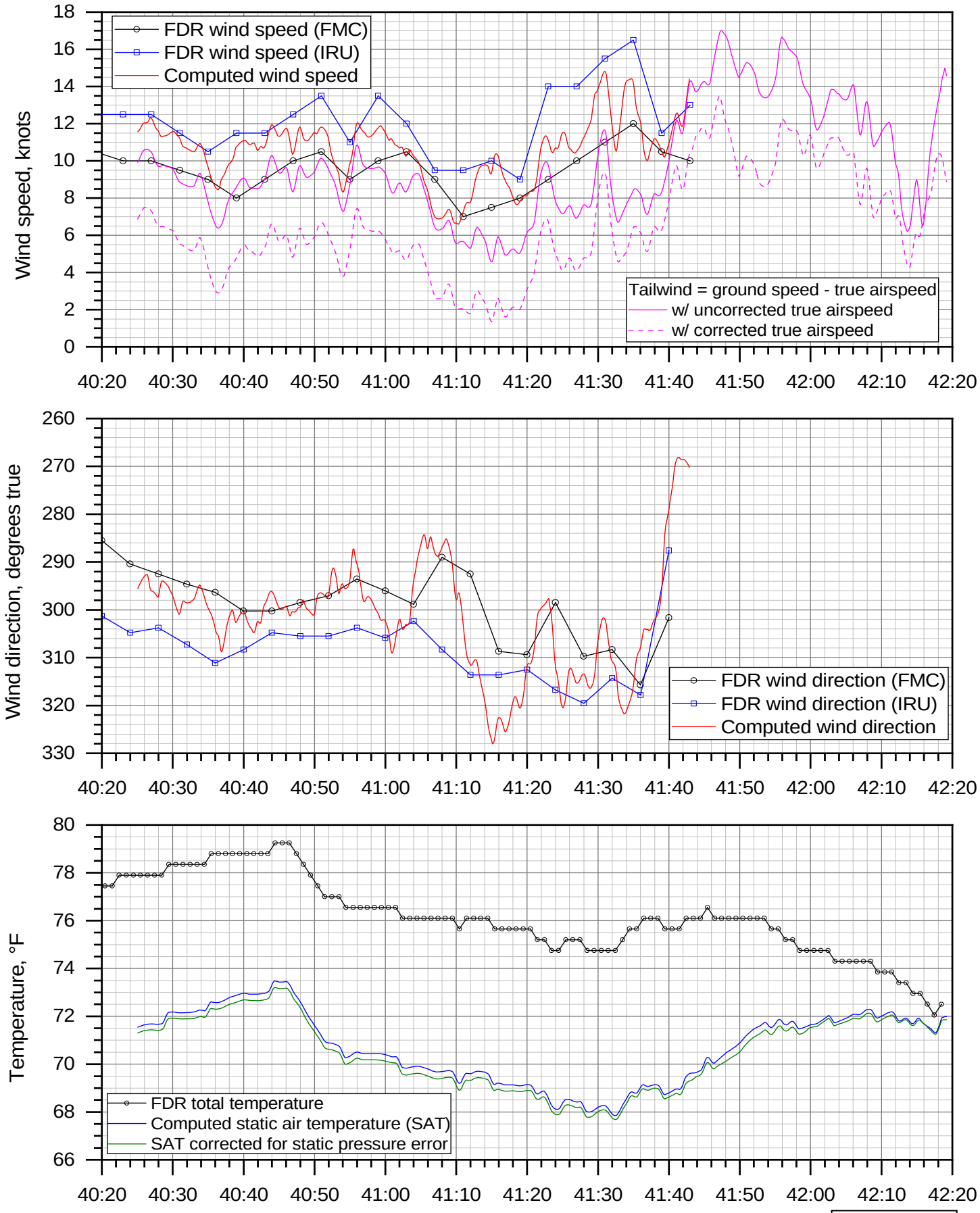

Figure 16.

DCA19MA143: Miami Air flight 293, Boeing 737-800 N732MA, Jacksonville, FL, May 3, 2019

Flight controls during approach, landing and rollout

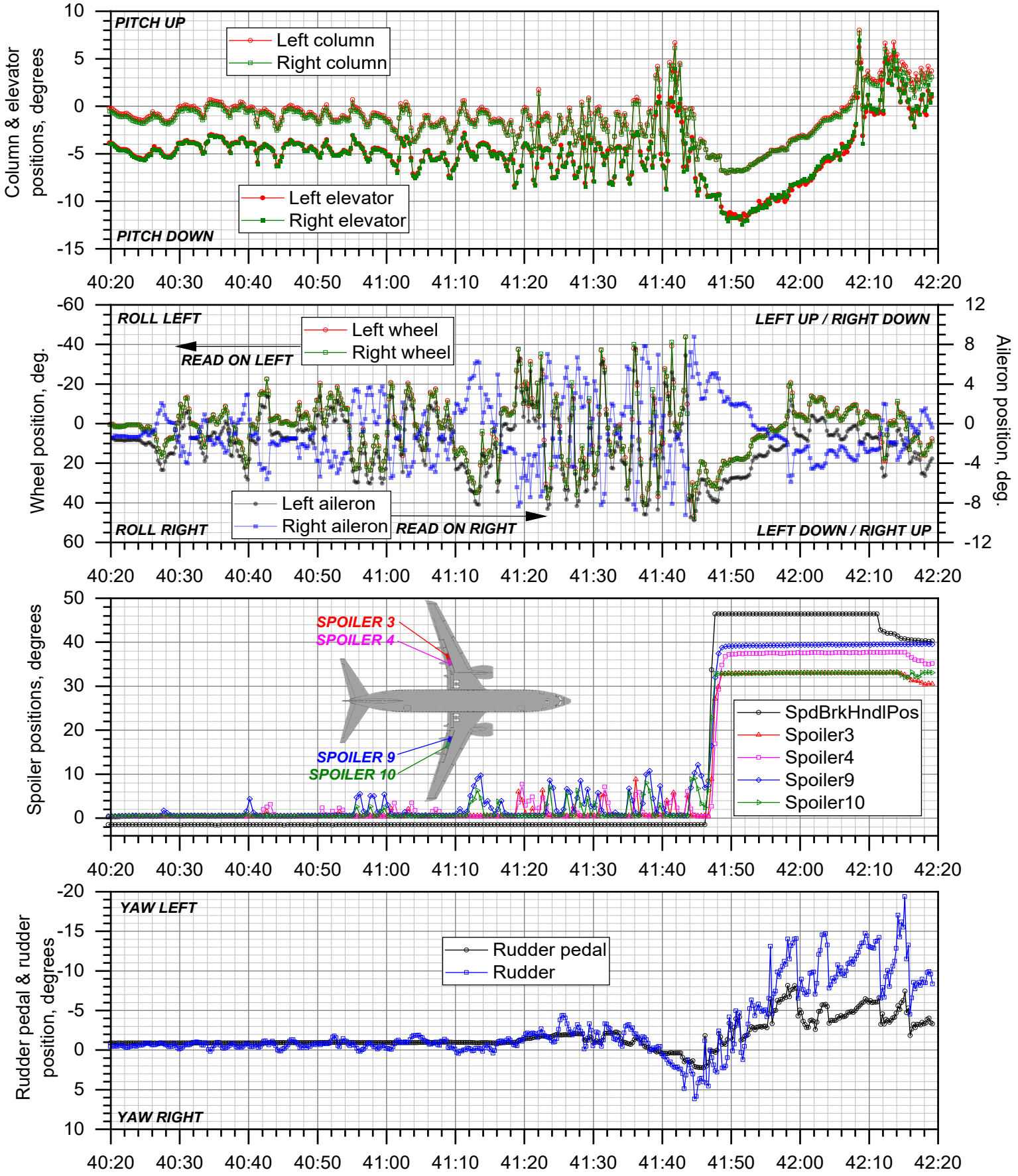

Figure 17a.

DCA19MA143: Miami Air flight 293, Boeing 737-800 N732MA, Jacksonville, FL, May 3, 2019

Flight controls during approach, landing and rollout (detail)

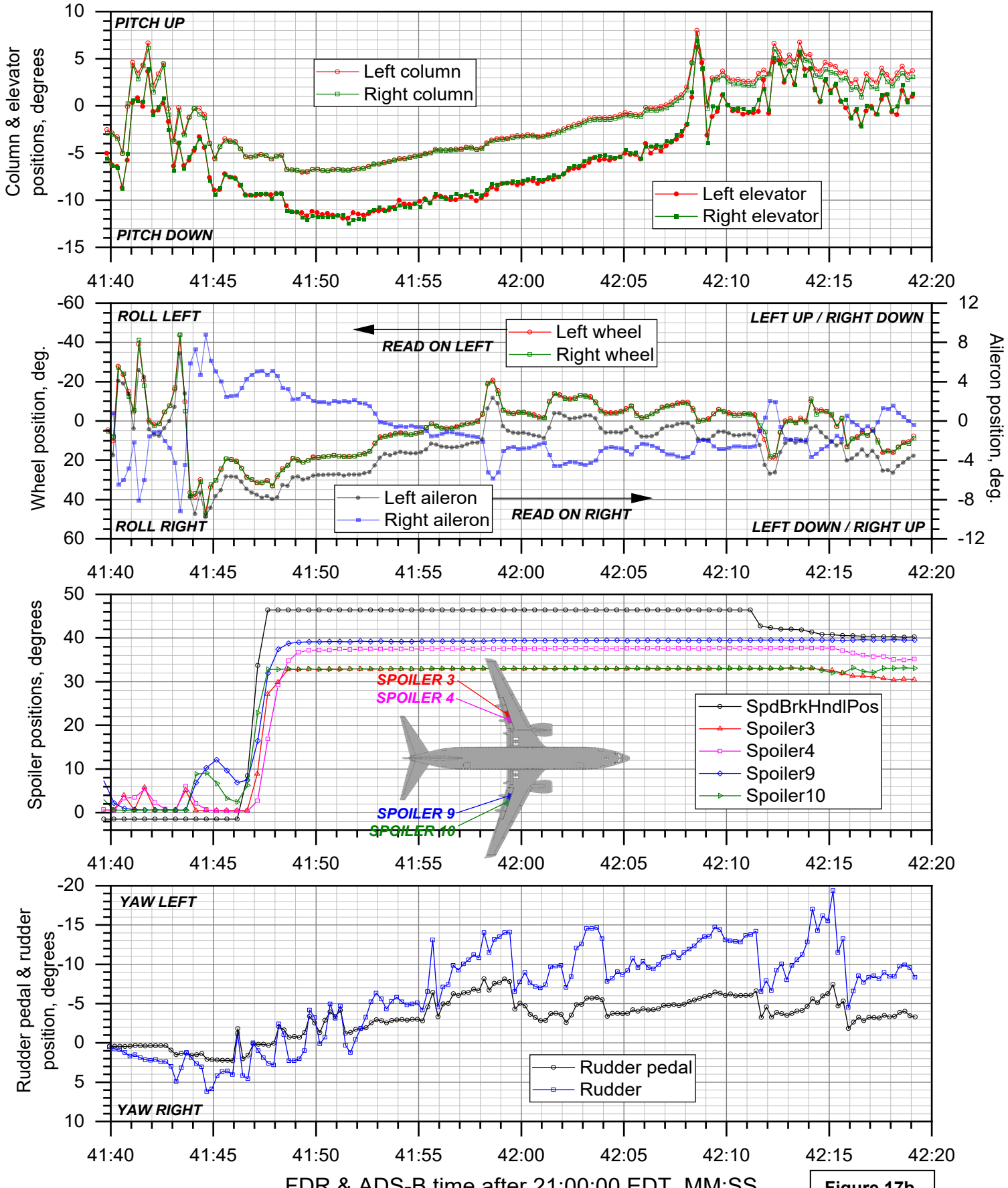

Figure 17b.

DCA19MA143: Miami Air flight 293, Boeing 737-800 N732MA, Jacksonville, FL, May 3, 2019

Deceleration performance during landing and rollout

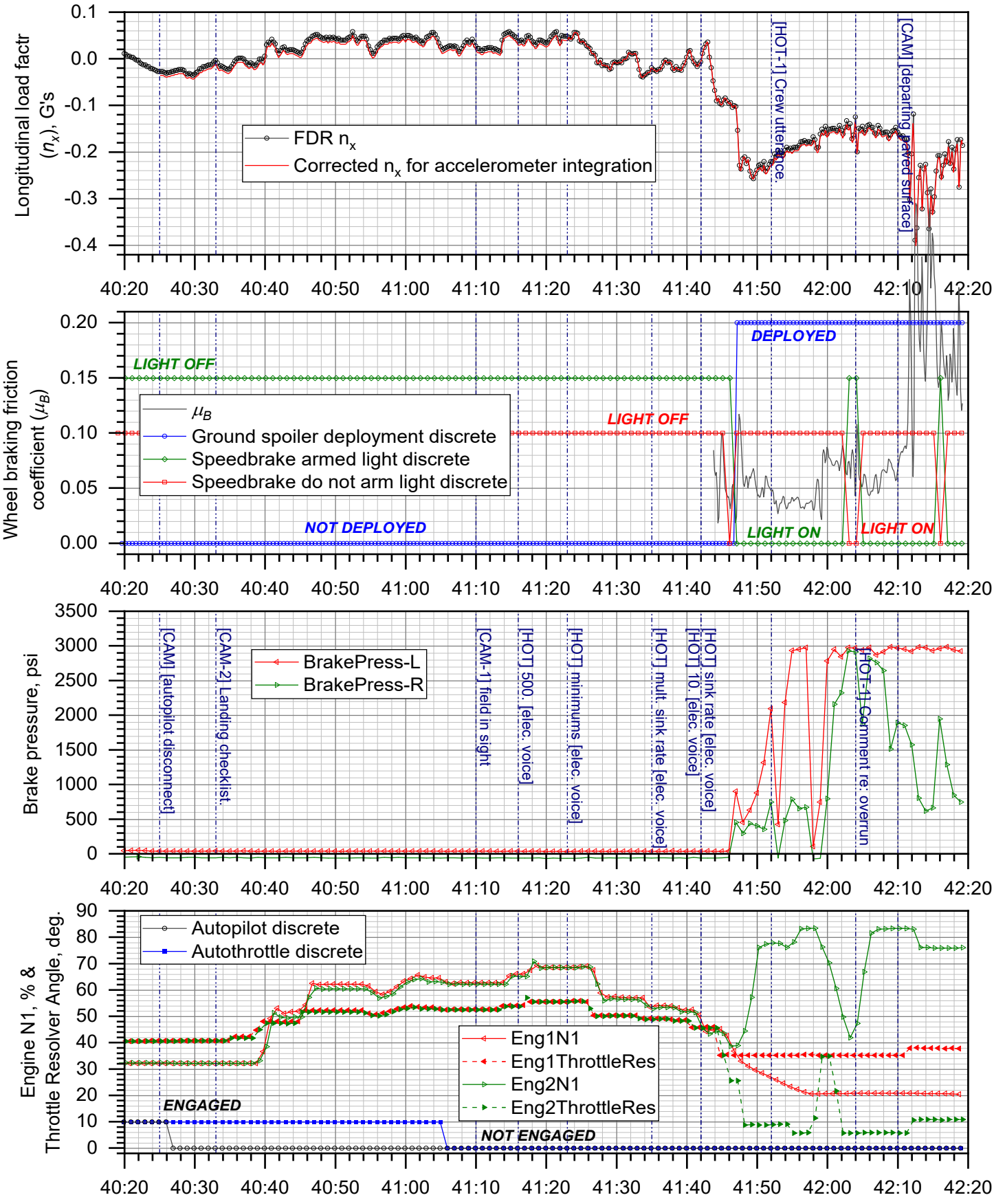

Figure 18.

DCA19MA143: Miami Air flight 293, Boeing 737-800 N732MA, Jacksonville, FL, May 3, 2019

Deceleration performance during landing and rollout (detail)

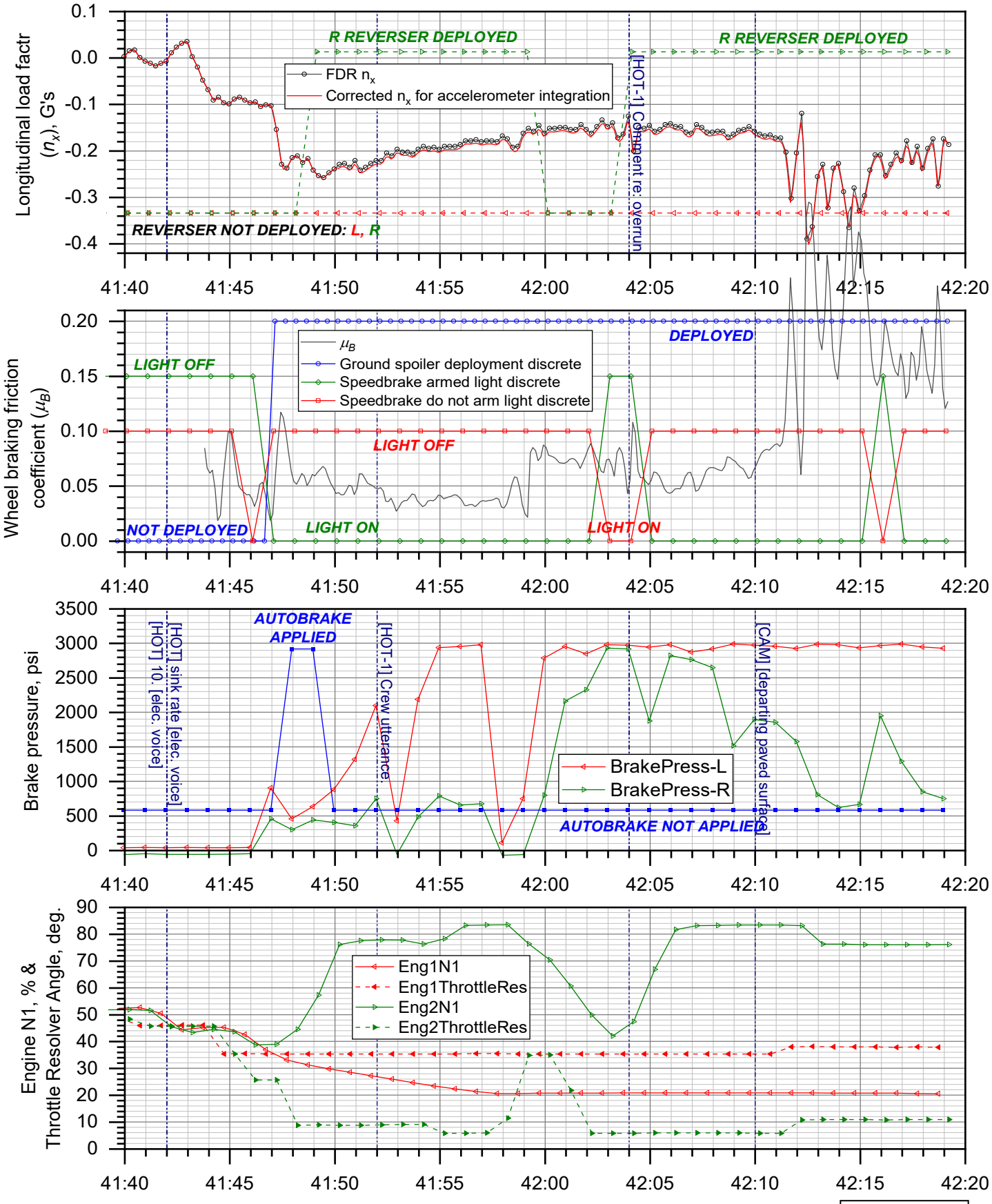

Figure 18b.

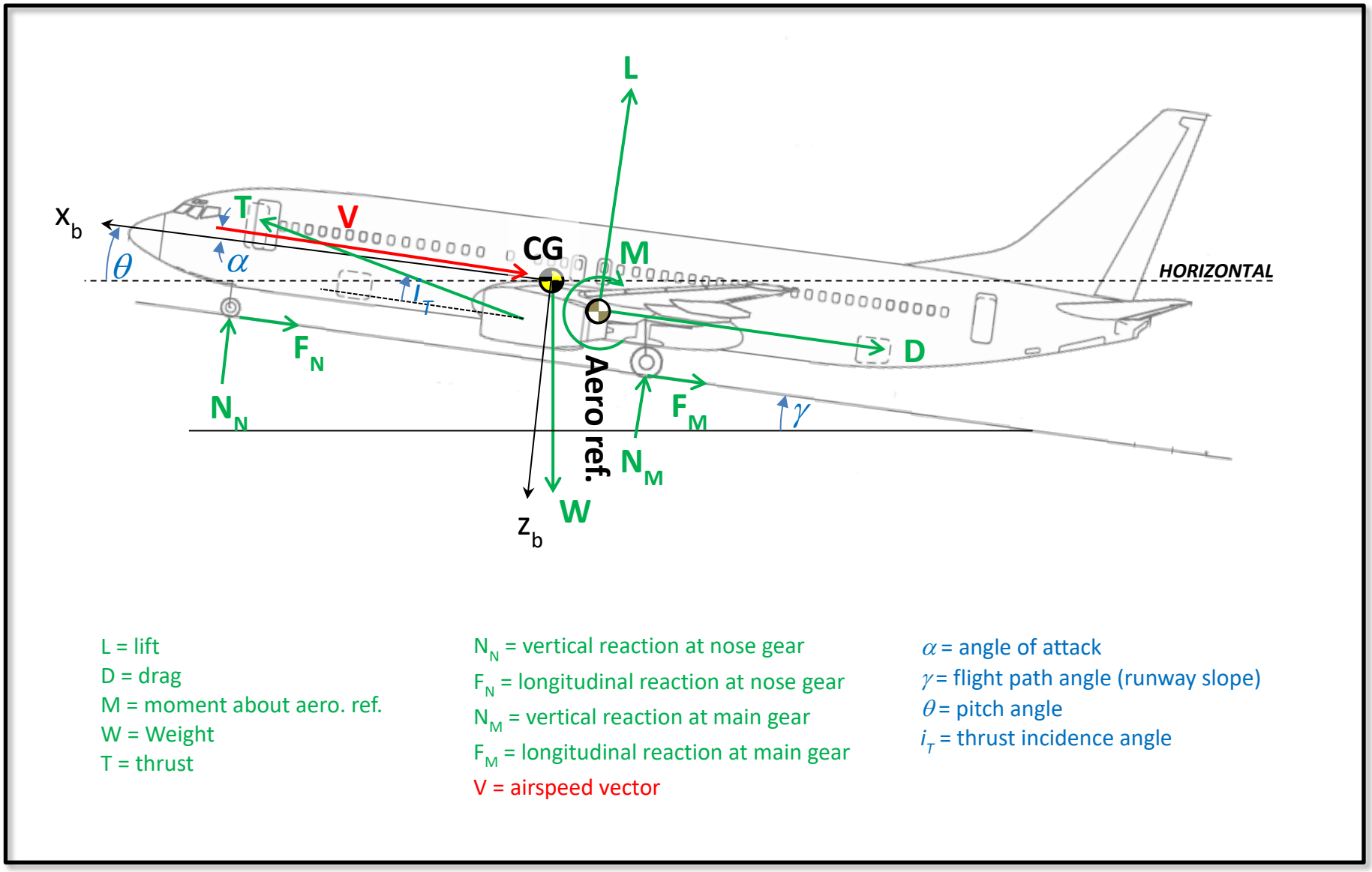

Figure 19. Free body diagram of forces on airplane during ground roll.

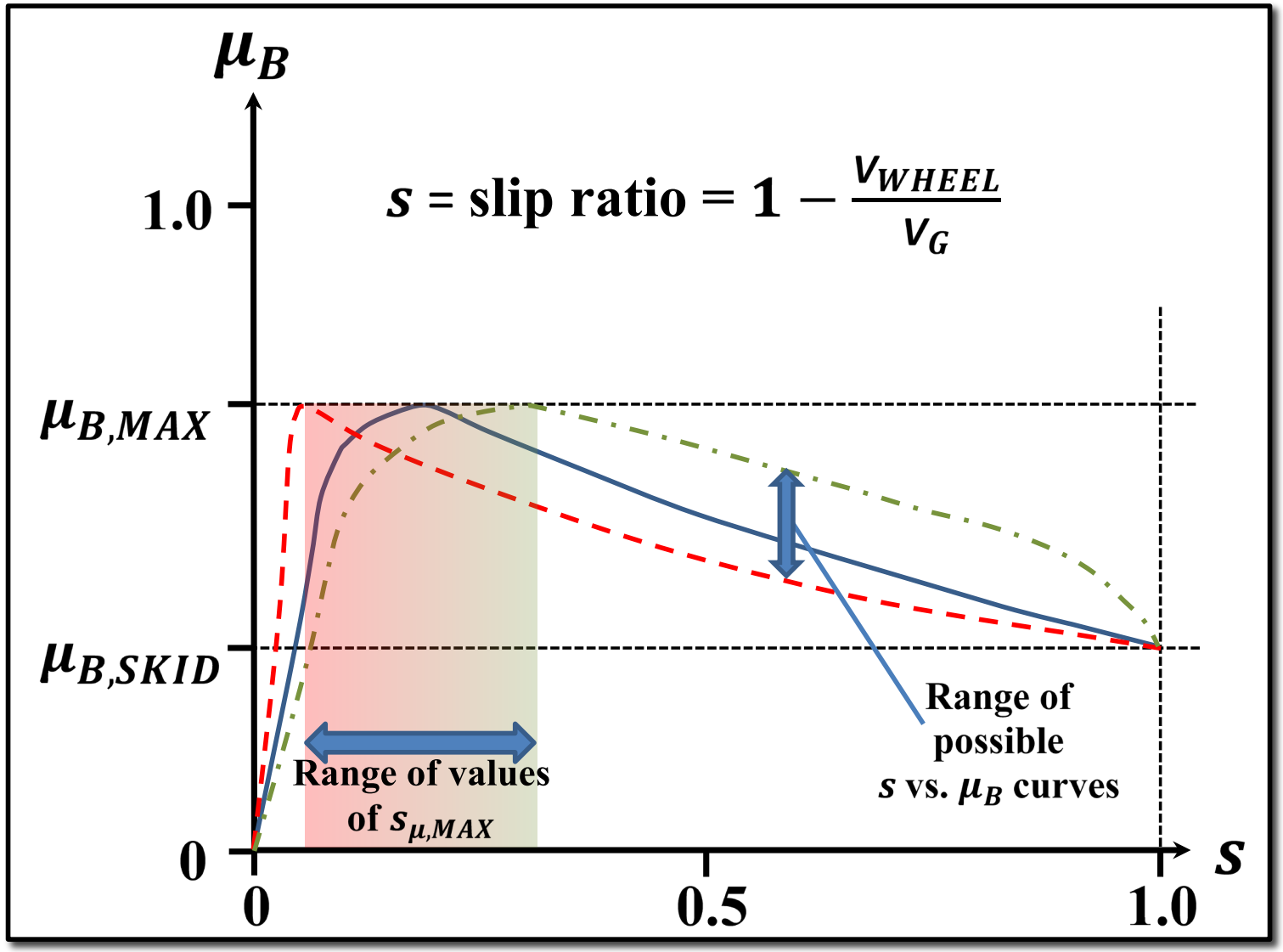

Figure 20. Effect of slip ratio s on the wheel braking friction coefficient μ_B.

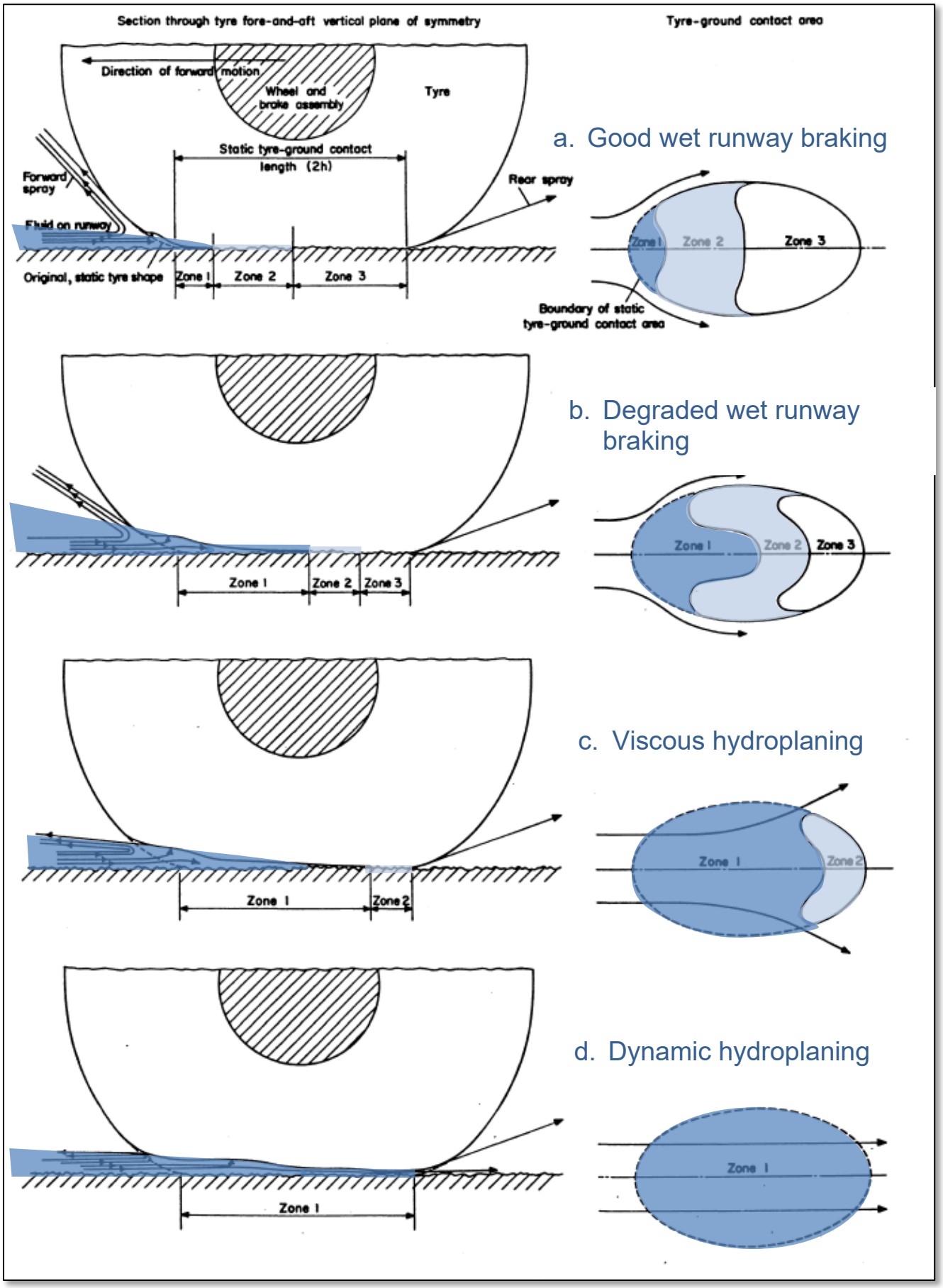

Figure 21. Effect of forward speed on the tire-ground contact area in wet conditions, from Reference 21.

DCA19MA143: Miami Air flight 293, Boeing 737-800 N732MA, Jacksonville, FL, May 3, 2019

Rainfall rate per KNIP 1 and 5 minute ASOS observations

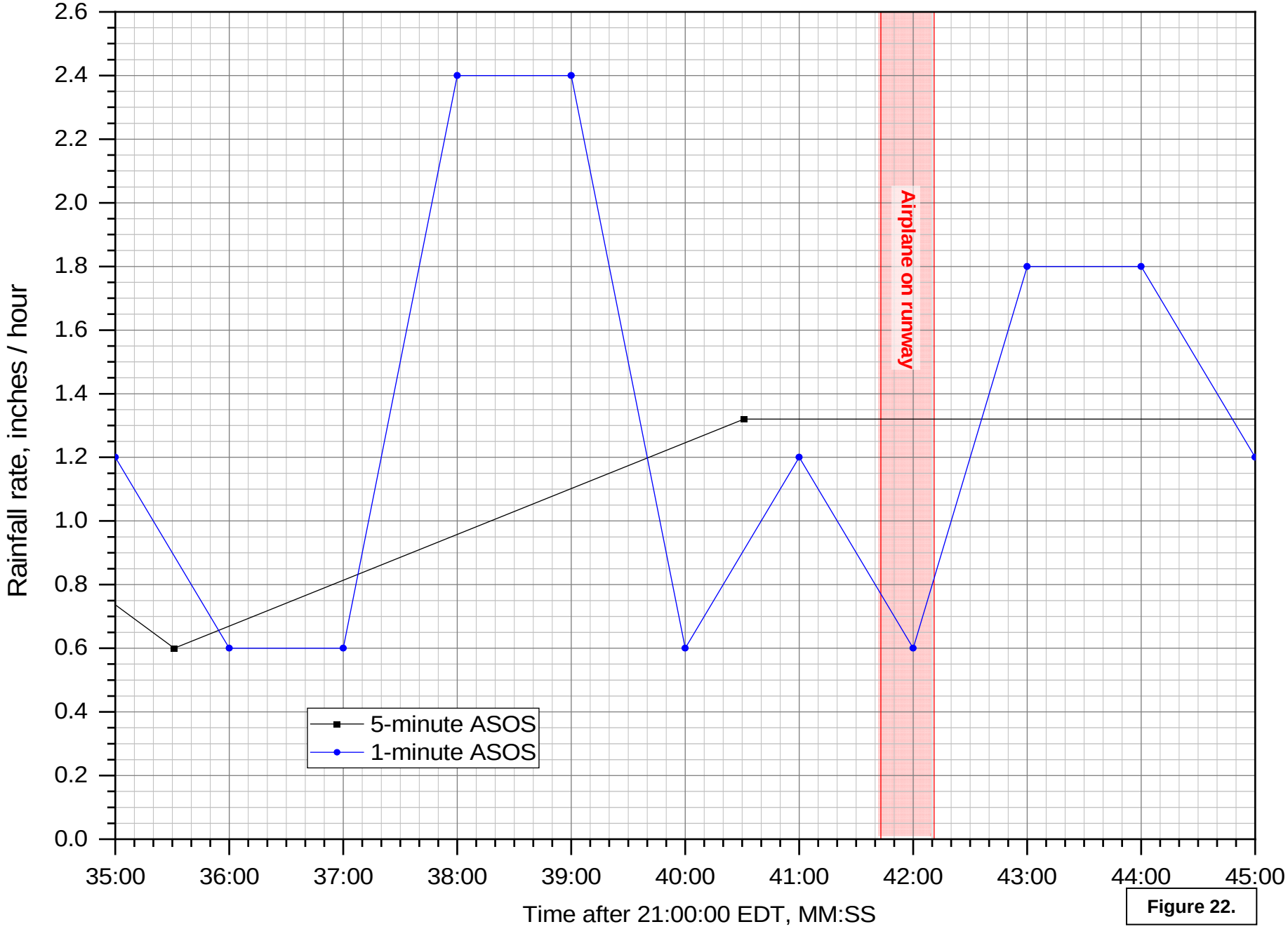

Figure 22.

Water depth on runway, based on TTI model and measured runway texture depth and cross-slope

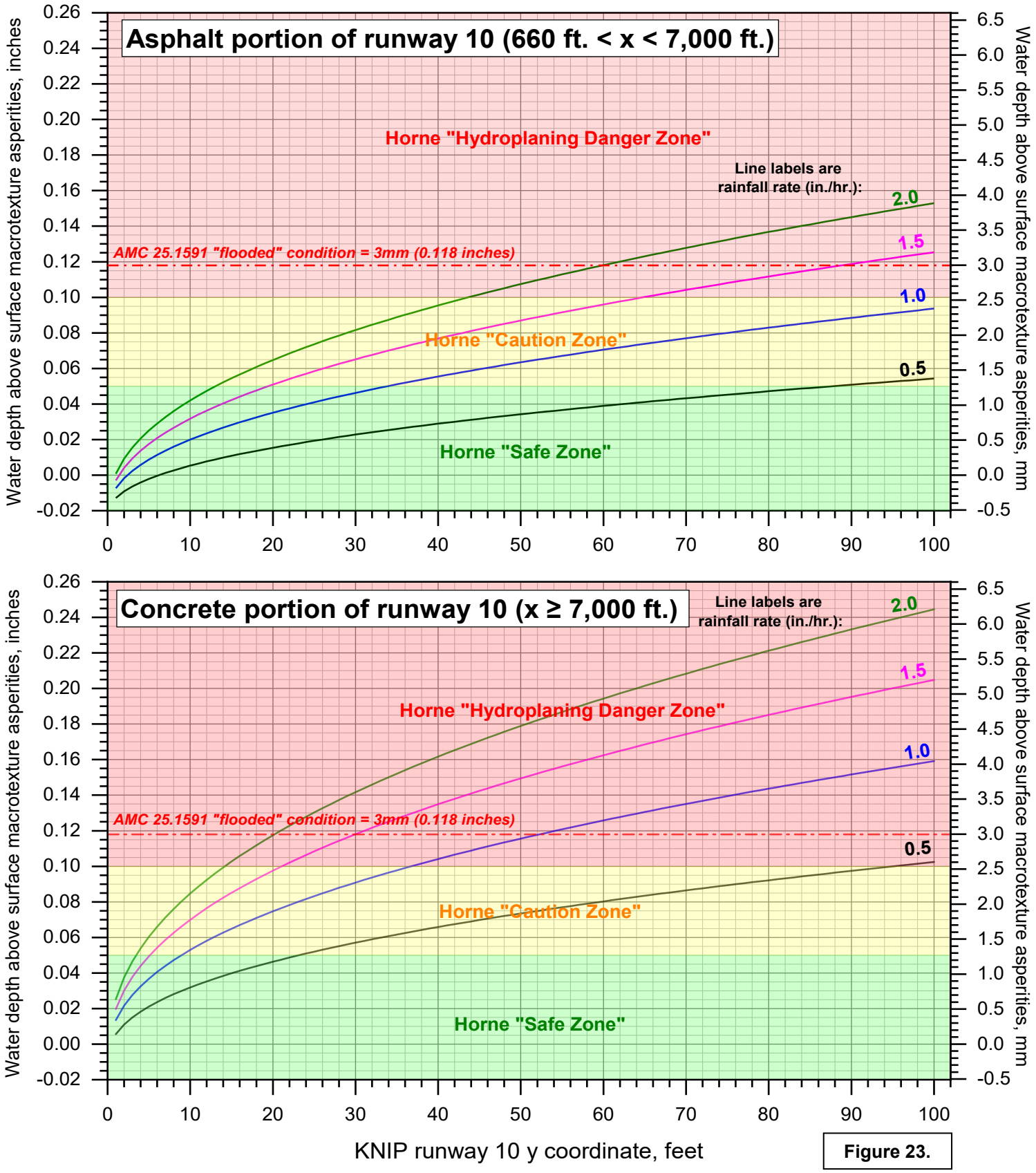

Figure 23.

DCA19MA143: Miami Air flight 293, Boeing 737-800 N732MA, Jacksonville, FL, May 3, 2019

μ_B comparisons vs. ground speed

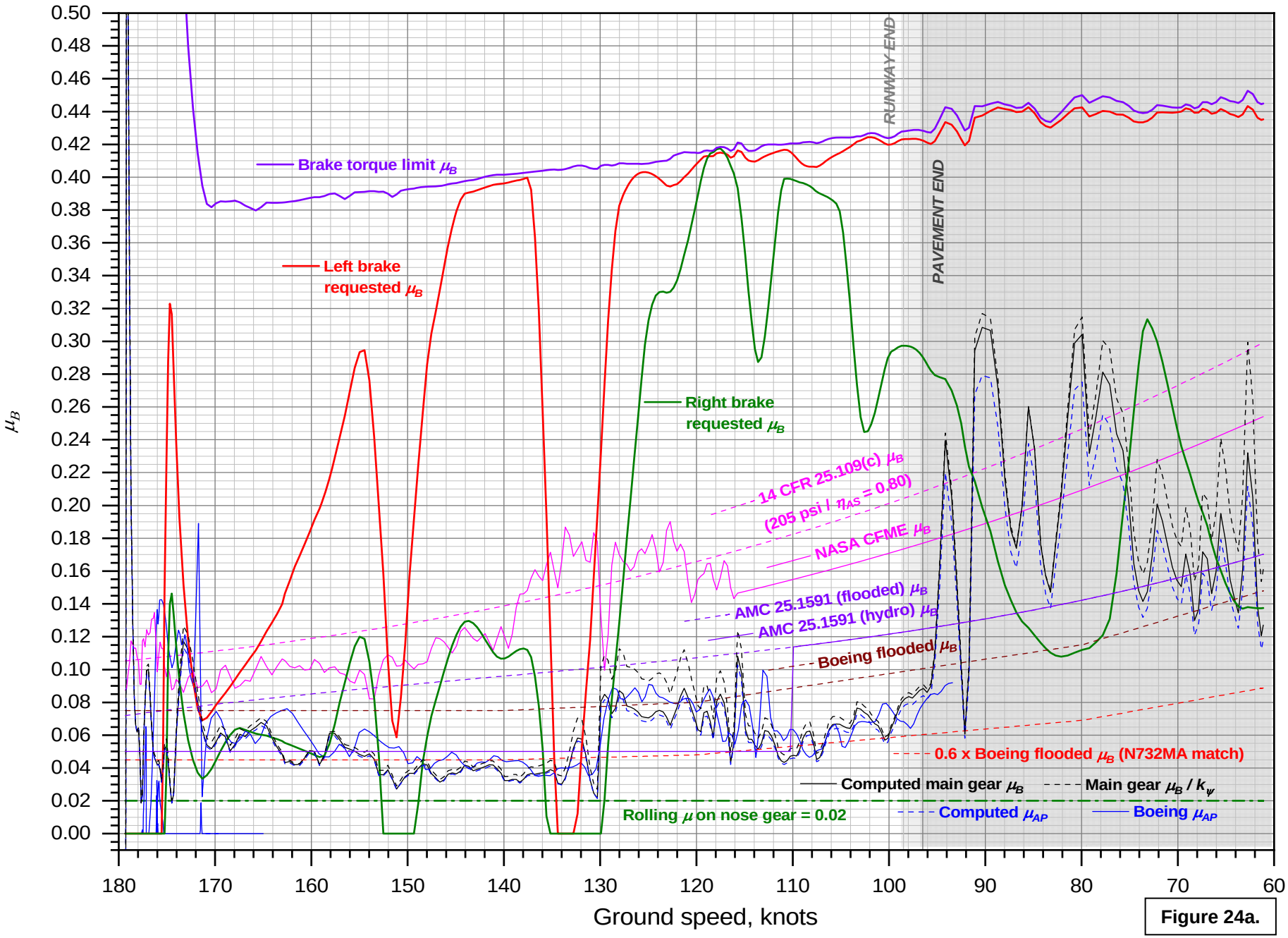

Figure 24a.

DCA19MA143: Miami Air flight 293, Boeing 737-800 N732MA, Jacksonville, FL, May 3, 2019

μ_B comparisons vs. ground speed - zero reverse thrust

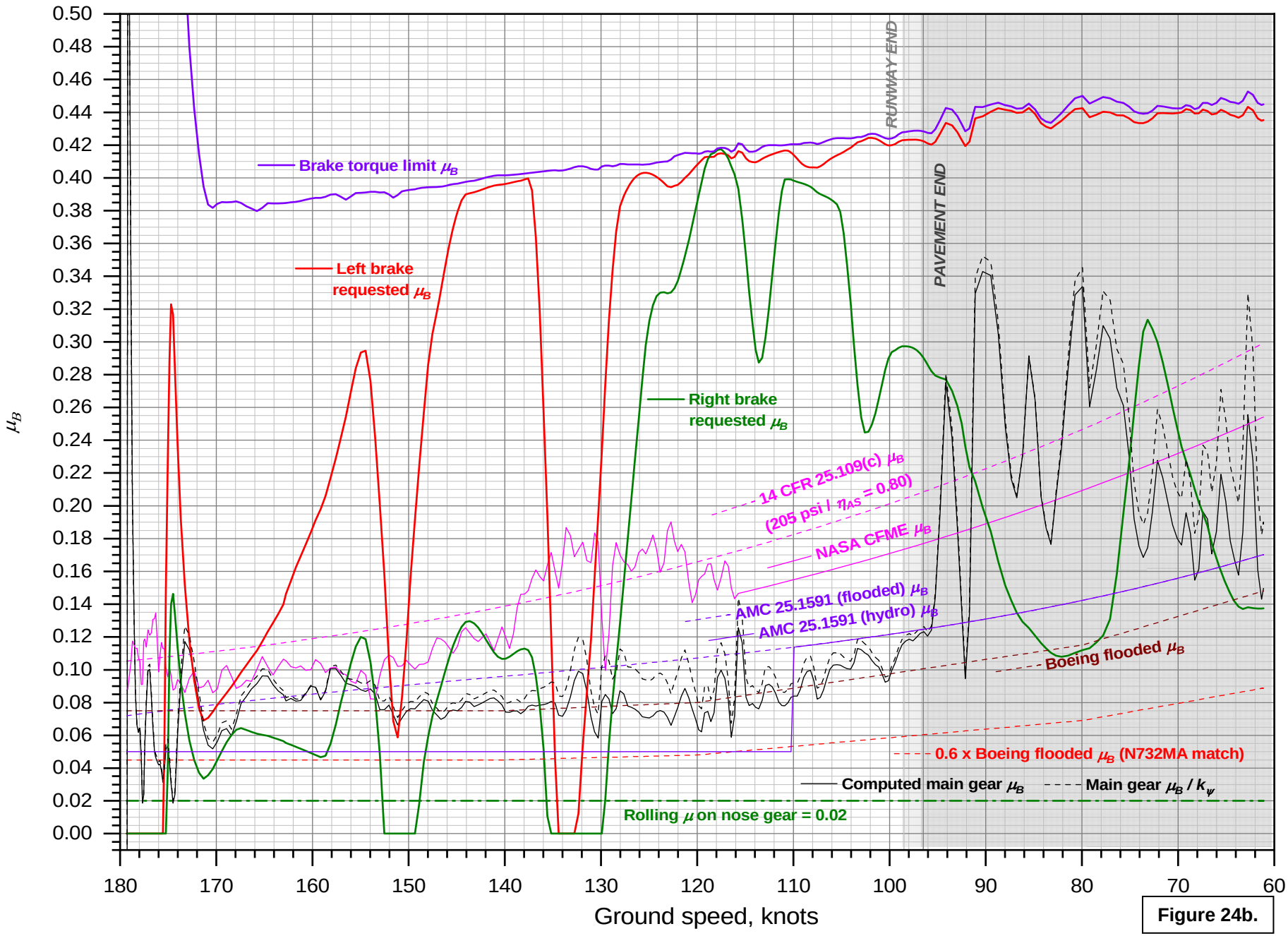

Figure 24b.

DCA19MA143: Miami Air flight 293, Boeing 737-800 N732MA, Jacksonville, FL, May 3, 2019

μ_B comparisons vs. distance from threshold

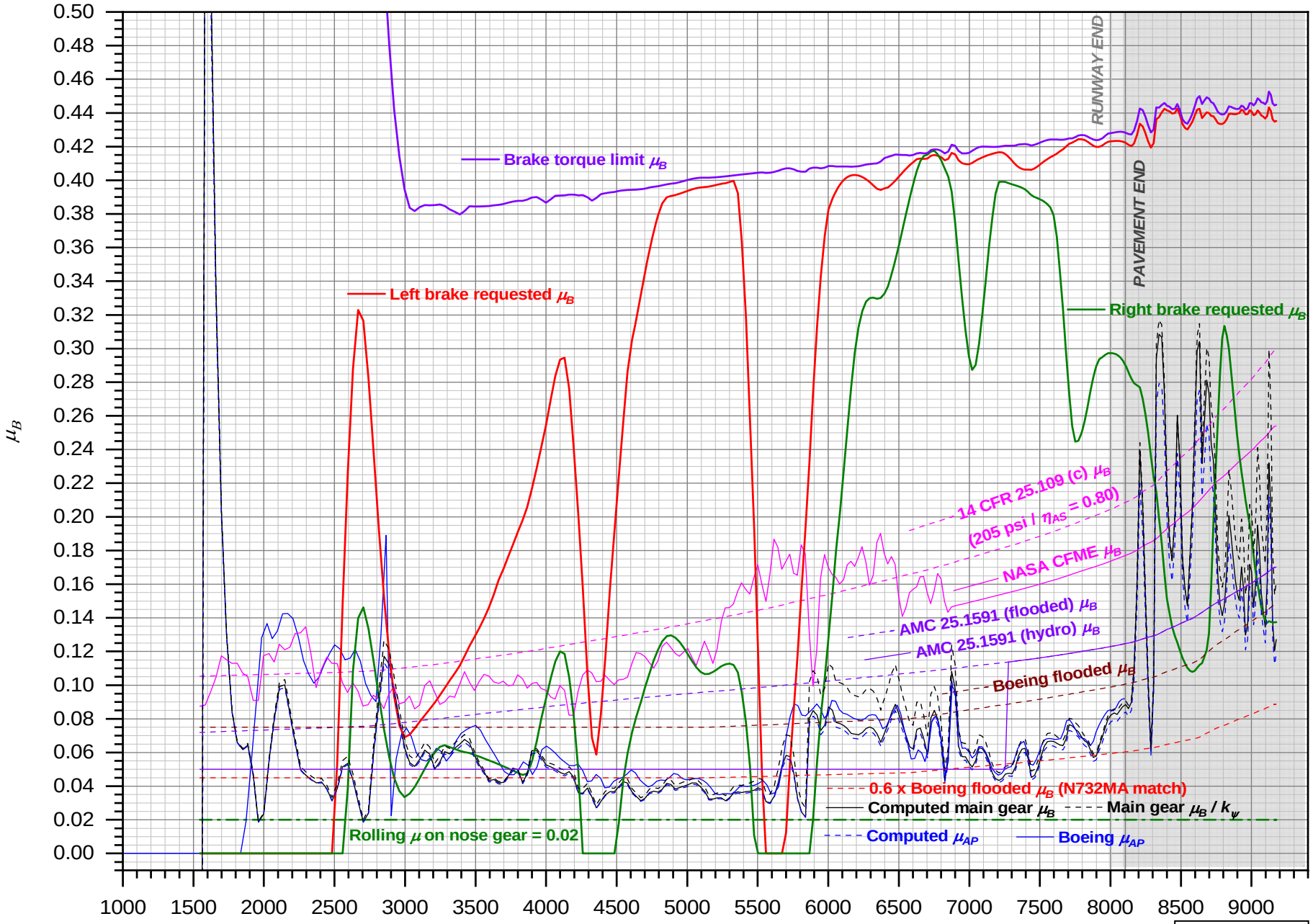

Figure 25a.

DCA19MA143: Miami Air flight 293, Boeing 737-800 N732MA, Jacksonville, FL, May 3, 2019

μ_B comparisons vs. distance from threshold - zero reverse thrust

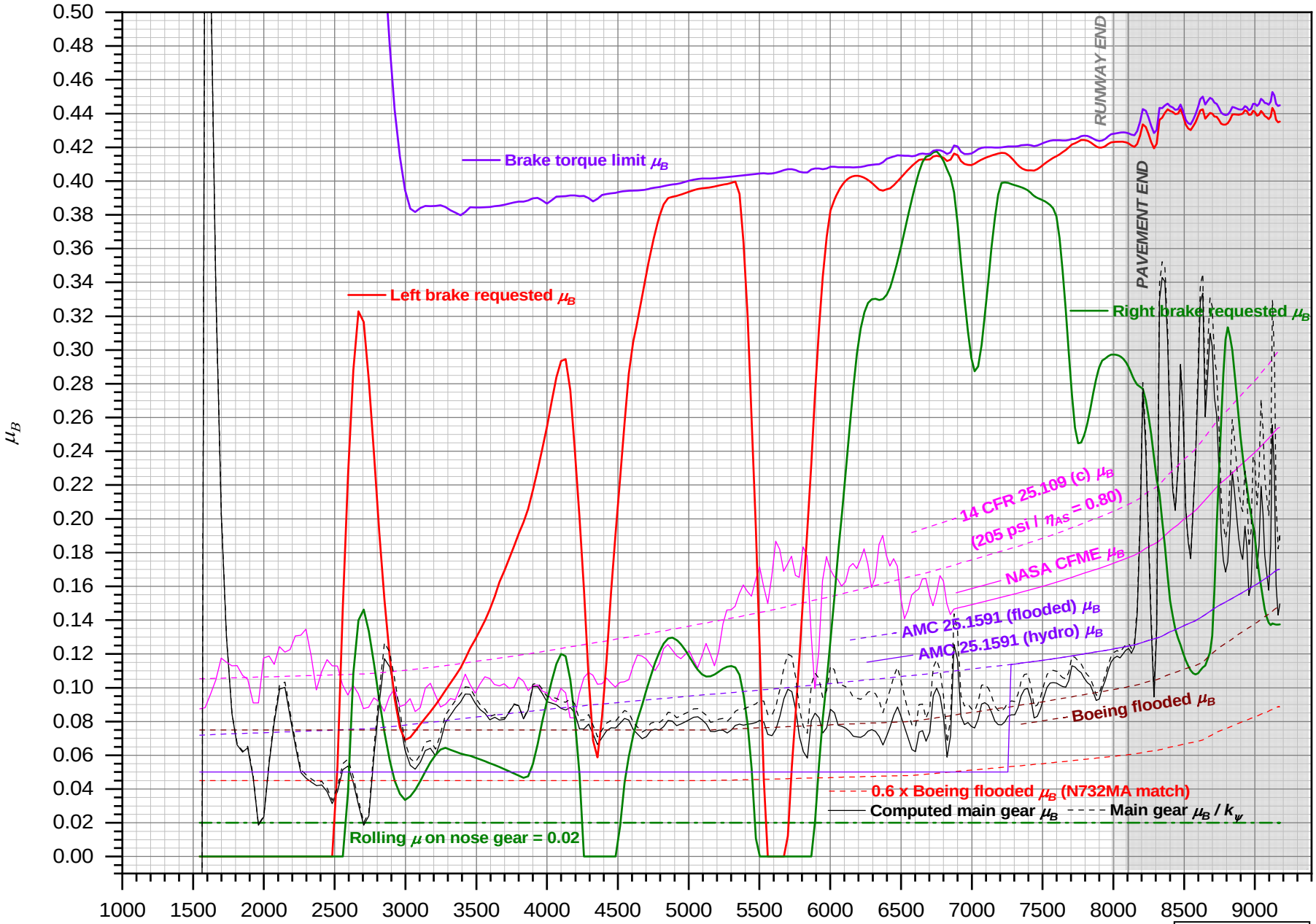

Figure 25b.

DCA19MA143: Miami Air flight 293, Boeing 737-800 N732MA, Jacksonville, FL, May 3, 2019

Stopping distance vs. ground speed for different μ_B models

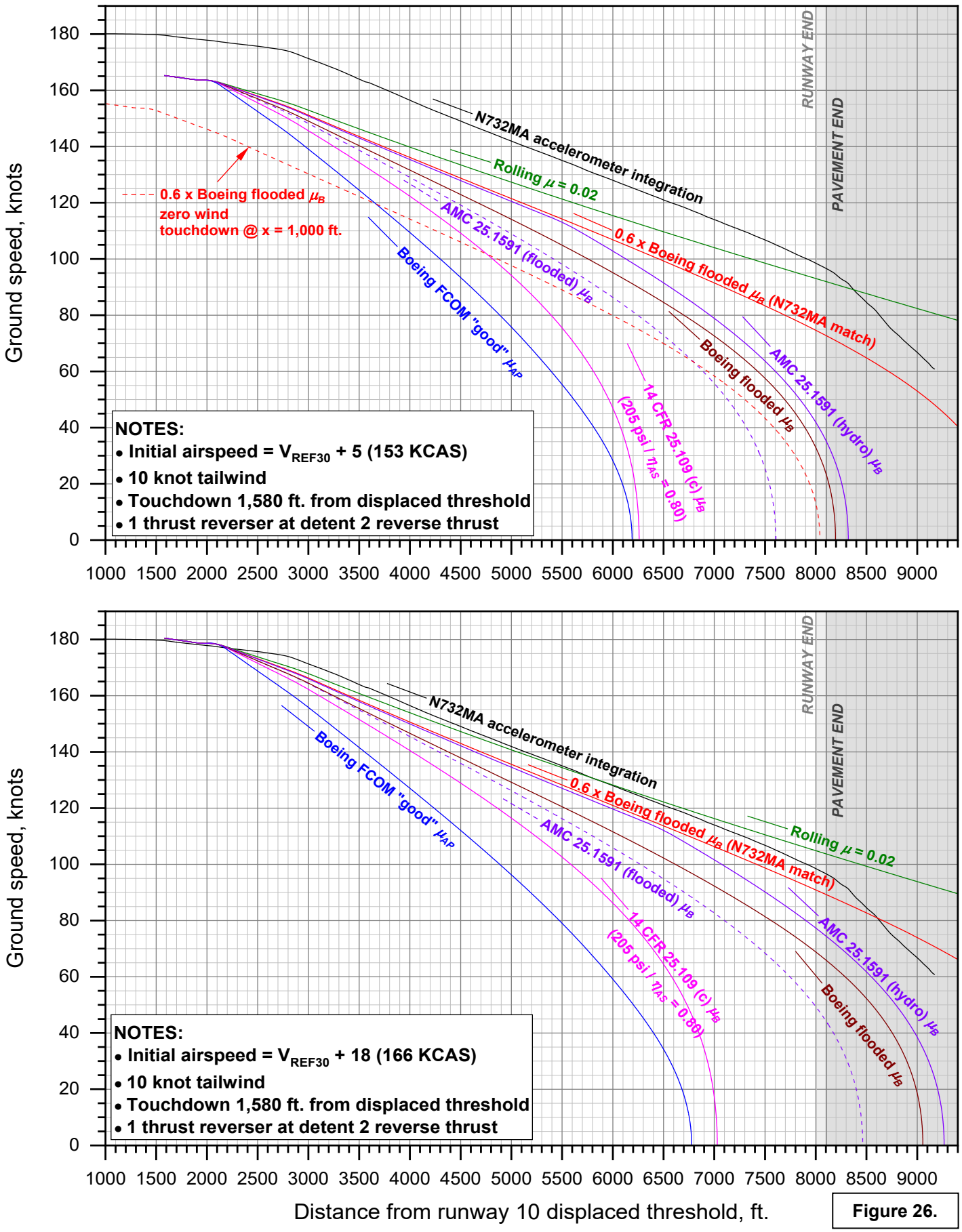

Figure 26.

DCA19MA143: Miami Air flight 293, Boeing 737-800 N732MA, Jacksonville, FL, May 3, 2019

CFME test run paths

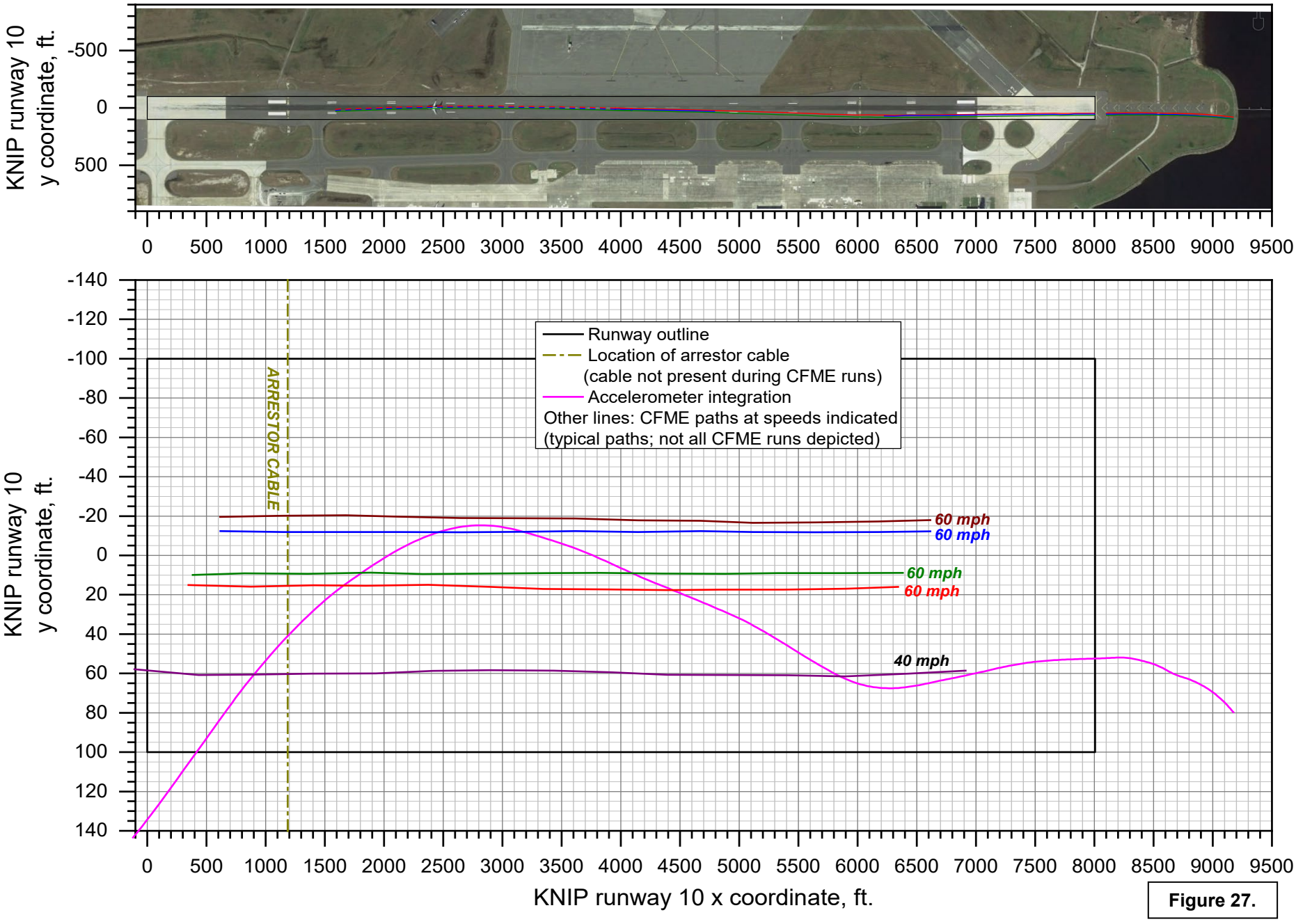

Figure 27.

DCA19MA143: Miami Air flight 293, Boeing 737-800 N732MA, Jacksonville, FL, May 3, 2019

μ measured by CFME @ 40 & 60 mph

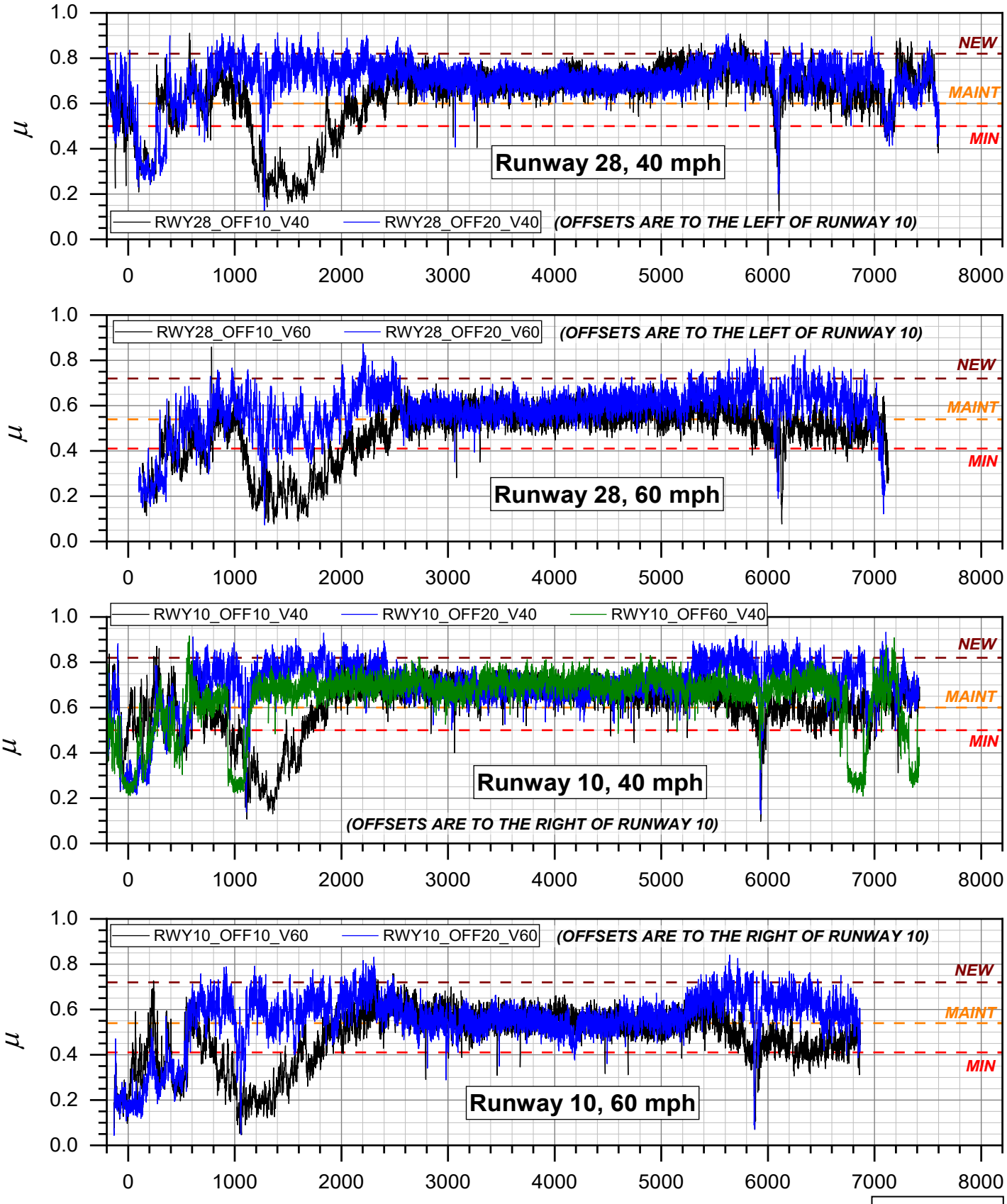

Figure 28.

	40 mph			60 mph		
	Minimum	Maintenance Planning	New Design/ Construction	Minimum	Maintenance Planning	New Design/ Construction
Mu Meter	.42	.52	.72	.26	.38	.66
Dynatest Consulting, Inc. Runway Friction Tester	.50	.60	.82	.41	.54	.72
Airport Equipment Co. Skiddometer	.50	.60	.82	.34	.47	.74
Airport Surface Friction Tester	.50	.60	.82	.34	.47	.74
Airport Technology USA Safegate Friction Tester	.50	.60	.82	.34	.47	.74
Findlay, Irvine, Ltd. Griptester Friction Meter	.43	.53	.74	.24	.36	.64
Tatra Friction Tester	.48	.57	.76	.42	.52	.67
Norsemeter RUNAR (operated at fixed 16% slip)	.45	.52	.69	.32	.42	.63

Figure 29. Friction level classification for runway pavement surfaces (Table 3-2 in Reference 32).

DCA19MA143: Miami Air flight 293, Boeing 737-800 N732MA, Jacksonville, FL, May 3, 2019

k_B of runway based on CFME measurements

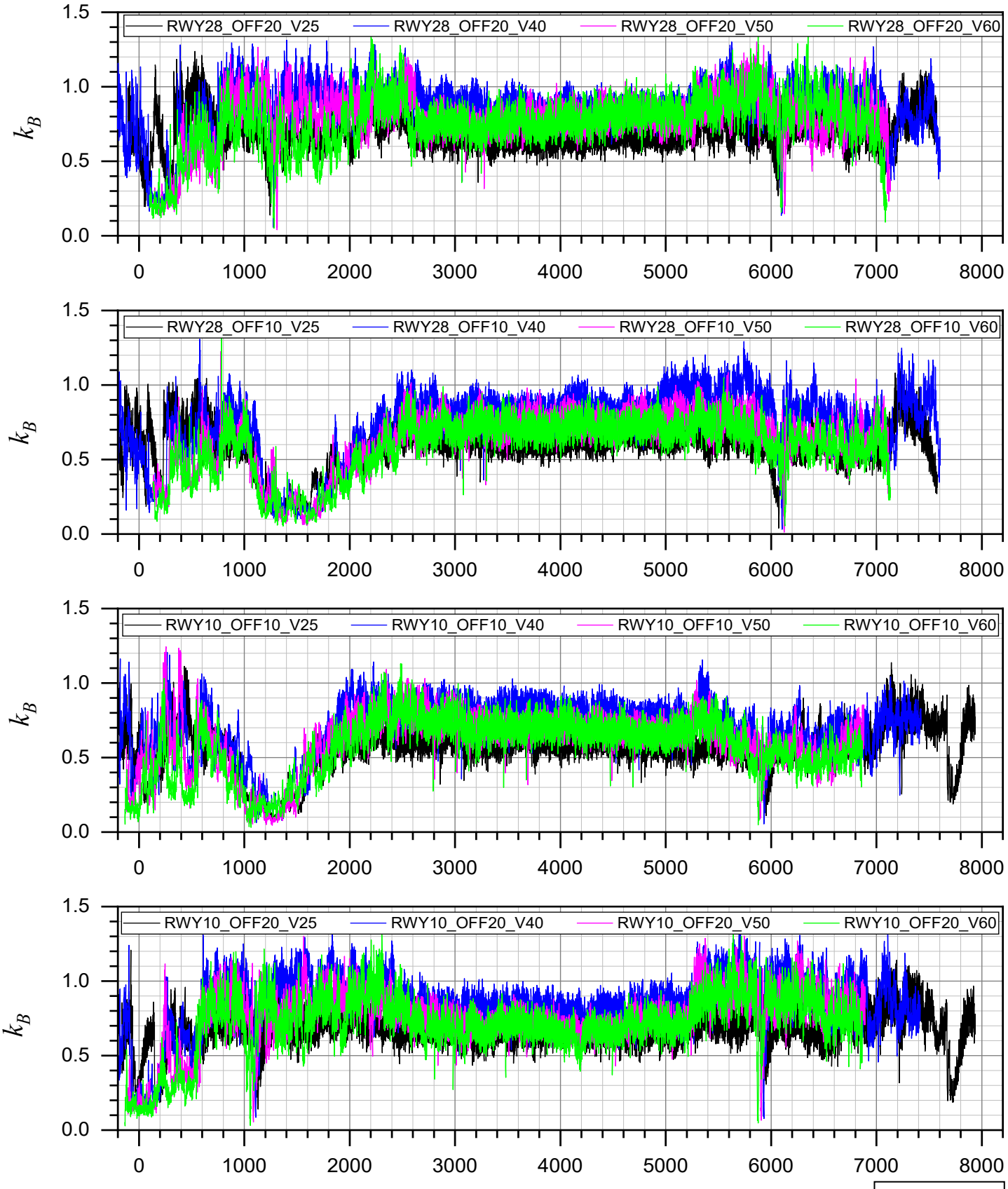

Figure 30a.

DCA19MA143: Miami Air flight 293, Boeing 737-800 N732MA, Jacksonville, FL, May 3, 2019

Filtered k_B of runway based on CFME measurements

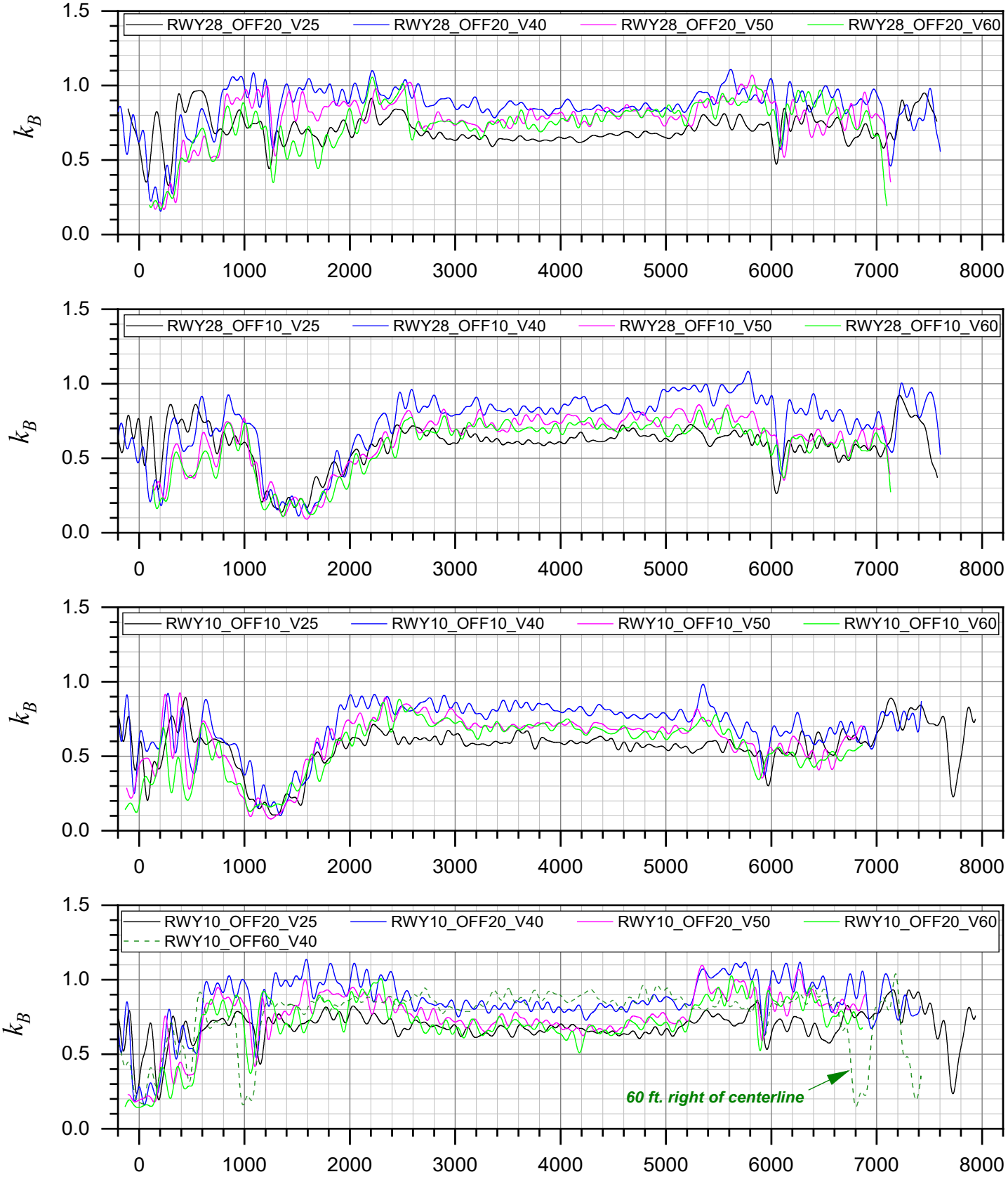

Figure 30b.

DCA19MA143: Miami Air flight 293, Boeing 737-800 N732MA, Jacksonville, FL, May 3, 2019

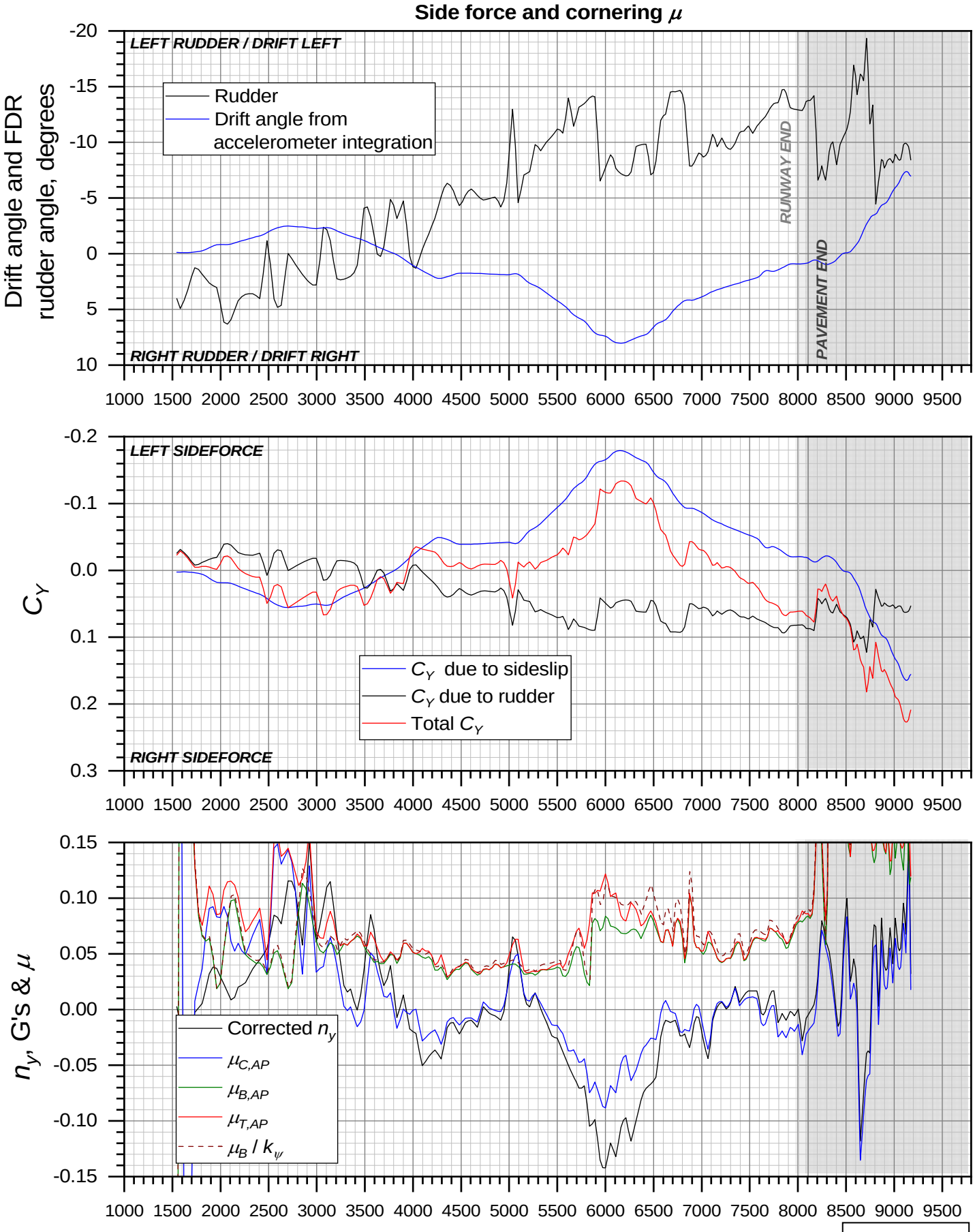

Figure 31.

Figure 32: Runway Surface Condition–Pilot Reported Braking Action—Wheel Braking Coefficient Correlation Matrix, from AC 25-32

Runway Condition Code	Runway Surface Condition Description	Pilot-Reported Braking Action	Wheel Braking Coefficient
6	• Dry	—	90% of certified value used to comply with § 25.125[1].
5	• Frost • Wet (includes damp and ⅛″ (3 mm) depth or less of water) ⅛″ (3 mm) depth or less of: • Slush • Dry snow • Wet snow	Good	Per method defined in § 25.109(c).
4	-15 °C and colder outside air temperature: • Compacted snow	Good to Medium[2]	0.20[3]
3	• Wet (“Slippery When Wet” runway) • Dry snow or wet snow (any depth) over compacted snow Greater than ⅛″ (3 mm) depth of: • Dry snow • Wet snow Warmer than -15 °C outside air temperature: • Compacted snow	Medium[2]	0.16[3]
2	Greater than ⅛″ (3 mm) depth of: • Water • Slush	Medium[2] to Poor	(1) For speeds below 85% of the hydroplaning speed[4]: 50% of the wheel braking coefficient determined in accordance with § 25109(c), but no greater than 0.16[3]; and (2) For speeds at 85% of the hydroplaning speed[4] and above: 0.05[3].
1	• Ice	Poor	0.08[3]
0	• Wet ice • Water on top of compacted snow • Dry snow or wet snow over ice	Nil	Not applicable. (No operations in Nil conditions.)

[1] 100% of the wheel braking coefficient used to comply with § 25.125 may be used if the testing from which that braking coefficient was derived was conducted on portions of runways containing operationally representative amounts of rubber contamination and paint stripes.

[2] The braking action term “FAIR” is in the process of being changed to “MEDIUM” throughout the FAA. Until an official change is published, the term “FAIR” may be used.

[3] These wheel braking coefficients assume a fully modulating anti-skid system. For quasi-modulating systems, multiply the listed braking coefficient by 0.625. For on-off systems, multiply the listed braking coefficient by 0.375. (See AC 25-7C to determine the classification of an anti-skid system.) Airplanes without anti-skid systems will need to be addressed separately on a case-by-case basis.

[4] The hydroplaning speed, V_P, may be estimated by the equation $V_P = 9\sqrt{P}$, where V_P is the ground speed in knots and P is the tire pressure in lb/in^2.

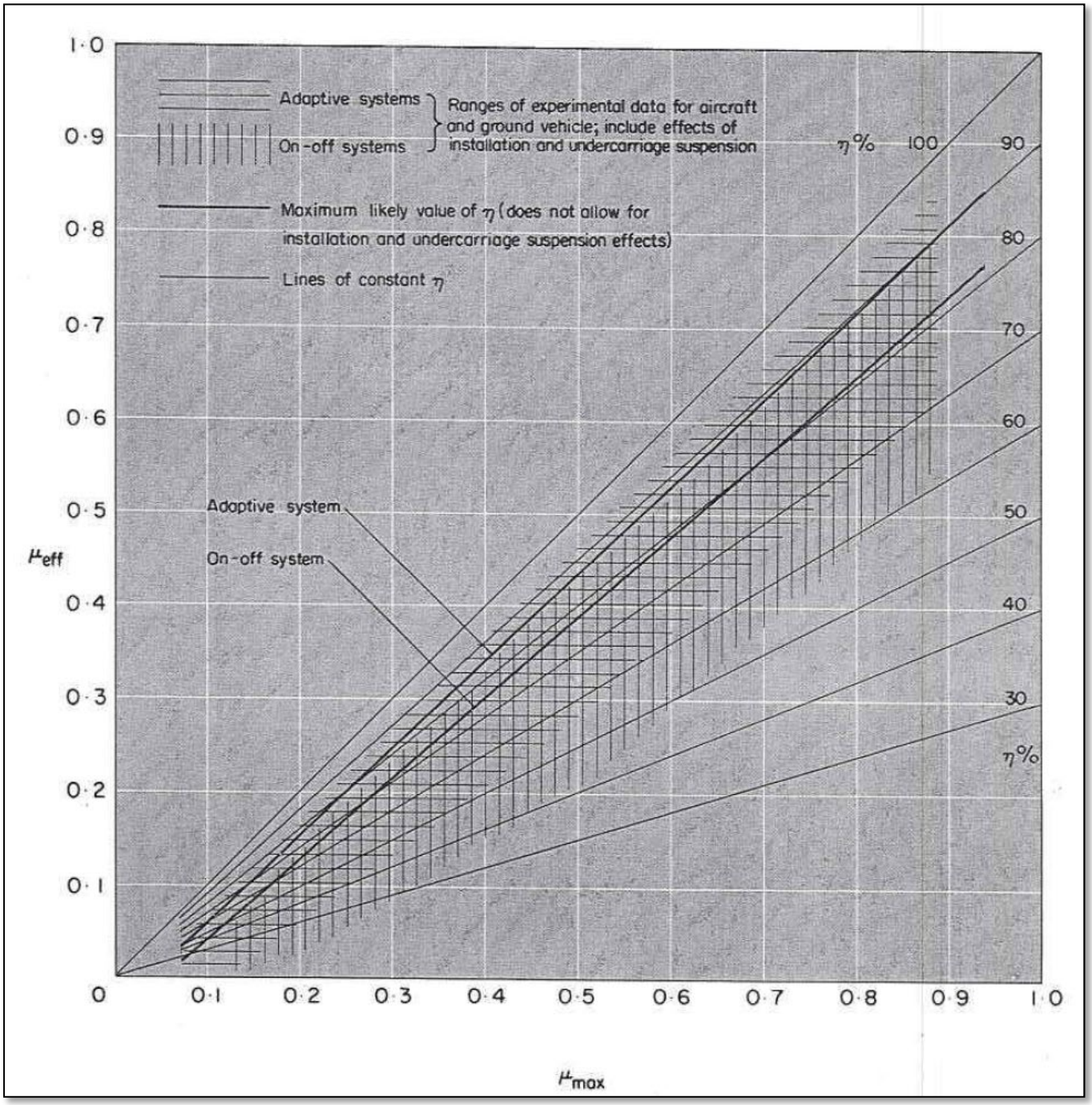

Figure 33. Brake system anti-skid efficiency (η_{AS}), from ESDU 71026 (Reference 29).

DCA19MA143: Miami Air flight 293, Boeing 737-800 N732MA, Jacksonville, FL, May 3, 2019

ESDU 05011 μ_{max} and implied accident η_{AS}

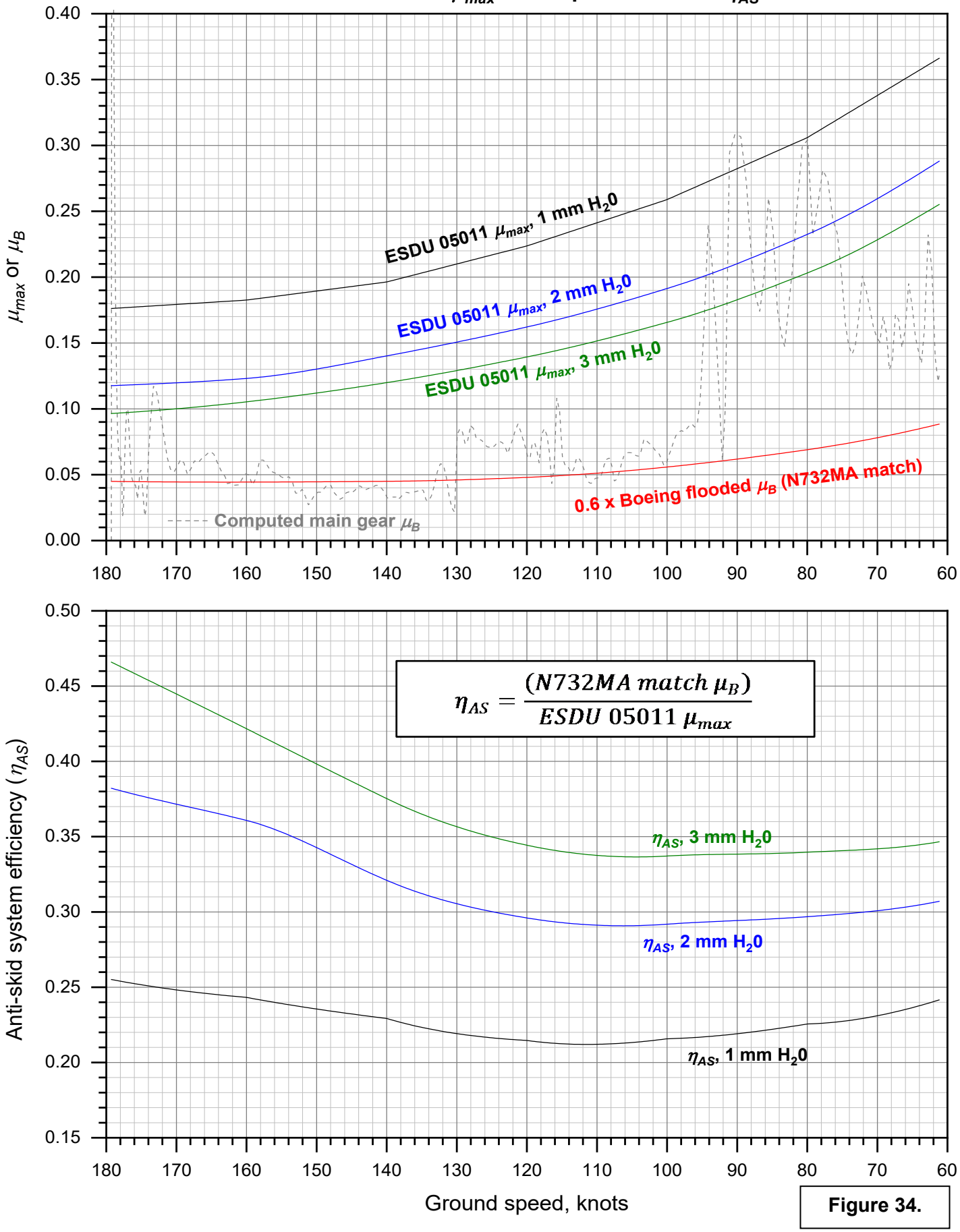

Figure 34.

DCA19MA143: Miami Air flight 293, Boeing 737-800 N732MA, Jacksonville, FL, May 3, 2019

ESDU 05011 μ_B vs. slip ratio s for different speeds and runway water depths

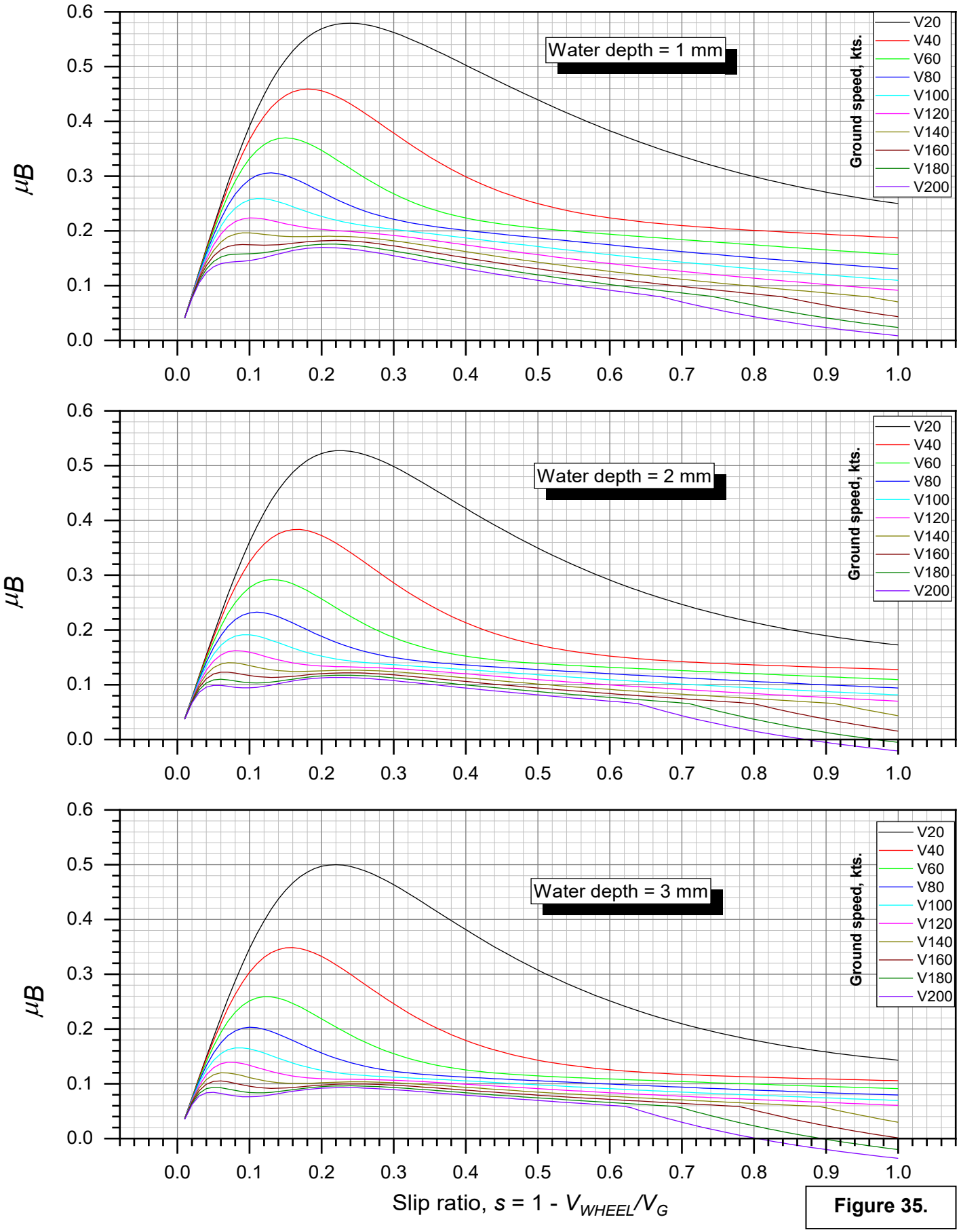

Figure 35.

DCA19MA143: Miami Air flight 293, Boeing 737-800 N732MA, Jacksonville, FL, May 3, 2019

μ_B computed for previous landing at MUGM

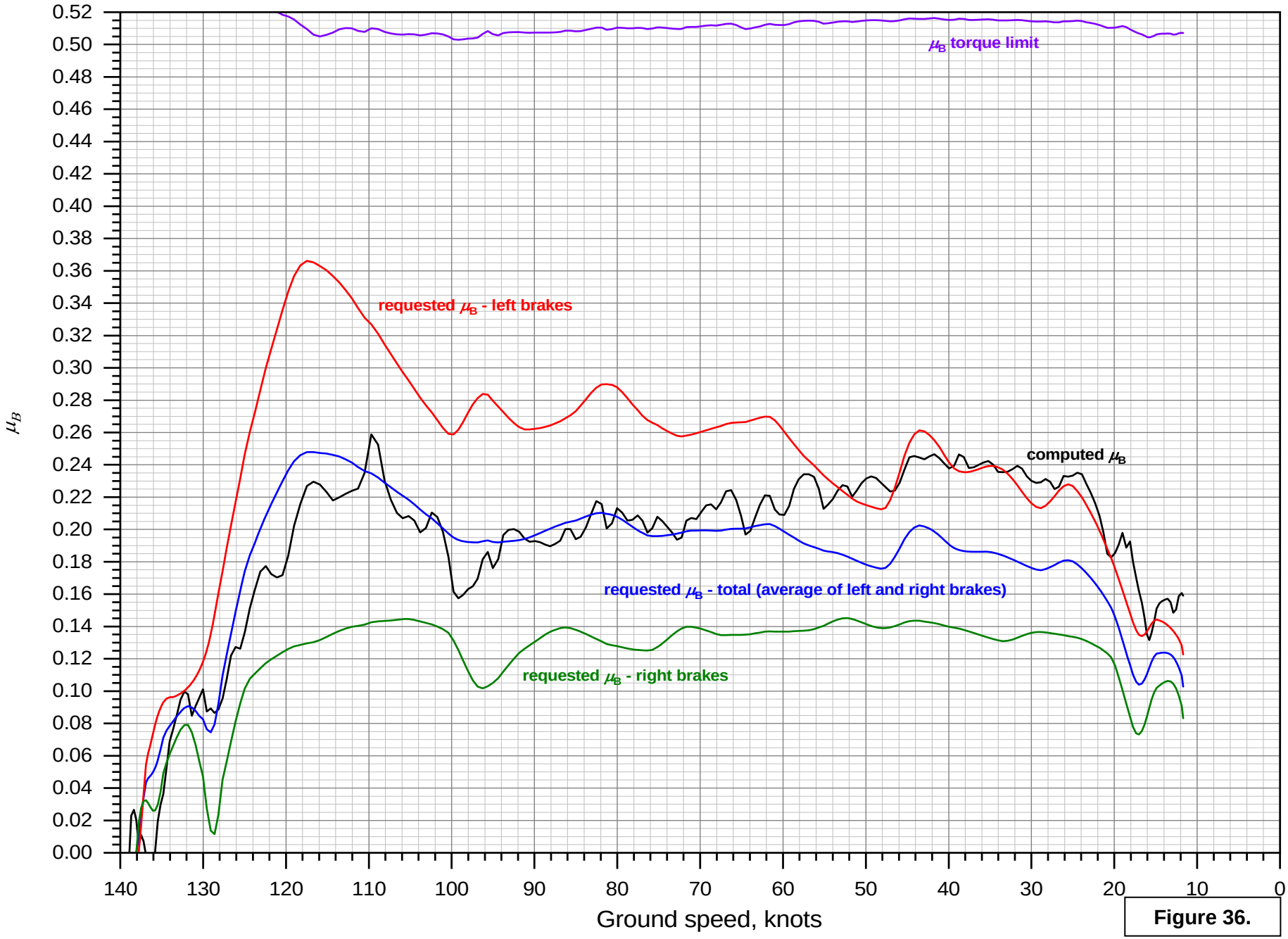

Figure 36.

(a)

(b)

Figure 37. Photographs of KNIP runway 10 provided by a Miami Air pilot following a landing on 12/20/2019.

DCA19MA143: Miami Air flight 293, Boeing 737-800 N732MA, Jacksonville, FL, May 3, 2019

Requested & achieved μ_B during 12/20/2019 N773MA landing @ KNIP

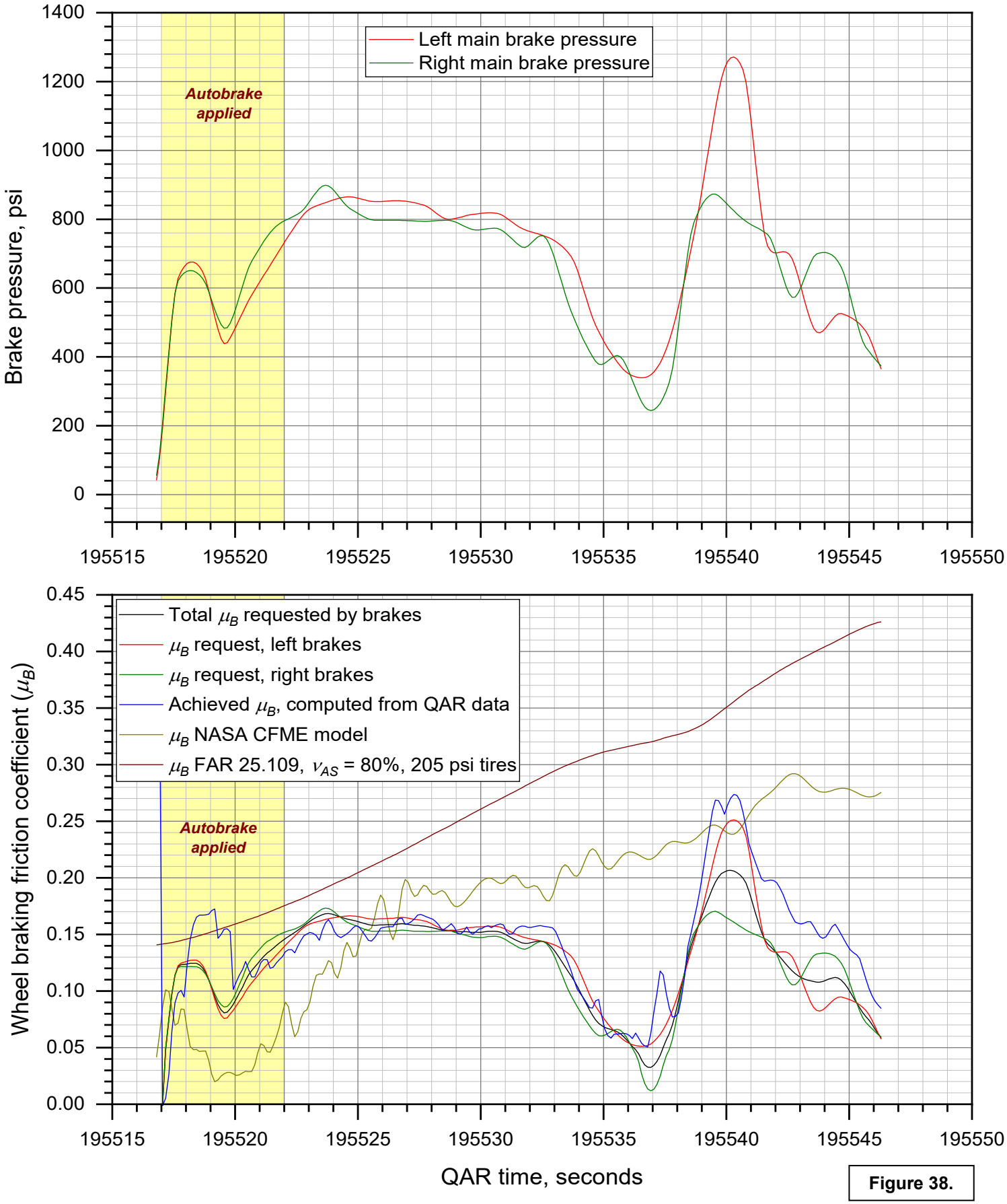

Figure 38.

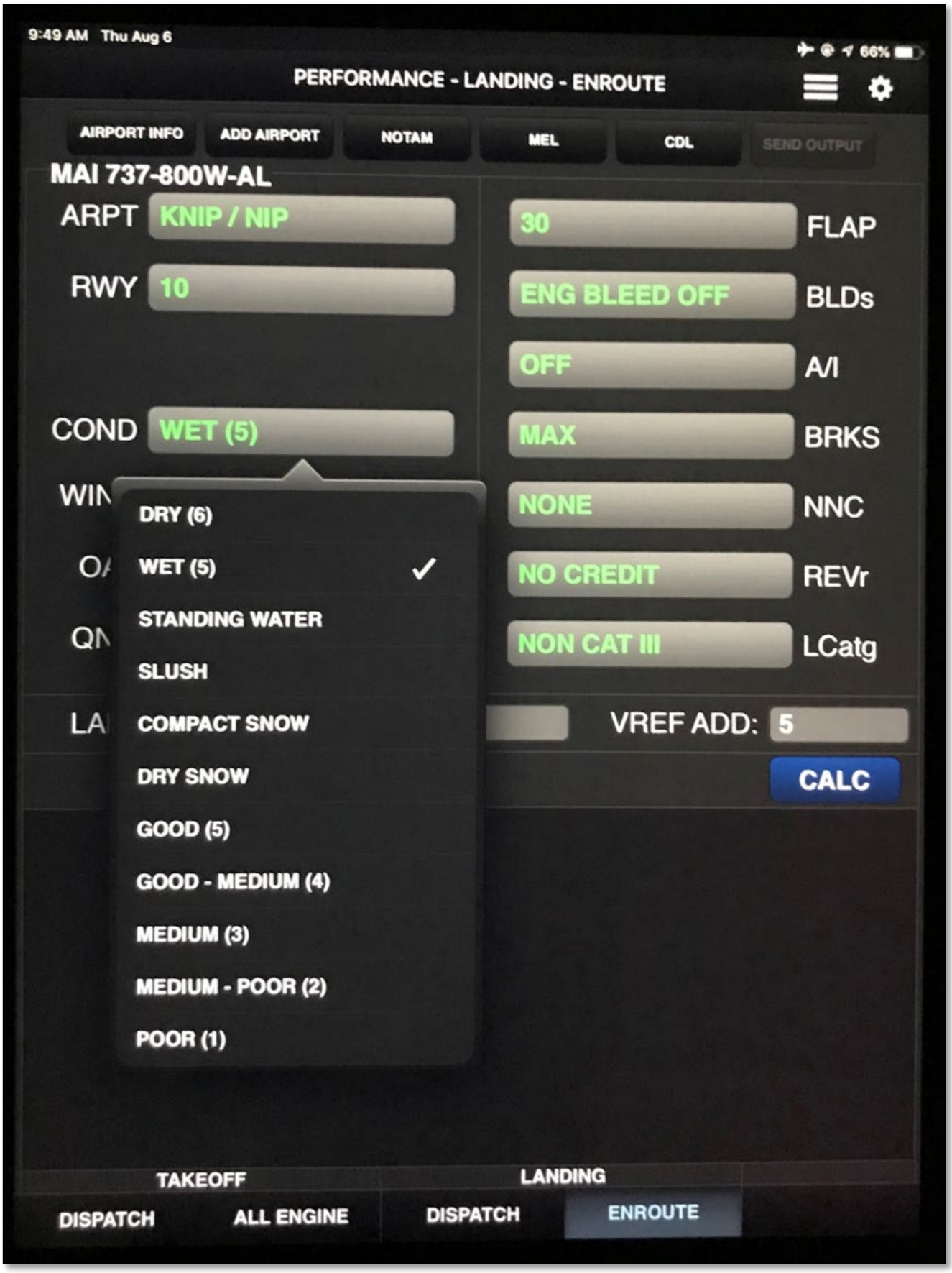

Figure 39. Runway condition options in the Miami Air Operational Performance Tool (OPT).

THIS PAGE DELIBERATELY LEFT BLANK

APPENDIX A:

KNIP airport diagram and other information

A2

KNIP Jacksonville Naval Air Station (Towers Field)

Jacksonville, Florida, USA

FAA INFORMATION EFFECTIVE 25 APRIL 2019

Location

FAA Identifier: NIP
Lat/Long: 30-14-01.3417N / 081-40-33.8059W
30-14.022362N / 081-40.563432W
30.2337060 / -81.6760572
(estimated)
Elevation: 22.5 ft. / 7 m (estimated)
Variation: 06W (2010)
From city: 4 miles S of JACKSONVILLE, FL
Time zone: UTC -4 (UTC -5 during Standard Time)
Zip code: 32212

Loc | Ops | Rwys | IFR | FBO | Links
Com | Nav | Svcs | Stats | Notes

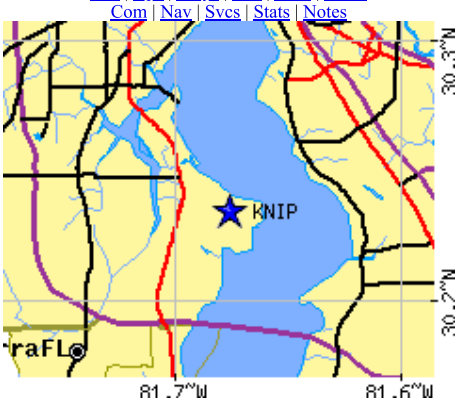

Road maps at: MapQuest Bing Google

Aerial photo

WARNING: Photo may not be current or correct

Do you have a better or more recent aerial photo of Jacksonville Naval Air Station (Towers Field) that you would like to share? If so, please **send us your photo**.

Sectional chart

Airport Operations

Airport use: Private use. Permission required prior to landing
Activation date: 05/1941
Control tower: yes
ARTCC: JACKSONVILLE CENTER
FSS: GAINESVILLE FLIGHT SERVICE STATION
NOTAMs facility: NIP (NOTAM-D service available)
Attendance: CONTINUOUS
OPR 24/7, SEE FLIP AP/1 SUPPLEMENT ARPT INFO.
CLOSURES PUBLISHED VIA NOTAM.
Pattern altitude: TRAN JET ACFT EXP RGT TFC RWY 10.
Segmented circle: no
Lights: ACTVT HIRL RWY 10/28 - 134.775.
Beacon: white-white-green (lighted military airport)
Operates sunset to sunrise.

Airport Communications

CTAF: 125.15
ATIS: 290.425
NAVY JACKSONVILLE GROUND: 128.6 336.4 [24 HRS. SEE FLIP AP/1 SUPPLEMENT ARPT INFO.

	CLOSURES PUBLISHED VIA NOTAM.]
NAVY JACKSONVILLE TOWER:	125.15 340.2 307.325 [24 HRS. SEE FLIP AP/1 SUPPLEMENT ARPT INFO. CLOSURES PUBLISHED VIA NOTAM.]
JACKSONVILLE APPROACH:	127.775
JACKSONVILLE DEPARTURE:	127.775 RWY 27
CLEARANCE DELIVERY:	134.775 353.675
ATCOM (SSB):	6723FM
EMERG:	121.5 243.0
NAVY JAX FLT PLN:	134.775 310.2
PMSV METRO:	343.5
RADAR:	127.7X 134.1X 266.8X 276.4 278.8X 299.6X 305.8 314.8X 315.4 325.2X 328.4 337.2X 348.0X 350.8X 354.8X 363.0X 379.225X
WX AWOS-3 at HEG (7 nm W):	119.275 (904-695-0334)
WX ASOS at CRG (10 nm NE):	PHONE 904-646-4670
WX AWOS-3 at VQQ (10 nm W):	125.275 (904-778-6934)
WX ASOS at JAX (16 nm N):	PHONE 904-741-4304

- SFA.
- SEE TERMINAL FLIP FOR RADAR MINIMA.

Nearby radio navigation aids

VOR radial/distance	VOR name	Freq	Var
CRGr237/10.7	CRAIG VORTAC	114.50	03W
VQQr087/(11.2)	CECIL VOR	117.90	03W
SGJr319/24.5	ST AUGUSTINE VOR/DME	109.40	06W

NDB name	Hdg/Dist	Freq	Var	ID
REYNOLDS	004/16.0	338	07W	RYD .-. -.-- -..

Airport Services

Airframe service:	NONE
Powerplant service:	NONE
Bottled oxygen:	NONE
Bulk oxygen:	NONE

Runway Information

Runway 10/28

Dimensions:	9003 x 200 ft. / 2744 x 61 m	
Surface:	asphalt, in fair condition	
Weight bearing capacity:	PCN 61 /R/C/W/T	
Runway edge lights:	high intensity	
Operational restrictions:	RY 10/28 CLSD 1000-1230Z++ FOR CENTERLINE MAINTENANCE.	
	RUNWAY 10	**RUNWAY 28**
Latitude:	30-13.895333N	30-13.904000N
Longitude:	081-41.576167W	081-39.865833W

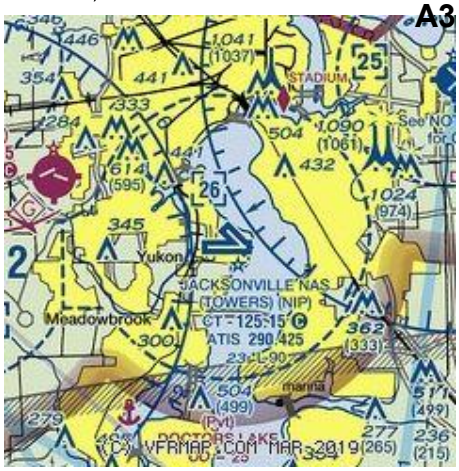

Airport diagram

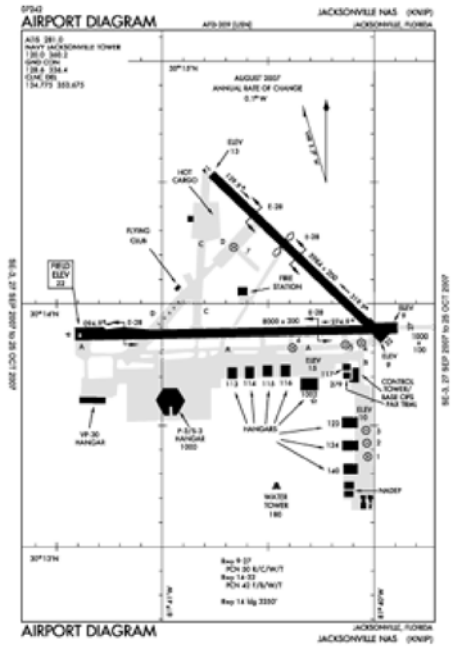

Download PDF
of official airport diagram from the FAA

Airport distance calculator

Flying to Jacksonville Naval Air Station (Towers Field)? Find the distance to fly.

From to KNIP

CALCULATE DISTANCE

Sunrise and sunset

Times for 07-May-2019

	Local (UTC-4)	Zulu (UTC)
Morning civil twilight	06:14	10:14
Sunrise	06:39	10:39
Sunset	20:07	00:07
Evening civil twilight	20:33	00:33

Current date and time

Zulu (UTC)	07-May-2019 16:12:31
Local (UTC-4)	07-May-2019 12:12:31

A4

Elevation:	22.5 ft.	7.9 ft.
Traffic pattern:	left	left
Displaced threshold:	997 ft.	no
Declared distances:		TORA:8002 TODA:8002 ASDA:9003 LDA:9003
Markings:	precision, in fair condition	precision, in fair condition
Visual slope indicator:	4-light PAPI on left (3.00 degrees glide path) OPTICAL LANDING SYSTEM (OLS) & WAVE-OFF	4-light PAPI on left (3.00 degrees glide path) OPTICAL LANDING SYSTEM (OLS) & WAVE-OFF
Approach lights:	ALSF1: standard 2,400 foot high intensity approach lighting system with centerline sequenced flashers (category I)	ALSF1: standard 2,400 foot high intensity approach lighting system with centerline sequenced flashers (category I)
Runway end identifier lights:	yes	yes
Centerline lights:	yes	yes
Touchdown point:	yes, no lights	yes, no lights

Runway 14/32

Dimensions:	5979 x 200 ft. / 1822 x 61 m	
Surface:	asphalt, in fair condition	
Weight bearing capacity:	PCN 48 /F/B/W/T	
Runway edge lights:	high intensity	
	RUNWAY 14	**RUNWAY 32**
Latitude:	30-14.554000N	30-13.860500N
Longitude:	081-40.730050W	081-39.922333W
Elevation:	12.4 ft.	7.4 ft.
Traffic pattern:	left	left
Runway heading:	141 magnetic, 135 true	321 magnetic, 315 true
Displaced threshold:	2734 ft.	no
Declared distances:	LDA:3245	TORA:3245 LDA:3245
Markings:	precision, in fair condition	precision, in fair condition
Approach lights:		OLS & WAVE-OFF
Runway end identifier lights:	no	yes
Touchdown point:	yes, no lights	yes, no lights

Airport Ownership and Management from official FAA records

Ownership: U.S. Navy
Owner: US NAVY
OCEANOGRAPHIC OFC-CODE 3142
WASHINGTON, DC 20373
Manager: COMMANDING OFFICER
NAVAL AIR STATION
JACKSONVILLE, FL 32212

Additional Remarks

METAR

KNIP	071553Z 11007KT 10SM SCT040 SCT250 29/18 A3011 RMK AO2 SLP192 T02890178
KHEG 7nm W	071555Z AUTO 08005G10KT 8SM FEW036 SCT048 BKN060 29/18 A3013 RMK AO2
KCRG 10nm NE	071553Z 10008KT 10SM SCT024 SCT035 28/21 A3012 RMK AO2 SLP198 T02780211
KVQQ 11nm W	071550Z 16005KT 10SM SCT048 31/19 A3011
KJAX 16nm N	071556Z 09009KT 10SM SCT030 BKN250 28/20 A3010 RMK AO2 SLP194 T02780200
KNRB 16nm NE	071552Z 07008KT 10SM SCT030 SCT250 27/22 A3012 RMK AO2 SLP198 T02720222

TAF

KNIP	0707/0807 VRB05KT 9999 SCT035 SCT250 QNH2996INS BECMG 0714/0716 10009KT 9999 SCT035 SCT250 QNH2999INS T21/0710Z T29/0720Z FN00205
KCRG 10nm NE	071300Z 0713/0812 08007KT P6SM SCT012 TEMPO 0713/0715 BKN012 FM071500 09008KT P6SM FEW025 SCT050 FM071800 11012KT P6SM FEW050 SCT250 FM080200 10006KT P6SM SCT250
KVQQ 11nm W	071405Z 0714/0812 08008KT P6SM BKN015 FM071600 09008KT P6SM FEW025 SCT050 FM071900 11010KT P6SM FEW060 SCT250 FM080200 09003KT P6SM SCT250
KJAX 16nm N	071301Z 0713/0812 08006KT P6SM SCT012 TEMPO 0713/0715 BKN012 FM071500 09008KT P6SM FEW025 SCT050 FM071900 11011KT P6SM SCT050 SCT250 FM080200 10005KT P6SM SCT250
KNRB 16nm NE	0707/0807 VRB06KT 9999 SCT035 SCT250 QNH2997INS BECMG 0714/0716 10011KT 9999 SCT035 SCT250 QNH3000INS AUTOMATED SENSOR METWATCH 0707 TIL 0709 T22/0710Z T27/0720Z FN00205

NOTAMs

Click for the latest **NOTAMs**

NOTAMs are issued by the DoD/FAA and will open in a separate window not controlled by AirNav.

E60- HOOK E28(B) (2984 FT)
32
E60- HOOK E28(B) (1992 FT)
28
E60- HOOK E28(B) (1190 FT)
10
E60- HOOK E28(B) 1229 FT)
14

- JASU: 1(NCPP-105) 2(NC-8)
- FUEL: J5
- FLUID: LOCAL SQUADRONS CTC FUELS DIV FOR LOX SVC, DSN 942-3906, C904-542-3906, 1300-2030Z++ MON-FRI. LOX SERVICE IS NOT AVAILABLE FOR TRANSIENT AIRCRAFT.
- TRANS ALERT: LTD TRAN MAINT AND SVC AVBL DUR NML WORKING HR, EXP 2 HR FUEL DELAY. ACFT STAIRS AVBL 1100-0200Z++ DLY WITH 24 HR NTC, QUALIFIED AIRCREW RQRD.
- RSTD: TRAN JET ACFT VFR TOUCH AND GO NA. ALL ACFT CTC FLT PLNG 310.2, 134.775 15 MIN PRIOR TO LNDG. RY 14 AVBL FOR ARR F/W CAT A AND R/W ACFT.
- CAUTION: EXER EXTREME VIGILANCE DUR IFR APCH RY 10 IN VMC DUE TO GENERAL AVIATION ACFT VICINITY CECIL FLD.
- CAUTION: UNSHIELDED LGT AT BALLFIELD NIP 216/2.4 NM ON RY 10 APCH.
- AFLD CLSD 2ND WED OF EV MONTH FOR AFLD MAINT FR 1400-1600Z++. AFLD CLSD 2ND WED IN JAN, APR, & OCT FOR FOD WALKDOWN FM 1230-1400Z++. 48 HR PPR NTC REQ EXC AIREVAC, JOSAC, NALO, AND LIFEFLTS, CTC BASEOPS DSN 942-5211, C904-542-2511. BOQ DSN 942-3138/3427/3139.
- NS ABTMT: STOP LDG ONLY MON-SAT BTN 0300-1300Z++ & SUN BTN 0300-1700Z++ DUE TO QUIET HRS.
- CSTMS/AG/IMG: ACFT RQR INSPECTION CTC AFLD MGR DSN 942-3176, C904-542-3176 AT LEAST 48 HRS PRIOR TO ARR TO COORD INSPECTION SETUP.
- MISC: VIP ACFT CTC BASE OPS PRIOR LDG.
- CAUTION: TO PRECLUDE TAIL HOOK SKIP DURING A-GEAR ENGAGEMENT, AVOID RY 10/28 CNTRLN LGTS LOCATED 24 INCHES SOUTH OF RWY CNTRL. MAXIMUM SAFE OFF-CNTR ARRESTMENT 40 FT.
- RSTD: RY 14 NOT AVBL FOR LDG BTN SS AND SR. AFLD CLSD 2ND WED OF EVERY MONTH FOR AFLD MAINT FR 1230-1400Z++. AFLD CLSD 2ND WED IN JAN, APR, JUL AND OCT FOR FOD WALKDOWN FR 1230-1400Z++.
- RSTD: PPR FOR ALL TRAN ACFT EXC AIREVAC, JOSAC, NALO AND LIFEFLTS, CTC AFLD MGR 48 HR PRIOR TO ARR FOR PPR NR, DSN 942-3176, C904-542-3176. BOQ DSN 942-3138/3427/3139.
- MISC: CTC NAVAL ATLANTIC MET FAC JACKSONVILLE FOR WX ADVSY OR WX FCST DSN 942-2541, C904-542-2541.
- CAUTION: MAT AREAS BTN RY 10/28 & RY 14/32 NOT AUTHORIZED FOR ACFT USE.
- CAUTION: EXTREME BIRD HAZ DUR SUMMER MONTHS. CTC TWR FOR CURRENT BASH COND.
- CAUTION: SKYDIVING AND GLIDER OPERATIONS , SFC TO 10,000 FT, 7MILES, IN VICINITY OF HERLONG AIRPORT, BTN SR & SS.
- MISC: AIRCREWS ARE RESPONSIBLE FOR THEIR ON/OFF BASE TRANSPORTATION. AIRCREWS COORDINATE FOR CLASSIFIED MATERIAL STORGE WITH NCTAMSLANT AT DSN 942-3777.
- CAUTION: EXER EXTREME VIGILANCE DUR IFR APCH RY 10 IN VMC DUE TO GENERAL AVATION ACFT INVOF CECIL FLD.
- MISC: WX FCST SVC AVBL 0900-0100Z++ MON-FRI. ALL OTHER HOURS WX OBSERVER ONLY. CTC FWC-N AVN CP JAX AT DSN 942-2535 C904-542-2535. CTC NAVAL AVAITION FCST CNTR FOR WX ADVSY OR WX FCST DSN 564-2594, C757-444-2594 DURING OTHER HRS.

Instrument Procedures

NOTE: All procedures below are presented as PDF files. If you need a reader for these files, you should download the free Adobe Reader.

NOT FOR NAVIGATION. Please procure official charts for flight.
FAA instrument procedures published for use from 25 April 2019 at 0901Z to 23 May 2019 at

0900Z.

STARs - Standard Terminal Arrivals

ALMA TWO	download (111KB)
HOTAR ONE (RNAV)	download (217KB)
POGIE ONE	download (189KB)
TAYLOR TWO	download (173KB)

IAPs - Instrument Approach Procedures

RNAV (GPS) RWY 10 ****CHANGED****	download (134KB)
RNAV (GPS) RWY 28 ****CHANGED****	download (118KB)
HI-TACAN RWY 10 ****CHANGED****	download (133KB)
HI-TACAN RWY 28 ****CHANGED****	download (137KB)
TACAN RWY 10 ****CHANGED****	download (103KB)
TACAN RWY 28 ****CHANGED****	download (103KB)
Radar Approach Procedures available	download (236KB)
NOTE: Special Take-Off Minimums/Departure Procedures apply	download (238KB)

Other nearby airports with instrument procedures:

KHEG - Herlong Recreational Airport (7 nm W)
KCRG - Jacksonville Executive Airport at Craig (10 nm NE)
KVQQ - Cecil Airport (10 nm W)
KJAX - Jacksonville International Airport (16 nm N)
KNRB - Mayport Naval Station (Adm David L. McDonald Field) (16 nm NE)

Would you like to see your business listed on this page?

If your business provides an interesting product or service to pilots, flight crews, aircraft, or users of the Jacksonville Naval Air Station (Towers Field), you should consider listing it here. To start the listing process, click on the button below

ADD YOUR BUSINESS OR SERVICE

Other Pages about Jacksonville Naval Air Station (Towers Field)

www.nasjax.navy.mil

UPDATE, REMOVE OR ADD A LINK

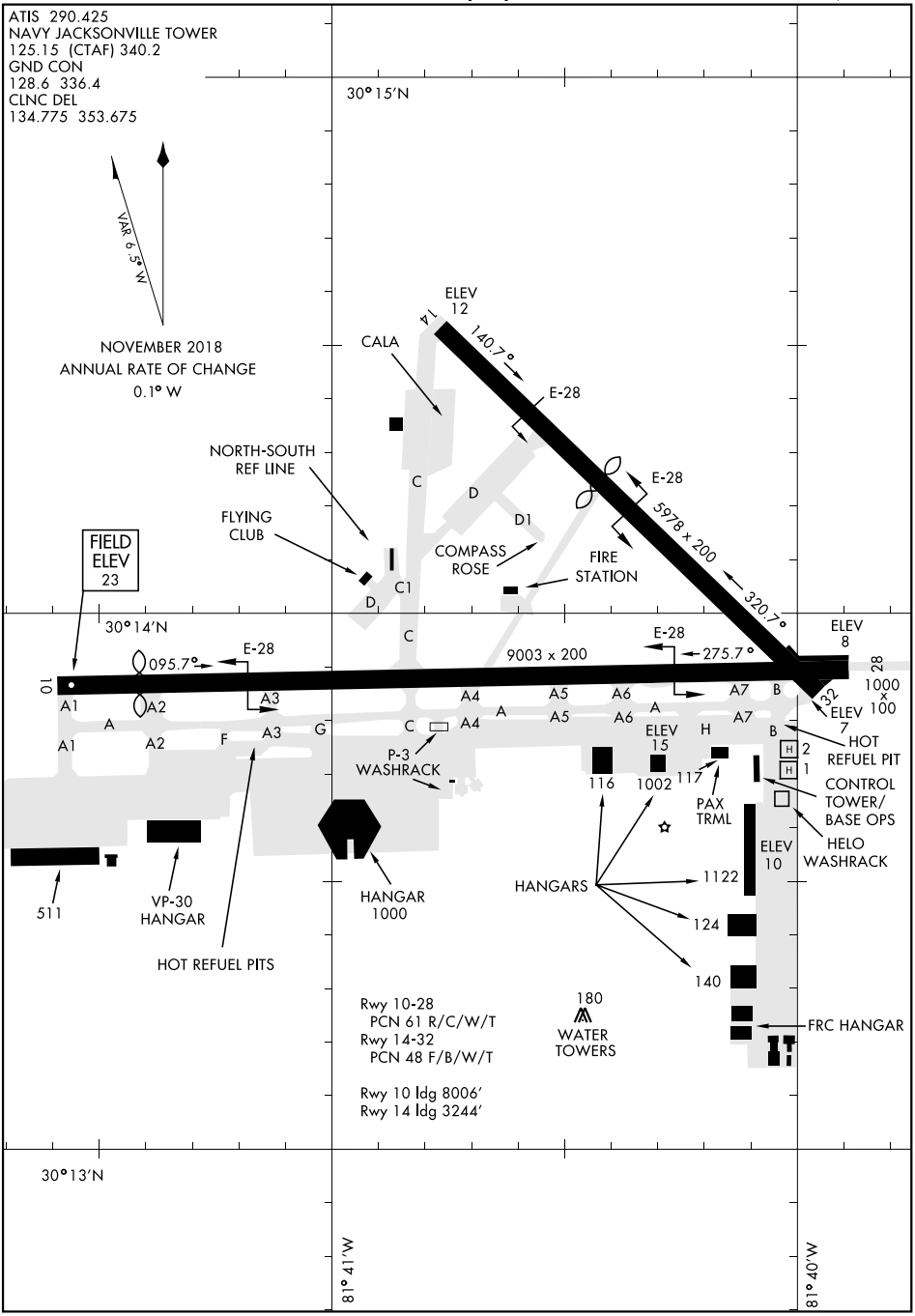

SE-3, 25 APR 2019 to 23 MAY 2019

SE-3, 25 APR 2019 to 23 MAY 2019

eNASR

Cycle: Current (2019-07-18) Resource: Airport Query Screen

Airport NIP

General | Location | Associated FAA Facilities | Contacts | Services and Facilities | Usage, Rules, and Regulations | Pad Rwy | Linear Rwy

Item 1 of 2

Status:	EXISTING	**Rwy ID:**	10/28	**Gross Wt SW:**		**Gross Wt DW:**		**Gross Wt DTW:**	
Gross Wt DDTW:		**PCN Number:**	61	**Pavement Type:**	R - RIGID	**Subgrade Strength Category:**	C - LOW	**Tire Pressure:**	W - UNLIMITED
Evaluation Method:	T - TECHNICAL EVAL								

Rwy General

Edge Intensity:	HIGH	**Length:**	9003	**Length Source:**	MILITARY	**Length Source Date:**	2016-05-16
Width:	200						

Rwy Surface

Condition:	FAIR	**Surface Type:**	ASPH	**Treatment:**	

Base Rwy End

Rwy End ID: 10

Arresting Systems

System Code
E28

Apch Lights:	ALSF1	**Centerline:**		**Marking Cond:**	FAIR	**Marking Type:**	PIR
REIL:		**RVR:**		**RVV:**		**TDZ:**	
Thr Crossing Hgt:	51	**VGSI:**	P4L	**Visual Glide Angle:**	3.0		

Obstruction

Clearance Slope:		**Close In:**		**Cntrln Offset**		**Ctlg Obstn:**	
				Offset:		**Displaced Thr Len:**	997
				Direction:			
Dist From Rwy End:		**FAR 77 Category:**		**Hgt Above Rwy End:**		**Marked Lighted:**	
						Slope to Displaced Thr:	

Displaced Threshold

Elevation

Elevation ft:	21.1
Source:	MILITARY
Source Date:	2016-05-16
Datum:	EGM96

Position

Latitude:	30-13-53.78N
Longitude:	81-41-23.21W
Source:	MILITARY
Source Date:	2016-05-16

Runway End

Elevation

Elevation ft:	22.5
Source:	MILITARY
Source Date:	2016-05-16
Datum:	EGM96

Position

Latitude:	30-13-53.72N
Longitude:	81-41-34.57W
Source:	MILITARY
Source Date:	2016-05-16

Touchdown Zone

Elevation ft:	21.1	**Source:**	MILITARY
Source Date:	2016-05-16	**Datum:**	EGM96

Rwy Distances

Aclt Stop Dist Avbl:	**Lndg Dist Avbl:**
Overrun Len:	**Stopway Len:**
Tkof Dist Avbl:	**Tkof Run Avbl:**

LAHSO

Hold Short of

Rwy End General

Gradient:	**Grad Drctn:**

LAHSO Lndg Dist: **Intersecting Rwy:**

Hold Short of Other:

Hold Short Point
Latitude:
Longitude:
Source:
Source Date:

Right Traffic: **True Heading:**

Reciprocal Rwy End

Rwy End ID: 28

Arresting Systems

System Code
E28

Apch Lights: ALSF1 **Centerline:** **Marking Cond:** FAIR **Marking Type:** PIR **REIL:**

RVR: **RVV:** **TDZ:** **Thr Crossing Hgt:** 62 **VGSI:** P4L

Visual Glide Angle: 3.0

Obstruction

Clearance Slope: **Close In:**

Cntrln Offset
Offset:
Direction:

Ctlg Obstn: **Displaced Thr Len:**

Dist From Rwy End: **FAR 77 Category:** **Hgt Above Rwy End:** **Marked Lighted:** **Slope to Displaced Thr:**

Displaced Threshold

Elevation
Elevation ft:
Source:
Source Date:
Datum:

Position
Latitude:
Longitude:
Source:
Source Date:

Runway End

Elevation
Elevation ft: 7.9
Source: MILITARY
Source Date: 2016-05-16
Datum: EGM96

Position
Latitude: 30-13-54.24N
Longitude: 81-39-51.95W
Source: MILITARY
Source Date: 2016-05-16

Touchdown Zone

Elevation ft: 12.7 **Source:** MILITARY
Source Date: 2016-05-16 **Datum:** EGM96

Rwy Distances

Aclt Stop Dist Avbl: 9003 **Lndg Dist Avbl:** 9003
Overrun Len: **Stopway Len:**
Tkof Dist Avbl: 8002 **Tkof Run Avbl:** 8002

LAHSO

LAHSO Lndg Dist: **Hold Short of Intersecting Rwy:**

Hold Short of Other:

Hold Short Point
Latitude:
Longitude:
Source:
Source Date:

Rwy End General

Gradient: **Grad Drctn:**
Right Traffic: **True Heading:**

APPENDIX B:

Data Reduction Procedures for Using Ground Vehicle Friction Measurements to Calculate Aircraft Tire Friction Performance (NASA CFME μ_B Model)

Tom Yager
Distinguished Research Associate (retired)
NASA Langley Research Center

Data Reduction Procedures

For

Using Ground Vehicle Friction Measurements

To

Calculate Aircraft Tire Friction Performance

Tom Yager, NASA Langley Research Center

Basic Data Requirements –

1. Accurate and suitable ground vehicle friction measurements must be collected through a speed range (e.g. 10-60 mph) for each wet surface condition evaluated.

2. The test tire(s) operating mode and inflation pressure must be properly maintained and documented

3. The test tire(s) operating mode should be selected to provide one of three friction boundary conditions: locked-wheel skidding, peak braked rolling, or peak yawed (cornering) rolling

4. A characteristic dry friction coefficient, μ_{cd} must be determined experimentally for each ground vehicle test tire operating mode by conducting test runs at very low speed (<3 mph)

5. The aircraft main landing gear tire inflation pressure value must be known

Overall Tire Friction Methodology – See figure 1

Data Reduction Procedures –

STEP 1 - Determine best fit curve for aircraft and ground vehicle friction- speed gradient data. Figure 2 provides an example of the friction data range obtained on a wet slurry seal asphalt surface with the NASA instrumental B-737 aircraft and four different ground test vehicles: a diagonal-braked vehicle, a mu-meter, a Saab friction tester, and a BV-11 skiddometer.

STEP 2 – For each test vehicle, calculate the minimum tire dynamic hydroplaning spin down speed using the following equation (see table I)

$$Vp, Knots = 9\sqrt{p} \quad (1a)$$

$$Vp, mph = 10.35\sqrt{p} \quad (1b)$$

where Vp, tire dynamic hydroplaning spindown speed

$p, tire\ inflation\ pressure, psi$

NOTE: Experimental data obtained with the mu-meter trailer indicates a Vp value of 45 mph rather than the 33 mph derived from eq. 1b. Use $Vp = 45mph$ for mu-meter calculations.

STEP 3 – Tabulate characteristic dry friction coefficient values obtained experimentally for each ground vehicle test tire (see table I).

STEP 4 – Calculate characteristic dry friction coefficient value for air craft main gear tire using the following equation:

$$\mu_{cd} = 0.93 - 0.0011\ p \quad (2)$$

where, μ_{cd} characteristic dry friction coefficient

$p, tire\ inflation\ pressure, psi$

NOTE: Table I gives these values for both the B-737 and B-727 aircraft together with the pertinent ground vehicle tire friction parameters.

STEP 5 – Select and tabulate an appropriate number (minimum 5) of the friction coefficient and ground speed values to properly define the friction-speed gradient data measured by each ground test vehicle. Determine the ground speed/hydroplaning speed ratio associated with each of the selected friction coefficient values (see table II).

STEP 6 – Determine ground vehicle tire hydroplaning parameter values using the following general relationship:

$$\overline{y} = \frac{\mu_{wet}}{\mu_{cd}} \quad (3)$$

where $\overline{y}$, tire hydroplaning parameter

μ_{wet} , Experimental or predicted wet pavement friction coefficient value

μ_{cd} , characteristic dry friction coefficient value

In determining the tire hydroplaning parameter, distinction is made between two types of tire operating modes-non rotating and rotating. For locked-wheel, sliding (non rotating) tire friction data (e.g. DBV), the tire hydroplaning parameter is labeled $\overline{y}_L$. For braked or yawed rolling (rotating) tire friction data (e.g. BV-11, SFT and Mu-meter), the tire hydroplaning parameter is labeled $\overline{y}_R$The relationship between $\overline{y}_L$ and $\overline{y}_R$, which was empirically derived from NASA track aircraft tire test data, is given in table III. Hence, knowing one tire hydroplaning parameter allows determination of the other (see table III).

STEP 7 – Calculate aircraft tire maximum braking friction coefficient, μ_{max} , values by simply multiplying the $\overline{y}_R$ values determined in STEP 6 by the aircraft tire characteristic dry friction coefficient value determined for eq. 2 in STEP 4 (see table II).

STEP 8 – Determine estimated aircraft tire effective braking coefficient, μ_{eff} , values by use of the following equations:

For $\mu \max < 0.7$; $\mu_{eff} = 0.2\,\mu_{\max} + 0.7143\,\mu_{max\,2}$ (4a)

For $\mu_{max} \overline{>} 0.7$; μ_{eff} = 0.7 μ_{max} (4b)

These relationships between aircraft tire maximum braking and effective braking friction coefficient are based on the assumption that the total aircraft braking system (tires, brakes, hydraulics, gear, and antiskid) efficiency can be generalized by a single curve defined by equations 4 a and b. Values derived for B-737 aircraft are listed in table II.

STEP 9 – Calculate an equivalent aircraft ground speed associated with each μ_{eff} value by multiplying the appropriate ground vehicle speed ratio obtained in STEP 5 by the aircraft tire hydroplaning speed determined in STEP 2 (see table II).

STEP 10 – Compare estimated aircraft tire friction performance to actual measured performance (see figure 3).

<u>Supplemental Data Analysis</u> –

1. Statistical methods should be used to identify data set tolerances and degree of confidence in data correlation.

2. Parameter sensitivity studies should be performed to define effects on data correlation agreement.

Table I.- Compilation of test aircraft and ground vehicle tire friction parameters

TEST PARAMETER	TEST AIRCRAFT		GROUND TEST VEHICLES			
	B-737	B-727	DIAGONAL BRAKED	MU-METER	FRICTION TESTER	BV-11 SKIDDOMETER
Tire: Size Infl. Press. kPa (psi) Tread design	Main gear 40 x 14 1069 (155) 4-Groove	Main gear 49 x 17 931 (135) 6-Groove	ASTM E524 G78 x 15 165 (24) Smooth	RL-2 4.00 - 8 69 (10) Smooth	RL-2 4.00 - 8 207 (30) Smooth	RL-2 4.00 - 8 207 (30) Smooth
Braking method	Maximum Antiskid	Maximum Antiskid	Locked Wheel	None (7.5° yaw)	Constant 10% Slip	Constant 17% Slip
Friction reading	μ_{EFF}	μ_{EFF}	μ_{SKID}	μ_{SIDE}	μ_{DRAG}	μ_{DRAG}
Spin-down hydroplaning Speed, V_p, knots (mph)	112* (129)	105* (121)	44.1* (50.8)	39.1 (45)	49.3* (56.7)	49.3* (56.7)
Low speed characteristic dry friction, μ_{cd}	0.76*	0.78*	1.20	0.90	1.10	1.10

* Calculated values using:

(V_p) spin-down $= 3.43\sqrt{p}$ for SI Units $\mu_{cd} = 0.93 - 1.6 \times 10^{-4}\ p$

(V_p) spin-down $= 9\sqrt{p}$ for U.S. Customary Units $\mu_{cd} = 0.93 - 1.1 \times 10^{-3}\ p$

where p, tire inflation pressure, kPa (psi)

Table II - Compilation of parameter values used to estimate aircraft braking performance from ground vehicle data
(a) Slurry seal asphalt surface; Track wetted; Water depth 0.51mm (0.02in.)

GROUND TEST VEHICLE	FAIRED μ	SPEED, V_G		V_G/V_p	TIRE HYDROPLANING PARAMETERS		ESTIMATED B-737 AIRCRAFT BRAKING			ACTUAL B-737 A/C
		KNOTS	MPH		$\bar{Y}_L$	$\bar{Y}_R$	μ_{MAX}	μ_{EFF}	V_G, KNOTS	μ_{EFF}
Diagonal	0.77	10	12	0.227	0.642	0.895	0.680	0.466	25.4	—
Braked	.59	20	23	.454	.492	.742	.564	.340	50.8	0.365
Vehicle	.47	30	34	.680	.392	.642	.488	.268	76.2	.290
(DBV)	.38	40	46	.907	.317	.564	.429	.217	101.6	—
↓	.31	50	58	1.134	.258	.495	.376	.176	126.6	—
	.24	60	69	1.361	.200	.412	.313	.133	152.4	—
Saab	—	10	12	.203	—	—	—	—	22.7	—
Friction	.93	20	23	.406	.581	.845	.642	.423	45.5	.380
Tester	.78	30	34	.609	.460	.709	.539	.315	68.2	.315
(SFT)	.66	40	46	.811	.350	.600	.456	.240	90.8	.250
↓	.54	50	58	1.014	.255	.491	.373	.174	113.6	—
	.43	60	69	1.217	.188	.391	.297	.122	136.3	—
BV-11	—	10	12	.203	—	—	—	—	22.7	—
Skiddometer	.93	20	23	.406	.581	.845	.642	.423	45.5	.380
	.80	30	34	.609	.478	.727	.553	.329	68.2	.315
	.67	40	46	.811	.359	.609	.463	.246	90.8	.250
	.55	50	58	1.014	.262	.500	.380	.179	113.6	—
↓	.44	60	69	1.217	.193	.400	.304	.127	136.3	—
Mu-meter	.88	10	12	.256	.873	.978	.743	.520	28.7	.430
	.83	20	23	.512	.689	.922	.701	.491	57.3	.345
	.78	30	34	.767	.604	.867	.659	.442	85.9	.260
	.72	40	46	1.023	.544	.800	.608	.386	114.6	—
	.67	50	58	1.279	.494	.744	.565	.341	143.2	—
↓	.62	60	69	1.535	.441	.689	.524	.301	171.9	—

Table III. - Relationship between rotating ($\bar{Y}_R$) and nonrotating ($\bar{Y}_L$) tire hydroplaning parameters.

$\bar{Y}_R$	$\bar{Y}_L$	$\bar{Y}_R$	$\bar{Y}_L$	$\bar{Y}_R$	$\bar{Y}_L$	$\bar{Y}_R$	$\bar{Y}_L$	$\bar{Y}_R$	$\bar{Y}_L$
0.000	0.000	.200	.095	.400	.193	.600	.350	.800	.544
.005	.002	.205	.097	.405	.196	.605	.355	.805	.548
.010	.005	.210	.099	.410	.199	.610	.360	.810	.551
.015	.007	.215	.101	.415	.202	.615	.365	.815	.555
.020	.010	.220	.104	.420	.205	.620	.370	.820	.560
.025	.012	.225	.106	.425	.208	.625	.375	.825	.564
.030	.015	.230	.108	.430	.211	.630	.380	.830	.568
.035	.017	.235	.111	.435	.215	.635	.385	.835	.572
.040	.019	.240	.113	.440	.218	.640	.390	.840	.576
.045	.021	.245	.116	.445	.221	.645	.395	.845	.581
.050	.024	.250	.118	.450	.225	.650	.400	.850	.586
.055	.026	.255	.120	.455	.228	.655	.405	.855	.591
.060	.028	.260	.122	.460	.232	.660	.410	.860	.597
.065	.030	.265	.125	.465	.235	.665	.415	.865	.602
.070	.033	.270	.127	.470	.239	.670	.421	.870	.608
.075	.035	.275	.130	.475	.243	.675	.426	.875	.614
.080	.038	.280	.132	.480	.247	.680	.431	.880	.620
.085	.040	.285	.134	.485	.250	.685	.437	.885	.626
.090	.043	.290	.137	.490	.254	.690	.442	.890	.634
.095	.045	.295	.139	.495	.258	.695	.447	.895	.642
.100	.047	.300	.141	.500	.262	.700	.451	.900	.650
.105	.050	.305	.144	.505	.266	.705	.456	.905	.659
.110	.052	.310	.146	.510	.270	.710	.461	.910	.667
.115	.054	.315	.148	.515	.274	.715	.466	.915	.677
.120	.057	.320	.151	.520	.279	.720	.471	.920	.687
.125	.059	.325	.154	.525	.283	.725	.476	.925	.698
.130	.062	.330	.156	.530	.287	.730	.481	.930	.709
.135	.064	.335	.158	.535	.292	.735	.485	.935	.720
.140	.066	.340	.161	.540	.296	.740	.490	.940	.734
.145	.068	.345	.163	.545	.300	.745	.495	.945	.748
.150	.071	.350	.166	.550	.305	.750	.500	.950	.762
.155	.073	.355	.168	.555	.309	.755	.504	.955	.779
.160	.075	.360	.170	.560	.314	.760	.509	.960	.795
.165	.078	.365	.173	.565	.318	.765	.514	.965	.815
.170	.080	.370	.175	.570	.322	.770	.518	.970	.835
.175	.083	.375	.178	.575	.327	.775	.523	.975	.859
.180	.085	.380	.181	.580	.332	.780	.527	.980	.882
.185	.087	.385	.184	.585	.336	.785	.531	.985	.910
.190	.090	.390	.187	.590	.340	.790	.535	.990	.940
.195	.092	.395	.190	.595	.345	.795	.540	.995	.975
								1.000	1.000

Figure 1.- Methodology used to estimate aircraft tire friction performance.

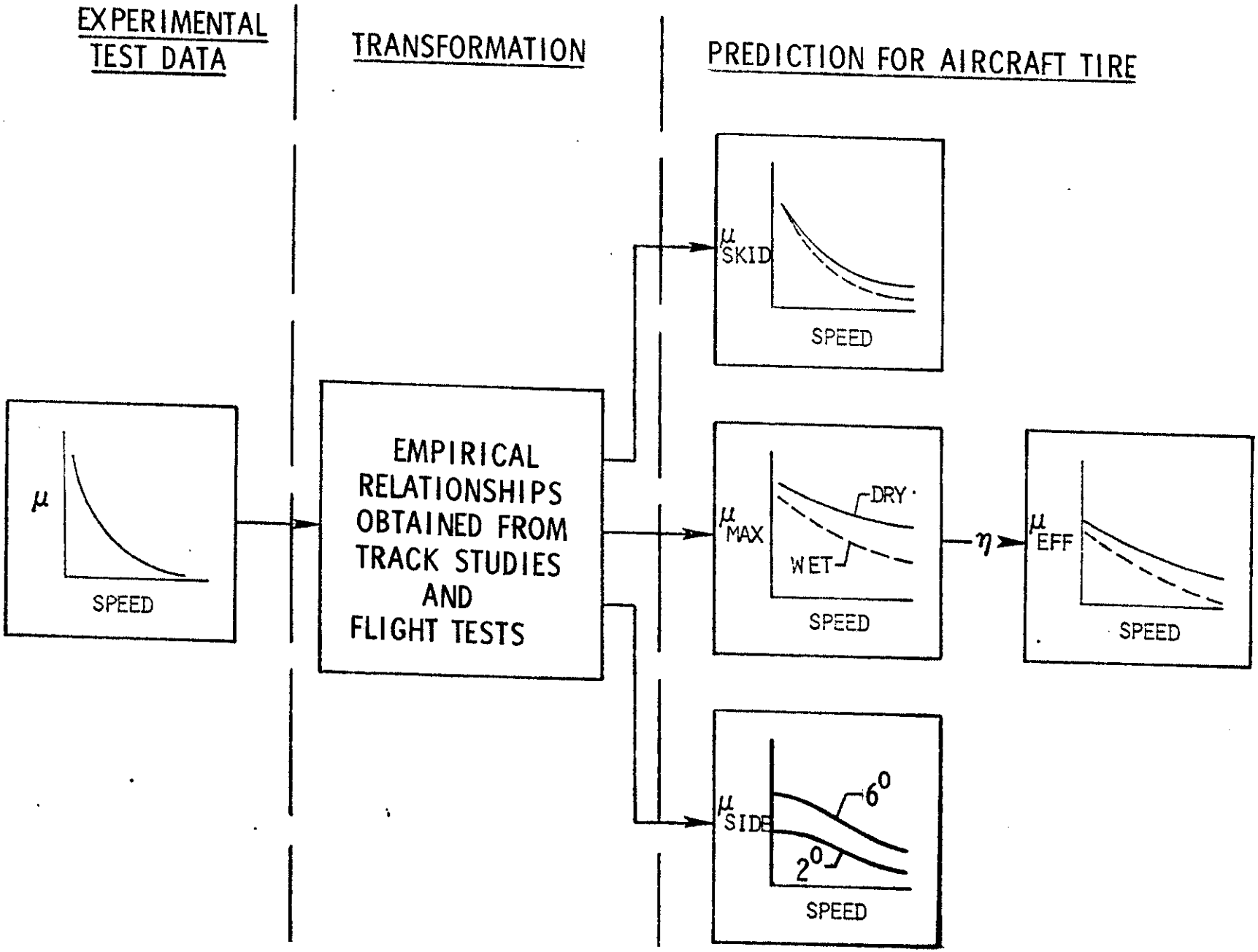

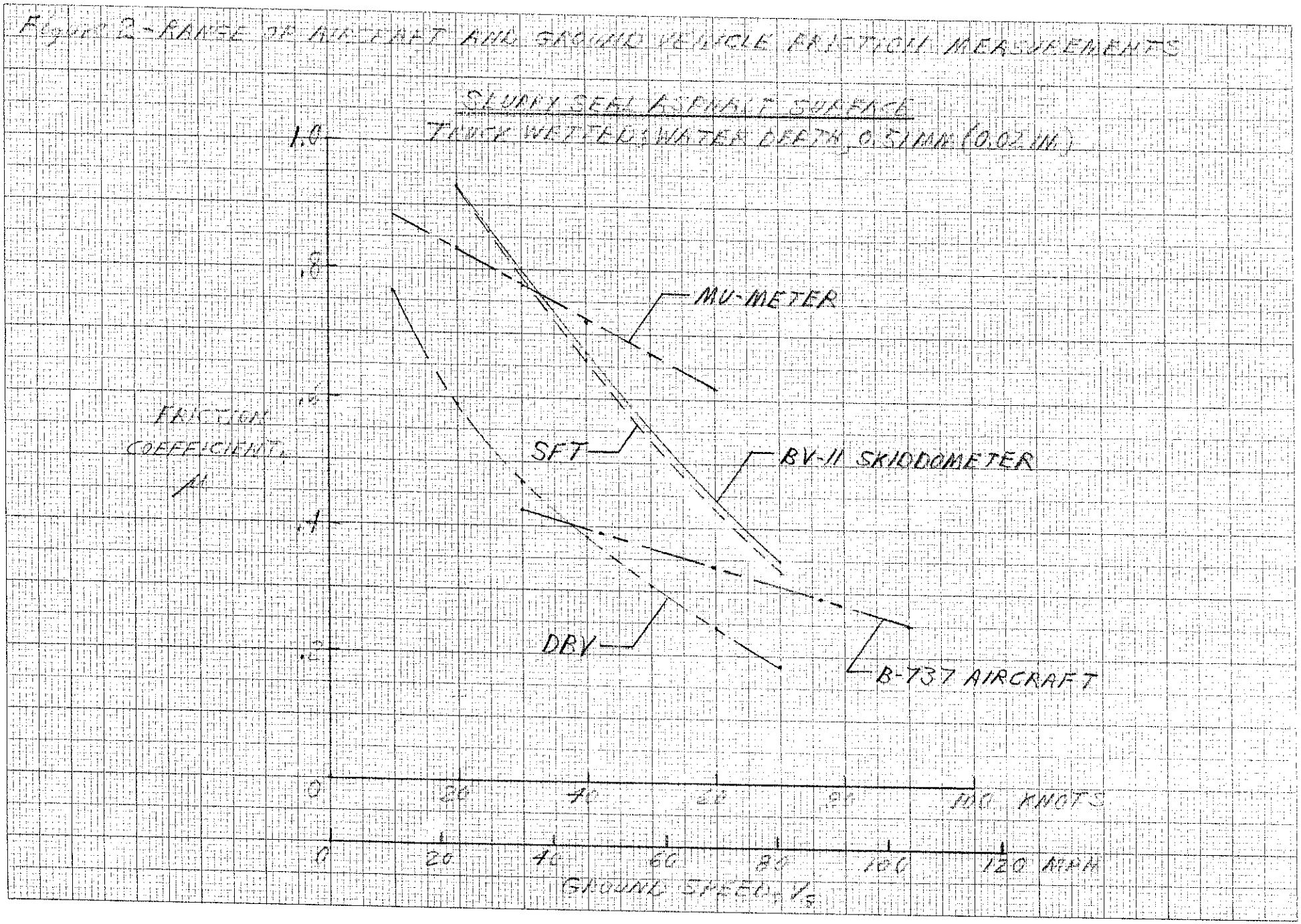

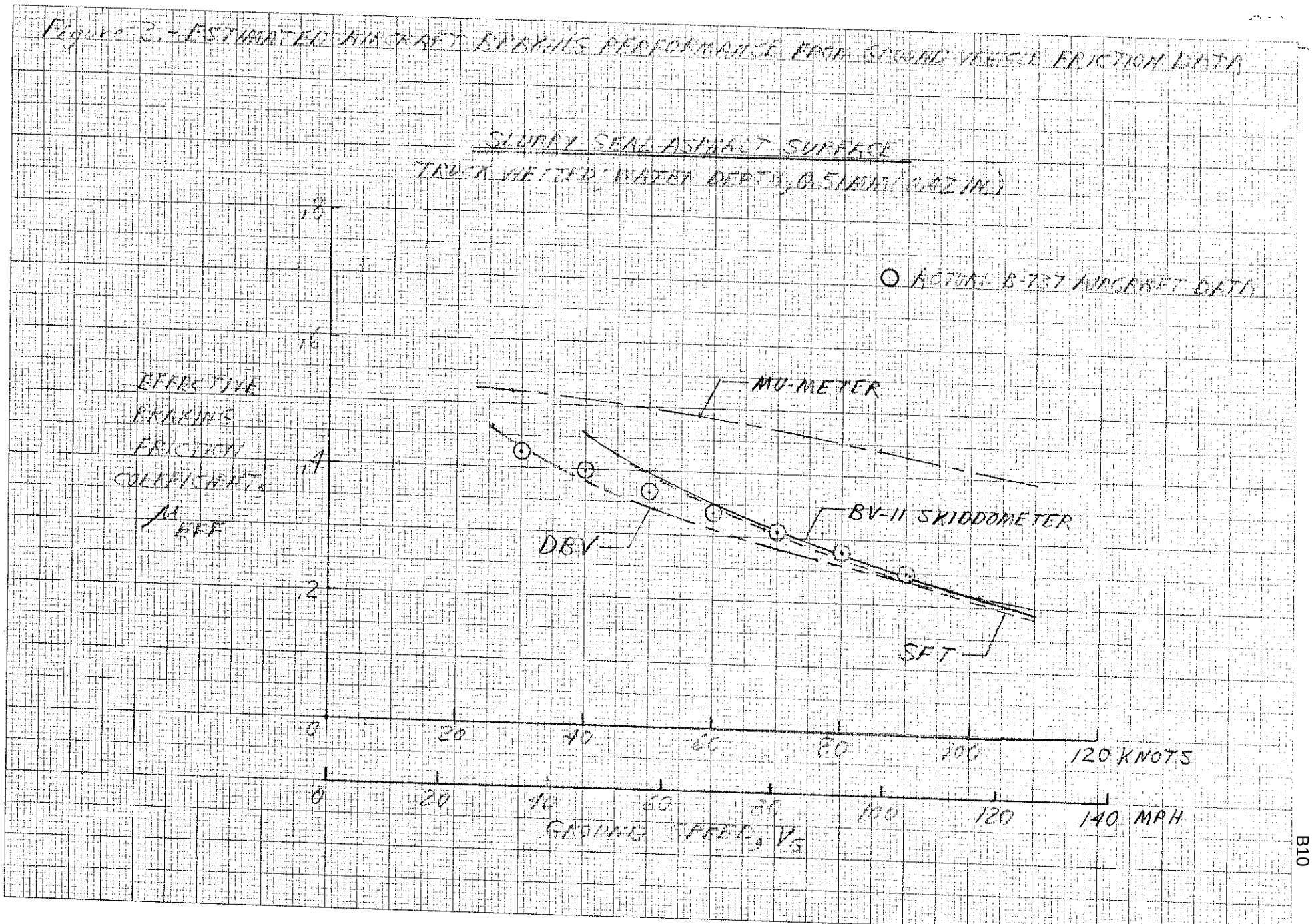

ONA TONNA, MN; R/W 30; July 31, 2008

SFT $\mu_{DRY} = 1.10$; $V_p = 56.8$ mph

A/C $\mu_{MAX} = 0.77$; $V_p = 107$ knots

RUNWAY SURFACE	SURF. COND.	SPEED, MPH	AVERAGE μ_{MAX}	V_G/V_p	$\bar{Y}_L$	$\bar{V}_R$	GA 125-800A Aircraft			
							μ_{SKID}	μ_{MAX}	μ_{EFF}	V_G, KNOTS
Ungrooved	0.1 mm	60	0.39	1.001	0.168	0.355	0.129	0.273	0.108	107
Concrete	(0.04 in)	50	0.45	0.880	0.199	0.409	0.153	0.315	0.134	94
		40	0.51	0.704	0.235	0.464	0.357	0.357	0.162	75
		30	0.58	0.528	0.295	0.527	0.219	0.406	0.199	56
		20	0.65	0.352	0.342	0.591	0.263	0.455	0.239	38
↓	↓	10	0.70	0.176	0.380	0.636	0.297	0.490	0.270	19
		70	0.31	1.232	0.133	0.282	0.102	0.217	0.090	132

NASA-Langley Form 10 (AUG 1969)

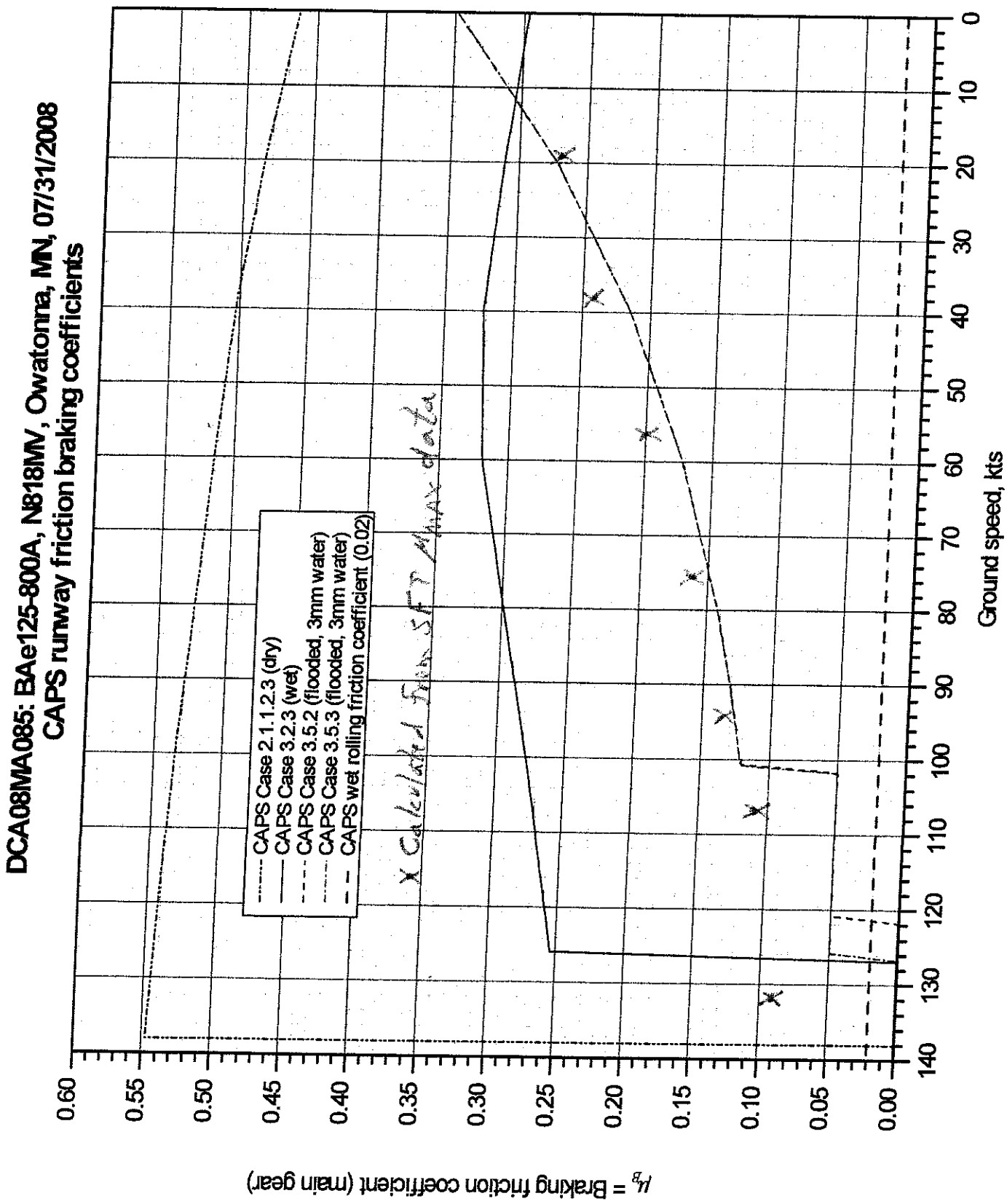
DCA08MA085: BAe125-800A, N818MV, Owatonna, MN, 07/31/2008
CAPS runway friction braking coefficients
CAPS Case 2.1.1.2.3 (dry)
CAPS Case 3.2.3 (wet)
CAPS Case 3.5.2 (flooded, 3mm water)
CAPS Case 3.5.3 (flooded, 3mm water)
CAPS wet rolling friction coefficient (0.02)
Calculated from SFT μMAX data
μB = Braking friction coefficient (main gear)
Ground speed, kts
0.60
0.55
0.50
0.45
0.40
0.35
0.30
0.25
0.20
0.15
0.10
0.05
0.00
140
130
120
110
100
90
80
70
60
50
40
30
20
10
0

APPENDIX C:

FAA SAFO 19001:
Landing Performance Assessments at Time of Arrival

U.S. Department
of Transportation
Federal Aviation
Administration

SAFO

Safety Alert for Operators

SAFO 19001
DATE: 3/11/19

Flight Standards Service
Washington, DC

http://www.faa.gov/other_visit/aviation_industry/airline_operators/airline_safety/safo

A SAFO contains important safety information and may include recommended action. SAFO content should be especially valuable to air carriers in meeting their statutory duty to provide service with the highest possible degree of safety in the public interest. Besides the specific action recommended in a SAFO, an alternative action may be as effective in addressing the safety issue named in the SAFO.

Subject: Landing Performance Assessments at Time of Arrival

Purpose: This SAFO replaces cancelled SAFO 06012 and provides recommendations for airplane operators at airports reporting runway conditions following the procedures in AC 150/5200-30 (Airport Field Condition Assessments and Winter Operations Safety). This information is provided to assist operators in developing methods to ensure sufficient landing distance exists to safely make a full stop landing.

Background: After a Boeing 737-700 runway overrun accident at Chicago Midway Airport in December 2005, the FAA convened the Takeoff and Landing Performance Assessment (TALPA) Aviation Rulemaking Committee (ARC). The Federal Aviation Administration (FAA) adopted certain recommendations of the ARC (which became known as "TALPA"), and implemented them into the National Airspace System on October 1, 2016. This SAFO provides information and guidelines to airplane operators on utilizing the safety benefits TALPA provides.

Applicability: This SAFO is applicable to all Title 14 of the Code of Federal Regulations (14 CFR) part 121, part 125, part 135, and part 91 airplane operators. This guidance is independent of the preflight landing distance-planning requirements of §§ 121.195, 135.385, and 91.1037.

Terminology: The following terms are specific to this guidance and may differ with definitions contained in other published references.

a. Landing Distance at Time of Arrival. These distances are advisory performance data (i.e., not required by regulation) intended to provide a more accurate assessment of actual landing distance at time of arrival, considering factors that cannot be accurately predicted at time of preflight, such as runway contaminants, winds, speed additives, and touchdown points. These distances may be based upon the use of reverse thrust, ground spoilers, autobrakes, etc.

b. Pilot Braking Action Report. A Pilot Report (PIREP) reflecting the brake contribution to the airplane's deceleration. A PIREP Braking Action Report reflects the pilots' impression of the available wheel braking. The report may also be based on directional control feedback. The parameters are as follows;

- Good – Braking deceleration is normal for the wheel braking effort applied, and directional control is normal.

- Good to Medium – Braking deceleration OR directional control is between Good and Medium; i.e. Braking deceleration is between "normal and noticeably reduced for the wheel braking effort applied" AND "directional control is between normal and noticeably reduced".

- Medium – Braking deceleration is noticeably reduced for the wheel braking effort applied OR directional control is noticeably reduced.

- Medium to Poor – Braking deceleration OR directional control is between Medium and Poor; i.e., Braking deceleration is between "noticeably reduced and significantly reduced for the wheel braking effort applied" AND "directional control is between noticeably reduced and significantly reduced".

- Poor – Braking deceleration is significantly reduced for the wheel braking effort applied OR directional control is significantly reduced.

- Nil – Braking deceleration is minimal to non-existent for the wheel braking effort applied OR directional control is uncertain.

c. Reliable Braking Action Report. Items to be considered to determine if the braking action report is reliable:

- Similar weight and class of airplane. An example would be the Boeing 737 and Airbus 320, where the weight and gear track are similar.
- Time since braking action report was given. For example, stable conditions with cold temperature and no active precipitation will likely be reliable for a longer time than reports provided during an active precipitation event with temperatures near 0-degrees Celsius.

d. Airplane Ground Deceleration Devices. Any devices used to aid in the onset or rate of airplane deceleration on the ground during the landing roll out. These would include, but are not limited to: brakes (either manual braking or autobrakes), spoilers, and thrust reversers.

e. At Time of Arrival. For the purpose of this guidance, Time of Arrival is a point in time close enough to the airport to allow the crew to obtain the most current meteorological and runway surface conditions considering pilot workload and traffic surveillance, but no later than the commencement of the approach procedures or visual approach pattern.

f. Landing Distance Available. The length of the runway declared available and suitable for landing an aircraft.

g. Runway Surface Conditions. The state of the runway surface: dry, wet, or contaminated.

- A dry runway is one that is clear of contaminants and visible moisture within the required length and the width being used.

- A wet runway is one that is neither dry nor contaminated.
- A contaminated runway is one where the runway surface conditions report includes the type and depth (if applicable) of the substance on the runway surface (e.g., water, dry snow, wet snow, slush, ice, frost, sanded, or chemical treatment).

The FAA acknowledges that there are situations where the flightcrew needs to know the absolute performance capability of the airplane. These situations include abnormal configurations of the airplane or during emergencies such as engine failure or flight control malfunctions. In such circumstances, the pilot must consider whether it is safer to remain in the air or to land immediately and should know the actual landing performance capability (without an added safety margin) when making these evaluations. This guidance is not intended to curtail such evaluations from being made for these situations (e.g., a pilot in command's (PIC) authority to exercise § 91.3(b).

h. Unfactored Certificated Airplane Flight Manual (AFM) Landing Distance. The landing distance required by § 25.125 without any factors applied. This landing distance is based on dry runway wheel braking and does not need to include runway slope or air temperature accountability, or approach speed additives. It may be based on aggressive flight test techniques when determining the air distance, and does not take credit for reverse thrust or account for the effect of autobrakes. The Unfactored Certified AFM Landing Distance may be used with the factors from Table 1 below to determine a factored time of arrival landing distance.

Discussion: The TALPA ARC was formed in 2008 to address issues associated with landing operations at the time of arrival and with takeoff on non-dry, non-wet runways. The committee consisted of airport operators, aircraft operators, aircraft manufacturers as well as their FAA and other regulatory agency counterparts.

a. The TALPA ARC discovered significant gaps in information needed to determine if a safe landing can be made. The ARC produced consistent terminology and runway assessment criteria, and recommended usage of non-dry, non-wet performance data for takeoff and time of arrival landing calculations. The TALPA ARC did not recommend any changes in the *preflight* landing distance requirements.

b. The following ACs and Orders were revised or created in support of the TALPA ARC implementation:

1. AC 150/5200-30D, Airport Field Conditions Assessments and Winter operations Safety
2. AC 150/5200-28F, Notices to Airmen (NOTAMs) for Airport Operators
3. AC 25-31, Takeoff Performance Data for Operations on Contaminated Runways
4. AC 25-32, Landing Performance Data for Time-of-Arrival Landing Performance Assessments
5. AC 91-79a, Mitigating the Risks of a Runway Overrun Upon landing
6. FAA Order 7930.2R Notices to Airmen (NOTAMs)
7. FAA Order 8900.1 Volume 4 Chapter 3 Section 1 Safety Assurance System: Airplane Performance Computation Rules, paragraph 4-494 Takeoff From a Runway which is Wet or Contaminated, and paragraph 4-503 Landing Distances at the Time of Arrival.
8. SAFO 15009 Turbojet Braking Performance on Wet Runways

These references may be consulted for definitions, Runway Condition Assessment Matrix (RCAM), Runway Condition Code (RwyCC) assignments etc.

c. 14 CFR part 139 certificated and/or federally obligated airports use the procedures in AC 150/5200-30D to report runway surface conditions when they are not dry. These conditions may be reported using the RCAM in AC 150/5200-30D, when airport operators receive pilot braking action reports, or when surface conditions are other than dry. Friction measuring equipment values are no longer used to determine and report surface conditions because joint industry and multi-national government tests have not established a reliable correlation between runway friction values and the relationship to airplane braking performance.

d. The basis for time of arrival landing distance as defined by the TALPA ARC reflects the recommended method of operationally landing and stopping an airplane in service. As such, it accounts for and quantifies many of the factors that may not be explicitly accounted for in the certificated (AFM) landing distance. Subparagraphs c. and d. Landing Distance Assessment at Time of Arrival (below) list the runway condition and aircraft performance factors that should be used for the time of arrival landing distance calculation.

e. Sections 121.195, 135.385 and 91.1037 wet or slippery landing data may not provide adequate runway length for landing on a wet or contaminated surface. Operators, through performance analysis, should identify those airports and aircraft that may be affected. In those cases, operators should take appropriate action to ensure the flightcrew will have sufficient runway for the conditions expected at the estimated time of arrival.

Landing Distance Assessment at Time of Arrival. There is no specific regulation requiring operators to assess landing distance requirements at time of arrival, however the FAA encourages operators to adopt such procedures to ensure that a safe landing can be made. Additionally, the FAA highly encourages operators to use their FAA-approved landing performance data and any associated manufacturer-provided supplemental/advisory data in concert with the AC 91-79-generated RCAM Braking Action Codes to conduct an adequate landing distance assessment at the time of arrival. This is particularly important when the landing runway is contaminated or not the same runway analyzed for preflight calculations. The following are best practices for conducting a landing distance assessment at time of arrival.

a. Timeliness. An assessment is initially performed when landing weather and field conditions are obtained, usually around Top of Descent (TOD). It is important to note the time of the latest Field Condition report and any associated reliable braking action reports. A number of overruns have occurred when pilots were provided with a runway condition that was no longer reliable given changes in meteorological conditions. Pilots are strongly advised to review the weather conditions and compare that to the time of the latest braking action report. The assessment should include consideration of how much deterioration in field conditions can be tolerated, the minimum RwyCC(s), and Field Condition (FICON) or Braking Action Reports needed to safely land, should those factors deteriorate from the ones used in the TOD landing distance

b. Source of Data. When possible, the Operational Landing Distance data used is advisory data based on the recommendations of AC 25-32. This data may be provided by the manufacturer. If it is not provided by the manufacturer, data developed by a performance data provider may be used.

1. If advisory data for a landing distance assessment at time-of-arrival is not available from the manufacturer, performance provider data may be used. If performance-provider data is not available, the landing distance factors (LDF) from Table 1, Landing Distance Factors, may be used. To find the Landing Distance Required (LDR), multiply the certificated (i.e., AFM dry, *unfactored*) Landing Distance by the applicable LDF in Table 1 for the runway conditions existing at the time of arrival. If the AFM landing distances are presented as *factored* landing distances, then those data must be adjusted to remove the applicable preflight factors applied to that data. The LDFs given in Table 1 include a 15 percent safety margin, an air distance representative of normal operational practices, a reasonable accounting for temperature, the effect of increased approach speed, reduced wheel braking, reverse thrust usage (or not), the additional effect of reduced wheel braking capability on altitude and wind distance adjustment.

2. Currently, the Small Airplane Directorate does not plan to provide aircraft manufacturers with advisory information similar to AC 25-32. In the absence of guidance to manufacturers of part 23 aircraft, Operational Landing Distance data may be based on the recommendations of AC 25-32. This data may be provided by the manufacturer or developed by a performance data provider if manufacturer data is not available. In the absence of guidance to part 23 aircraft manufacturers, the manufacturer or data provider may consider the recommendations in AC 25-32 when creating data for a time-of-arrival assessment. Manufacturer-provided guidance on the use of existing data with the runway condition codes (RwyCC) must be used when available.

Table 1. Landing Distance Factors

The following are multipliers to the unfactored certificated (AFM) landing distances

	Runway Condition Code						
Braking Action	6 (Dry)	5 Grooved /PFC Good	5 Smooth Good	4 Good to Medium	3 Medium	2 Medium to Poor	1 Poor
Turbojet, No Reverse	1.67	2.3	2.6	2.8	3.2	4.0	5.1
Turbojet, With Reverse	1.67	1.92	2.2	2.3	2.5	2.9	3.4
Turboprop Note 1	1.67	1.92	2.0	2.2	2.4	2.7	2.9
Reciprocating	1.67	2.3	2.6	2.8	3.2	4.0	5.1

Note 1: These LDFs apply only to turboprops where the AFM provides for a landing distance credit for the use of ground idle power lever position. Turboprops without this credit should use the Turbojet, No Reverse LDFs.

c. Runway Condition Considerations. When available for the portion of the runway that will be used for landing, the following are considered:

1) Runway condition code (RwyCC).
2) Expected runway conditions (contaminate type and depth).
3) Pilot braking action report.

d. Aircraft Performance Considerations. The following considerations may impact operational landing distance calculations:

1) Runway slope,
2) Airport elevation,
3) Wind,
4) Temperature,
5) Airplane weight and configuration,
6) Approach speed at threshold,
7) Adjustment to landing distance (such as autoland), and
8) Planned use of airplane ground deceleration devices.

e. Safety Margin. The operational landing distance (OLD) used for a time of arrival landing assessment includes a safety margin of at least 15 percent when based on manual wheel braking.

f. Autobrake Usage. While autobrakes are part of the aircraft's landing configuration, the landing distance assessment is not intended to force higher than necessary autobrake selection. For operations when the runway is dry or wet if the manual braking distance provides a 15 percent safety margin, then the braking technique may include a combination of autobrakes and manual braking even **IF** the selected autobrake landing data does not provide a 15 percent safety margin.

g. Touchdown Point. The touchdown point used in the performance data assessment reflects the assumed air distance. Operational landing data usually includes an allowance for 1,500 feet or 7 seconds of air distance from the threshold to touchdown. An air distance as short as 1,000 feet may be used **IF** an operator's landing assessment procedures include enhancements to minimize the risk of overruns or undershoots, including:

1) Training in touchdown control and short field landing techniques.
2) Identification of required touchdown point and training to assure go-around procedures are initiated if unable to achieve a suitable touchdown point.
3) Approach guidance and runway markings on the specific runway are consistent with a shorter air distance.
4) Operational data (without the need for interpolation) are provided to the crew for the specific runway, conditions, and aircraft landing configuration.
5) The flight techniques assumed in the creation of the performance data used for a shorter air distances are based on flight techniques to be used in the shorter air distance operation.

For example, the assumed speed bleed off used in the performance data needs to be consistent with the trained flight techniques for flaring the aircraft.

NOTE: If no other information is available, the autoland or other similar low visibility guidance system may be assumed to be consistent with the 7 second air distance.

h. Assessment Based on Preflight Criteria. When the runway is dry, or when the runway is wet and grooved or PFC, the assessment for turbojet airplanes with thrust reversers and turboprop airplanes with a landing distance credit for the use of ground idle may be as simple as confirming that the runway meets the criteria used for preflight.

i. Documentation and Training. Published material and training material include the assumptions and limitations on the use of data provided to do a landing distance assessment at the time of arrival.

1) The operator's flightcrew and dispatcher (part 121 Operations) training programs should include elements that provide knowledge in all aspects and assumptions used in landing distance performance determinations. This training should emphasize the airplane ground deceleration devices, settings, and piloting methods (e.g., air distance) used in determining landing distances for each make, model, and series of airplane. Elements such as braking action reports, airplane configuration, optimal stopping performance techniques, stopping margin, the effects of excess speed, delays in activating deceleration devices, and other pilot performance techniques should be addressed. All dispatchers and flightcrew members should be trained on these elements prior to operating on contaminated runway surfaces. This training should be accomplished in a manner consistent with the operator's methods for conveying similar knowledge to flight operations personnel. It may be conducted via operations/training bulletins or extended learning systems, if applicable to the operator's current methods of training.

2) Procedures for obtaining optimal stopping performance on contaminated runways should be included in flight training programs. All flight crewmembers should be made aware of these procedures for the make/model/series of airplane they operate. This training should be accomplished in a manner consistent with the operator's methods for conveying similar information to flight operations personnel. It may be conducted via operations/training bulletins or extended learning systems, if applicable to the operator's current methods of training. In addition, if not already included, these procedures should be incorporated into each airplane or simulator training curriculum for initial qualification on the make/model/series airplane, or differences training as appropriate. All flight crewmembers should have hands-on training and validate proficiency in these procedures during their next flight training event unless previously demonstrated with their current employer in that make/model/series of airplane.

Recommended Action: Directors of safety and directors of operations (part 121); directors of operations (part 135, and 125), program managers, (part 91K), and pilots (part 91) should take appropriate action within their operation to address the safety concerns with landing performance on wet or contaminated runways discussed in this SAFO. Operators should develop procedures for flightcrews to assess landing

performance based on conditions existing at time of arrival, distinct from conditions forecast prior to departure. Those conditions may include weather, Runway Condition Code (RwyCC) (if provided), FICON report (if provided), the airplane's weight, braking systems to be used, and any other conditions the operator deems necessary to conduct a safe landing, such as Pilot Reports of Braking action. Once the actual landing distance is determined at the time of arrival, an additional safety margin of at least 15 percent should be added to actual landing distance. Except under emergency conditions flight crews should not attempt to land on runways that do not meet the assessment criteria and safety margins as specified in this SAFO.

Contact: Questions or comments regarding this SAFO should be directed to the Air Transportation Division at 202-267-8166.

APPENDIX D:

FAA SAFO 19003:
Turbojet Braking Performance on Wet Runways

U.S. Department
of Transportation
Federal Aviation
Administration

SAFO

Safety Alert for Operators

SAFO 19003
DATE: 7/2/19

Flight Standards Service
Washington, DC

http://www.faa.gov/other_visit/aviation_industry/airline_operators/airline_safety/safo

A SAFO contains important safety information and may include recommended action. SAFO content should be especially valuable to air carriers in meeting their statutory duty to provide service with the highest possible degree of safety in the public interest. Besides the specific action recommended in a SAFO, an alternative action may be as effective in addressing the safety issue named in the SAFO.

Subject: Turbojet Braking Performance on Wet Runways.

Purpose: This SAFO cancels and replaces SAFO 15009 and warns airplane operators and pilots that the advisory data for wet runway landings may not provide a safe stopping margin especially in conditions of Moderate or Heavy Rain.

Background: Landing overruns that occur on wet runways typically involve multiple contributing factors such as long touchdown, improper use of deceleration devices, tailwind and less available friction than expected. Several recent runway-landing incidents/accidents have raised concerns with wet runway stopping performance assumptions. Analysis of the stopping data from these incidents/accidents indicates the braking coefficient of friction in each case was significantly lower than expected for a wet runway as defined by Title 14 of the Code of Federal Regulations (14 CFR) part 25 § Section 25.109 and Advisory Circular (AC) 25-7D methods.

These incidents/accidents occurred on both grooved and un-grooved runways. The data indicates that applying a 15% safety margin to wet runway time-of-arrival advisory data, as recommended by SAFO 19001 (or current guidance), may be inadequate in certain wet runway conditions. Takeoff and Landing Performance Assessment (TALPA) procedures implemented by the FAA on October 1, 2016, added new insight as to how flightcrews can evaluate runway braking performance prior to landing. TALPA defines *WET* as "Includes damp and 1/8-inch depth or less of water," while *CONTAMINATED* is "greater than 1/8-inch of water."

Discussion: These overruns have occurred on grooved and smooth runways during periods of moderate to heavy rain. Analysis of these incidents/accidents indicates that the braking coefficient of friction in each case was significantly lower than expected, and that 30 to 40 percent of additional stopping distance may be required if the runway transitions from *wet* to *contaminated* based on the rainfall intensity or reported water contamination (greater than 1/8-inch depth). For the operational in-flight landing assessment, determining whether the runway is wet or potentially contaminated is the pilot's responsibility.

The FAA recommends that airports report "Wet" conditions. However, airports are not required to report when a runway is only *wet*. Further, an airport may not be able to generate a Field Condition NOTAM (FICON) for sudden rain showers that result in water on the runway more than 1/8 of an inch in depth (*contaminated*). Rainfall intensity may be the only indication available to the pilot that the water depth

present on the runway may be excessive. The 1/8-inch threshold that separates a wet runway with a RWYCC of 5 from runway contaminated with water depth greater than 1/8-inch a RWYCC of 2 is based on possibility of dynamic hydroplaning. This can be especially true in moderate rain if the runway is not properly crowned, grooved, constructed with a porous friction course (PFC) overlay, or when water run-off becomes overwhelmed. During heavy rain events, this may be true even on a properly maintained grooved or PFC runway.

The TALPA RCAM recommends using landing performance data associated with medium to poor braking or RwyCC of 2, if greater than 1/8-inch of water is anticipated to be on the runway. When planning to land on a smooth runway under conditions of moderate or heavy rain, or when landing on a grooved or PFC runway under heavy rain, pilots should consider that the surface may be contaminated with water at depth greater than 1/8 inch and adjust their landing distance assessment accordingly. Pilots should use all available resources to determine what condition they may expect upon landing to include Air Traffic Control (ATC), FICONs (as some airports do report Wet conditions), flight visibility, and/or onboard weather radar.

> **Note:** A Special Weather Observation (SPECI) will only be generated if a Thunderstorm begins. A SPECI is not generated when rainfall rates simply change.

Knowing ahead of time whether your aircraft can or cannot stop within the Landing Distance Available if runway conditions deteriorate to a medium to poor condition (RwyCC = 2) is critical when operating in moderate or heavy rain. Go-around, holding, or diversion may be necessary if rainfall intensity increases beyond what might be acceptable for the intended operation.

Some of the wet runway braking shortfalls have occurred at US airports where 14 CFR Part 139 runway design and maintenance standards apply. Operators should be aware that the aforementioned runway design and maintenance standards might not be met in other countries. Many countries' standards for design, construction and/or maintenance of runways are based on International Civil Aviation Organization (ICAO) Annex 14 runway design and maintenance standards, however they may lack oversight in implementation of these standards. Outside of the United States, there is often less usage of grooving or PFC overlay which, when present, will normally aid in drainage and mitigate the risk of hydroplaning during active precipitation, thus improving braking action.

Unless the pilot or operator is knowledgeable of the runway's maintenance program, and that the runway is grooved or is a PFC surface that can provide good runway friction during periods of active moderate or heavy rain, they should consider basing their time-of-arrival assessment on the above recommendations. Aircraft operators should also clarify their reporting needs to the airport operator as it relates to "Wet" runway conditions.

As stated initially, the other common contributing factors for wet runway excursions include, but are not limited to delayed touchdown, improper application of deceleration devices and tailwind landings. Aircraft operators should review their flight training programs to ensure flight crews are familiar with the assumptions used in creating the data used for the time-of-arrival assessment, such as the assumed distance from threshold to touchdown and recommended uses of deceleration devices. 14 CFR Part 121 aircraft operators should also ensure flight crews are aware of the wind assumed in the original dispatch

calculations for the flight. Advisory Circular 91-79A addresses these issues, and operators should review the guidance contained therein.

Recommended Action: Directors of Safety and Directors of Operations (Part 121); Directors of Operations (parts 135, and 125), Program Managers, (Part 91K), and Pilots (Part 91) should ensure pilots verify, prior to initiating an approach, that the aircraft can stop within the Landing Distance Available using a RwyCC of "2" whenever there is the likelihood of moderate or greater rain on a smooth runway or heavy rain on a grooved/PFC runway.

Contact: Questions or comments regarding this SAFO should be directed to the Air Transportation Division's Air Carrier Operations Branch at (202) 267-8166.